OIL AND GAS INVESTIGATION 19

OIL AND GAS POTENTIAL OF THE SOUTHERN TYEE BASIN, SOUTHERN OREGON COAST RANGE

by

In-Chang Ryu, Alan R. Niem, and Wendy A. Niem
Oregon State University

With a section on
STRUCTURAL AND STRATIGRAPHIC PLAYS
by Alan R. Niem, Ray E. Wells, and In-Chang Ryu

and Plate 1,
INTERPRETED NORTH-SOUTH SEISMIC-REFLECTION PROFILE
ACROSS THE SOUTHERN TYEE BASIN,
by Peter O. Hales, In-Chang Ryu, and Alan R. Niem

1996

STATE OF OREGON
DEPARTMENT OF GEOLOGY AND MINERAL INDUSTRIES
965 State Office Building, 800 NE Oregon Street # 28
Portland, Oregon 97232

STATE OF OREGON
DEPARTMENT OF GEOLOGY AND MINERAL INDUSTRIES
965 State Office Building, 800 NE Oregon Street # 28
Portland, Oregon 97232

OIL AND GAS INVESTIGATION 19

OIL AND GAS POTENTIAL OF THE SOUTHERN TYEE BASIN, SOUTHERN OREGON COAST RANGE

by

In-Chang Ryu, Alan R. Niem, and Wendy A. Niem
Oregon State University

With a section on
STRUCTURAL AND STRATIGRAPHIC PLAYS
by Alan R. Niem, Ray E. Wells, and In-Chang Ryu

and Plate 1,
INTERPRETED NORTH-SOUTH SEISMIC-REFLECTION PROFILE
ACROSS THE SOUTHERN TYEE BASIN,
by Peter O. Hales, In-Chang Ryu, and Alan R. Niem

1996

Conducted and published in conformance with ORS 516.030

Oregon Department of Geology and Mineral Industries Oil and Gas Investigations, ISSN 0078–5741

Funded in part by contributions from

Douglas County Industrial Development Board
GCO Minerals Company
Oregon Department of Geology and Mineral Industries
State of Oregon Lottery Funds
Menasha Corporation
Oregon Natural Gas Development Corporation
Seneca Timber Company
U.S. Bureau of Land Management
USDA Forest Service
Weyerhaeuser Corporation

ABSTRACT

Sequence stratigraphic relationships of Eocene forearc and subduction zone strata in the southern Tyee basin of southwestern Oregon record a complex depositional and tectonic history in an active convergent margin. Several stratigraphic revisions and new members and formations are proposed based on new basinwide lithostratigraphic correlations in a fence diagram which was constructed from logs of several exploration wells, seismic-reflection profiles, and dozens of measured sections in conjunction with recent geologic mapping and biostratigraphic studies (coccoliths and foraminifers). Four depositional sequences, separated by sequence boundaries, are recognized in the 25,000-ft thick section. Syntectonic fan delta, slope, and submarine fan strata of sequence I (lower Umpqua Group) represent a partially subducted accretionary wedge deposited in a "trench" (Umpqua marginal basin). This marginal basin formed as a result of oblique convergence of the North American plate (northern Klamath Mountains) and the Farallon plate (Siletz River Volcanics). Wave- and tide-dominated deltas of sequence II (upper Umpqua Group, White Tail Ridge Formation, Camas Valley Formation) filled irregular lows and thinned over submarine highs (e.g., Reston high) created by intrabasin, imbricate thrust faulting. Farther north, sequences I and II rapidly thin and onlap oceanic basalt islands and seamounts of the older Paleocene to lower Eocene Siletz River Volcanics (Umpqua arch) to form a deep-marine condensed section and then thicken again northward in the Smith River subbasin in the subsurface. These sequences are overlain by a tectonism-forced transgressive systems tract (Camas Valley Formation) deposited during an onlap caused by tectonic subsidence and clockwise rotation of the basin approximately 50 Ma. By middle Eocene, wave- and tide-dominated deltas and deep-sea fans of sequences III and IV (Tyee, Elkton, Bateman, and Spencer formations) prograded northward down the axis of the Tyee forearc basin across the NE-SW structural trend of sequences I and II. Periods of deformation and uplift occurred in the early-middle and late Eocene and late-middle Miocene-Pliocene as a result of rapid plate convergence.

Organic geochemistry (e.g., Rock -Eval, TOC, TAI, and R_O) indicates that most marine mudstone and sandstone units are thermally immature and contain lean, gas-prone Type III kerogen. However, a few nonmarine beds (coals), carbonaceous mudstone, and mélange units of the adjacent Klamath Mountains are sufficiently organic-rich to be sources of biogenic and thermogenic methane discovered in numerous seeps. A computer-generated maturation model (BasinMod) predicts that some strata of sequences I and II have been matured in previously more deeply buried areas of the basin. Complex diagenesis in the lithic and arkosic sandstones has filled much of the primary porosity with zeolite, clay, and quartz cement, thus diminishing the permeability of these potential reservoir units. Reservoir-quality porosity, permeability, and some secondary porosity are identified in a few delta front and turbidite sandstone units (e.g., White Tail Ridge and Spencer formations and Tyee Mountain Member of the Tyee Formation).

Although the overall hydrocarbon potential of the basin is moderately low, several requirements for commercial accumulations of hydrocarbons probably exist together locally within and adjacent to the southern Tyee basin. Three petroleum systems are identified with five structural and stratigraphic plays. The first petroleum system appears near the southern border with the Mesozoic Klamath Mountains and is related to a proposed subduction zone maturation mechanism and migration of hydrocarbons along thrust faults. Potential reservoir units include members of the White Tail Ridge Formation. The seal includes the Camas Valley Formation. The second petroleum system is centered in the northern part of the study area and may be associated with unconventional plays associated with basin-center gas in overpressured zones in turbidite sandstones of the Tyee Mountain Member. The third petroleum system lies near the eastern border of the basin where maturation is related to local heating by sills and

migration of hydrothermal fluids associated with mid-Tertiary volcanism in the Western Cascade arc. The Spencer Formation and members of the White Tail Ridge Formation represent potential reservoir units. Four structural plays include the Williams River-Burnt Ridge anticline, Western Cascades foothills and Bonanza thrust, Tyee Mountain anticline play, and anticlinal and subthrust plays in the Myrtle Point-Sutherlin subbasin. Further exploration drilling appears warranted.

TABLE OF CONTENTS

PLATES — folded separately

1. Interpreted north-south seismic-reflection profile across the southern Tyee basin. The extended geologic cross section was constructed from maps of Black and others (in prep.) and Niem and Niem (1990). Two wells (Amoco Weyerhaeuser B-1 and Northwest Sawyer Rapids) provided subsurface control.
   By *Peter O. Hales, Alan R. Niem, and In-Chang Ryu*

2A. Stratigraphic distribution of sandstone and conglomerate samples

2B. Stratigraphic distribution of porosity

2C. Stratigraphic distribution of permeability

3A. Stratigraphic distribution of source rock samples

3B. Stratigraphic distribution of TOC

3C. Stratigraphic distribution of vitrinite reflectance ($\%R_O$)

3D. Stratigraphic distribution of T_{max}

4. Index map of fence diagram

FIGURES

Page

TABLES

DEDICATION

This publication is dedicated to the memory of the late C. M. "K" Molenaar who, along with emeritus professor Ewart Baldwin (University of Oregon), was instrumental over the years in enlightening geologists and constructing the geologic framework of the Tyee basin. With quiet demeanor, "K" stimulated vigorous discussions on sequence and basin stratigraphy and field visitations that greatly assisted us in further unraveling the complex geology of the basin.

ACKNOWLEDGEMENTS

The authors thank the staff of the Oregon Department of Geology and Mineral Industries (DOGAMI), particularly G. L. Black and Beverly Vogt for editorial advice and review, Dan Wermiel who initiated the project, and Dennis Olmstead who provided cores and cuttings of exploration wells in the basin. We acknowledge the many enlightening, informal discussions in the field with R. E. Wells, Angela Jayko, and Bob McLaughlin (U.S. Geological Survey), Gerald Black and Tom Wiley (DOGAMI), Peter O. Hales (Weyerhaeuser Co.), the late C. M. "K" Molenaar (U.S. Geological Survey), Ewart Baldwin (emeritus professor, University of Oregon), and Parke D. Snavely, Jr. (emeritus geologist, U.S. Geological Survey). David Bukry (emeritus geologist, U.S. Geological Survey), Daniel McKeel (consulting micropaleontologist), and Ellen J. Moore (emeritus geologist, U.S. Geological Survey) provided invaluable advice on coccolith, foraminiferal, and molluscan biostratigraphy. Elli Brouwers (U.S. Geological Survey), Louis Marinkovich (emeritus geologist, U.S. Geological Survey), and Bob Linder (University of Oregon) added information on ostracods, mollusks, and echinoids. Peter O. Hales (Weyerhaeuser) and Bill Seeley (Mobil Oil Corporation) provided subsurface data and seismic-reflection profiles as well as informative unpublished field mapping and company reports on the geology of the area. Keith Kvenvolden, Paul Lillis, Tom Lorenson, and Mark Pawlewicz of the U.S. Geological Survey and Dave Long (Portland State University) analyzed numerous organic geochemistry samples (source rocks and gases from seeps) and advised us on interpretation of the data. J. Reed Glasmann (courtesy professor, Oregon State University) helped in preparation, analysis, and interpretation of clay mineralogy and reviewed the sandstone petrography section of this report. Rauno Perttu (consulting geologist) and Dave Weatherby (former graduate student, University of Oregon) ran informative field trips in their respective thesis areas.

We also acknowledge support and advice over the years from George Priest (DOGAMI), H. Jack Meyer (Northwest Natural Gas Co.), Don Hull (Oregon State Geologist), John Beaulieu (Oregon Deputy State Geologist), Ben Law and Chuck Spencer (U.S. Geological Survey), Nancy Ketrenos (U.S. Bureau of Land Management), and Bob Fujimoto (U.S. Forest Service). Reviews by Parke Snavely, Ray Wells, Jerry Black, and Peter Hales improved the original typescript.

OIL AND GAS POTENTIAL OF THE SOUTHERN TYEE BASIN SOUTHERN OREGON COAST RANGE

by
In-Chang Ryu, A. R. Niem, and W. A. Niem

INTRODUCTION

This study is a culmination of a 5-year program to evaluate the oil and natural gas potential of the southern Tyee basin (Fig. 1.1). Interim reports include a preliminary compilation geologic map of the basin (scale 1:125,000) by Niem and Niem (1990) which summarized and made a preliminary interpretation of available data on oil, gas, and coal resources from industry and state and federal agencies. A fence diagram of 24 measured sections and 11 exploration wells and an accompanying interpretation by Ryu and others (1992) used a revised stratigraphy of the basin (Fig. 1.2). Details of those two reports will not be repeated here; the reader is urged to review those publications before reading this report. Those two investigations built upon the pioneering work of Diller (1898), Baldwin (1974), Baldwin's graduate students at the University of Oregon, student theses at Oregon State University and Portland State University, Molenaar (1985), Chan (1982), Heller (1983), Chan and Dott (1983), Ryberg (1984), and Heller and Dickinson (1985).

Other pertinent studies completed during this 5-year program include an interpretation of sequence stratigraphy of the basin by Ryu and Niem (1993, 1994) and by Ryu (1995), a sedimentologic study of the Bateman Formation by Weatherby (1991), and 25 geologic maps of 7.5-minute quadrangles in the Roseburg 30-minute by 60-minute sheet. These include maps of the Reston, Kenyon Mountain, and Remote quadrangles by Black (1990; 1994a; 1994b), of the Tenmile quadrangle by Wiley and Black (1994), of the Camas Valley quadrangle by Black and Priest (1993), of the Mount Gurney quadrangle by Wiley and others (1994), and of the Dora and Sitkum quadrangles by Wiley (1995). Eighteen 7.5-minute quadrangles in the eastern half of the Roseburg sheet will be published by the U.S. Geological Survey (Jayko, 1995a, 1995b; Jayko and Wells, 1996; Wells, 1996a-i; Wells and others, 1996a, 1996b; Wells and Niem, 1996). This report should be read with a copy of the geologic map of the Tyee basin (1:100,000) by Black and others (in prep.).

In order to better evaluate the oil and gas potential of the southern Tyee basin, this investigation uses the sequence stratigraphic terminology of Van Wagoner and others (1990), adapted for the Tyee basin by Ryu and others (1992) and Ryu and Niem (1993, 1994). Eocene lithostratigraphic units of the Tyee basin (i.e., members and formations) are grouped into unconformity-bounded depositional sequences of related sedimentary facies. Basinward, the unconformities become conformable. Each depositional sequence consists of lowstand, transgressive, and highstand systems tracts.

In evaluating the oil and gas potential of the basin, six topics will be considered. They are:

(1) Location and geologic setting, Eocene stratigraphy, and regional structure;
(2) Reservoir potential: sandstone petrography, diagenesis, and evolution of porosity and permeability;
(3) Source rock and maturation;
(4) Timing of maturation and burial history;
(5) Delineation of areas in which these factors are optimal for exploration success, utilizing the petroleum system and play concepts of Magoon (1988);
(6) Structural and stratigraphic plays.

Location and Geologic Setting

The southern Tyee basin is located in the southern Oregon Coast Range and is bounded by the northern margin of the Mesozoic Klamath Mountains (Fig. 1.1). The Tertiary sequence overlaps the tectonic boundary or suture between these two terrains. The basin extends 130 miles north to the latitude of Salem and Lincoln City (Snavely and others, 1964; Chan and Dott, 1983; Niem and others, 1992b), but only the southern 75 miles of the basin are considered in this report. It is this part of the basin that has the

highest potential for oil and gas. Major geographic features in the study area are the towns of Roseburg, Powers, Myrtle Point, Reedsport, and Florence, the Umpqua and Coquille rivers, and the Tyee escarpment. Access is provided by Interstate 5 (I-5) and Oregon Highway 42 (OR 42).

The basin is as much as 55 miles wide and is overlapped on the east by upper Eocene to Miocene volcanics of the Western Cascade arc (Fig. 1.1). The basin is partially bounded on the west by upper Eocene to middle Miocene deltaic to deep-marine siliciclastics of the Coos Bay forearc basin. The southern Tyee basin is a composite of two basins; the NE-SW-trending early Eocene Umpqua basin and the north-south-trending middle Eocene Tyee forearc basin (Fig. 1.1). The Umpqua basin is subdivided into two subbasins by a NE-SW-trending buried volcanic high, named the Umpqua arch by Ryu and others (1992). The Myrtle Point-Sutherlin subbasin lies south of the arch; the Smith River subbasin is north of the arch.

An aggregate thickness of more than 25,000 feet of lower to upper Eocene strata is preserved in the Umpqua basin although no more than 10,000 to 15,000 feet of strata are preserved at any one location. These strata overlie and, in part, interfinger with the Siletz River Volcanics, a thick sequence of Paleocene to lower Eocene pillow basalt flows and breccias (Figs. 1.1 and 1.2). The Siletz River Volcanics consist of oceanic basaltic crust formed of seamounts and oceanic islands (Snavely and others, 1968; Wells and others, 1984). The oceanic basaltic crust was accreted during the late-early Eocene to the North American continent, represented by the Mesozoic rocks of the northern Klamath Mountains (Fig. 1.1). Blake and others (1985) and Niem and Niem (1990) used the name Sixes River Terrane for the Dothan Formation of Ramp (1972) in the northern margin of the Klamath Mountains. The U.S. Geological Survey has returned to calling these rocks Dothan Formation in mapping in progress (R. E. Wells, 1995, pers. commun.); and, therefore, this report refers to those rocks as Dothan Formation also.

Geophysicists estimate that the Siletz River Volcanics is more than 25 km thick in the central Oregon Coast Range (Trehu and others, 1992). In the Umpqua basin, Mobil Oil Corporation drilled more than two miles of Siletz River basalt in the Sutherlin No. 1 well in 1979. Therefore, this unit is generally considered to be economic basement. However, some natural gas seeps and oil shows occur where Siletz River flows and intrusions are intercalated with or are in thrust contact with lower Eocene Umpqua strata or in thrust contact with Mesozoic rocks of the Klamath Mountains (Kvenvolden and others, 1995; Lillis and others, 1995). The volcanics form buried highs, such as the Umpqua arch.

The Umpqua arch is a subsurface volcanic high of Siletz River seamounts and oceanic islands. In seismic-reflection profiles, well-stratified soft palagonite in the Siletz River Volcanics is nearly accoustically transparent; volcanic breccias and hard pillow lavas, on the other hand are strong accoustical reflectors. Umpqua Group strata lap onto and thin across these highs (Peter Hales, Weyerhaeuser, 1989, pers. commun.; Niem and Niem, 1990) (Plate 1). The volcanics that comprise the arch are exposed northeast and southwest of the Tyee forearc basin in the cores of the Dickinson Mountain, Drain, and Jack Creek anticlines (Hoover, 1963).

Eocene Stratigraphy

This study uses the revised stratigraphic nomenclature for the Eocene Tyee basin developed from new mapping and facies studies of the southern Coast Range by Molenaar (1985), Ryu and Niem (1993, 1994), Black (1990, 1994a, 1994b), Black and Priest (1993), Jayko (1995a, 1995b), and Wells (1995a-i). Overlying and interfingering with the upper part of the Siletz River Volcanics is the lower Eocene Umpqua Group which includes the Bushnell Rock and Tenmile formations (Fig. 1.2). To the north, the laterally equivalent lithofacies is informally referred to as undifferentiated Umpqua Group. This undifferentiated unit is a thick sequence of well-indurated, lithic turbidites and dark gray, deep-marine mudstone. These strata were deposited as middle to outer submarine fans and basin plain facies, possibly in a trench or subduction zone setting (Baldwin and Perttu, 1980; Heller and Ryberg, 1983) or in a rifted continental margin setting (Wells and others, 1984; Snavely, 1984).

The 250- to 4,000-ft thick Bushnell Rock Formation is composed of well-indurated, thick to very thick, amalgamated beds of polymict pebble-

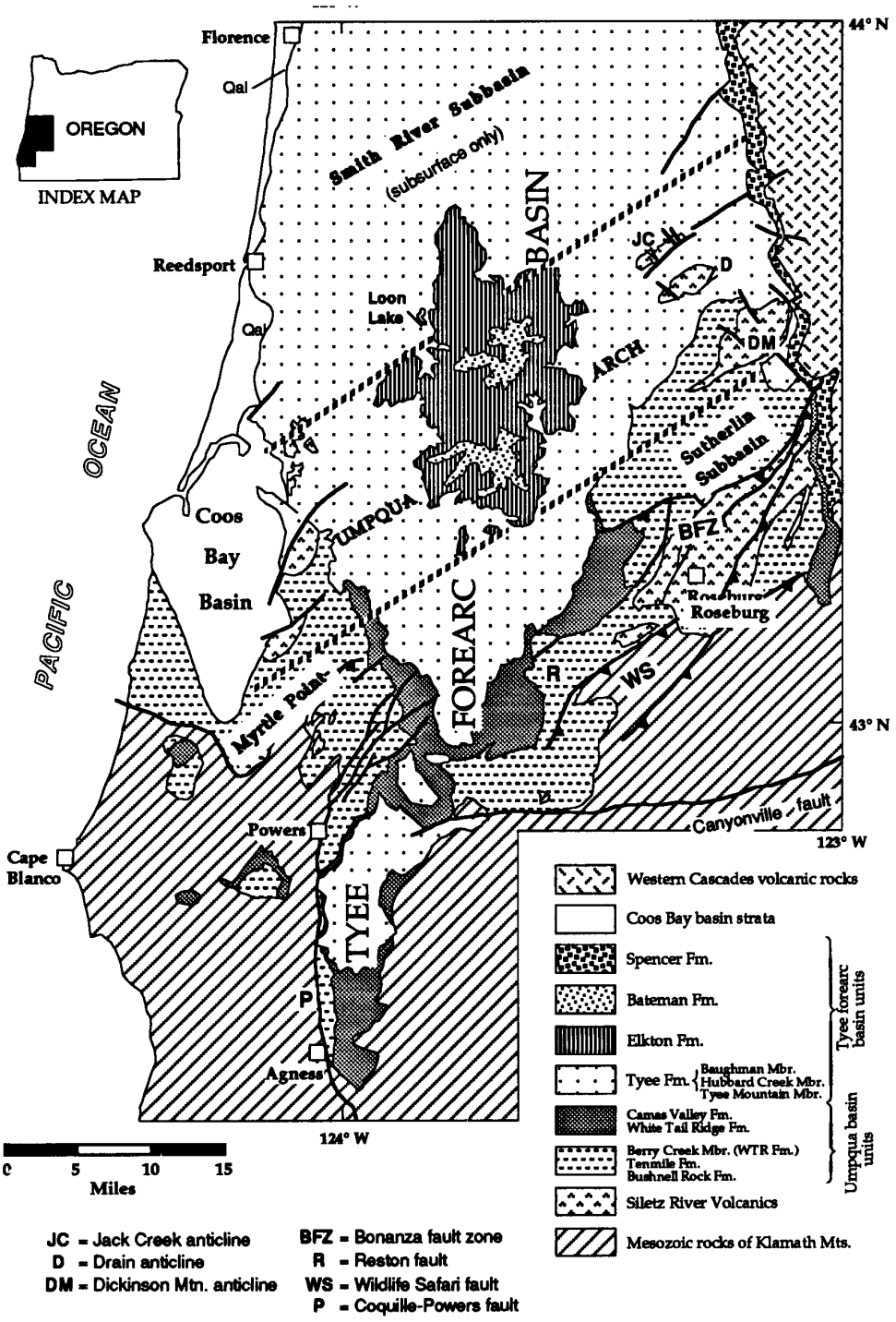

Fig. 1.1 Index map of general geology and tectonic features of the southern Tyee basin, SW Oregon. Note the NE-SW structural trend of the Paleocene to early Eocene subsurface Umpqua arch of Siletz River Volcanics. Lower Eocene Umpqua basin (Myrtle Point-Sutherlin and Smith River subbasins) strata lie parallel to the NE-SW trend; lower to middle Eocene Tyee forearc basin strata show a N-S. trend.

cobble-boulder conglomerate and subordinate, poorly sorted, very coarse-grained lithic sandstone. These lithofacies are conformably overlain by very thick-bedded, shallow-marine, fine-grained lithic sandstone of the 2,000-ft thick Slater Creek Member (Ryu and others, 1992). The well-indurated, syntectonic conglomerate and thick lithic sandstone formed as alluvial fans, fan deltas, beach gravels and inner shelf sands, and as deep-sea fan channels and canyon fills. These strata were derived from sedimentary, igneous, and metamorphic Mesozoic accreted terranes of the tectonically active Klamath Mountains to the south. The coarse-grained, wedge-shaped deposits thin rapidly and are missing in correlative sections of undifferentiated Umpqua Group in a distance of only 5 to 10 miles to the north (Ryberg, 1984; Ryu and others, 1992)(Fig. 1.3).

Conformably overlying the Bushnell Rock conglomerate is the 3,000-ft thick Tenmile Formation which consists of rhythmically interstratified, thin to very thin beds of graded, coarse-grained, lithic turbidites and dark gray slope mudstone. Thick, channelized beds of pebble-cobble-boulder polymict conglomerate and an upper thick, massive shelf mudstone comprise a minor part of this formation (Ryu and others, 1992).

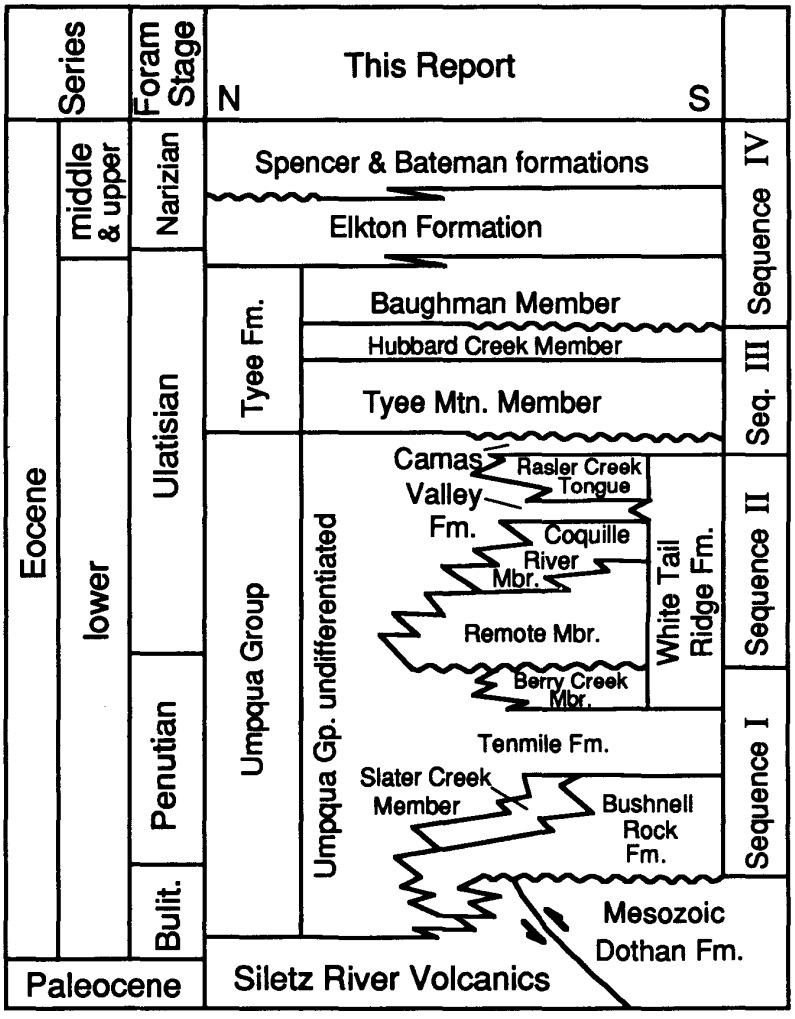

Fig. 1.2 Stratigraphic column of Tyee and Umpqua basins, southern Oregon Coast Range after Ryu and others (1992).

These units partially fill the Myrtle Point-Sutherlin subbasin and onlap the Umpqua arch. North of the arch, hemipelagic basinal mudstone of the undifferentiated Umpqua Group filled the Smith River subbasin during the early Eocene.

Using the sequence stratigraphic concepts of Van Wagoner and others (1990), the Bushnell Rock and Tenmile formations together with the overlying Berry Creek Member of the White Tail Ridge Formation comprise Depositional Sequence I of Ryu and others (1992) (Fig. 1.2). Some of these units (e.g., Bushnell Rock and Tenmile) locally overlie an unconformity on the Klamath Mountains terranes and Siletz River Volcanics in the southern part of the Umpqua basin (Baldwin and Beaulieu, 1973; Baldwin, 1974) (Fig. 1.3). Northward into the Myrtle Point-Sutherlin subbasin, these strata interfinger with middle and outer fan lithic turbidite strata and with slope and basin plain mudstone of the undifferentiated Umpqua Group which is several thousand feet thick (Molenaar, 1985; Ryu and others, 1992).

Overlying the lower Umpqua Group are the lower Eocene White Tail Ridge Formation and Camas Valley Formation (Fig. 1.2). The White Tail Ridge Formation has been further subdivided by Ryu and others (1992) into the Berry Creek Member, Remote Member, Coquille River Member, and Rasler Creek Tongue. These units are quartzo-feldspathic lithic sandstone, siltstone, coal, and mudstone. The Remote Member, Coquille River Member and Rasler Creek Tongue comprise Depositional Sequence II of Ryu and others (1992).

The coal-bearing White Tail Ridge Formation is a 4,000-ft thick deltaic sequence. The Berry Creek and Coquille River members contain thickening-upward parasequences of delta front sandstone formed during highstands. The delta front sandstones are hummocky bedded, bioturbated, and mollusk-bearing. Subbituminous coal and oyster-bearing estuarine siltstone are subordinate facies. The Remote Member consists of multi-stacked sequences of pebble-cobble-boulder polymict conglomerate and pebbly, cross-bedded, fluvial to distributary channel sandstone formed during a lowstand. Root-bioturbated overbank siltstone and coal beds also are present. The 2,200-ft thick Remote Member was deposited during a period of tectonic instability; the unit is locally incised into and overlies an angular unconformity on older lower Umpqua Group units in the southern Coast Range (e.g., on Fig. 1.3 between section 8 and well #16; Reston high of Ryu and others, 1992; Black and others, in prep.). The basal contact of the Remote Member forms a sequence boundary between depositional sequences I and II. The Rasler Creek Tongue is a thickening-upward parasequence of highstand, wave-dominated delta front sandstone and minor paralic coal that pinches out to the north into massive, fossiliferous, shelf to slope mudstone of the Camas Valley Formation (Fig. 1.3). The 1800-ft thick Camas Valley mudstone also overlies all deltaic members of the White Tail Ridge Formation (Figs. 1.2 and 1.3). This mudstone unit represents a tectonism-forced transgressive systems tract (Ryu and Niem, 1994).

During accretion of the Coast Range block (Siletz River Volcanics and Umpqua basin sequences I and II) in the early-middle Eocene, a new subduction zone formed to the west in the present position on the outer continental shelf-upper slope of Oregon (Heller and Ryberg, 1983; Wells and Heller, 1988; Niem and others, 1992a) (Fig. 1.4B). Subsidence of the area between this new subduction zone and the developing calcalkaline volcanic arc (Clarno volcanics of central Oregon?) created the Tyee forearc basin in which more than 10,000 ft of micaceous, lithic arkosic sandstone, mudstone, and minor coal were deposited (Snavely and others, 1964; Lovell, 1969). These younger strata are less deformed than the underlying folded and thrust-faulted Umpqua Group. These units form depositional sequences III and IV and cut across the structural grain of the earlier accreted NE-SW-trending Umpqua basin (Figs. 1.1 and 1.2) (Ryu and Niem, 1994). Clockwise rotation of the Coast Range-northern Klamath block about a pivot point in northwestern Oregon began about this time (Wells and Heller, 1988).

The Tyee Mountain and Hubbard Creek members of the Tyee Formation comprise Depositional Sequence III (Fig. 1.2). The middle Eocene Tyee Mountain Member consists of 3,000 to 6,000 feet of widespread, very thick-bedded, rhythmic, fine-grained, micaceous volcanic arkosic sandstone and deep-marine mudstone (Fig. 1.3). The member formed as a lowstand, sand-rich submarine fan (Chan and Dott, 1983) or as a submarine ramp (Heller and Dickinson, 1985)(Figs. 1.5A, 1.5B, and 1.6A). The overlying

Figure 1.3 Reduced fence diagram of southern Tyee basin, illustrating distribution and geometry of stratigraphic units (from Ryu and others, 1992).

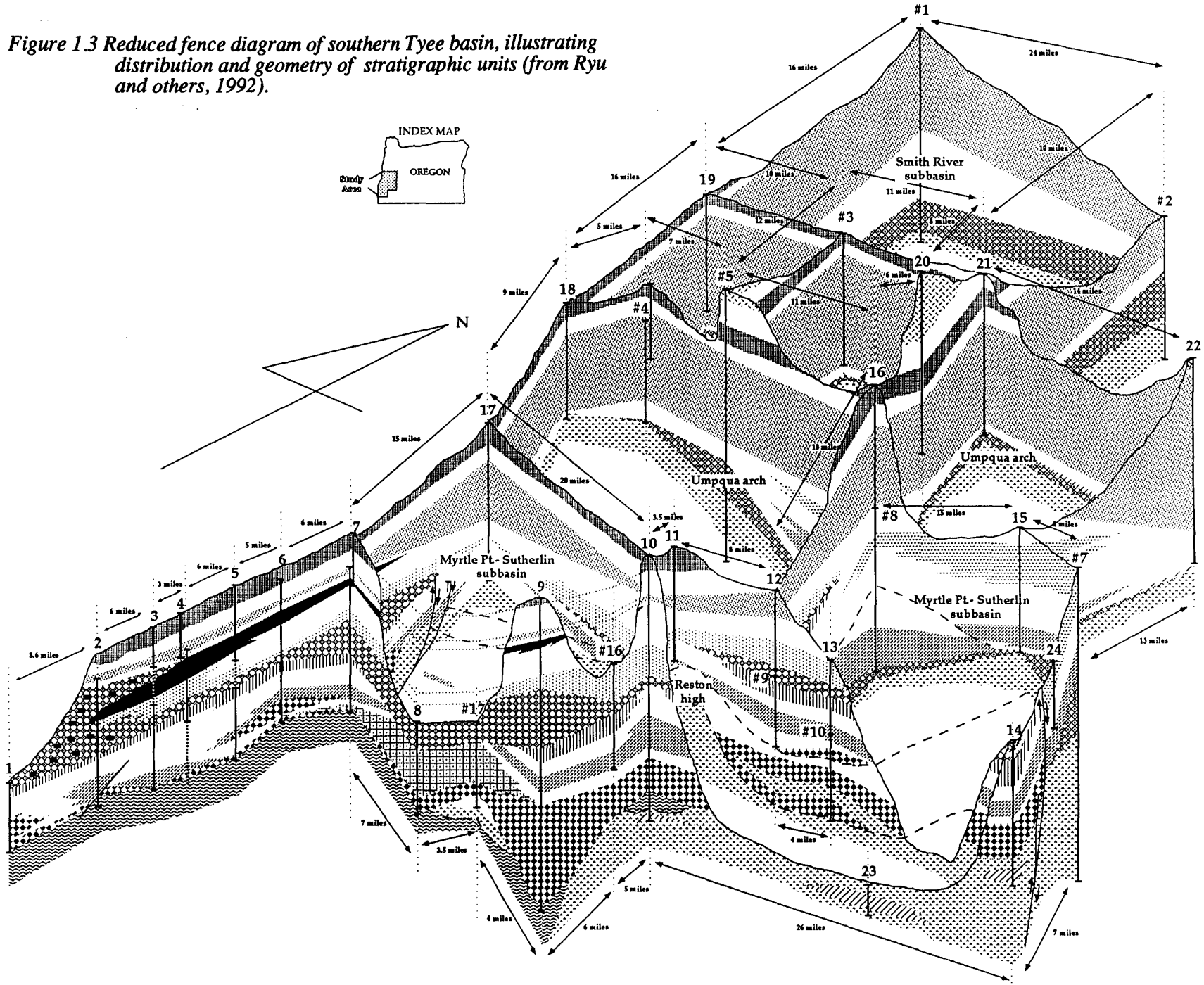

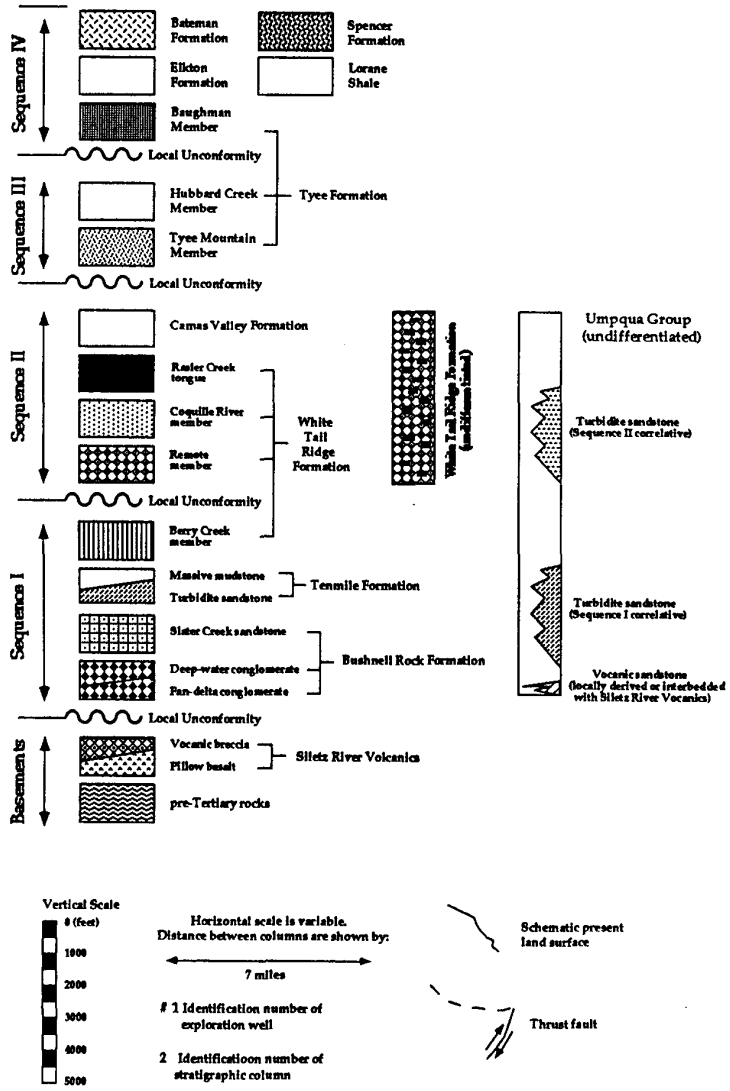
Sequence IV
Bateman Formation
Spencer Formation
Elkton Formation
Lorane Shale
Baughman Member
Local Unconformity
Sequence III
Hubbard Creek Member
Tyee Formation
Tyee Mountain Member
Local Unconformity
Sequence II
Camas Valley Formation
Rasler Creek tongue
Coquille River member
Remote member
White Tail Ridge Formation
White Tail Ridge Formation (subsurface only)
Umpqua Group (undifferentiated)
Turbidite sandstone (Sequence II correlative)
Local Unconformity
Sequence I
Berry Creek member
Massive mudstone
Turbidite sandstone
Tenmile Formation
Turbidite sandstone (Sequence I correlative)
Sister Creek sandstone
Deep-water conglomerate
Fan-delta conglomerate
Bushnell Rock Formation
Volcanic sandstone (locally derived or interbedded with Siletz River Volcanics)
Local Unconformity
Basements
Volcanic breccia
Pillow basalt
Siletz River Volcanics
pre-Tertiary rocks
Vertical Scale
0 (feet)
1000
2000
3000
4000
5000
Horizontal scale is variable.
Distance between columns are shown by:
7 miles
1 Identification number of exploration well
2 Identificatioon number of stratigraphic column
Schematic present land surface
Thrust fault

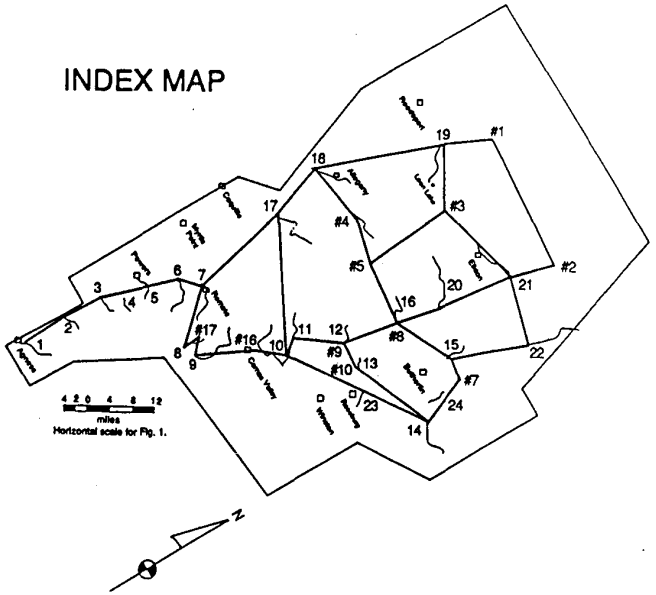
INDEX MAP
#1
#2
#3
#4
#5
#6
#7
#8
#9
#10
#16
#17
1
2
3
4
5
6
7
8
9
10
11
12
13
14
15
16
17
18
19
20
21
22
23
24
4 2 0 4 8 12
miles
Horizontal scale for Fig. 1.
N

Hubbard Creek Member is 600 to 1000 ft of thin, well-bedded to massive, micaceous, laminated mudstone and some thin, nested channels filled with turbidite sandstone. The unit represents a lowstand and transgressive systems tract (Figs. 1.6B and 1.6C).

The Baughman Member of the Tyee Formation and the Elkton, Bateman, and Spencer formations form Depositional Sequence IV (Fig. 1.2). Locally resting on an unconformity eroded into the Hubbard Creek Member, the 2,000-ft thick Baughman Member contains cross-bedded, medium- to coarse-grained, micaceous, lithic arkosic sandstone. Minor mollusk-bearing siltstones and subbituminous coals occur in this well-indurated, sandstone-dominated unit which forms prominent cliffs. The Baughman represents a lowstand delta and alluvial plain (Fig. 1.6B). The middle Eocene Elkton Formation is 1500 feet of deep-marine, laminated, micaceous mudstone and minor channelized micaceous arkosic sandstone. The unit reflects an overlying transgressive systems tract of shelfal and slope mudstone (Fig. 1.6C). The Elkton and overlying 2500-ft thick Bateman Formation crop out only in the middle of the forearc basin. The Bateman Formation is probably correlative to or slightly older than the middle and upper Eocene Spencer Formation which is exposed on the eastern flank

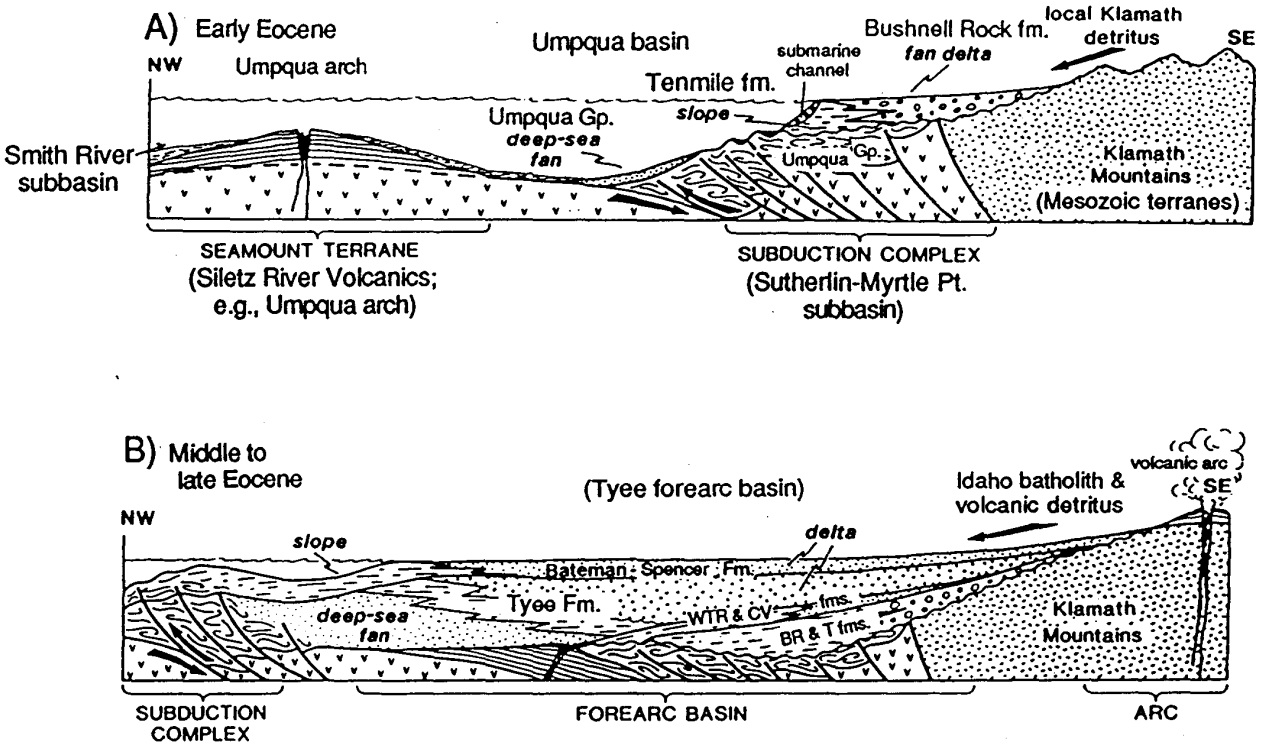

Figure 1.4 Depotectonic setting of Eocene rock units in the southern Tyee basin (modified slightly from Heller and Ryberg, 1983). A) Early Eocene lithic deep-sea fan of the Umpqua Group and Tenmile Formation slope facies fed by fan deltas of the Bushnell Rock Formation. These units were simultaneously deposited and subducted (i.e., accretionary wedge with imbricate thrusts) in the subduction complex (Myrtle Point-Sutherlin subbasin). B) After accretion and clogging of the subduction zone by thickened oceanic crust, a new subduction complex formed to the northwest.
Abbreviations: WTR & CV fms. = White Tail Ridge and Camas Valley formations; BR & T fms. - Bushnell Rock and Tenmile formations. Arkosic micaceous sandstone and mudstone of the Tyee, Elkton, and Bateman-Spencer formations accumulated in the subsequent forearc basin on top of the Umpqua basin accretionary wedge.

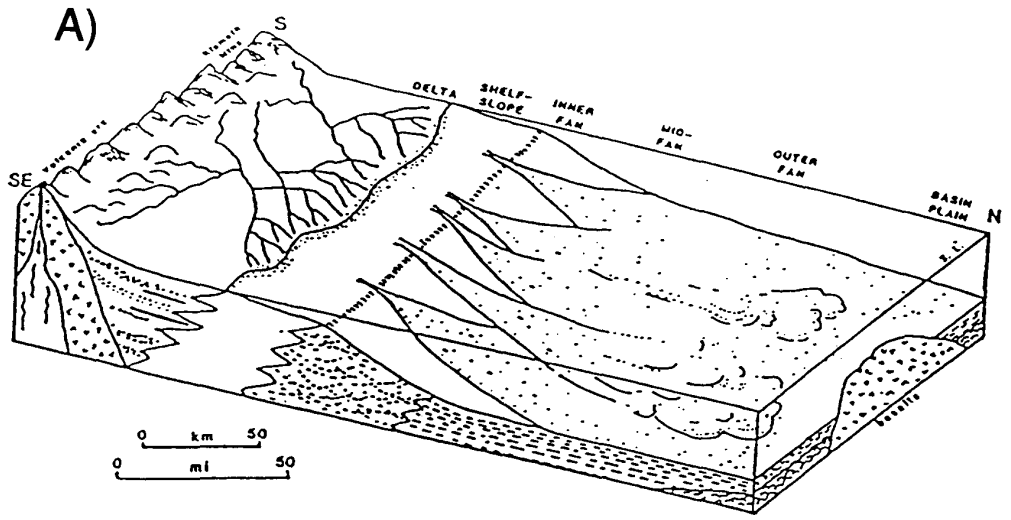

Early Eocene Tyee depositional model for deltaic shelf sands in line source cascade into deep water to form a sand-rich submarine fan (from Chan and Dott, 1983).

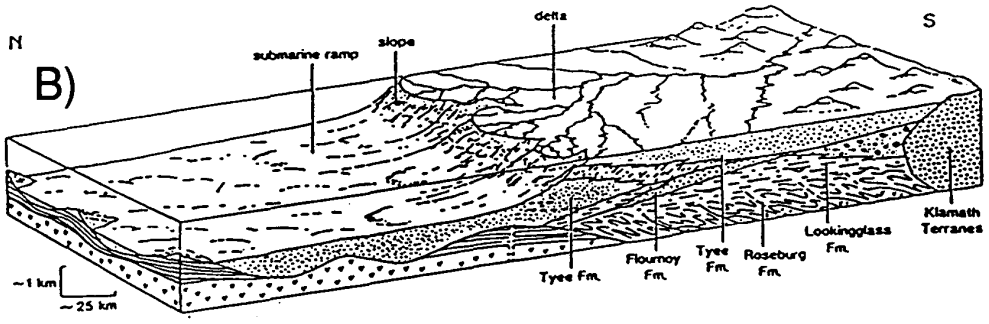

Paleogeographic reconstruction of the southern part of the Oregon Coast Range during Eocene deposition of the Tyee Formation (from Heller and Dickinson, 1985).

Figure 1.5 Comparison of depositional models proposed for the Tyee Formation. Diagram A is the sand-rich submarine fan model of Chan and Dott (1983); diagram B is the submarine ramp model of Heller and Dickinson (1985).

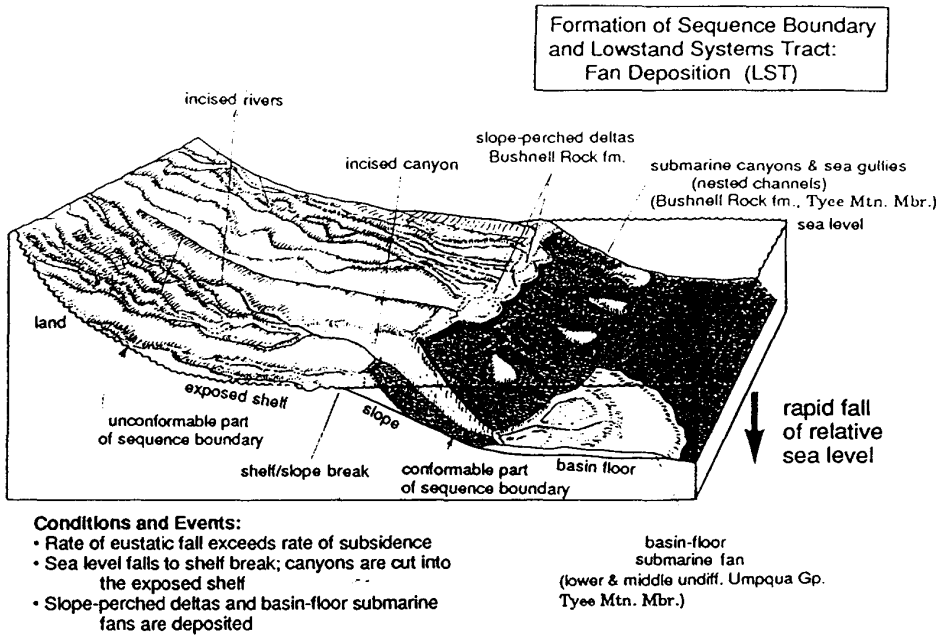

Figure 1.6A Formation of a sequence boundary, lowstand systems tract (LST), and lowstand basin-floor fan due to rapid relative fall of sea level resulting from a high rate of tectonic uplift and/or eustatic sea level fall (modified slightly from Van Wagoner and others, 1990).

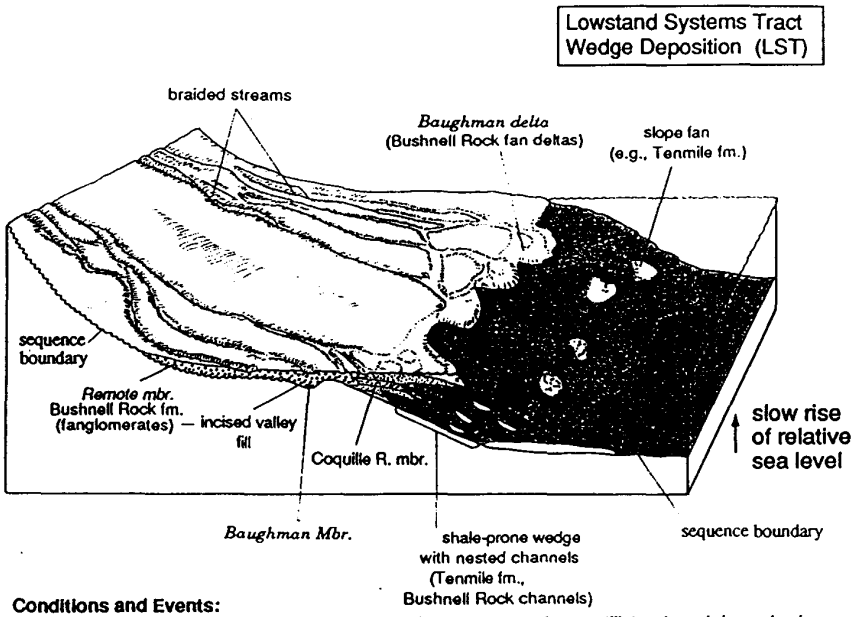

Figure 1.6B Lowstand systems tract (LST): a lowstand slope-wedge forms as a result of a slow fall of relative sea level, followed by a stillstand, and then slow rise of relative sea level (modified slightly from Van Wagoner and others, 1990).

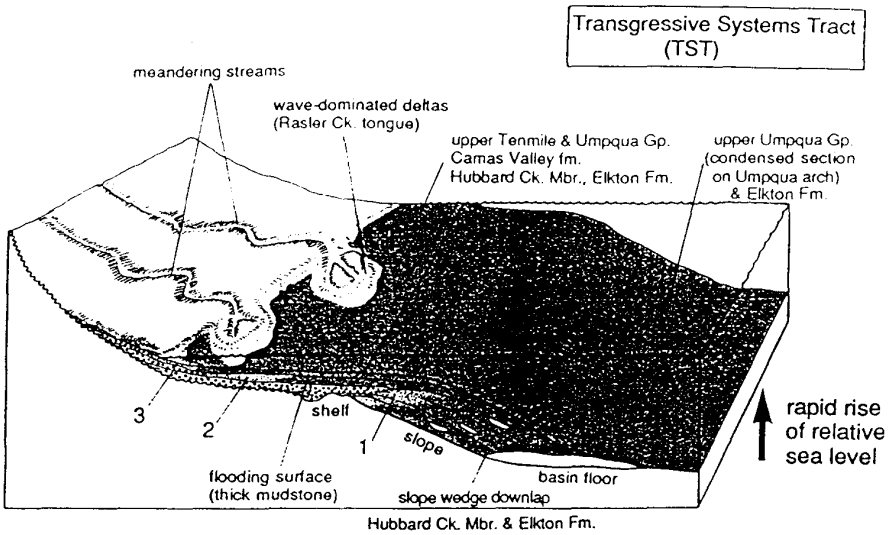

Conditions and Events:

- Rate of eustatic and/or tectonic rise is at a maximum
- During brief slowdowns in rate of rise, parasequences (e.g., delta front sandstones) prograde; but overall stack in backstepping pattern (i.e., shift from position 1 to 2 to 3).
- Thin, organic-rich facies (condensed section) moves up onto the shelf
- Fluvial systems typically shift from a braided to meandering pattern

Figure 1.6C Formation of a transgressive systems tract (TST) due to a rapid rise of sea level, resulting from increased tectonic subsidence rate and/or rapid eustatic sea level rise (modified slightly from Van Wagoner and others, 1990).

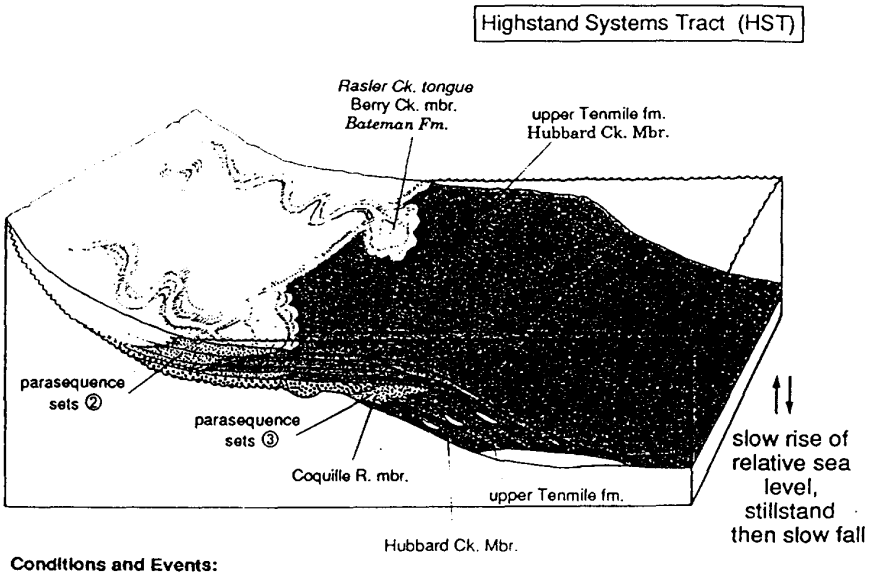

Conditions and Events:

- Rate of eustatic rise is at a minimum and in the late highstand, fall slowly
- Rates of deposition greater than the rates of sea level rise, parasequences (coarsening-upward sequences of delta front sandstones) build basinward in aggradational to progradational parasequence sets of the highstand systems tract ②
- Parasequences downlap onto the condensed section ③

Figure 1.6D Creation of a highstand systems tract (HST) by a slow relative rise, a stillstand, and a slow fall of relative sea level as a result of tectonic uplift and/or eustatic sea level drop (modified slightly from Van Wagoner and others, 1990).

of the basin adjacent to the Western Cascades arc (Fig. 1.1). Both the Bateman and Spencer consist of thickening-upward parasequences of moderately friable, laminated to hummocky bedded, arkosic, micaceous sandstone, mudstone, and coal (Weatherby, 1991; Ryu and others, 1992). The major source areas for the micaceous quartzo-feldspathic (K-feldspar) volcanogenic sandstones of the Tyee Mountain Member submarine fan of sequence III and the highstand, wave-dominated deltaic units of sequence IV (Baughman Member; Bateman and Spencer formations) are probably the Idaho Batholith and an active volcanic arc (Fig. 1.4B; Chan, 1982, 1985; Heller and Ryberg, 1983; Heller and others, 1985, 1992). Subdued Klamath Mountains terrane sources also contributed minor detritus.

Chan and Dott (1983) and Heller and Dickinson (1985) interpreted the facies of the Tyee Formation (i.e., Baughman, Tyee Mountain, and Hubbard Creek members), based on Walther's law of conformable units, as a sand-rich delta system that fed a multisource sandy submarine fan or deep-marine ramp facies to the north. Based on new detailed geologic mapping (Black and others, in prep.), seismic-reflection profiles, and subsurface sections (Ryu and others, 1992; Ryu, 1995), we now recognize a local unconformity at the base of the Baughman Member and a thick, widespread mudstone unit (Hubbard Creek Member) that separates the Tyee Mountain submarine fan from the deltaic Baughman Member (Figs. 1.2 and 1.3). Sequence stratigraphic concepts suggest that the Tyee Mountain submarine fan formed earlier during a lowstand, followed by deposition of slope to shelf mudstones of the Hubbard Creek transgressive systems tract (sequence III) (Figs. 1.6A, 1.6B, and 1.6C). A later lowstand event deposited the deltaic Baughman Member at the start of sequence IV (Fig. 1.6B).

Flanking the Tyee basin on the west, the Coos Bay basin contains the 6,000- to 7,000-ft thick upper Eocene (late Narizian) deltaic Coaledo Formation which is correlative to the Spencer Formation and possibly to the slightly older(?) Bateman Formation (Fig. 1.1). These upper Eocene units represent a widespread late Eocene delta-coastal plain that extended from Coos Bay northward to the Puget Lowland of Washington and may have once covered Tyee basin strata (Snavely and Wagner, 1963; Dott, 1966).

The overlying Oligocene to middle Miocene marine strata of the Coos Bay basin are not preserved in the Tyee forearc basin. They were either never deposited there or have been eroded since uplift of the basin. Very thick upper Eocene to Miocene nonmarine lava and pyroclastics in the adjacent Western Cascades arc flank the basin on the east and overlie an angular unconformity on the Tyee and Umpqua basin strata (Fig. 1.1).

Starting in the late-middle Miocene, a period of rapid plate subduction and reorganization on the Oregon outer continental shelf resulted in E-W compression and some oblique-slip, normal, and reverse faulting of the Tyee Basin strata (Niem and Niem, 1990). This resulted in uplift and rapid erosion of the Coast Range. Major rivers (e.g., Umpqua) formed entrenched meanders during the Pleistocene and Holocene. Personius (1993) showed evidence that compression folding has slightly deformed Holocene river terraces along the Siuslaw River east of Florence.

Regional Structure

The tectonic boundary between the Tertiary southern Oregon Coast Range and the Mesozoic northern Klamath Mountains is delineated, in part, by major thrust and transcurrent faults, including the northeast-southwest Wildlife Safari fault, the east-west Canyonville fault, and the north-south Coquille River-Powers fault (Diller, 1898; Perttu, 1976; Ryberg, 1984; Ramp and Moring, 1986) (Fig. 1.1). The Wildlife Safari fault is an oblique-slip reverse fault which has an estimated 3 miles of right-lateral separation (Ryberg, 1984). Carayon (1984) suggested that the northeastern segment of this fault may be a major thrust fault. Recent mapping of the 1:100,000 Roseburg sheet by Wells and others of the U.S. Geological Survey confirms that the Wildlife Safari fault is, in large part, a thrust fault which involves units as young as the White Tail Ridge Formation (Jayko and Wells, 1996; Wells and Niem, 1996).

The nearly east-west transcurrent Canyonville fault zone offsets various Cretaceous and Jurassic tectonostratigraphic terranes of the Klamath Mountains (Blake, 1984). Ryberg (1984) estimated >15 miles of right-lateral motion on the Canyonville fault. The half-mile-wide fault zone contains sheared serpentinite and slivers of

Cretaceous-Jurassic Riddle Formation and other terranes. Latest renewed motion on this fault may have involved members of the White Tail Ridge Formation before deposition of the deltaic Tyee Mountain Member of the middle Eocene Tyee Formation. This and other faults appear to have been sufficiently active in the late-early Eocene to have produced scarps of uplifted Klamath Mountains terrane rocks which were point sources of detritus during syntectonic deposition of the boulder-cobble conglomerate in the Remote Member of the White Tail Ridge Formation and the fan delta facies of the Bushnell Rock Formation (Perttu, 1976; Heller and Ryberg, 1983; Ryberg, 1984; Kugler, 1979). For example, A. Jayko of the U.S. Geological Survey has mapped a thick, basal, boulder conglomerate (largely granitic clasts) and lithic arkosic sandstone, probably Remote Member, overlying a Jurassic granodiorite pluton of the Klamath Mountains south of Glide (Buck Rock-White Rock area; Jayko, 1995a, 1995b).

Ryberg (1984), Baldwin and Hess (1971), and Ahmad (1981) reported that the north-south-trending Coquille River-Powers fault displays mainly reverse separation with as much as 5,000 feet of offset. This fault uplifts Klamath Mountains terranes on the west against Tyee, White Tail Ridge, and Tenmile strata on the east. It may be related to a major right-lateral northwest-trending fault in the Coos Bay basin which can be extended into the southwestern Tyee basin in T. 28 S., R. 12 W., offsetting Siletz River Volcanics against lower Umpqua and Tenmile strata (Baldwin, 1974).

The major structural features in the Myrtle Point-Sutherlin subbasin include the northeast-southwest-trending Bonanza fault zone, Reston fault, Wildlife Safari fault, and numerous folds. The Bonanza fault zone is a 5-mile wide system of NW-verging out-of-sequence thrust faults, some back thrusts, high-angle reverse faults, and northeast-southwest-trending asymmetrical anticlines cored with Siletz River Volcanics. Tight synclines within the thrust system involve lower Umpqua Group slope and basinal mudstone and middle to outer fan turbidite sandstone. The main thrust overrides the White Tail Ridge, Camas Valley, and Colestin formations in the Hinkle Creek 7.5-minute quadrangle (Wells, 1996b). Some thrusts in the subsurface appear to be be blind thrusts associated with fault-propagation folds (Plate 1). In an earlier interpretation, Niem and Niem (1990) postulated that some of these structures might be fault-bend folds. The principal folds north of the Bonanza fault zone, from north to south, are the Jack Creek anticline, Hardscrabble Creek syncline, Drain anticline, Yoncalla syncline, Dickinson Mountain (or Red Hill) anticline, Heavens Gate anticline, Calapooya (or Metz Hill) syncline, and Oakland anticline (Fig. 1.1) (Hoover, 1963; Niem and Niem, 1990; Wells, 1996g, 1996h). Mobil Oil Corporation drilled the Oakland anticline in 1979 (Sutherlin Unit No. 1) and penetrated <4,000 feet of Umpqua turbidite strata and >9,000 feet of Siletz River pillow basalt and some subaerial flows (Bill Seeley, Mobil Oil Corp., 1989, pers. commun.).

The imbricate thrust boundary and strike-slip faults of the southern Tyee basin have been interpreted as a collision boundary or suture zone between obliquely underthrusted oceanic crust (represented by the Siletz River Volcanics) and North American continental crust (represented by the Klamath Mountains terranes) (Heller and Ryberg, 1983; Ryberg, 1984; Carayon, 1984). The imbricate thrusting generally becomes less intense and generally younger to the north (R. E. Wells, 1994, pers. commun.). Suturing was largely completed by the early-middle Eocene (Snavely, 1987).

Field mapping and interpretation of seismic-reflection profiles indicate that much of the thrusting occurred prior to deposition of the middle Eocene Tyee Formation (Niem and Niem, 1990; Black, 1990; Black and Priest, 1993). Movement on some thrusts south of the Reston fault, for example, ceased before fan delta conglomerates of the Bushnell Rock Formation (as at Bushnell Rock) prograded into the basin. Renewed movement on the Reston thrust fault in the late-early Eocene created an anticlinal basement high (the Reston high) which uplifted Siletz River Volcanics and the lower Umpqua Group (Tenmile turbidites and Bushnell Rock conglomerate) (Black, 1990). Deltaic strata of the White Tail Ridge Formation thin over the Reston high, suggesting that in the late-early Eocene the high was an effective barrier which controlled the depositional pattern of the White Tail Ridge Formation in this area (Fig. 1.3) (Black, 1990; Ryu and others, 1992). Other faults appear to have been active contemporaneously with deposition of the lower Umpqua Group (Heller and Ryberg, 1983; Perttu and Benson, 1980), and

many younger faults deformed the White Tail Ridge Formation. For example, the White Tail Ridge Formation is involved in reactivated out-of-sequence thrusts near Glide and south of Tenmile (Wells and Niem, 1996; Wiley and Black, 1994).

In the northeastern part of the Myrtle Point-Sutherlin subbasin, the Bonanza fault zone can be mapped from the foothills of the Cascades east of Sutherlin to the Tyee escarpment west of Melrose (Fig. 1.1). Seismic-reflection profiling shows that the fault zone and associated folds extend beneath the forearc basin sequence in the central part of the southern Tyee basin (Fig. 1.1; Plate 1) (Peter Hales, Weyerhaeuser, 1989, pers. commun.). In the southwestern part of the subbasin west of Remote and Dora, NNE-SSW-trending thrusts and high-angle reverse/oblique-slip faults locally bound basalt-cored anticlines and are probably the exposed continuation of the Bonanza fault zone. In addition, NE-SW-trending basalt-cored anticlines mapped north of the Bonanza fault zone in the eastern part of the basin appear as discontinuous, NE-SW-trending, elongate anomalies on aeromagnetic maps beneath the Tyee Formation in the central part of the basin (Peter Hales, Weyerhaeuser, 1995, pers. commun.). A high-resolution aeromagnetic survey of the southern Tyee basin, to be flown by the US Geological Survey in 1996, should provide additional constraints on the subsurface structure.

Many faults in the southwestern part of the Myrtle Point-Sutherlin subbasin juxtapose mélange and broken formation, Dothan Formation, and serpentinite against Siletz River Volcanics and Umpqua-Tenmile turbidite fan and slope strata. Baldwin and Beaulieu (1973) and Baldwin (1974) originally mapped these faults as high-angle reverse and normal, and some thrust faults. Niem and Niem (1990) offered an alternative explanation that the Mesozoic rocks in this area are part of major overthrust sheets (or nappes) with serpentinite over Umpqua turbidite strata and Siletz River Volcanics. Subsequent uplift and erosion have left klippen of mélange (i.e., blocks of blueschist and greenstone) over undifferentiated lower Umpqua and Tenmile turbidite strata and Siletz River Volcanics. Parke Snavely in unpublished mapping and Robert McLaughlin of the U.S. Geological Survey (1995, pers. commun.), in recent mapping of the Bridge 7.5-minute quadrangle west of Remote, found Siletz River Volcanics thrust over Mesozoic Klamath Mountains rocks as well as high-angle, right-lateral oblique-slip and reverse faults. McLaughlin (1995, pers. commun.) interprets that there has been considerable tectonic shortening in this area. He also found Bushnell Rock conglomerate locally overlying an angular unconformity on Dothan Formation.

Carayon (1984) and Carayon and others (1984) showed in a cross section a small klippe of mélange (Dothan Formation?) thrust over lower Umpqua strata and Siletz River Volcanics in the Bushnell Rock-Reston area north of the Wildlife Safari fault. Baldwin (1984) proposed an alternative interpretation that the exotic blocks of pre-Tertiary strata, blueschist, and greenstone are olistostromal blocks that slid or slumped into the Umpqua marginal basin during the Eocene from uplifted Klamath Mountains terranes to the south. Large clasts of pre-Tertiary rocks in mud matrix support fill ancient channels near Agness and may be debris flow deposits in a submarine canyon head in the Umpqua Group-Tenmile Formation (Ryberg, 1984).

Ryberg found that some tectonic wedges of mélange with blocks of blueschist and disrupted Mesozoic rocks also contain blocks of mudstone with Paleocene foraminifers. Ryu (1995) sampled a sheared mudstone in the Slater Creek area which also yielded early Eocene(?) foraminifers. These early Tertiary foraminifers suggest that some Klamath Mountains "pre-Tertiary" mélange formed in the earliest Tertiary and may be equivalent to the Eocene coastal belt Franciscan of northern California. This mélange with exotic blocks may represent an uplifted segment of the more deeply subducted part of the Paleogene accretionary wedge.

Thus, some geologists have favored the idea of significant tectonic shortening via thrusting and subduction at the southern boundary of the southern Tyee basin. Eocene Umpqua Group turbidite strata involved in such a setting could extend as thrust slices far beneath the northern margin of the Mesozoic Klamath Mountains (Fig. 1.4A).

Ryberg (1984) presented an alternative structural interpretation that Umpqua Group turbidite strata and Siletz River Volcanics do not extend as thrust slices beneath the Mesozoic terranes but rather are abruptly terminated by

the oblique-slip Wildlife Safari fault. If the reader prefers the Ryberg model, then there are no Umpqua Group turbidite strata as a target for exploration or as potential source rocks beneath the Dothan Formation within a reasonable drilling depth. Recent detailed mapping of Eocene sedimentary units in the Roseburg area by Wells (1996e, 1996f) shows relatively minor thrusting and shortening (i.e., a few miles) on the Bonanza and Wildlife Safari faults, not tens to a hundred miles expected in a major subduction zone. Some seismic-reflection profiles also suggest minor net slip (e.g., Plate 1).

Wells (1996, pers. commun.) has recently hypothesized that this suture may be analogous to the suture between the Ontong Java Plateau and Solomon Islands in the southwest Pacific. He thinks that the oceanic plate (represented in the southern Oregon Coast Range by the thickened oceanic seamount crust of Siletz River Volcanics and lower Umpqua Group turbidite strata) may have split the continental plate (represented by the Mesozoic Klamath Mountains terranes) like a spear point, rather than slipping far beneath the edge of the continental plate. In this type of plate collision, slices of continental rocks are thrust partially over and partially under the oceanic plate. Tectonic shortening of the folded and thrusted Coast Range Siletz River Volcanics and Umpqua Group turbidites is relatively minor in the final stages of collision and accretion. The exact nature of the suture zone between the Umpqua Group of the Umpqua basin and the northern Klamath Mountains is presently a subject of detailed field investigations by the U.S. Geological Survey (R.E. Wells, R. McLaughlin, and A. Jayko, 1989-96, pers. communs.).

The forearc basin sequence (middle Eocene Tyee and younger formations) is less deformed than the Umpqua basin strata. This sequence overlies an angular unconformity on generally more intensively faulted and folded lower Umpqua strata (Fig. 1.1 and Plate 1). In the late-middle Miocene to the present, renewed underthrusting and subduction of the Juan de Fuca plate beneath the North American plate on the outer continental shelf and slope of Oregon created east-west compression of the basin (Snavely, 1987; Wells and Heller, 1988; Niem and others, 1992b). This produced the broad, open north-south-trending folds and high-angle faults in the forearc basin sequence in the central and northern parts of the study area (Niem and Niem, 1990; Black and others, in prep.). Toward the eastern flank of the basin, these north-south axes gradually become NE-SW-trending, subparallel to the older structural trend due to the buttress effect of uplifted Siletz River Volcanics during compression. Some of these folds and fault blocks have been explored (e.g., General Petroleum Long Bell No. 1, Florida Exploration Harris 1-4, and Northwest Exploration Sawyer Rapids wells).

On the geologic map of western Oregon, Wells and Peck (1961) showed a broad north-trending synclinal axis in the Tyee forearc strata, roughly bisecting the middle and upper Eocene Elkton and Bateman formations. Although Niem and Niem (1990) also followed that general outcrop pattern, they depicted many smaller structures superimposed on that structure. For example, NE- and N-trending folds gently deform the Elkton and Bateman formations, and E-W-trending left-lateral faults displace the synclinal axis south of Remote.

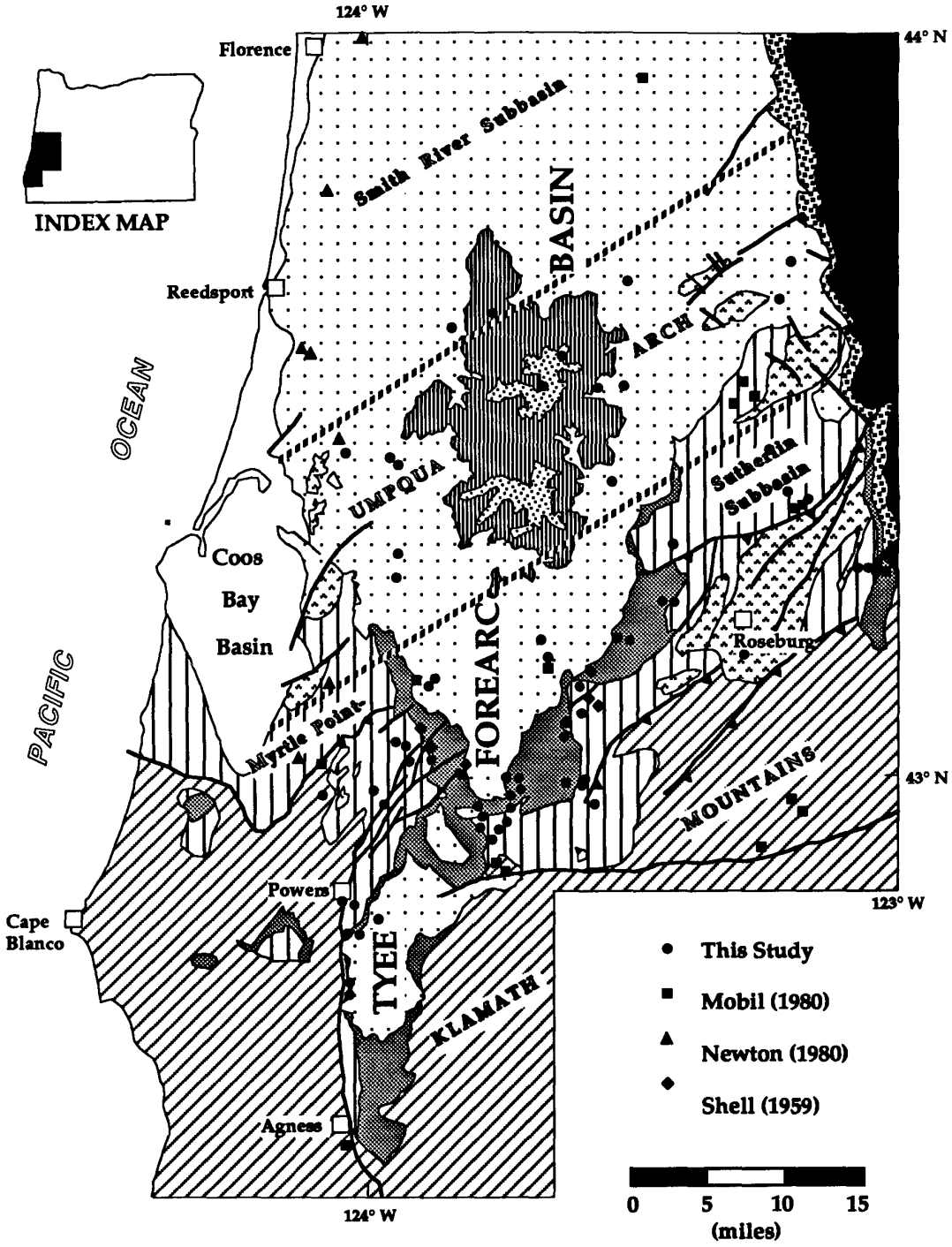

Figure 2.1 Geographic distribution of sandstone and conglomerate samples from the Eocene Tyee basin. Solid circles represent the locations of seventy sandstone samples petrographically analyzed for this study. Sandstone samples from other sources (e.g., Mobil, Newton, and Shell) also are plotted on the map.

SANDSTONE PETROGRAPHY

Framework Mode and Cements

The composition and diagenesis of some Tyee basin units have been analyzed by Burns and Ethridge (1979), Chan (1985), Heller and Ryberg (1983), Van Atta in Newton (1980), and by several MS and PhD theses completed at the University of Oregon (under the supervision of Ewart Baldwin), at Portland State University, and at Oregon State University (see list on compilation map of Niem and Niem, 1990). We expanded upon those studies and have included stratigraphic units not previously investigated.

Seventy sandstone and conglomerate samples were studied petrographically from the entire Eocene section throughout the southern Tyee basin (Fig. 2.1). These samples represent the 13 sandstone-dominated lithostratigraphic units in the basin. Most were collected from the measured stratigraphic sections described by Ryu and others (1992) (Plate 2A).

The average compositions of the framework grains, detrital matrix, cement, and porosity of each of the sandstone-dominated units are presented in Table 2.1. More than 400 points were counted in each thin section. Sandstones are mainly composed of quartz, plagioclase, K-feldspar, and varying proportions of sedimentary, volcanic, and metamorphic rock fragments. Clay matrix and cement are abundant. Framework grains (primarily rock fragments with sub-equal amounts of quartz and feldspar) are the dominant component, averaging 79% of each sample (Table 2.1).

Matrix commonly comprises 8% and ranges from 5 to 11%. Most sandstones are arenites (<10% clay matrix), but some turbidite sandstones (e.g., Tyee Mountain Member and Elkton Formation) are wackes (>10% clay matrix) in the classification of Williams and others (1954). Texturally, both primary detrital orthomatrix and secondary diagenetically formed epimatrix and pseudomatrix (developed from deep burial) are common in the sandstones (Dickinson, 1970). In many thin sections, it is difficult to distinguish between them. X-ray diffraction and scanning electron microscopy analyses indicate that these matrix clays are dominated by smectite, corrensite, chlorite, illite, and serpentine. Authigenic clays, zeolites, calcite, and quartz cements average 11% of the

			BULK COMPOSITION (%)			
SEQUENCE	STRATIGRAPHIC UNIT	NUMBER OF SAMPLES	FRAMEWORK GRAINS	DETRITAL MATRIX	CEMENT	VISUAL POROSITY
IV	Spencer Formation	2*	76.12	9.26	11.70	2.92
	Bateman Formation	2*	84.56	7.77	7.67	0.00
	Elkton Formation	1*	79.10	10.26	10.63	0.00
	Baughman Member	5	80.95	9.87	6.92	2.27
III	Tyee Mountain Member	13	76.66	11.06	10.56	1.72
II	Rasler Creek Tongue	2*	74.15	7.11	15.13	3.61
	Coquille River Member	8	80.46	4.70	12.09	2.75
	Remote & Upper Umpqua	12	79.65	7.38	11.57	1.40
	White Tail Ridge Formation	2*	71.50	8.93	18.43	1.15
I	Berry Creek Member	8	85.56	4.45	9.20	0.79
	Tenmile Formation	5	81.49	8.45	8.79	1.27
	Slater Creek Member	2*	82.23	5.79	11.68	0.30
	Bushnell & Lower Umpqua	7	78.03	8.73	10.65	2.60
Klamath Mtns.	Pre-Tertiary	1*	77.64	7.80	6.00	8.56
	AVERAGE		79.15	7.97	10.79	2.10

*Table 2.1. Overall composition of seventy Tyee basin sandstones and conglomerates analyzed in this study. * Additional compositions of Tyee sandstone and conglomerate units are reported in Burns and Ethridge (1979), Chan (1982), Heller (1983), Newton (1980), Ryberg (1984), and Weatherby (1991).*

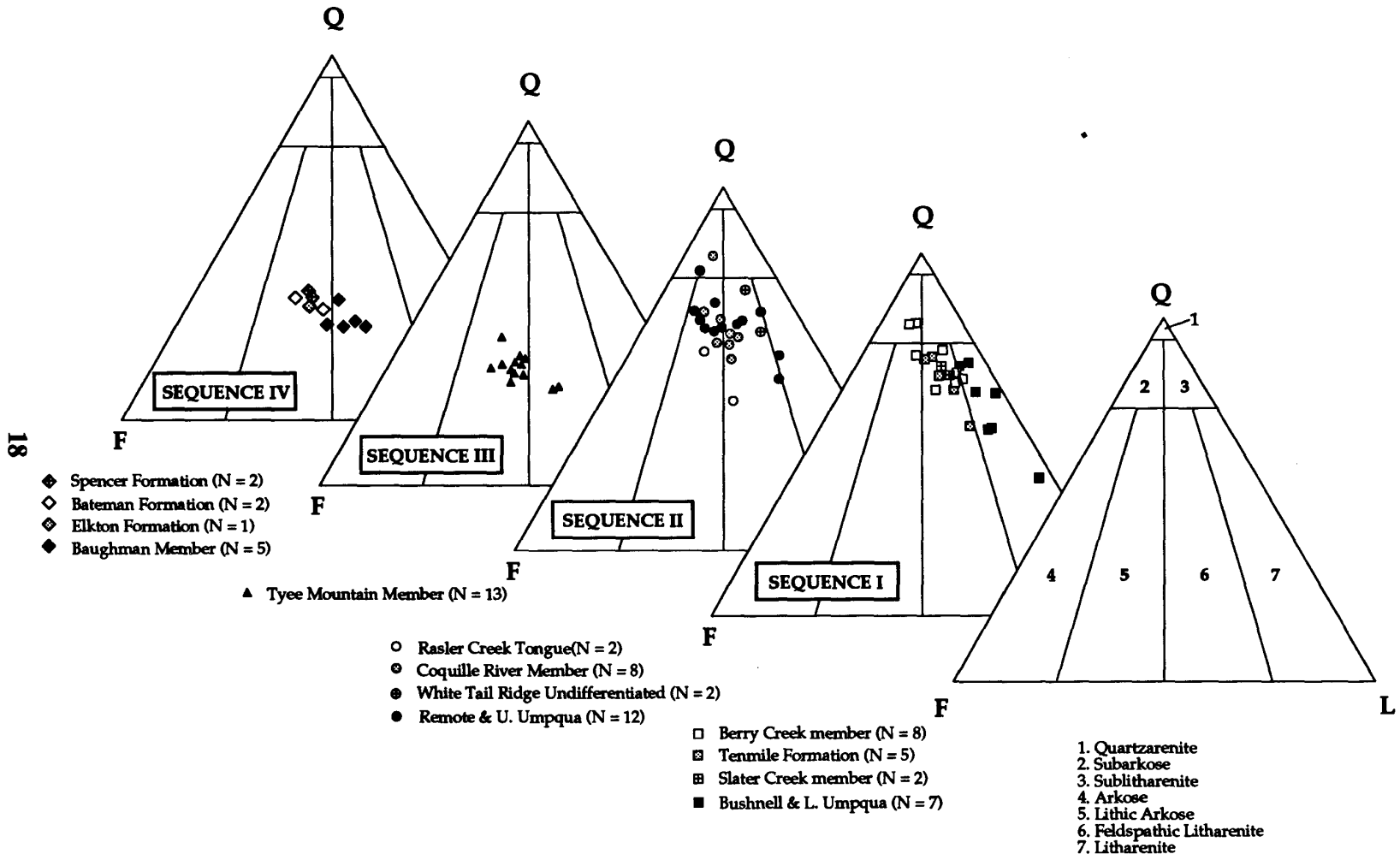

Figure 2.2 QFL classification (after Folk, 1974) of Eocene Tyee basin sandstones and conglomerates. Q is quartz; F is feldspar; L is lithic fragments.

sandstone bulk composition. Minor amounts of hematite and limonite cement also occur in some weathered samples. Authigenic clays are primarily corrensite and chlorite, but illite is also common. The textural and mineralogical characteristics of the various cements and clay matrix is further described in the Diagenesis section of this report.

One to three percent porosity was calculated from point counts of the sandstones (Table 2.1). Most pores are secondary intergranular and intragranular, formed by partial to complete dissolution of framework minerals, such as feldspars. Minor fracture porosity is also locally present. Higher porosities (averaging 11%) in the Tyee basin sandstones and conglomerates were measured in seventy samples by porosimeter by Goode Core Analysis Services of Bakersfield, California (Table 2.2). The difference between visual point count estimation and the quantitative laboratory measurement of the porosity might be due in part to microporosity in the sandstones, which cannot be accurately estimated using the petrographic microscope.

The composition of detrital framework grains varies significantly between lithostratigraphic units (Table 2.3 in Appendix). The dominance of rock fragments (<45%) over quartz (<30%) and feldspar (<24%) classifies most Tyee basin sandstones as lithic arkoses and feldspathic litharenites according to the scheme of Folk (1974), but lithic arenites and subarkoses also occur (Fig. 2.2).

SEQUENCE	STRATIGRAPHIC UNIT	NUMBER OF SAMPLES	POROSITY (%VOLUME)		PERMEABILITY (md)	
			Average	Range	Averge	Range
IV	Spencer Formation	2*	14.45	10.2-18.7	6.7	1.1-12.3
	Bateman Formation	2*	15.7	14.1-17.3	2.15	2.0-2.3
	Elkton Formation	1*	14.7	-	1.6	-
	Baughman Member	5	9.7	7.7-12.9	0.24	0.15-0.33
III	Tyee Mountain Member	13	10.88	7.3-16.9	0.53	0.01-3.1
		(26*)	(16.45*)	(7.9-38.2*)	(18.03*)	(0.01-154*)
II	Rasler Creek Tongue	2*	13.2	12.0-14.4	9.35	0.2-18.5
	Coquille River Member	8	12.9	10.9-16.9	9.59	0.13-40.5
	Remote & Upper Umpqua	12	10.45	5.4-16.3	2.93	0.05-18.5
		(14*)	(11.74*)	(5.4-32.2*)	(3.65*)	(0.05-18.5*)
	White Tail Ridge Formation	2*	8	6.1-9.9	0.15	0.08-0.22
I	Berry Creek Member	8	9.75	6.3-11.4	0.63	0.03-1.9
		(10*)	(9.52*)	(6.3-11.4*)	(0.63*)	(0.03-1.9*)
	Tenmile Formation	5	9.58	7.2-15.0	0.27	0.01-1.2
	Slater Creek Member	2*	7.4	7.1-7.7	0.03	0.02-0.03
	Bushnell & Lower Umpqua	7	8.33	4.7-12.7	1.67	0.05-5.2
		(9*)	(11.98*)	(4.7-28.3*)	(11.31*)	(0.05-32.6*)
Klamath Mountains	Pre-Tertiary	1*	16.6	16.6	16.6	16.6
		(13*)	(9.32*)	(4.3-23.2*)	(16.26*)	(0.03-90.0*)
	AVERAGE		10.73	5.0-18.7	2.76	0.01-40.5
			(12.25*)	(4.3-38.2*)	(8.80*)	(0.01-154*)

* includes porosity and permeability data from Shell (1959), Mobil (1980), and Newton (1980).

Table 2.2 Summary of porosity and permeability data measured by Goode Core Analysis Service (Bakersfield, California) for Eocene Tyee basin sandstones and conglomerates.
** Additional compositions of Tyee sandstone and conglomerate units are reported in Burns and Ethridge (1979), Chan (1982), Heller (1983), Newton (1980), Ryberg (1984), and Weatherby (1991).*

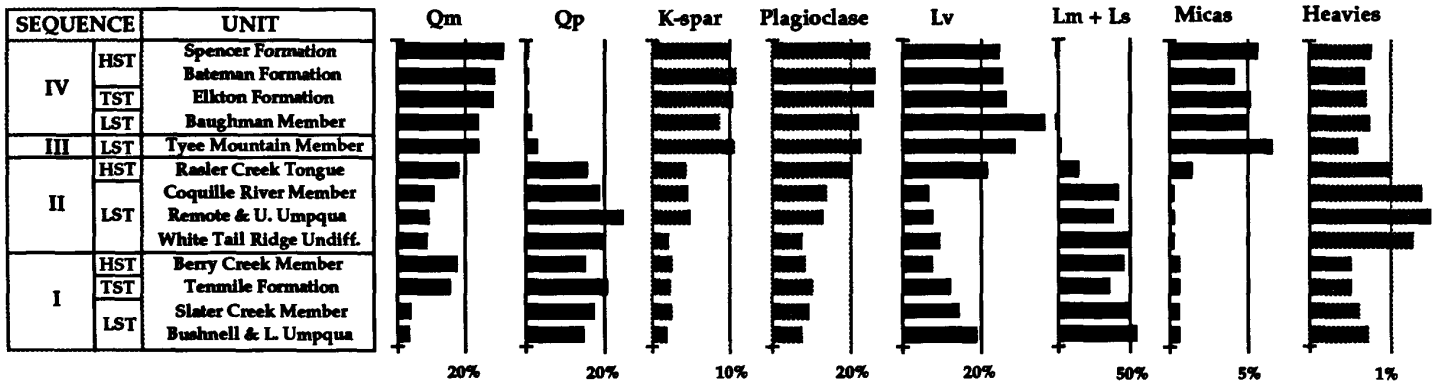

Figure 2.3 Relative abundance of major framework minerals from Eocene Tyee basin units. This diagram was modified from Heller and Ryberg (1983) based upon our stratigraphic and petrographic data. (LST=Lowstand Systems Tract; TST=Transgressive Systems Tract; HST=Highstand Systems Tract).

Lithic fragments constitute a significant proportion of the detrital fraction, averaging 44% of all sandstones (Fig. 2.3 and Table 2.3 in Appendix). The proportions of volcanic (Lv), metamorphic (Lm), and sedimentary rock fragments (Ls) vary from one lithostratigraphic unit to another (Fig. 2.3 and Table 2.3 in Appendix). Volcanic rock fragments are dominated by intermediate composition types displaying microlitic or pilotaxitic, and porphyritic textures. Metamorphic clasts (Lm) include quartz-mica schists, phyllites, metagraywacke, metagabbro, metaquartzite, and epidote-quartz aggregates. Rare acidic plutonic rock fragments (i.e., granitic) consist of interlocking coarse quartz-mica-feldspar aggregates. Sedimentary rock fragments (Ls) are dominated by light and dark unfossiliferous cherts and some radiolarian chert. Clasts of fine-grained sandstone, siltstone, mudstone, and carbonized plant fragments are also common.

Monocrystalline and polycrystalline quartz (Qm and Qp, respectively) comprise the second most abundant framework grain types, averaging 30% of the detrital fraction (Table 2.3 in Appendix). Monocrystalline quartz grains display straight to strongly undulose extinction and contain vacuoles and inclusions. Some monocrystalline quartz grains are embayed and euhedral, reflecting their silicic volcanic origin (Folk, 1974). Polycrystalline quartz grains also have straight to strongly undulose extinction. Crystal boundaries are commonly curved to sutured and crystal shapes are somewhat elongate and strained, suggesting a metamorphic origin. A minor amount of vein quartz and microveins in chert fragments also are present.

Feldspars (F) form 23% of the framework grains (Fig. 2.3 and Table 2.3 in Appendix). Plagioclase (P) generally exceeds K-feldspar (K) with a mean P/F ratio of 0.6 to 0.8 in most sandstone units. Plagioclase compositions range from nearly pure albite to andesine (average An content 1-40%) using the Michel-Levy method. Plagioclase grains are usually fresh, but many are partially altered to albite, sericite, clay, and/or zeolites. Dissolution of plagioclase has locally formed intragranular pores. For example, secondary pores formed by plagioclase dissolution are common in turbidite sandstones in the lower part of the Tyee Mountain Member. K-feldspars include orthoclase and microcline as well as perthite. They are extensively altered to sericite and clay and display a cloudy appearance. A few K-feldspar grains contain thin potassium feldspar overgrowths.

In some units, common accessory minerals are muscovite, biotite, and heavy minerals. Very coarse to coarse flakes of both muscovite and biotite characterize sandstones in the Tyee (e.g., Tyee Mountain and Baughman members), Elkton, Bateman, and Spencer formations and average 5% of the detrital fraction (Fig. 2.3 and Table 2.3 in Appendix). Pre-Tyee units (other than the Rasler Creek Tongue) generally lack coarse mica flakes and contain less than 1 percent fine sand-sized mica (Fig. 2.3 and Table 2.3 in Appendix). Large flakes of micas are severely bent and crushed due to compaction during burial. Many are altered to green chlorite. Some micas are partially replaced or pseudomorphosed by zeolites that display relict basal (001) mica cleavages. Heavy minerals include opaque iron oxides (magnetite and ilmenite) as well as non-opaque hornblende, epidote, sphene and garnet. They comprise 0.4 to 1.5 percent of framework grain fractions. Epidotes dominate the heavy mineral assemblage and are most abundant in the White Tail Ridge Formation (Fig. 2.3 and Table 2.3 in Appendix).

Compositional characteristics of sandstone units

Lower Umpqua Group sandstones (e.g., Bushnell Rock and Tenmile formations, and Berry Creek Member of White Tail Ridge Formation) and upper Umpqua sandstones (Remote Member, Coquille River Member, and Rasler Creek Tongue of White Tail Ridge Formation) are characterized by polycrystalline (vein and metamorphic) quartz, a low proportion of K-feldspar and plagioclase feldspar, monocrystalline quartz, micas, and volcanic rock fragments, and high amounts of metamorphic and sedimentary (mainly chert) rock fragments (Fig. 2.3). These sandstones are compositionally submature to immature (Folk, 1974). This mineralogy was largely locally derived from physical weathering and rapid erosion of Mesozoic sedimentary, volcanic, and low grade metamorphic terranes of the Klamath Mountains during the early Eocene (Burns and Ethridge, 1979; Koler, 1979; Heller and Ryberg, 1983; Ryberg, 1984; Niem and Niem, 1990). The rugged Klamath Mountains topography promoted rapid erosion (conglomerates are common) which removed detritus before extensive chemical

weathering and clay alteration could occur, even in the warm, semi-tropical climate that existed in the early Eocene.

In contrast, the younger strata of the Tyee forearc basin (i.e., Tyee Mountain Member to Spencer Formation) have a high proportion of monocrystalline quartz, little or no polycrystalline quartz, and a much higher abundance of K-feldspar and plagioclase, micas, and volcanic rock fragments (Fig. 2.3). This petrofacies, according to Heller and Ryberg (1983) and Chan (1985), reflects greater volumes of detritus from more distant, extrabasinal granitic sources (e.g., Idaho batholith) and an incipient calcalkaline volcanic arc (possibly Challis-Clarno volcanics) of eastern Oregon and Idaho. The finer grained forearc sand was transported via a major river system (i.e., ancestral Columbia River) prior to clockwise rotation of the Coast Range block (Wells and Heller, 1988) through low-lying Mesozoic Klamath terranes that contributed little metamorphic and sedimentary detritus to the Tyee forearc basin strata.

As a result, Tyee forearc basin sandstones (Tyee Mountain and Baughman members and Elkton, Bateman, and Spencer formations) more commonly plot as micaceous lithic (volcanic) arkosic sandstone (Fig. 2.2). They are typically fine- to medium-grained and moderately to poorly sorted. Some, such as the Tyee Mountain turbidite sandstones, are richer in detrital and diagenetic clay matrix. Coarser grained sandstones (such as those in the fluvial deltaic Baughman Member) tend to have more lithic fragments (i.e., volcanic) and less feldspar and quartz. These rocks plot on Folk's sandstone classification diagram (Fig. 2.2) as feldspathic volcanolithic sandstone (arenites). In contrast, most of the older Umpqua basin sandstone units (e.g., Bushnell Rock, Tenmile, and White Tail Ridge formations) are coarser grained, are more quartzose (due to higher proportions of polycrystalline vein and metamorphic quartz) and are enriched in metamorphic and sedimentary lithic fragments (mainly chert). They plot as feldspathic lithic (metamorphic-sedimentary) arenites and wackes (Fig. 2.2). The very coarse-grained sandstone and pebbly sandy conglomerate of the Bushnell Rock Formation plot as lithic (metamorphic-sedimentary) arenites and wackes on Folk's diagram (Fig. 2.2) as does the finer grained Slater Creek member. Very coarse- to coarse-grained Bushnell Rock sandstone and pebble conglomerate contain higher proportions of metabasalt rock fragments and polycrystalline quartz whereas carbonaceous phyllite is more abundant in medium- to coarse-grained Tenmile turbidite sandstone (Fig. 2.3). Fluvio-deltaic sandstones in the Berry Creek, Coquille River, and Remote members of White Tail Ridge Formation also are subarkosic to lithic arkosic in composition; they tend to be more quartzose and feldspathic than the underlying Bushnell Rock and Tenmile formations (Fig. 2.2).

Heavy minerals in these Umpqua basin sandstone units and in the overlying Tyee forearc basin units also reflect the two different source terrains. Umpqua basin sandstones commonly contain large amounts of epidote aggregates and epidote-polycrystalline quartz grains, derived from the Klamath Mountains metavolcanic and metasedimentary units. The heavy mineral assemblage in the overlying Tyee forearc strata is epidote-poor but contains more zircon, tourmaline, and opaque iron oxides derived from the Idaho batholith and intermediate volcanics.

The mineralogy of the Rasler Creek Tongue is transitional between Umpqua Group strata and the overlying Tyee forearc strata. It consists of a high proportion of both extrabasinal intermediate volcanic rock fragments, micas, and feldspars (both K-feldspar and plagioclase) and locally derived Klamath Mountains sedimentary and metamorphic rock fragments and polycrystalline quartz (Fig. 2.3).

Textural characteristics of sandstones

Well-indurated sandstone of the lower Umpqua Group (i.e., Bushnell Rock and Tenmile formations) is poorly to moderately sorted and is composed of subangular to subrounded framework clasts (Table 2.4 in Appendix). These rocks are moderately rich in clay matrix. They are texturally immature and reflect depositional processes and environments characterized by rapid deposition and burial (e.g., fan deltas and turbidites). Most are medium- to very coarse-grained, well-indurated, "dirty", dark gray sandstone in outcrop. Sandstones of the Slater Creek Member of the Bushnell Rock Formation are fine- to medium-grained and are slightly better sorted (Table 2.4 in Appendix). Less-indurated sandstones of the lower Umpqua Group (i.e., Berry Creek Member of White Tail

Ridge Formation) and upper Umpqua Group (e.g., Coquille River Member and Rasler Creek Tongue) are more moderately well-sorted, fine- to medium-grained, and cleaner and lighter grey in outcrop (tend to have less clay matrix). Therefore, these units are texturally more mature (Folk, 1974). The greater degree of textural maturity can be attributed to deposition in delta front environments that were extensively reworked by storm waves and longshore currents that winnowed detrital clays and sorted the grains.

The overlying moderately indurated Remote Member sandstone and well-indurated sandstones of the Baughman Member (Tyee Formation) are coarse- to very coarse-grained, locally conglomeratic, and more poorly sorted, reflecting rapid deposition and burial in fluvial and distributary channels and bars with infrequent reworking and sorting of the sediments by currents (Table 2.4 in Appendix). Well-indurated, finer grained turbidites of the Tyee Mountain Member and Elkton Formation are moderately sorted, rich in clay, and contain subangular to subrounded grains (Table 2.4 in Appendix). They are uniformly fine- to medium-grained with abundant mica and crushed carbonized plant fragments. Wave-dominated deltaic sandstones of the Bateman and Spencer formations are typically fine- to medium-grained, clean, friable, moderately sorted, and texturally mature (Table 2.4 in Appendix). Some Spencer fluvial to distributary channel sandstones are coarse- to very coarse-grained.

Tectonic provenances and stratigraphic variations of sandstones

Compositional variations of major framework grains plotted on normalized discriminant or ternary diagrams are a powerful tool for deciphering plate tectonic provenance and the evolutionary trends of sandstone compositions (Dickinson and Suczek, 1979; Dickinson et al., 1983). In a series of ternary diagrams, Dickinson and others (1983) outlined the compositional ranges of sandstones derived from various provenances. Data for Tyee basin sandstones are plotted on these ternary diagrams using different symbols to represent each lithostratigraphic unit (Figs. 2.4, 2.5. 2.6, 2.7, and 2.8). The lithostratigraphic nomenclature for the southern Tyee basin proposed by Ryu and others (1992) is used in this study.

Umpqua Group sandstones (sequences I and II) generally plot in the recycled orogenic provenance (e.g., Mesozoic Klamath Mountains sources) on QFL diagrams of Dickinson and others (1983). Sandstones from the overlying forearc Tyee, Elkton, Bateman, and Spencer formations (sequences III and IV) plot in the dissected magmatic arc provenance (e.g., Idaho batholith, Clarno-Challis arc sources) (Fig. 2.4). On a daughter-diagram, QmFLt, Umpqua Group sandstones are clustered closer to the total lithics (Lt) pole (Fig. 2.5). Also, sandstones of the White Tail Ridge Formation (Remote Member, Coquille River Member, and Rasler Creek Tongue) and the upper Umpqua Group (sequence II) are more widely scattered, plotting on the recycled orogenic, undissected magmatic arc, and transitional magmatic arc provenances on this ternary diagram (Fig. 2.5). This shift is mainly due to substantial amounts of polycrystalline quartz and chert in these upper Umpqua Group sandstones. QpLvLs diagrams demonstrate that Umpqua Group sandstones contain a higher proportion of polycrystalline quartz and chert in comparison to the Tyee and younger forearc units (Fig. 2.6). Point count data on the QmPK plots show clustering toward the Qm-P line with relatively little K present, particularly in Umpqua Group sandstones (Fig. 2.7). Potassium feldspar is more abundant in the Tyee Formation and post-Tyee units. Umpqua Group sandstones are widely scattered on the volcanic (Lv), metamorphic (Lm), and sedimentary (Ls) lithics diagram (Fig. 2.8). This is because these siliciclastic rocks contain subequal amounts of sedimentary and metamorphic rock fragments and subordinate volcanic rock fragments (mainly metavolcanics). In contrast, Tyee, Elkton, Bateman, and Spencer sandstones cluster toward the volcanic rock fragment pole; these rocks contain lower proportions of sedimentary and metamorphic rock fragments.

These compositional changes in the Eocene sandstones are reliable indicators of tectonic reconfiguring of the basin as well as tectonic events in the source areas. Lower Eocene strata (i.e., Umpqua Group units) which have been interpreted as forming in a subduction zone and marginal basin were derived from recycled orogenic, transitional, and undissected magmatic arc provenances. The overlying middle to upper Eocene strata (i.e., Tyee, Elkton, Bateman, and Spencer formations) formed in a forearc basin and consist of detritus eroded from dissected and

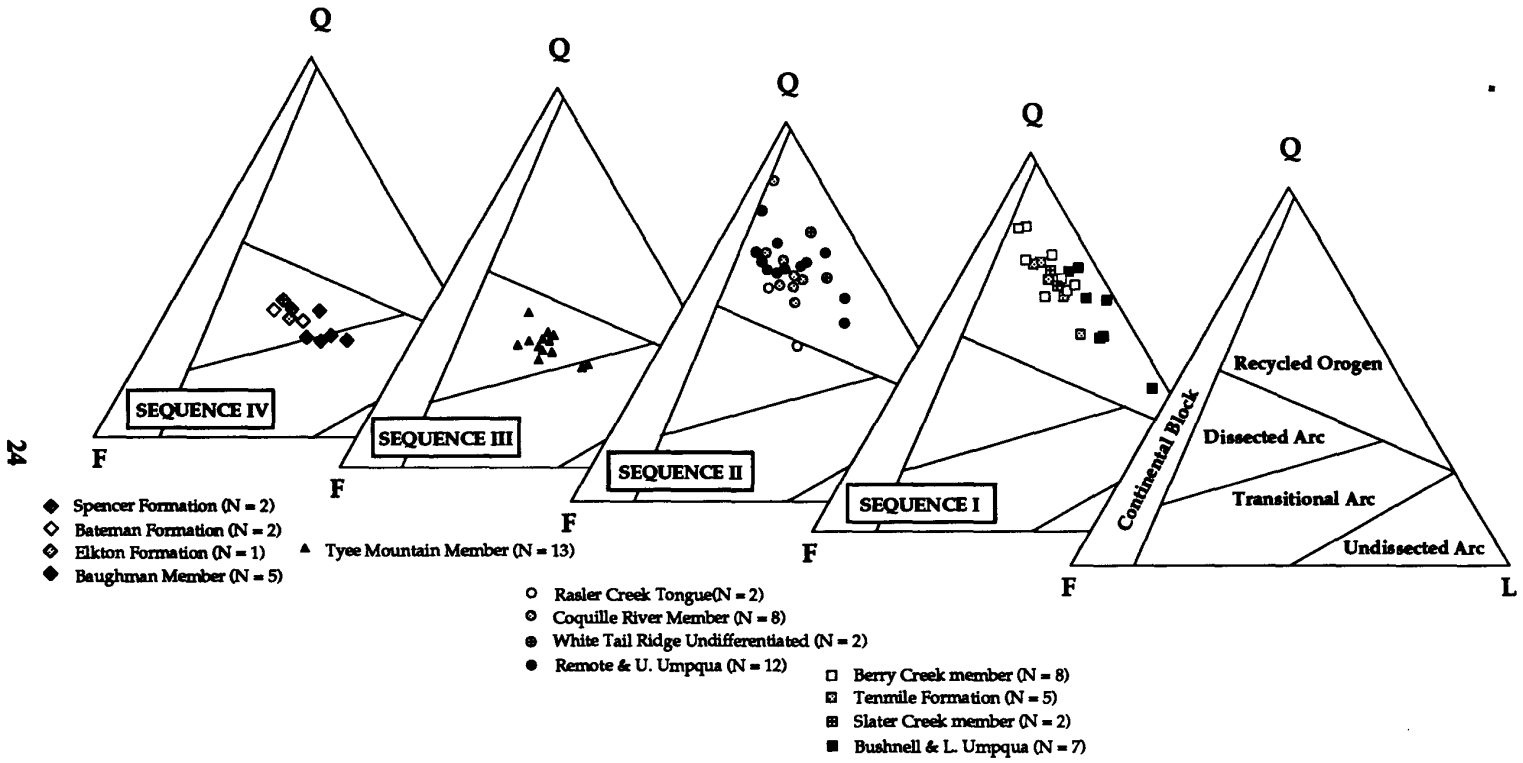

Figure 2.4 QFL plot of Tyee basin sandstones. Sandstones from Umpqua Group (Sequences I and II) generally plot in the recycled orogenic provenance, whereas sandstones from the overlying Tyee, Elkton, Bateman, and Spencer formations (Sequences III and IV) plot in the dissected magmatic arc provenance (Dickinson and others, 1988). Q = total quartz grains including polycrystalline lithic fragments such as chert and quartzite; F = monocrystalline feldspar grains; L = unstable polycrystalline lithic fragments.

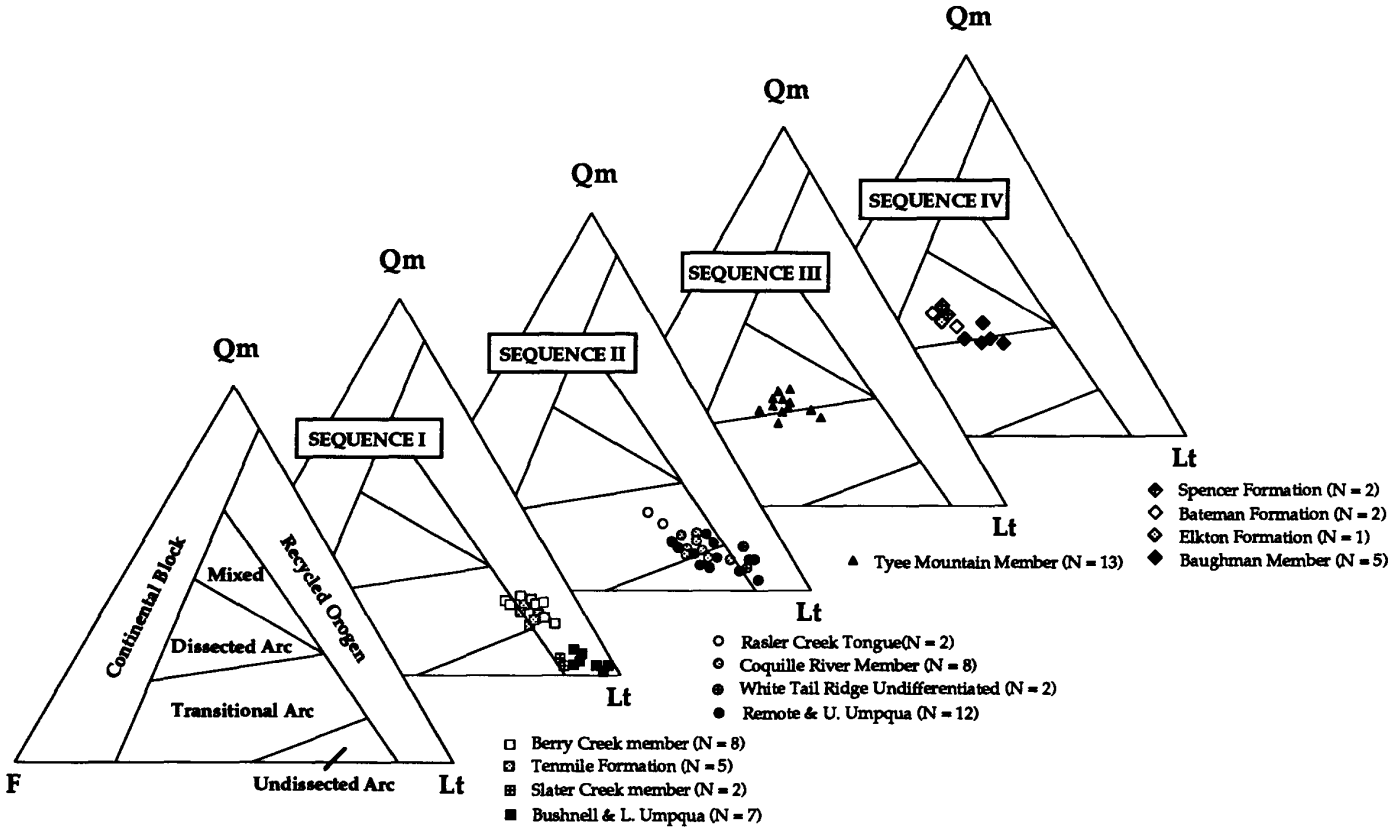

Figure 2.5 QmFLt plot of Tyee basin sandstones. Sandstones from lower Umpqua Group (Sequence I) plot in the recycled orogenic provenance, but sandstones from upper Umpqua Group (Sequence II) are more widely scattered on the recycled orogenic, undissected magmatic arc, and transitional magmatic arc provenances. The overlying forearc basin sandstones (Sequences III and IV) generally plot in the dissected magmatic arc provenance (Dickinson and others, 1988). Qm = monocrystalline quartz grains; F = feldspar grains; Lt = total polycrystalline lithic fragments.

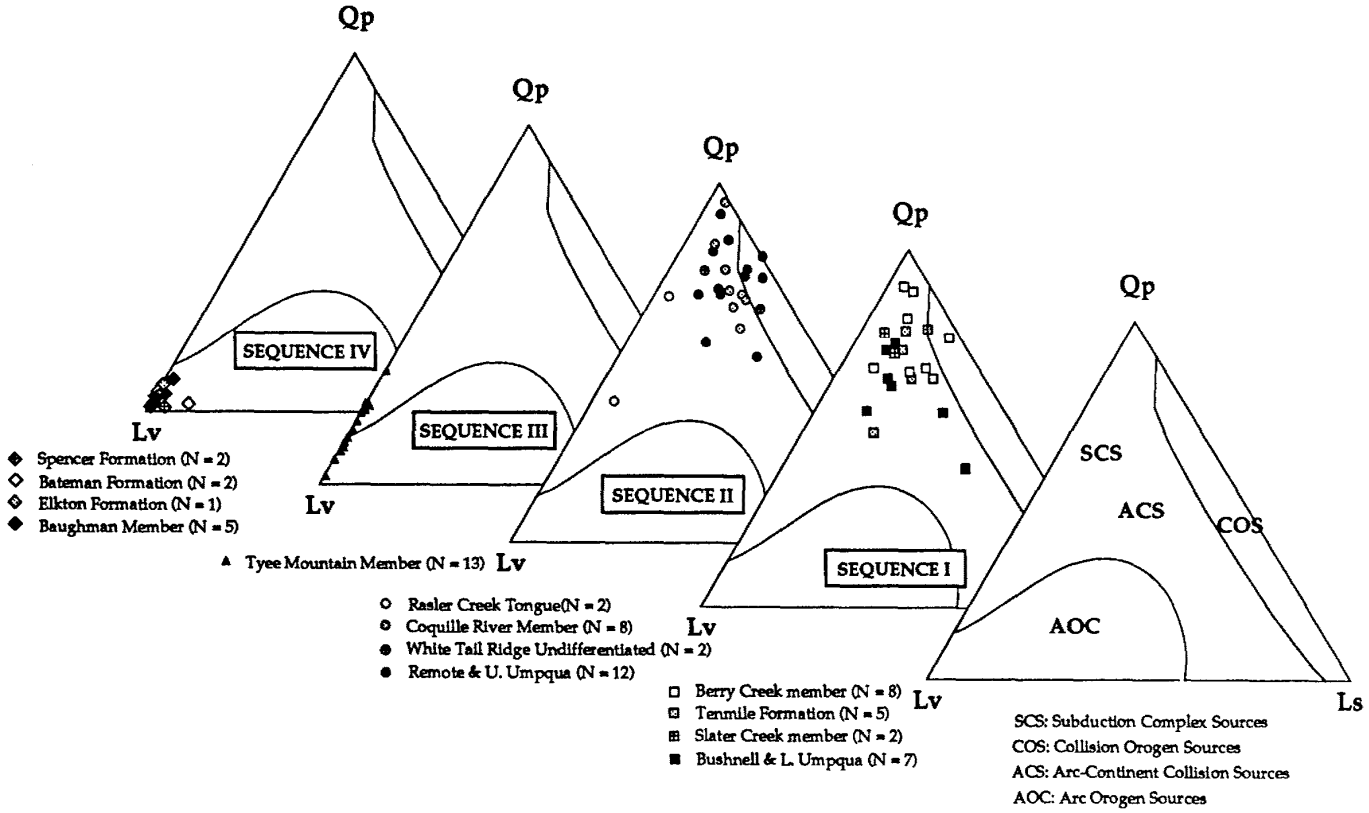

Figure 2.6 QpLvLs plot of Tyee basin sandstones. The Umpqua Group (Sequences I and II) sandstones contain a high amount of polycrystalline quartz and chert, whereas the Tyee and younger forearc sandstones (Sequences III and IV) contain a high amount of volcanic lithic fragments (Dickinson and Suczek, 1979). Qp = polycrystalline quartz grains; Lv = volcanic lithic fragments; Ls = sedimentary lithic fragments.

undissected magmatic arc provenances (Snavely and Wagner, 1963; Baldwin and Perttu, 1980; Heller and Ryberg, 1983; Snavely, 1984, 1987; Wells and others, 1984; Wells and Heller, 1988; Ryu and others, 1992; Ryu and Niem, 1993).

Heller and Ryberg (1983) also recognized major changes in sandstone composition. The lithic sandstones of the lower Eocene Roseburg and Lookingglass formations (Umpqua Group of Ryu and others, 1992) were derived from the uplifted orogenic Mesozoic Klamath Mountains terranes during syndepositional subduction and accretion of the Umpqua basin. The overlying, less deformed micaceous lithic arkosic (mainly volcanic) sandstones of the Tyee and Coaledo formations (middle and upper Eocene) were sourced from the Idaho batholith and from Clarno-Challis arc before the Oregon Coast Range and Tyee basin were rotated (Heller and others, 1985; Wells and Heller, 1988).

Resolution of lithostratigraphic problems

The differences in sandstone composition among the Eocene units also verify the new geologic mapping and lithostratigraphy of the southern Tyee basin established by Molenaar (1985), by Ryu and others (1992), and by Black and others (in prep.). In previous mapping, Baldwin (1974), Baldwin and Perttu (1980), and Niem and Niem (1990) depicted lateral equivalence between the deltaic facies of the Flournoy Formation (now called White Tail Ridge Formation) in the type area and the turbidite facies of the Flournoy Formation which crops out throughout the central Coast Range north of Loon Lake. They restricted the Tyee Formation to south of the Elkton-Loon Lake area. Chan and Dott (1983) and Heller and Dickinson (1985) used this definition in their reconstructions of the Eocene Tyee/Flournoy deltaic-turbidite depositional system.

However, recent field mapping (Black and others, in prep.) and lithostratigraphy (fence diagram of Ryu and others, 1992) show that the turbidite strata north of Loon Lake are part of the Tyee Formation (i.e., Tyee Mountain Member). This new mapping and litho- and biostratigraphic studies (e.g., Molenaar, 1985; Ryu and others, 1992; Ryu, 1995) show that Baldwin's (1974) type Flournoy (now called White Tail Ridge Formation) is a deltaic facies that pinches out northward into mudstone of the upper part of the undifferentiated Umpqua Group. These deltaic strata are not lithostratigraphically equivalent to the turbidites north of Loon Lake.

Thin sections of sandstone and conglomerate from the type area and type section of the Flournoy Formation reveal that these strata are non-micaceous, lithic (metamorphic and sedimentary) feldspathic arenites and wackes. They contain large proportions of polycrystalline quartz and only a few volcanic rock fragments (mostly Klamath-derived epidote-bearing metabasalt). In contrast, turbidite sandstones north of Loon Lake are much finer grained, richer in clay matrix, micaceous (very abundant, coarse flakes of muscovite and biotite) volcano-lithic arkoses. These turbidite sandstones are identical to the fine-grained, micaceous Tyee Formation sandstones at Tyee Mountain in the type area and along the Umpqua River south of Elkton and Drain.

Sequence stratigraphic implication

Sandstone compositions in the southern Tyee basin are controlled mainly by change in provenance and plate tectonic setting. Since the changes in provenance are basinwide and largely synchronous, compositional variations in the sandstones are also useful for regional correlation of stratigraphic units (Ingersoll, 1983). Moreover, application of sequence stratigraphic concepts in regional correlations can provide a more sophisticated interpretation to the compositional variations in the Tyee basin sandstones based on the relationship between sedimentation, eustacy, and tectonics.

Recent studies by Ryu and others (1992) and Ryu and Niem (1993, 1994) using sequence stratigraphic concepts of Van Wagoner and others (1990) indicate that Eocene strata in the basin consist of four third order depositional sequences numbered I to IV. Each depositional sequence is locally bounded on the basin margin by unconformities and by the correlative conformities toward the basin center. A sequence generally begins with a lowstand systems tract (LST) (either a prograding deltaic wedge and/or incised valley fill and/or slope-fan and basin-floor fan), overlain by a transgressive systems tract (TST) (typically a backstepping lowstand deltaic wedge and slope-fan with major marine flooding surface), and capped by a highstand systems

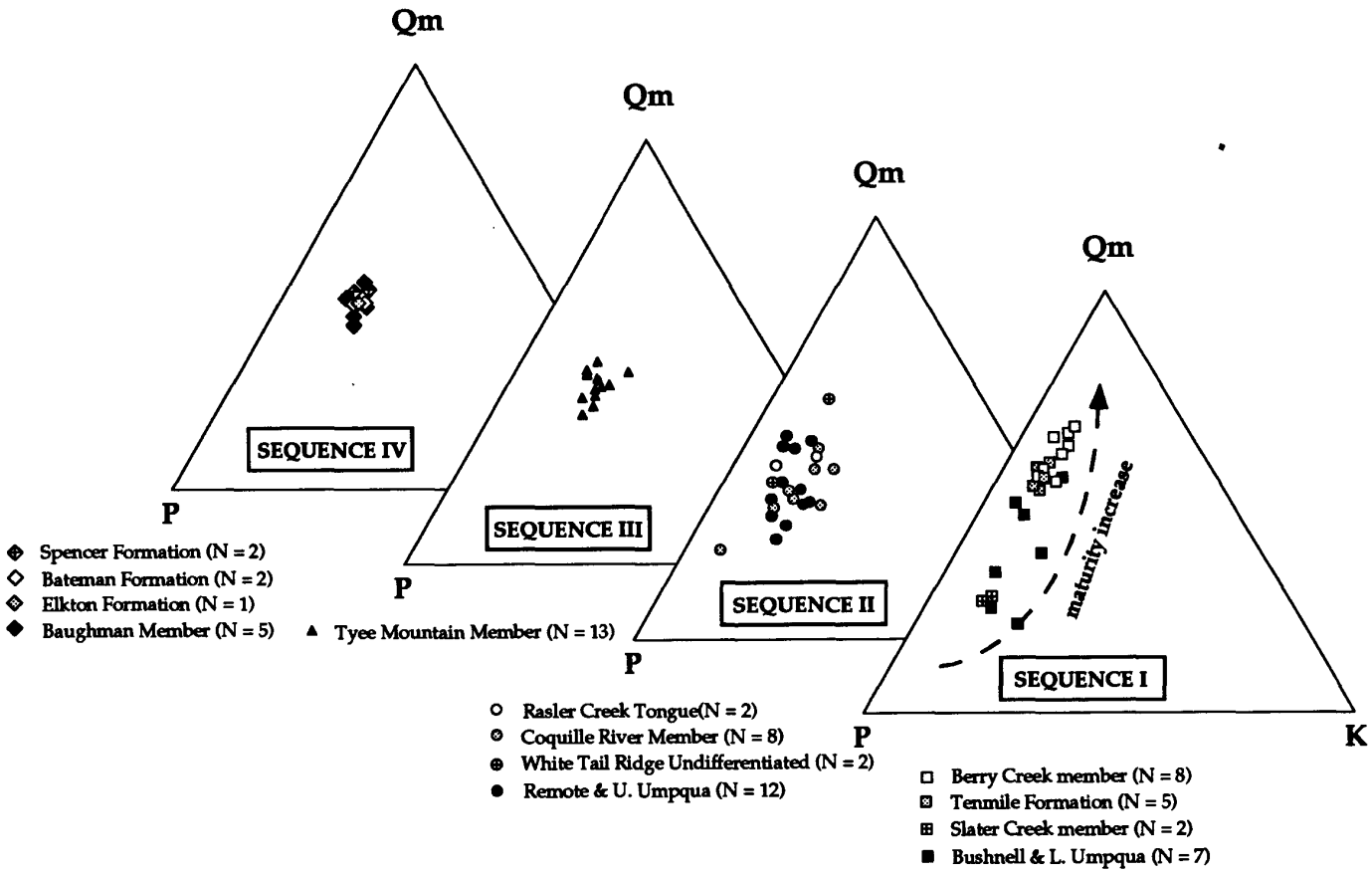

Figure 2.7 QmPK plot of Tyee basin sandstones. Qm = monocrystalline quartz grains; P = plagioclase; K = potassium feldspar.

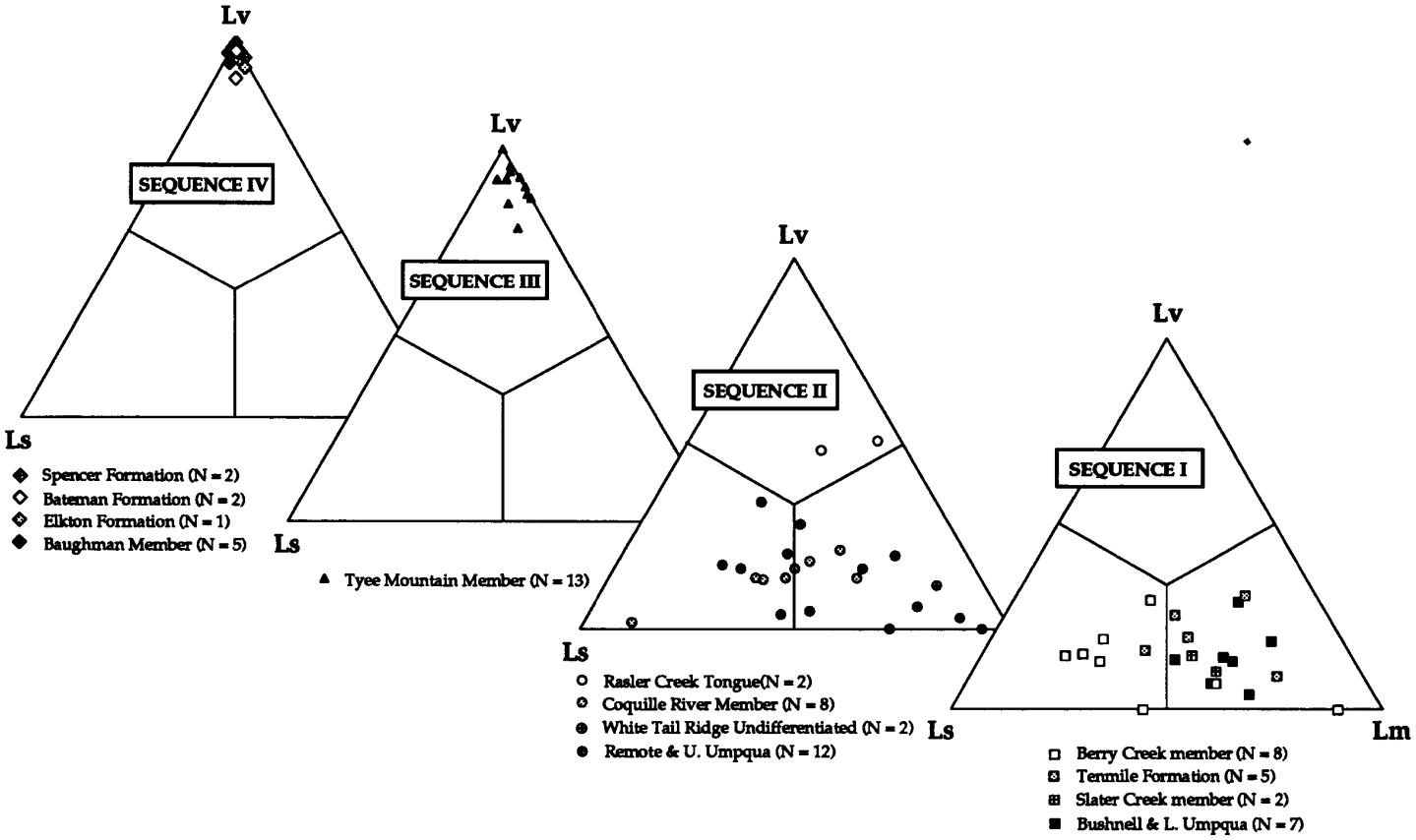

Figure 2.8 LvLmLs plot of Tyee basin sandstones. Umpqua sandstones (Sequences I and II) are widely scattered on the fields of sedimentary and metamorphic rock fragments. In contrast, Tyee and younger forearc sandstones cluster toward the volcanic lithic fragment pole. Lv = volcanic lithic fragments; Ls = sedimentary lithic fragments; Lm = metamorphic lithic fragments.

tract (HST) (typically a prograding wave- to tide-dominated delta).

Depositional sequence I includes the lower Umpqua Group (slope-fan to basin-floor fan), the Bushnell Rock Formation and the Slater Creek Member (incised valley fill and prograding deltaic wedge of a lowstand systems tract), the Tenmile Formation (a backstepping slope-fan and a transgressive systems tract), and the Berry Creek Member of the White Tail Ridge Formation (a prograding delta of highstand systems tract). Depositional sequence II consists of the upper Umpqua Group (slope-fan to basin-floor fan), the Remote Member (an incised valley fill), the Coquille River Member (prograding and backstepping deltaic wedge), the Camas Valley Formation (transgressive systems tract), and the Rasler Creek Tongue (a prograding delta of a highstand systems tract). Depositional sequence III consists of the Tyee Mountain Member (an incised valley or canyon fill, slope-fan, and basin-floor fan) and the Hubbard Creek Member (a transgressive systems tract and outer shelf/slope mudstone with nested channel sandstones of a highstand systems tract). Depositional sequence IV contains the Baughman Member (a prograding deltaic wedge), the Elkton Formation (a transgressive systems tract), and the Bateman and Spencer formations (prograding wave-dominated delta of a highstand systems tract).

Our detailed comparison of the relative abundance of major framework grains in each depositional sequence provides further explanation of the variation in sandstone composition due to changes in rates of sedimentation, depositional environment, eustacy, and tectonism within the basin as well as in the provenance. Sequences I and II (Umpqua Group lithic petrofacies) are primarily composed of polycrystalline quartz, metamorphic rock fragments, and sedimentary rock fragments (Fig. 2.3). Sequences III and IV (Tyee and post-Tyee lithic arkosic petrofacies) typically have a higher abundance of monocrystalline quartz, K-feldspar, plagioclase, volcanic rock fragments, and micas (Fig. 2.3). This petrofacies change supports the interpretation of a regional change in provenance from a local Klamath Mountains source to a more distant Idaho batholith-Clarno volcanic arc source (Heller and Ryberg, 1983). Furthermore, the composition of framework grains varies systematically from the LST to the HST in each sequence. These compositional changes reflect the varying competence of transport processes in lower energy environments (in the LST) compared to high-energy depositional environments (in the HST) to sort, winnow, and abrade grains.

For example, monocrystalline quartz grains are relatively abundant in HST sandstones (e.g., the Berry Creek Member, Rasler Creek Tongue, and Bateman and Spencer formations; Fig. 2.3). However, the abundance of polycrystalline quartz grains generally decreases from the LST to the HST. The relative increase of monocrystalline quartz grains in concert with decrease of polycrystalline quartz grains within a depositional sequence reflects that polycrystalline quartz grains are more effectively abraded and destroyed by the higher energy processes (e.g., waves, tides, and longshore currents) that are prevalent in the HST depositional environments (e.g., wave-dominated delta). This results in concentration of monocrystalline quartz grains in HST sandstones.

The proportions of K-feldspar and plagioclase in these sandstones may be controlled either by the relative abundance of those feldspars in the source rocks or by depositional and weathering processes. Feldspars are most abundant (up to 35% of detrital fraction) in sequences III and IV (Fig. 2.3 and Table 2.3 in Appendix). The substantial increase of feldspar abundance from sequences I and II to sequences III and IV is compatible with the regional change in provenance (Figs 2.4 and 2.5). However, no systematic variation of feldspar abundance is recognized within any of the sequences (Fig. 2.3). This suggests that the abundance of feldspar is more effectively controlled by rock types and by weathering processes in the provenance than by reworking processes within the basin of deposition.

The abundance of volcanic rock fragments decreases toward the HST within sequence I (Fig. 2.3). Sequence II shows a similar decrease of volcanic rock fragment abundance, but the HST in sequence II (the Rasler Creek Tongue) contains many volcanic rock fragments (up to 20%). The HST is usually characterized by a higher concentration of quartz (i.e., monocrystalline quartz) due to prolonged reworking of the sands by high-energy depositional processes (e.g., waves). The higher

concentration of volcanic rock fragments in the Rasler Creek Tongue, for example, probably reflects the contribution of a developing volcanic arc provenance (e.g., Clarno-Challis volcanics) before deposition of sequence III (e.g., Tyee Formation). Wells and Heller (1988) demonstrated that the southern Oregon Coast Range started to rotate clockwise approximately at this time (49 Ma). Paleomagnetic data indicate that rotation was accompanied by change of tectonic setting from subduction and accretion of the Umpqua basin strata to forearc basin subsidence (Heller and Ryberg, 1983).

A systematic variation of proportions of volcanic rock fragments (both in composition and in texture) also appears within sequences III and IV (Fig. 2.9). Intermediate volcanic rock fragments with porphyritic texture (plagioclase phenocrysts) are much more abundant in the LSTs (e.g., the Tyee Mountain Member and the Baughman Member; Fig. 2.9). This type of volcanic rock fragment dramatically decreases toward the HST (e.g., the Bateman and Spencer formations; Fig. 2.9). In contrast, intermediate finely crystalline volcanic (lava) rock fragments with pilotaxitic textures are less abundant in the HST sandstones, but greatly increase (up to 60%) toward the HST (Fig. 2.9). The proportion of the two textural types of volcanic rock fragments in these sandstones is a result of variations of lava composition and textures in the provenance and energy of the depositional processes. For example, prolonged high-energy processes, such as waves, preferentially destroy less abrasion-resistant pilotaxitic volcanic grains.

Metamorphic rock fragments are less abundant in the HST than in the LST of sequence II, although this change is not apparent in sequence I (Fig. 2.10). This may be due to the relative abundance and varying hardness of different metamorphic rock fragment types in each sequence. Abrasion-resistant metaquartzite, quartz-mica schist, and quartz-mica-feldspar aggregates are more abundant in the coarse-grained sandstones of sequence I, whereas sequence II contains more clasts of softer phyllite, sheared graywacke, and epidote-quartz greenschist. Sedimentary rock fragments are more abundant toward the HST (e.g., Berry Creek and Coquille River members). The higher abundance of sedimentary rock fragments in the HST is mainly due to the concentration of abrasion-resistant chert in sequences I and II (Fig. 2.3). It is concentrated by constant reworking by wave and tidal processes in these wave-dominated delta front sands as softer metamorphic and sedimentary rock fragments are preferentially destroyed.

The compositional variations of the detrital framework grains in the sandstones reflect the variety of tectonic settings, the predominant rock types in the source area, and the dominant transport and reworking processes operating in the basin of deposition. Within a depositional sequence, LST sandstones (formed in lower energy environments; such as, alluvial and submarine fans) contain more, chemically unstable framework grains, such as volcanic and metamorphic rock fragments and polycrystalline quartz, compared to HST sandstones that were deposited in higher energy depositional environments (e.g., beaches). Since an LST is created by a rapid fall of relative sea level, much of the continental shelf is exposed during that time. Alluvial fans, rivers and submarine canyons are locally incised into the exposed shelf and upper slope. Lithic sediments derived from the surrounding mountainous tectonically active source terranes are rapidly transported by gravity transport processes (e.g., debris flow and turbidity current) through sea gullies and submarine canyons to form a basin-floor fan. Due to rapid burial and lack of further reworking, these lithic-rich sands are compositionally and texturally immature.

HST sandstones are characterized by a higher concentration of abrasion-resistant quartz (i.e., monocrystalline quartz and chert) and feldspar as framework grains, compared to LST sandstones. During highstand sea-level stage, a deltaic depositional system is well-developed and actively prograding onto the shelf because the rate of sedimentation exceeds the rate of accommodation (Posamentier and others, 1988). Softer and chemically unstable framework grains (e.g., volcanic and metamorphic rock fragments) are more effectively abraded and destroyed by waves, tides, and longshore currents during progradation of wave-dominated deltas. However, a high influx of chemically unstable framework grains (e.g., volcanic rock fragments) due to an abrupt change in the provenance may be recorded as an unusual concentration of unstable framework grains even during HST deposition. This suggests that the patterns of sedimentation and sandstone composition can be

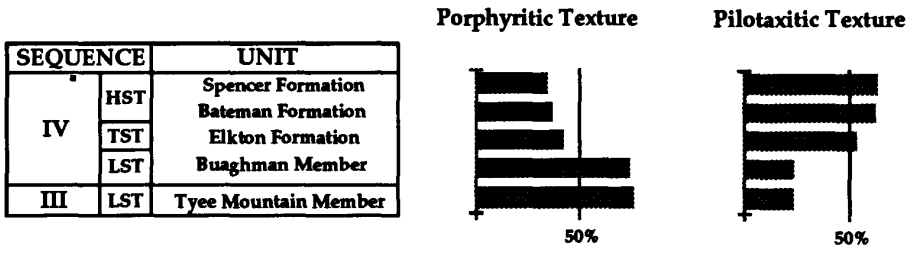

Figure 2.9 Compositional variation of volcanic rock fragments in Sequence III & IV. (LST=Lowstand Systems Tract; TST=Transgressive Systems Tract; HST=Highstand Systems Tract).

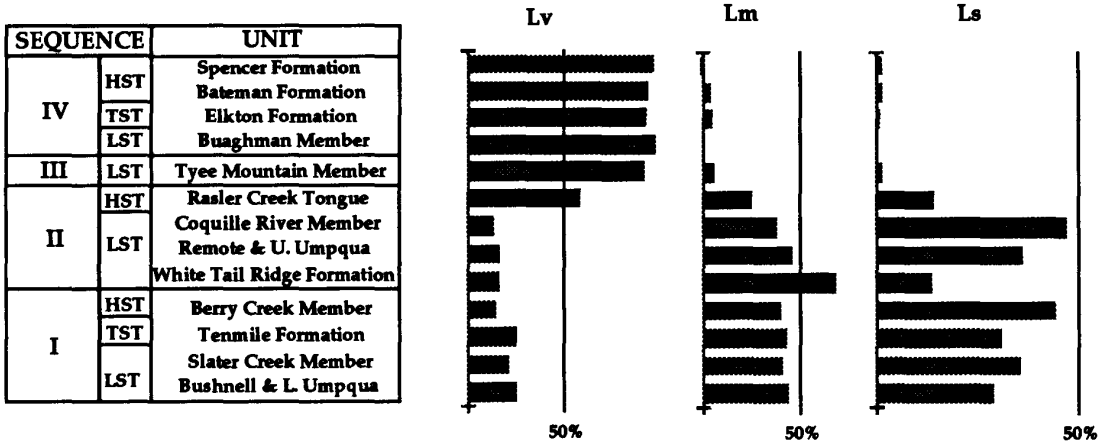

Figure 2.10 Relative abundance of rock fragments types in Tyee basin sandstones. (LST=Lowstand Systems Tract; TST=Transgressive Systems Tract; HST=Highstand Systems Tract; Lv = Volcanic Rock Fragments; Lm = Metamorphic Rock Fragments; Ls = Sedimentary Rock Fragments).

normally affected by relative changes in sea-level, but the composition of sandstone is more strongly controlled by tectonic uplift in the provenance, where tectonic factors greatly exceed eustatic effects in the depositional basin (e.g., the Rasler Creek Tongue; Ryu and others, 1992; Ryu and Niem, 1993, 1994).

Diagenesis

Sandstone diagenesis for some Eocene units in the Tyee basin has been previously described by Burns and Ethridge (1979) and Chan (1985) and briefly discussed by numerous MS theses at the University of Oregon, Portland State University, and Oregon State University (see list on compilation map in Niem and Niem, 1990). This section summarizes the previous investigations and elaborates on the diagenesis of sandstones and conglomerates in the Tyee basin units based upon our regional study of 70 additional thin sections.

Sandstones in the Tyee basin display a variety of diagenetic features in thin section and under the scanning electron microscope which reflect the effects of seven diagenetic processes. These processes are: (1) mechanical compaction, (2) alteration of framework grains, (3) cementation by zeolites, quartz, and feldspar (4) formation of authigenic clay minerals, (5) dissolution of framework grains and formation of secondary porosity, (6) late-stage calcite replacement, and (7) other diagenetic effects (i.e., detached clay coats).

Mechanical compaction

Mechanical compaction is the main diagenetic process that has reduced porosity and permeability in Tyee basin sandstones. Mechanical reduction of primary pore space during shallow burial included minor grain rotation and readjustment to a more stable grain packing. Deeper burial of the older stratigraphic units has resulted in more extensive compaction and deformation of framework grains and a greater reduction of primary intergranular pore space. The effect of compaction is most strongly displayed by ductile coarse mica flakes, particularly biotite and chlorite. These grains are elongate, straight, undeformed to slightly warped in the shallow-buried sandstone units (e.g., Spencer and Elkton formations). Grain boundaries between framework clasts and lithic fragments in the younger shallow buried units are delicate point or straight, and large intergranular pore spaces remain. Mica flakes are increasingly bent and contorted or crushed between brittle framework grains, such as quartz and feldspar, in more deeply buried lithic-feldspathic sandstone units (e.g., Baughman and Tyee Mountain members) (Fig. 2.11). Carbonized wood and ductile rock fragments, such as carbonaceous phyllite, mudstone, and clay-altered volcanics, have also deformed plastically and flowed into remaining primary intergranular pore space to form pseudomatrix in deeper-buried lithic sandstone units (e.g., Bushnell Rock, Tenmile, and White Tail Ridge formations). Sutured and interpenetrating to concave-convex grain boundaries between brittle mono- and polycrystalline quartz grains resulting from pressure solution and lithostatic compaction are common in the deepest buried sandstone-dominated units of the lower Umpqua Group (Fig. 2.12).

Alteration of framework grains

Diagenetic products resulting from alteration of framework grains vary among sandstone units in the Tyee basin due to primary compositional differences. Alteration processes include zeolitization, albitization and partial dissolution of plagioclase, and alteration of lithic fragments to clay minerals.

Albitization of plagioclase is characterized by a dusty to mottled appearance of plagioclase grains in thin section. It is extensive in the feldspathic Spencer, Bateman, Elkton, and Tyee formations. Some plagioclase clasts are partly replaced by authigenic mixed-layer chlorite/smectite clay or authigenic zeolite. Albitization has been documented as an important reaction in the diagenesis of feldspathic sandstones (Boles, 1982; Gold, 1987; Milliken, 1988). Albitization is closely associated with crystallization of authigenic zeolites in pore spaces in feldspathic sandstones (Helmold and Van de Kamp, 1984). Other alteration products, such as sericite, are associated with albitization of plagioclase clasts.

The groundmass of glassy lava fragments is commonly altered to smectite clays. Lath-like plagioclase microlites and phenocrysts are surrounded by a groundmass of clay minerals. Other formerly glassy clasts (e.g., pumice,

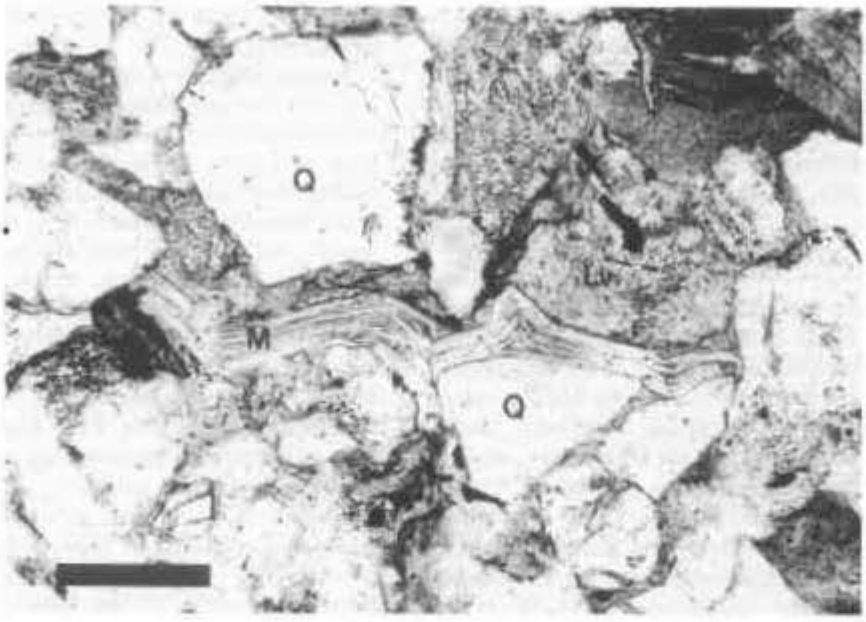

Figure 2.11 Photomicrograph of mechanically contorted and crushed, elongate muscovite flake (M) between brittle quartz (Q) and volcanic lithic (Lv) framework grains. Compaction has significantly reduced primary intergranular porosity in deeply buried Tyee Mountain turbidite sandstones. Sample RN-91-361, plane-polarized light, 6X, scale bar = 0.2 mm.

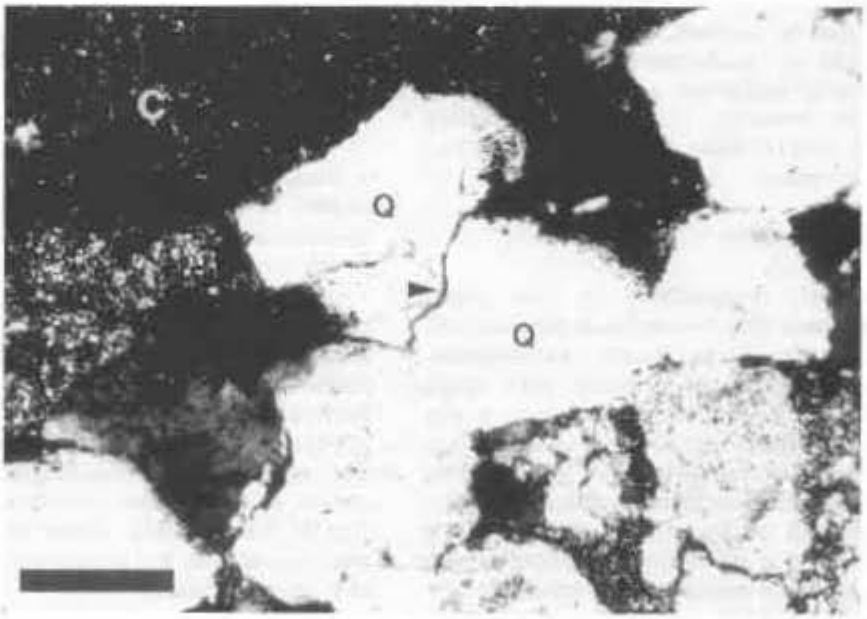

Figure 2.12 Photomicrograph of angular to jagged, mono- and polycrystalline quartz (Q) and chert (C) (microcrystalline quartz) grains in a Coquille River Member sandstone. Note the straight and interpenetrating (or sutured) contacts between these grains, due to intense compaction by deep burial that has greatly reduced primary intergranular pore space. Sample RN-91-307, crossed nicols, 6X, scale bar = 0.2 mm.

amygdules, or rare shards) are severely altered and compacted to elongate greenish fibrous celadonite, iron-rich smectite and chlorite clays.

Cementation by zeolites, quartz, and feldspar

Diagenetic zeolites, silica, feldspar, and calcite are the main cements in Tyee basin sandstones. These cements occur as overgrowths and as extensive pore-fillings. Some partially replace framework grains and lithic fragments.

(i) Zeolites: Authigenic zeolites include heulandite/clinoptilolite and laumontite. These occur as extensive pore-filling cements and minor replacements of framework grains in sandstones of the Tyee Formation.

Heulandite/clinoptilolite is recognized only in sandstones in the upper part of the Baughman Member. Heulandite/clinoptilolite has been commonly reported as an alteration product of glassy clasts in volcanogenic sandstones and usually occurs as authigenic minute coffin-shaped crystals to prismatic crystal aggregates (less than 10 μm in size) that partially fill primary intergranular pore space (Boles and Coombs, 1975; Surdam and Boles, 1979). In the Baughman Member, this zeolite is present mainly as a late-stage pore-filling cement without obvious glass precursors (Fig. 2.13). Heulandite/clinoptilolite cements post-date early formed smectite clay coats/rims in these sandstones.

Laumontite is common as a pore-filling cement and replacement mineral of plagioclase in sandstone in most of the Tyee Formation. In lower Baughman sandstones, laumontite cement completely fills the remaining large primary intergranular pore spaces. These pore spaces are also commonly lined by thin radiating fibrous greenish smectite and corrensite clay coats or rim cement. This textural or paragenetic relationship indicates that pore-filling laumontite post-dated the earlier formed diagenetic smectite/corrensite clay rim cement. However, it is not clearly evident that heulandite/clinoptilolite cement pre-dated pore-filling laumontite cement because they largely occur in separate sandstones of the Baughman Member. Vertical stratigraphic

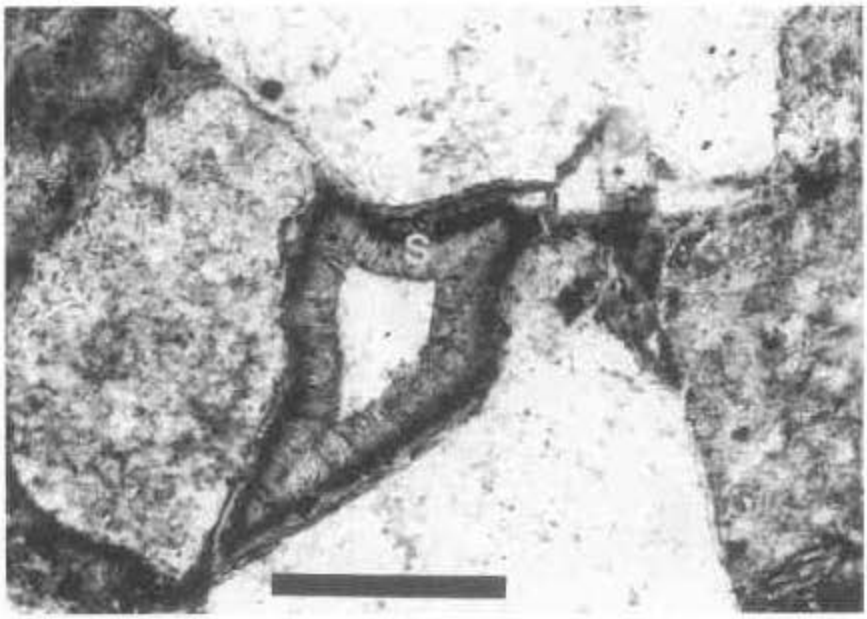

Figure 2.13 High magnification of two clay coats (early burial stage = dark line and thick, fibrous smectite(S)) that rim angular and rounded framework grains. Clay coats fill inward toward the center of a former, large, primary intergranular pore. Center of pore is filled with later stage granoblastic heulandite/clinoptilolite cement (low birefringence). Baughman Member, Sample RN-91-401, crossed nicols, 10X, scale bar = 0.2 mm.

distribution of these zeolites suggests that pore-filling laumontite cement post-dated heulandite/clinoptilolite cement although some are nearly coeval. Chan (1985) and this study, for example, found heulandite/clinoptilolite cement only in shallow-buried upper Baughman and Bateman sandstones of sequence IV. Laumontite cement is well-developed in the more deeply buried sandstones of the lower Baughman and Tyee Mountain members of sequences III and IV. However, there is some overlap of the stratigraphic distribution of heulandite/clinoptilolite and laumontite cements as demonstrated by some Baughman sandstone beds in which some pores are filled with heulandite/clinoptilolite while other pores are filled with laumontite. Boles and Coombs (1978) showed that laumontite cement is typically more stable thermodynamically than heulandite/clinoptilolite and gradually replaced heulandite/clinoptilolite in more deeply burial Triassic-Jurassic volcanic rocks of the Southland Syncline, New Zealand.

Laumontite replacement shows two distinctive modes of occurrence: replacement of earlier formed smectite and corrensite clay rim cements and replacement of detrital framework grains. Laumontite replacement of early smectite and corrensite clay rim cements is relatively rare in Baughman sandstones. However, downsection, laumontite replaced both early-stage clay rim cements and late-stage clay pore-fills (Fig. 2.14). Some relict clay rim textures are partially preserved as thin dark linings. Laumontite replacement of framework grains varies from patchy alteration within a framework grain to complete replacement and is the most common mode of occurrence of laumontite in Tyee Mountain Member sandstones. Patches of laumontite are usually found within detrital plagioclase grains (Fig. 2.15) but are also common in volcanic rock fragments. Complete replacement of framework grains occurs in the lower part of the Tyee Mountain Member. Textural or paragenetic relationships between framework grains and clay rim cement replacement by laumontite are not evident in individual thin sections, but their vertical stratigraphic distribution suggests that replacement of smectite and corrensite clay coats/rim cements occurs prior to replacement of

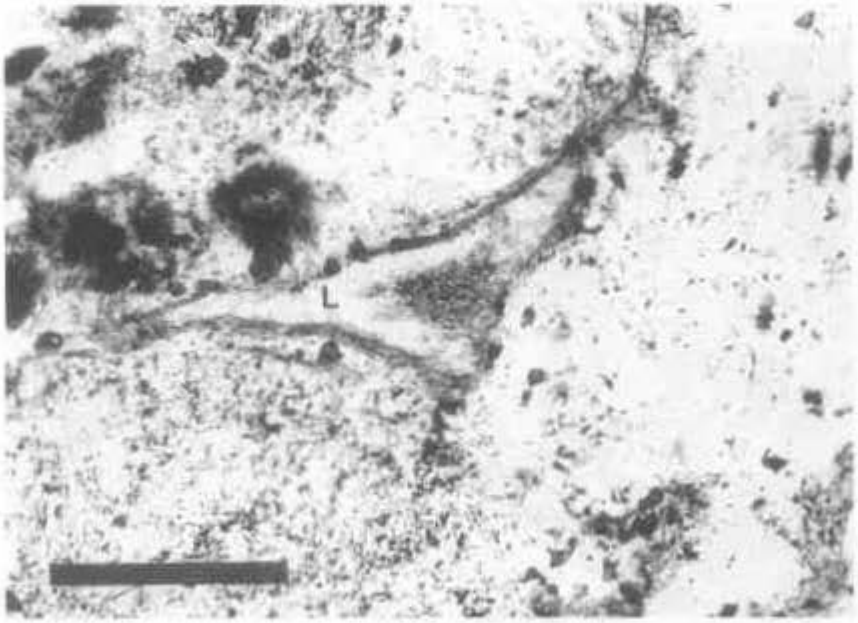

Figure 2.14 Photomicrograph of laumontite (L) cement that partially replaces fibrous smectite/corrensite rim cements. Earlier stage thin clay coat (dark line) that lines pore boundaries appears to be unaffected by the laumontite replacement, suggesting slight differences in chemical composition between the thin coats and the later stage more extensive fibrous, pore-filling clay rim cements. The later stage smectite/corrensite (sc) pore-filling cements are partially preserved in the center of pores. Baughman member, Sample RN-91-115, plane-polarized light, 10X, scale bar = 0.2 mm.

Figure 2.15 White, patchy laumontite (L) (low birefringence) replacing albite-twinned calcic plagioclase in Tyee Mountain turbidite sandstone. Sample RN-91-021, crossed nicols, 10X, scale bar = 0.2 mm.

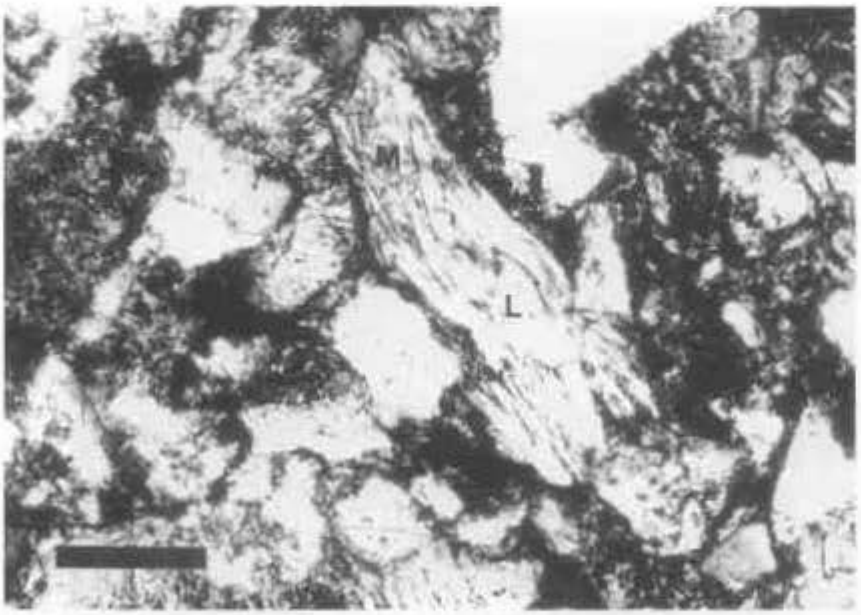

Figure 2.16 Muscovite (M) flake partially replaced by laumontite (L). Note the early, dark smectite/ corrensite clays that have extensively infilled intergranular pores and have clogged pore throats between angular framework grains of feldspar and volcanic rock fragments, and effectively destroyed most primary porosity. Tyee Mountain Member, Sample RN-90-184, crossed nicols, 10X, scale bar = 0.2 mm.

detrital framework grains. Laumontite and sericite are also found as displacive patches along the cleavages of detrital mica flakes in all the Tyee sandstones (Fig. 2.16).

Burns and Ethridge (1979) reported that zeolites are present as pore-fill cements in Umpqua sandstones of sequences I and II. However, our petrographic investigation indicates that, instead of zeolite cements, quartz cement and quartz overgrowths are pervasive in Umpqua sandstone units. Scanning electron microscope study using electron dispersive X-rays shows that these overgrowths and cements are exclusively composed of silicon with no Ca, Na, or Al cations such as found in zeolite cements higher in the section in sequences III and IV. This discrepancy may partially stem from a miscorrelation of lithostratigraphy in the basin. In spite of this discrepancy, the possibility of zeolite cement in the lower Umpqua sandstones could not be excluded because zeolite cement is usually formed by *in situ* rock-fluid reaction in sandstone containing abundant volcanic rock fragments. Some lower Umpqua sandstones (e.g., Bushnell Rock Formation) have a substantial amount of metavolcanic rock fragments. If this is the case, laumontite pore-filling cement may be locally developed in some sandstones by *in situ* reaction between volcanic rock fragments and pore fluids in the lower Umpqua sandstones.

(ii) Quartz: Quartz cement is common only in Umpqua sandstones of sequences I and II. It occurs as overgrowths that are usually separated from the detrital quartz host grains by very thin dust rims and/or early formed diagenetic clay coats. The overgrowths show optical discontinuity and a different extinction position from the host grains in crossed nicols. Many, however, lack any differentiation from the detrital grain and are solely recognized by the presence of euhedral hexagonal crystal faces projecting into the pore space (Fig. 2.17). In upper Umpqua sandstones of sequence II (e.g., Rasler Creek Tongue) where some primary and secondary porosity are preserved, minor euhedral individual quartz crystals occur in pores. Traces of early formed quartz overgrowths may be destroyed in some deeper-buried Umpqua sandstones of sequences I and II where effects of pressure solution are extensive.

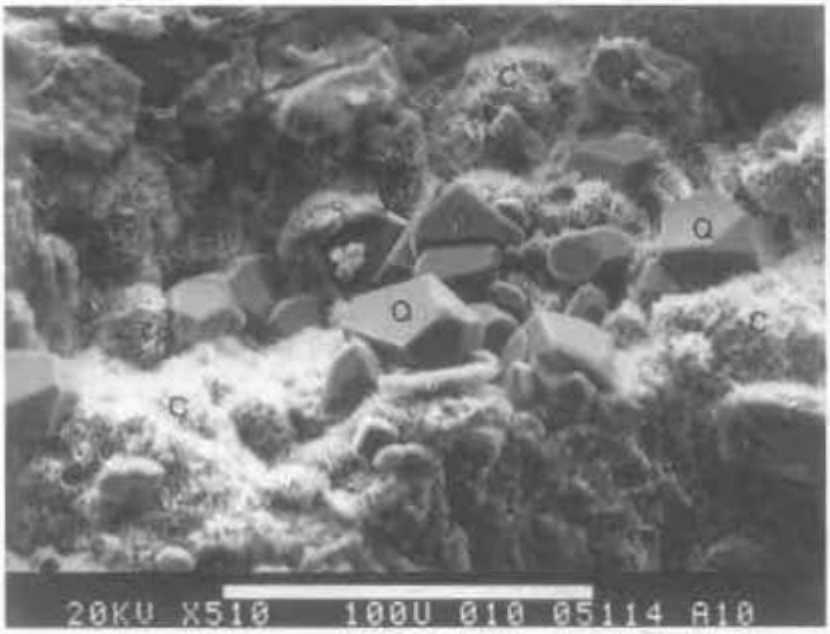

Figure 2.17 SEM photomicrograph of secondary quartz overgrowth (Q). Euhedral quartz crystals overgrow and project into pore spaces. Finer fibrous crystals of corrensite (C) also are present as pore-filling clay cements (fine, honeycomb-texture). Remote Member, Sample RN-90-267. Bar scale is 100 microns.

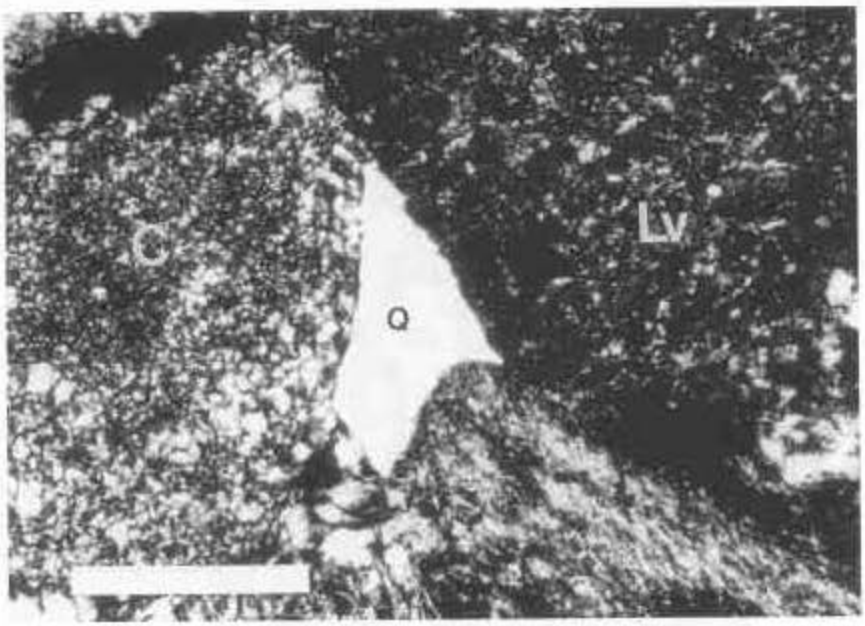

Figure 2.18 Single crystal of quartz (Q) cement completely infills and obliterates large primary intergranular pore between volcanic rock fragment (Lv) and chert (C) in sandstone of the Rasler Creek Tongue. Sample R-92-024, crossed nicols, 10X, scale bar = 0.2 mm.

Quartz cement is present as uniform single crystal pore-fillings and as multiple crystal pore-fillings (Figs. 2.18 and 2.19). Optically single crystal pore-fillings are much more common than polycrystalline quartz cement in the Umpqua sandstones of sequences I and II. Polycrystalline quartz cement is associated with earlier formed thin fibrous corrensite clay coats and has been observed only in fluvial sandstones of the Remote Member of sequence II and fan delta pebbly lithic sandstones and conglomerates of the Bushnell Rock Formation of Sequence I (Fig. 2.19). These clays may have originated during burial from infiltration of detrital clay minerals which subsequently recrystallized to early diagenetic fibrous clay radiating away from the clay rim boundary. On the other hand, monocrystalline quartz cement is present in pores that lack thin clay coats or rim cement and mainly occurs in more feldspathic delta front sandstones. In delta front environments, detrital clays are effectively winnowed out and rock fragments are abraded and destroyed by prolonged strong waves and tidal action (Fig. 2.18).

The form of quartz cement, whether monocrystalline or polycrystalline, may be a function of the permeability of the sandstones. In fluvial and fan delta sandstones, thin, early diagenetic, nearly opaque, well-developed clay coats and rim cements in pore throats greatly reduce primary permeability and effective porosity. Clay coats and rim cements could retard the continuous supply of silicon cations to large pore spaces by blocking the migration paths of pore fluids, thus, inhibiting formation of large, continuous phase single crystal pore-fillings. In the cleaner delta front sandstones, such as the Coquille River Member of sequence II, clay coats are absent or insignificant; and greater volumes of silica-saturated pore fluid could migrate freely through these sandstones. Under these conditions, a continuous supply of silicon cations would flow through pores, and large uniform single-crystal quartz pore-fillings could form (Fig. 2.18). Therefore, it is inferred that retardation of silica-bearing pore fluids may result in multiple-crystal quartz pore-fillings in sandstones that have low permeability and porosity. Alternatively, the minute spaces between fibers of the earlier formed corrensite clay rim may have provided abundant nucleation sites for growth of multiple-crystal quartz pore-fillings from a limited supply of silicon-saturated pore fluids.

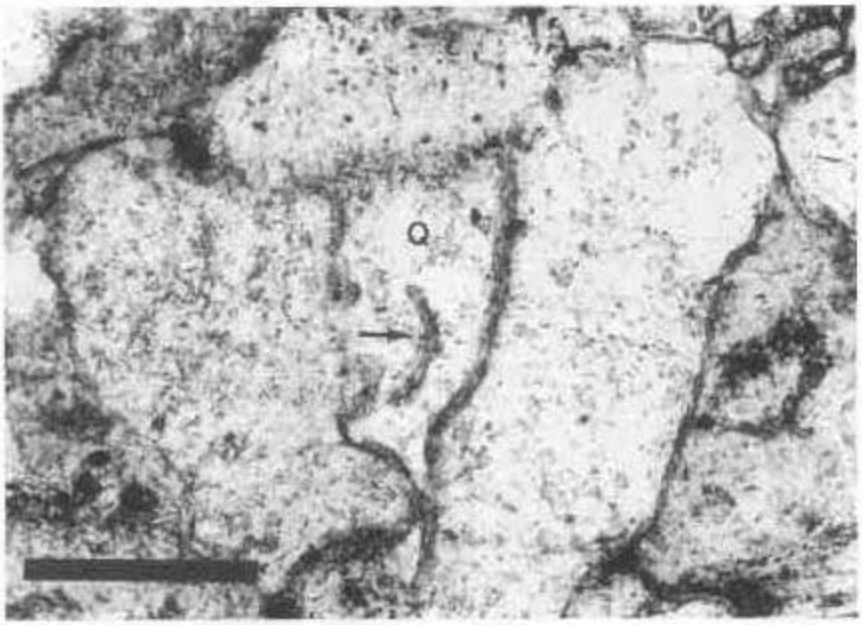

Figure 2.19 Multiple crystals of quartz (Q) grew inward from thin, fibrous, corrensite clay lining cement (dark line) and infilled center of intergranular pore in tightly cemented fluvial channel sandstone of Remote Member. Some earlier formed diagenetic corrensite clay coats became detached and were broken (arrow) during compaction and subsequently engulfed and cemented by the later stage pore-filling polycrystalline quartz cement. Remote Member. Sample R-89-002, plane-polarized light, 10X, scale bar = 0.2 mm.

(iii) Feldspar: Authigenic feldspar occurs as minor K-feldspar and plagioclase overgrowths in some intergranular pores. These authigenic minerals are present in Spencer and Bateman sandstones, but are rare. The overgrowths display a marked optical discontinuity with the host feldspar grain of the same composition and are up to 0.01 mm thick. Most feldspar overgrowths are not perceptible in thin section due to their thinness.

Formation of authigenic clays

Clay minerals (<2μm) identified in Tyee basin sandstones by X-ray diffraction (XRD) and scanning electron microscope (SEM) analysis are mainly smectite, corrensite (mixed-layer chlorite/smectite), and minor chlorite, serpentine, and mica (Fig. 2.21). The clay-sized micas and chlorite are largely detrital in origin (i. e., crushed metamorphic lithics and/or coarse flakes of mica) because they show sharp, tall peaks in XRD patterns (Fig. 2.21) (J. R. Glasmann, 1994, pers. commun.). Detrital muscovite, biotite, and chlorite are abundant as fine to coarse flakes in the Rasler Creek Tongue and younger sandstone units (e.g., Tyee Formation) of sequences III and IV. In older Umpqua sandstone units of sequences I and II, very fine detrital mica and chlorite are present in the abundant metamorphic and sedimentary rock fragments.

The smectite (S) and corrensite (mixed chlorite/smectite, C/S) appear to be largely authigenic, based upon their well-crystallized forms. These clay minerals form greenish to green-brown clay coats/rims and pore-filling cements (Figs. 2.20 and 2.21). In the Tyee Formation, for example, authigenic smectite/corrensite is present in three textural forms based upon thin section paragenetic relationships (Chan, 1985): (1) very thin, dark dust rims, possibly formed by infiltrated detrital clay during early burial (Fig. 2.13); (2) thicker rims of later stage, well-crystallized fibers of smectite/corrensite that are oriented perpendicular to the boundaries of framework grains (Fig. 2.13); and (3) late-stage randomly oriented, greenish brown crystals that infill the centers of larger intergranular pores (Fig. 2.14). These earlier diagenetic, authigenic clays are responsible for destroying much of the primary intergranular porosity and permeability, particularly in sequences III and IV.

Semi-quantitative analysis of X-ray diffraction patterns of 20 Tyee basin sandstones by Jeff Schatz and Jim McConkey (OSU undergraduate students) shows that the abundance of smectite decreases downsection while the abundance of mixed-layer smectite/chlorite (corrensite) increases downsection (Fig. 2.20). A similar downsection transition from authigenic smectite (S) to chlorite (C) or illite (I), involving an intermediate mixed-layer chlorite/smectite (C/S) or illite/smectite (I/S) phase, has been documented in many Tertiary sandstones along the Pacific Rim (e.g., Santa Ynez Mountains; Helmold and Van de Kamp, 1984).

Although the abundance of chlorite and illite also initially increases downsection from Spencer sandstones, it neither increases nor decreases systematically farther downsection. Thus, it is very difficult to assess whether or not all the clay-sized chlorite and illite in Tyee basin sandstones are detrital or in part authigenic. These clay minerals are obviously not related in a systematic way to burial depth, unlike the smectite and corrensite trends (Fig. 2.20). It is probable that clay-sized micas and chlorites in the sandstones are largely detrital in origin, but some may have formed as authigenic cement during diagenesis. Burns and Ethridge (1979), for example, reported some fibrous chlorite clay cement in Umpqua Group sandstone; we believe this is largely corrensite (mixed-layer smectite/chlorite) based on XRD.

In addition, a minor amount of serpentine is recognized from XRD analysis in some upper Umpqua Group sandstone (e.g., Remote and Coquille River members). Clay-sized serpentine is interpreted to be detrital in origin, eroded from serpentinite intrusions in the Mesozoic Klamath Mountains.

Third order peaks suggest that the diagenetic smectite cements are Fe-rich (i.e., nontronite). The nontronite formed largely by alteration of glassy volcanic rock fragments during early burial. In thin section, the groundmass of many mafic and intermediate volcanic rock fragments has been altered to greenish brown iron-rich

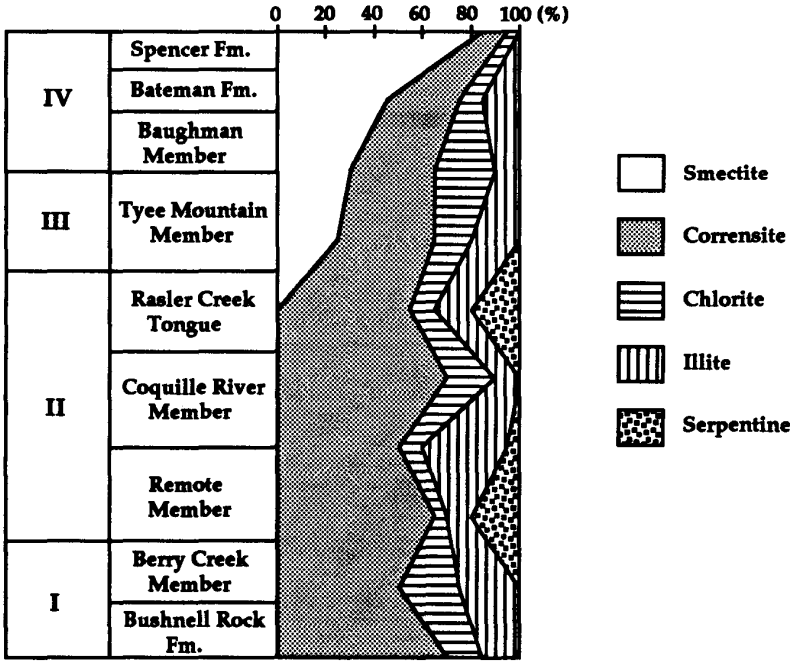

Figure 2.20 Relative abundance of authigenic and detrital clay minerals in twenty sandstones from Eocene Tyee basin. The relative abundance of clay minerals was determined using the methods of Reynolds (1980) and Hower (1981). A clay mineral transition from smectite to mixed-layer chlorite/smectite occurs with increasing depth.

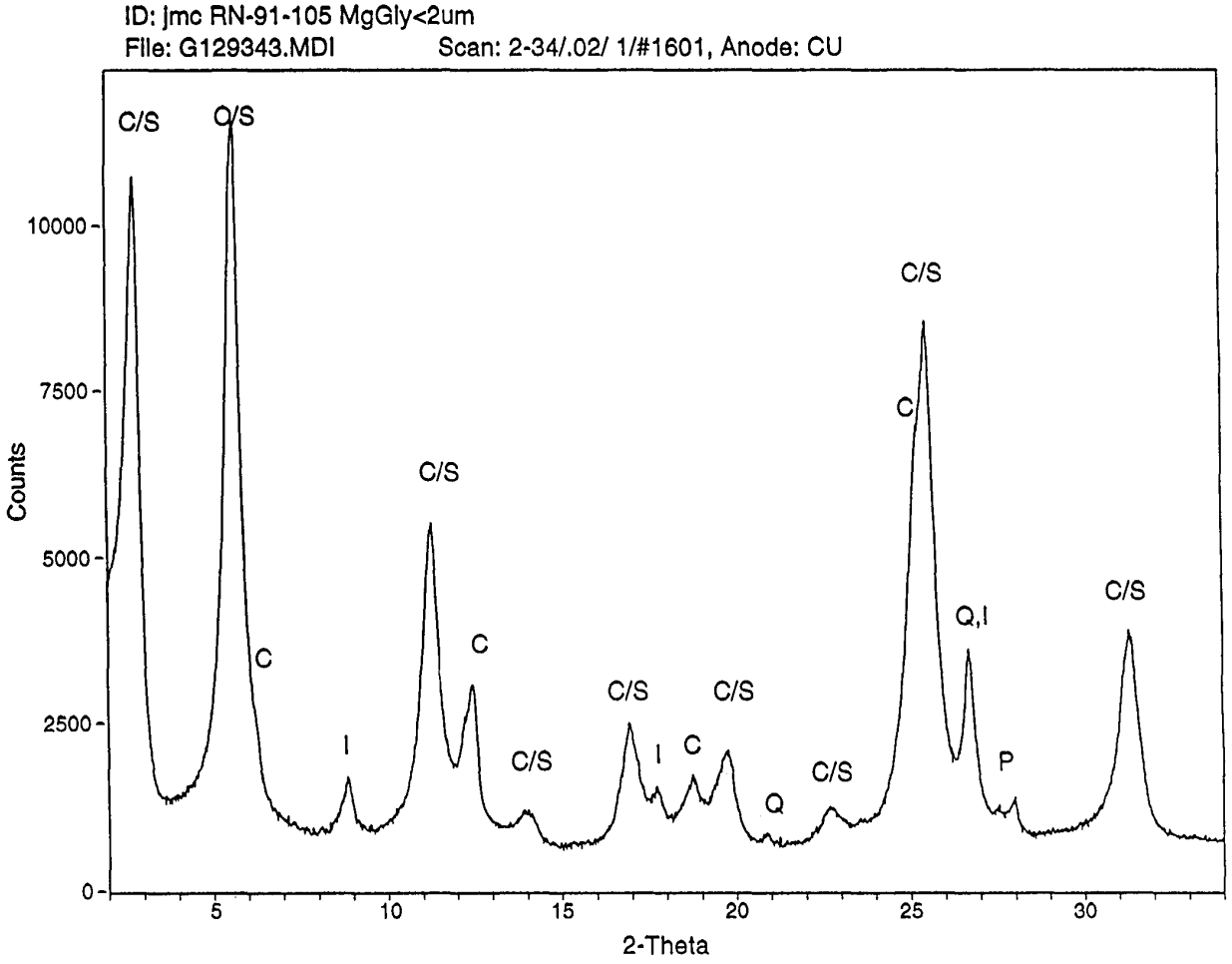

Figure 2.21 X-ray diffraction pattern of the White Tail Ridge sandstone. Mixed-layer chlorite-smectite (C/S) clays are abundant. Chlorite (C) and illite (I), which may be detrital, also are present. P is plagioclase and Q is quartz.

smectite which grades into iron-rich smectite pseudomatrix in the pores (Dickinson, 1970) (Fig. 2.16). This diagenetic pseudomatrix formed by compaction of soft, altered volcanic rock fragments and has obliterated much of the primary intergranular porosity of the sandstones. The squashed smectite flowed into and filled pore spaces, and is particularly evident in Tyee Mountain, Baughman, and Spencer sandstones. Iron-rich smectite (nontronite) clay rims and pore-filling cements occur mainly in the shallow-buried sandstone units (e.g., Spencer Formation and Rasler Creek Tongue).

Mixed-layer chlorite/smectite (corrensite) clays are most abundant in deeper-buried sandstone units as an authigenic cement (e.g., Rasler Creek Tongue and Bushnell Rock Formation). This downsection clay mineral change from authigenic smectite to corrensite may reflect a change in the composition of the parent grains. For example, from an abundance of intermediate and mafic volcanic rock fragments in the younger units of sequences III and IV to mainly metasedimentary (e.g., phyllite) and metavolcanic (e.g., greenstone) rock fragments in the older units. Furthermore, altered and partially dissolved pyroxenes and amphiboles in metavolcanic rock fragments and other metamorphic rock fragments may have supplied Fe and Mg ions for formation of mixed-layer corrensite.

Dissolution of framework grains and formation of secondary porosity

Secondary porosity is present as dissolved framework grains and cements or as tectonically formed fractures. Most Tyee basin sandstones are tightly cemented by smectite clays, quartz, and zeolites and contain little primary porosity in thin section (less than 2%) (Table 2.1). However, some sandstone units show evidence of partial dissolution of framework grains and earlier diagenetic cements that has created minor secondary porosity (Fig. 2.22).

Most secondary porosity occurs as enlarged intergranular or intragranular primary pores in sandstones of the lower Tyee Mountain Member, Rasler Creek Tongue, and Coquille River Member. In most cases, calcic plagioclase and volcanic framework grains have been partially dissolved. A minor amount of fracture porosity and channel porosity due to tectonic deformation and uplift is present in Bushnell Rock pebbly sandstones. Calculation of sandstone porosity from Formation Density and Compensated Neutron logs in the Sawyer Rapids well shows that an abrupt increase of porosity occurs in the subsurface in the lower part of the Tyee Mountain Member (Fig. 2.23). These data confirm that the secondary porosity in thin sections of sandstone from outcrops is not a product of surface weathering but is, instead, the result of partial dissolution of framework grains during diagenesis under deep burial.

Late-stage calcite replacement

Sparry calcite cement is volumetrically minor but is found locally as late-stage pore-filling cement and as a replacement product in concretions and calcareous sandstone beds (Fig 2.24). It is also randomly present throughout the stratigraphic section as isolated partial replacements of plagioclase grains, volcanic rock fragments, and other earlier formed cements. This calcite formed during a late-stage diagenetic event, as evidenced by its replacement of all earlier formed cements (e.g., quartz and zeolites) and alteration products of framework minerals. For example, late-stage calcite replacement of authigenic smectite and corrensite clay coats or clay rim is recognized by its relict rim-like form in thin section (Fig. 2.24).

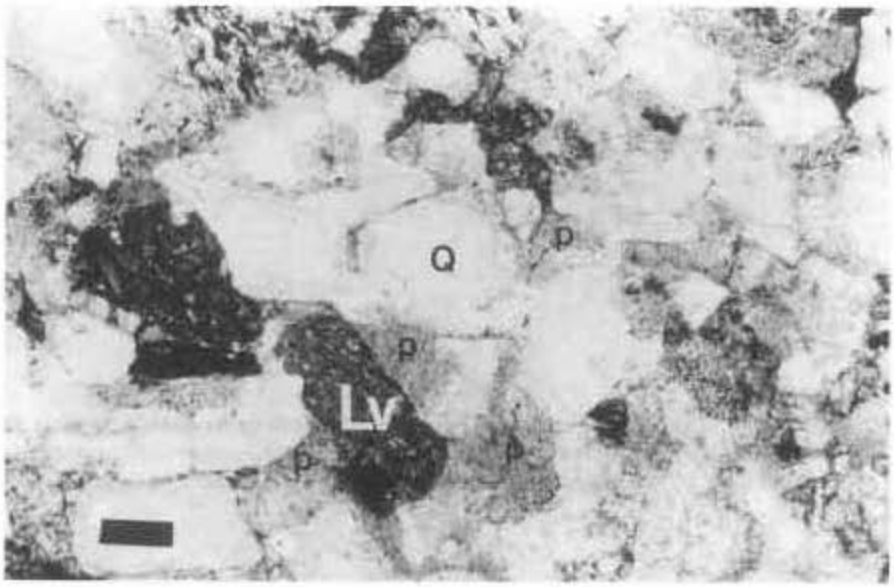

Figure 2.22 Abundant, secondary pores (P) in delta front lithic arkosic sandstone in the Rasler Creek Tongue. Note fine volcanic rock fragments (Lv). Sandstones in the Rasler Creek, Coquille River, and lower part of the Tyee Mountain members show the best development of secondary porosity. Sample R-92-024, plane-polarized light, 2.5X, scale bar = 0.2 mm.

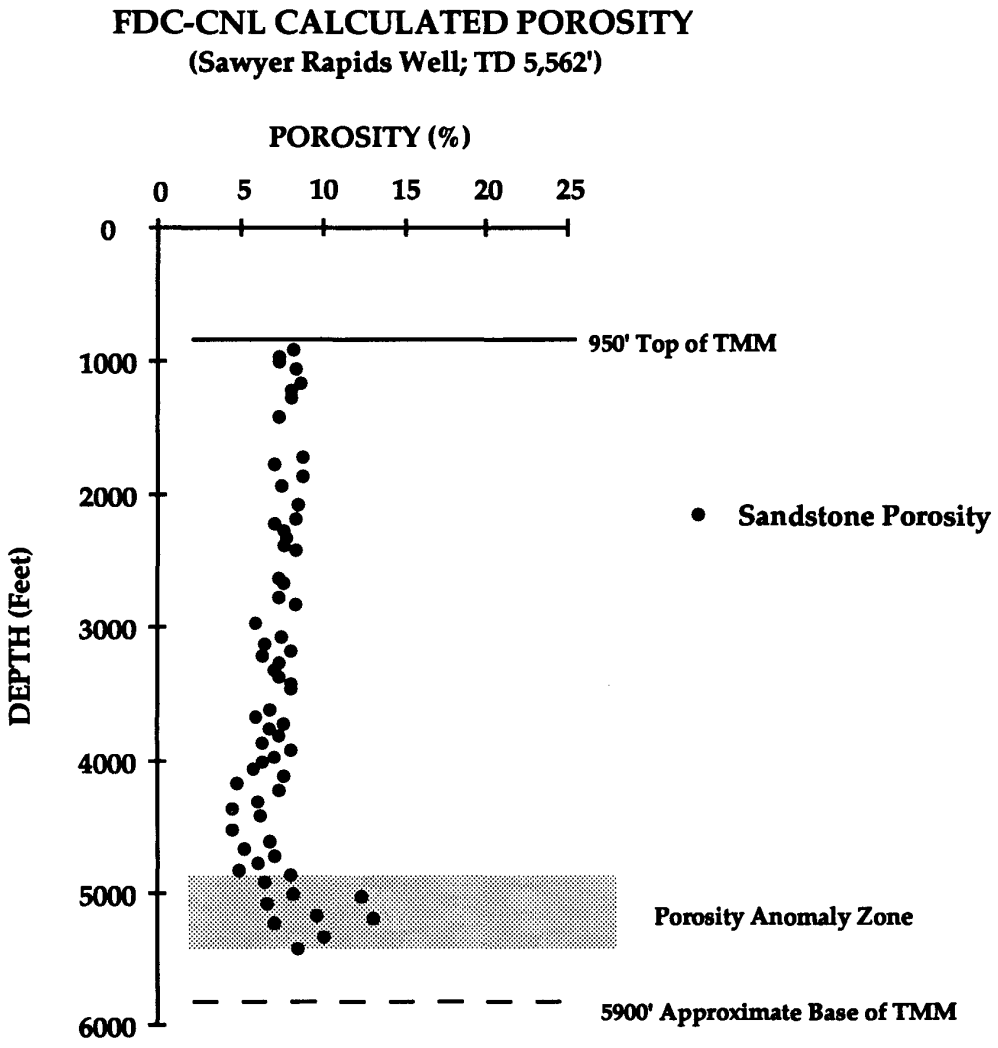

Figure 2.23 FDC-CNL calculated porosity from Sawyer Rapids well. Note the porosity anomaly zone in the lower part of the Tyee Mountain Member (TMM). The apparent increase of porosity in this anomaly zone may be due to development of secondary porosity during diagenesis.

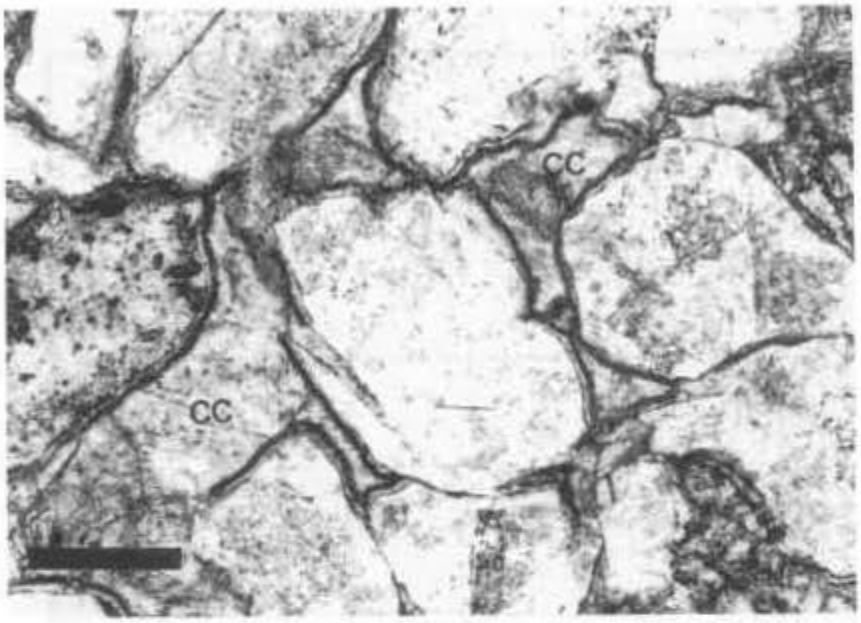

Figure 2.24 Late-stage calcite cement (CC) replaced early-formed iron-rich smectite clay rim cement (dark line) and completely filled intergranular pores. Spencer sandstone, Sample R-92-026, plane-polarized light, 6X, scale bar = 0.2 mm.

Other diagenetic effects

Detached clay coats (or broken clay coats) locally occur in fluvial pebbly lithic arkosic sandstones of the Remote Member and in fan delta lithic sandstones of the Bushnell Rock Formation. They are usually associated with polycrystalline quartz cement (Fig. 2.19). Corrensite clay coats may have become detached when migrating pore fluids forcibly pushed the clay coats along congested pore throats. The fluid force may have eventually ripped parts of the authigenic clay coats off framework grain boundaries. As a consequence, detached clay coats have been incorporated and surrounded by late-stage quartz cement. Similar detached clay coats have been documented in the Upper Cretaceous Tuscaloosa Sandstone of Louisiana (Pittman and others, 1992).

Another possible explanation for detached clay coats is that they may be developed by dehydration processes during diagenetic transformation of clay minerals (Moraes and de Ros, 1990). A change in clay composition from smectite to mixed-layer chlorite-smectite occurs with increasing depth in Tyee basin sandstones (Fig. 2.21). These reactions cause the release of water and produce shrinkage of the framework grains. As a result, clay coats become detached along some framework grain surfaces.

Iron-oxide cements (hematite and limonite) are also locally developed in fluvial sandstones of the Remote Member and the Bushnell Rock Formation. They are a product of oxidation during deposition and early burial and/or present weathering processes by oxidation of iron-bearing minerals by groundwater.

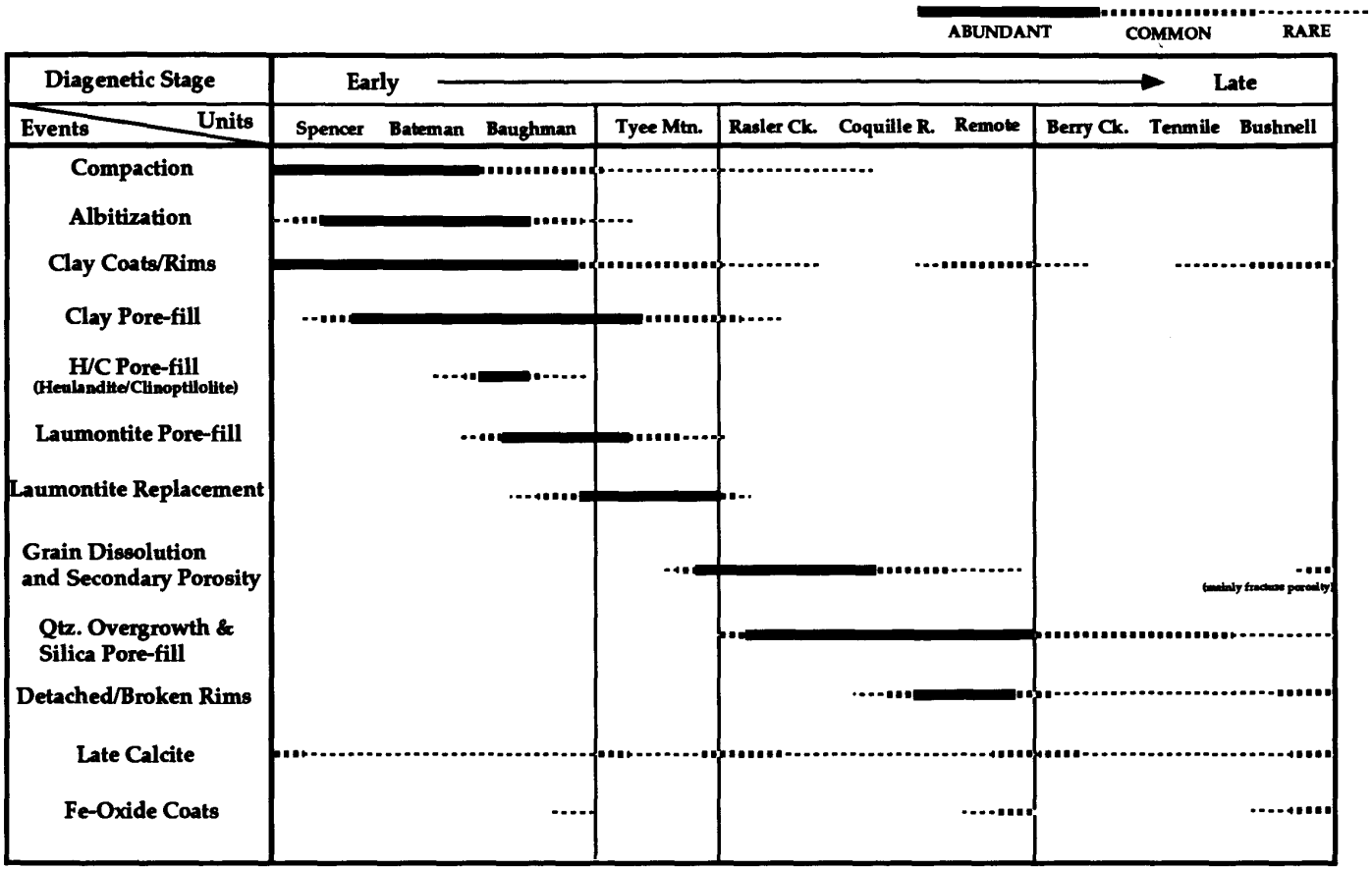

Figure 2.25 Paragenetic sequence of diagenetic events for Tyee basin units.

Paragenetic sequence

The textural relationships between authigenic minerals and cements in thin section and SEM photomicrographs and their stratigraphic distribution (Ryu and others, 1992) suggest the following paragenetic sequence (Fig. 2.25): (1) an early stage of mechanical compaction, (2) early clay coats and clay rim development, (3) an early smectite clay pore-fill which was altered to corrensite with deeper burial, (4) albitization and partial dissolution of plagioclase grains to form secondary porosity, (5) early heulandite/clinoptilolite pore-fill followed by laumontite pore-fill, (6) intermediate-stage laumontite replacement, (7) intermediate-stage dissolution of framework grains creating additional secondary porosity, (8) late-stage precipitation of quartz overgrowths, (9) detached broken clay rim cement, (10) late-stage calcite replacement of detrital grains and earlier formed clay, zeolites, and quartz cements, and (11) late-stage uplift, oxidation, and formation of minor iron-oxide cement by weathering (Fig. 2.25).

Sandstones from the Tyee, Elkton, Bateman, and Spencer formations were largely derived from volcanic arc and granitic batholith provenances. They contain abundant volcanic rock fragments, unidentifiable glassy detritus, and plagioclase (Table 2.1) that are chemically reactive with pore fluids during diagenesis and burial. Due to mechanical compaction, "soft" iron-rich smectite clay-altered ductile volcanic rock fragments were rotated and squeezed into pore spaces during early to moderately deep burial, forming pseudomatrix (Dickinson, 1970) (e.g., Tyee, Bateman, and Spencer formations). Unidentifiable former glassy volcanic fragments were subsequently altered entirely to "soft" ductile green smectite clay that was then remobilized and squashed to fill primary pore space during early compaction due to deeper burial. Some pore-filling heulandite/clinoptilolite cement, together with the smectite rim cement, formed from diagenetic alteration of glassy volcanic fragments in the sandstones of sequence IV. Also larger crystals of authigenic heulandite/clinoptilolite later infilled the center of some intergranular pores that were rimmed by the earlier formed fibrous smectite cement (Fig. 2.13).

During the early stage of diagenesis, highly alkaline pore fluids were enriched in Na^+, Al^{++}, Ca^{++}, and other metal cations derived from dewatering of interbedded smectite-rich mudstones. XRD analysis shows that mudstones of the Elkton Formation, Hubbard Creek Member, and Camas Valley Formation, for example, are largely composed of smectite and illite. Under these conditions a continuous supply of Na^+ would have been delivered to the sandstones by migrating pore fluids during early compaction of the muds, resulting in partial dissolution and albitization of calcic plagioclase grains (e.g., andesine and labradorite) which, in turn, supplied Ca^{++} ions necessary for formation of early heulandite/clinoptilolite and laumontite cements that infill the adjacent primary intergranular pores. Alternatively, pore-filling laumontite cement might have been formed directly from the earlier-formed heulandite with subsequent deeper burial by the following chemical reaction according to Noh and Boles (1993):

$$Ca_{3.75}Al_{7.5}Si_{28.5}O_{72}24H_2O + 3.35Ca^{++} + 6.7Al(OH)_4 = 7.1CaAl_2Si_4O_{12}4H_2O + 9H_2O$$

heulandite laumontite

Although incipient albitization is apparent in the younger sandstone units (e.g., Baughman Member) which contain early-stage laumontite cement, more extensive albitization occurred in the underlying sandstone units (e.g., Tyee Mountain Member) which contain mixed-layer chlorite/smectite (corrensite) clay instead of smectite clay. During deeper burial, this more active albitization may result in late-stage laumontite replacement of the plagioclase by the following chemical reaction according to Boles and Coombs (1977), Helmold and Van de Kamp (1984), and Noh and Boles (1993):

$$Na_{0.7}Ca_{0.3}Al_{1.3}Si_{2.7}O_8 + 0.6H_4SiO_4 = 0.7NaAlSi_3O_8 + 0.3CaAl_2Si_4O_{12}4H_2O$$

plagioclase albite laumontite

Clay mineral conversion of smectite clay to mixed-layer C/S clay probably produced the corrosive silicic acid (H_4SiO_4) necessary for the above reaction (Noh and Boles, 1993).

At greater burial depths, further dissolution of calcic plagioclase grains and volcanic rock fragments resulted in formation of minor secondary porosity (e.g., in the lower Tyee Mountain Member). Smectite clay rim cements and pseudomatrix were also mostly converted to mixed-layer chlorite/smectite (corrensite) clays at these depths (Fig. 2.21). Silicic acid (H_4SiO_4) pore fluid produced from these chemical reactions may be, in part, the source for the excess silicon cations that resulted in precipitation of late-stage polycrystalline and monocrystalline quartz cement which fills pore space in the underlying deeply buried Umpqua sandstones of sequences I and II.

Precipitation of quartz cement was also governed by the mineral composition of the sandstones. For example, concurrent albitization of plagioclase and production of laumontite and heulandite/clinoptilolite cements is commonly evident in the micaceous lithic arkosic Tyee Formation sandstones which contain abundant volcanic rock fragments and plagioclase grains. These processes may consume excess $H_4SiO_4^+$ in pore fluids which combines with Al^{++} and Ca^{++} cations to form zeolites released in the albitization process. Due to precipitation of laumontite, pore fluids were undersaturated in hydrosilicic acid H_4SiO_4, and quartz cement and quartz overgrowths could not be precipitated in the pores. However, albitization and precipitation of laumontite cement were absent or insignificant in the Umpqua sandstones which are more quartzose in composition. As a result, pore fluids were oversaturated in $H_4SiO_4^+$ and quartz cement was precipitated as euhedral hexagonal or trigonal crystals in pore space (Fig. 2.17). McBride and others (1987) showed that hexagonal or trigonal quartz crystals grew as overgrowths into large secondary pores during late-stage burial diagenesis in the deeply buried Jurassic Norphlet Formation of Mississippi. Bodine and Madsen (1987) also demonstrated that quartz cement and corrensite were produced during smectite clay transformation in the Paradox Member of the Hermosa Formation in Utah. This process is coincident with our SEM observations of abundant euhedral quartz crystals and underlying corrensite clays in the Umpqua sandstones (Fig. 2.17).

Another possible silica source for quartz cement includes pressure solution of the abundant detrital polycrystalline quartz grains of the lower Umpqua sandstones as a result of deep burial (Fig. 2.12). Dissolution of more soluble opal-A siliceous microorganisms (e.g., diatoms, radiolarians, and sponge spicules) in the interbedded marine mudstones by pore water could also be a source for silica which migrated into the overlying Umpqua sandstone units. Other local sources of silica for the quartz cement could be Cascades volcanic arc-related intrusions. Umpqua lithic sandstones are locally bleached white due to mercury sulfide (cinnabar) mineralization along the eastern boundary of the Umpqua basin and border with the Western Cascades arc (Wells and Waters, 1934). However, this mechanism does not explain abundant quartz overgrowths in the western part of the Umpqua basin.

Discussion of Controls on Authigenic Mineral Reaction and Cement Distribution

One of the most important factors controlling the abundance and types of authigenic minerals in Tyee basin sandstones is the composition of the dominant framework grains. Zeolites are restricted to sandstones of the younger forearc sequences (e.g., Tyee, Bateman, and Spencer formations) which contain abundant intermediate and mafic volcanic rock fragments and calcic plagioclase. The underlying Klamath Mountains-derived lithic sandstones of sequences I and II are composed of dominantly polycrystalline quartz, chert, sedimentary and metamorphic rock fragments, and authigenic minerals and pore-filling quartz cements. This compositional difference suggests that zeolites and quartz cements were not the result of the introduction of zeolite- or silica-precipitating solutions from outside the formations, but rather were the results of *in situ* rock-fluid reactions.

Eocene sandstones in the study area exhibit a vertical zonation of authigenic minerals and cements, consisting of early formed heulandite/clinoptilolite to laumontite, and finally to quartz as well as transformation of iron-rich smectite to mixed-layer smectite/chlorite (corrensite) with increasing burial depth. This vertical zonation of authigenic minerals probably resulted, in part, from variations in pore fluid composition in time and space. For example, Tyee Formation sandstone containing pore fluids undersaturated in $H_4SiO_4^+$ and enriched in Al^{++}, Ca^{++}, and Na^+, is characterized by albitization and zeolite cement, whereas Umpqua Group sandstone containing pore fluids oversaturated in $HSiO_4^+$ and lack of other competing metal cations is characterized by quartz cement and overgrowths and absence or insignificant albitization.

Because diagenetic reactions require a significant amount of transfer of cations and anions to and from reaction sites, permeability and porosity variations may be important in controlling the distribution of authigenic minerals in Tyee basin sandstones. Without adequate permeability and effective porosity, pore fluid flow is restricted, thereby decreasing mass transfer of cations and anions and, consequently, inhibiting reactions. The importance of permeability is suggested by textural control of quartz cements.

In addition, increasing temperature and depth of burial probably influenced the formation of authigenic minerals in Tyee basin sandstones. Vitrinite reflectance values for mudstone and coal samples from the surface and subsurface in the study area (average $\%R_0$ = 0.40-0.77) indicate that paleotemperatures ranged between 50°C and 115°C (see Source Rocks section). This implies that paleotemperatures for diagenesis of the sandstones were no greater than 115°C throughout the Eocene section. Based on the measured temperatures of deep wells in the Niigata oil field of Japan, Iijima (1978) suggested that heulandite and laumontite cements formed at about 100°C. Also, precipitation of late-stage quartz, where silica likely is released by clay transformation and pressure solution, requires a temperature range between 80°C and 120°C (Surdam and Crossey, 1987). Paleotemperatures in the Eocene section were also adequate for formation of authigenic smectite and corrensite clay minerals.

RESERVOIR POTENTIAL

Distribution of Porosity and Permeability

Prior to this investigation, data on porosity and permeability of potential reservoir sandstones in the southern Tyee basin were limited (Mobil, 1980; Newton, 1980; Niem and Niem, 1990). Outcrop samples were haphazardly distributed across the basin, and most samples were concentrated in a few potential reservoir units (e.g., Tyee Mountain Member, lower Umpqua Group, and pre-Tertiary sandstones; see map in Niem and Niem, 1990). In addition, there were far too few (27 analyses from 22 widely scattered localities) to make generalizations about the reservoir potential of all the stratigraphic units in the basin.

An additional seventy sandstone and conglomerate samples were collected for thin section and porosity and permeability analysis during the course of this investigation. Those samples are keyed to the measured sections of Ryu and others (1992; Fig. 2.1 and Plate 2A). Samples were chosen from the freshest exposures of each stratigraphic unit and were quantitatively analyzed for porosity and permeability by Goode Core Analysis Service of Bakersfield, California. They drilled plugs of the sandstone and conglomerate samples, using fresh water as the bit coolant. Prior to measurement of porosity and permeability in air, the samples were dried at 235°F. Grain volume was determined by Boyle's Law method using helium as the gaseous medium. Bulk volume was measured by mercury displacement at ambient conditions. A confining pressure of 500 psig was used for permeability measurements. Individual porosity and permeability analyses are listed in an appendix in Ryu (1995). The porosity and permeability are averaged by formation in Table 2.2.

Permeabilities are highest in sequence II (range 0.05 to 40.5 md, average 5.51 md for 24 samples). The next most permeable rocks are in sequence IV (range 0.2 to 12.3 md, average 2.67 md for 10 samples). Permeabilities of the other sequences are very low: sequence I (range 0.01 to 5.2 md, average 0.65 md for 22 samples); sequence III (range 0.01 to 3.1 md, average 0.53 md for 13 samples). One sample from an isolated outlier of "pre-Tertiary sandstone", mapped by Niem and Niem (1990) in the southwestern part of the Tyee basin, shows relatively high porosity (16.60%) and permeability (16.60 md).

Controls on Distribution of Porosity and Permeability

A bar graph is useful to show stratigraphic variations of average porosity and permeability among Tyee basin units (Fig. 3.1). Porosity generally increases a few percent from lowstand systems tract sandstone and pebbly conglomerates (LST) to highstand systems tract sandstones (HST) within a depositional sequence although there are exceptions (Fig. 3.1). As discussed in the sandstone petrography section above, a lowstand systems tract contains numerous gravity flow deposits (e.g., turbidites and debris flows) and fluvial channel-fills that are composed of poorly sorted, "dirty" graywacke sandstone and lithic conglomerate. These deposits are typically a mixture of diagenetically unstable rock and mineral fragments and abundant fine detrital clay/silt matrix. This texture is a result of rapid sedimentation and burial with little or no reworking by currents on a fan surface (e.g., in alluvial fan and in deep-sea fan environments). In contrast, highstand systems tract units in the Tyee basin contain abundant delta front sandstones that are generally more quartzose (i.e., chemically more stable) and better sorted. Softer, chemically unstable lithic framework grains (e.g., volcanics and carbonaceous phyllite) were effectively abraded and destroyed by prolonged reworking by waves, longshore currents, and tides during progradation of a wave-dominated delta. Also, fine detrital sediments, such as clay and silt, which could fill primary intergranular pores are winnowed out by these processes. Thus, the depositional or primary porosity of highstand systems tract delta front sandstones is generally greater than that of lowstand systems tract sandstones and conglomerates. The abundance of primary porosity is partly related to texture (grain size, shape, sorting, abundance of detrital clay matrix) which, in turn, reflects the depositional environment.

Primary porosity is also controlled by the compositional variation of the sandstones (e.g., lithic versus arkosic). Primary porosity in lithic turbidite sandstone and conglomerate of a lowstand systems tract is much more effectively destroyed than primary porosity in a quartzose-arkosic delta front sandstone of a highstand systems tract. Porosity is reduced because chemically unstable framework grains (e.g., volcanic rock fragments and soft metamorphic fragments) are more abundant in lithic sandstones. These grains are more susceptible to chemical alteration to pore-filling clay and zeolite cements and to greater mechanical compaction during burial or loading by tectonic events (e.g., thrusting).

Permeability in the sandstones is not only controlled by depositional processes and mineral composition, but also constrained by secondary diagenetic processes. In an ideal case in which the distribution of porosity and permeability is solely controlled by depositional processes (i.e., controlled by grain size and sorting), the highest porosity is most likely to be accompanied by the highest permeability. If this is the case, the cross-plot of porosity versus permeability shows a very good one-to-one correlation (R = 1). However, sandstone porosity is reduced or enhanced (i.e., secondary porosity; Schmidt and MacDonald, 1979) due to diagenetic processes such as mechanical compaction and dissolution of unstable framework grains during deeper burial. This may result in deterioration of the ideal one-to-one correlation between porosity and permeability. It may be inferred, therefore, that the correlation coefficient (R) between porosity and permeability decreases as sandstones undergo progressively more diagenetic modification.

Best fit lines on cross-plots of porosity versus permeability of each depositional sequence reveal that there is a fairly good correlation (R = 0.74) in the shallower buried depositional sequence IV. In contrast, the more deeply buried and diagenetically altered sequences I, II, and III have relatively low correlation coefficients (R = 0.18 to 0.30) (Fig. 3.2). This implies that the distribution of porosity and permeability in sequence IV still reflects the depositional processes that controlled grain size and sorting

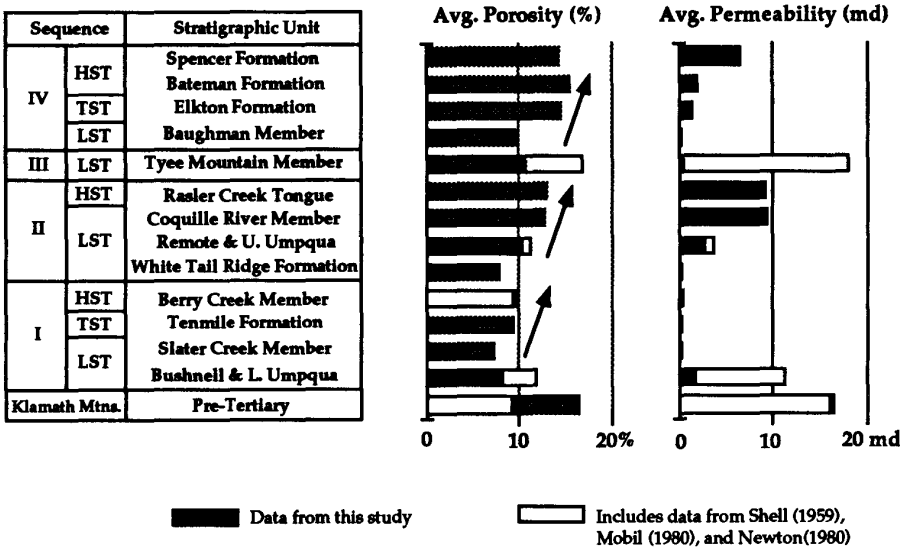

Figure 3.1 Average porosity and permeability of Tyee basin units; (LST=Lowstand Systems Tract, TST= Transgressive Systems Tract, HST=Highstand Systems Tract). Arrows indicate increasing porosity in each systems tract. Data from Newton (1980) for the Tyee Mountain Member (unshaded bar) are anomalously high compared to porosity and permeability data acquired during this study. The disparity of values may be a function of differences in techniques between laboratories.

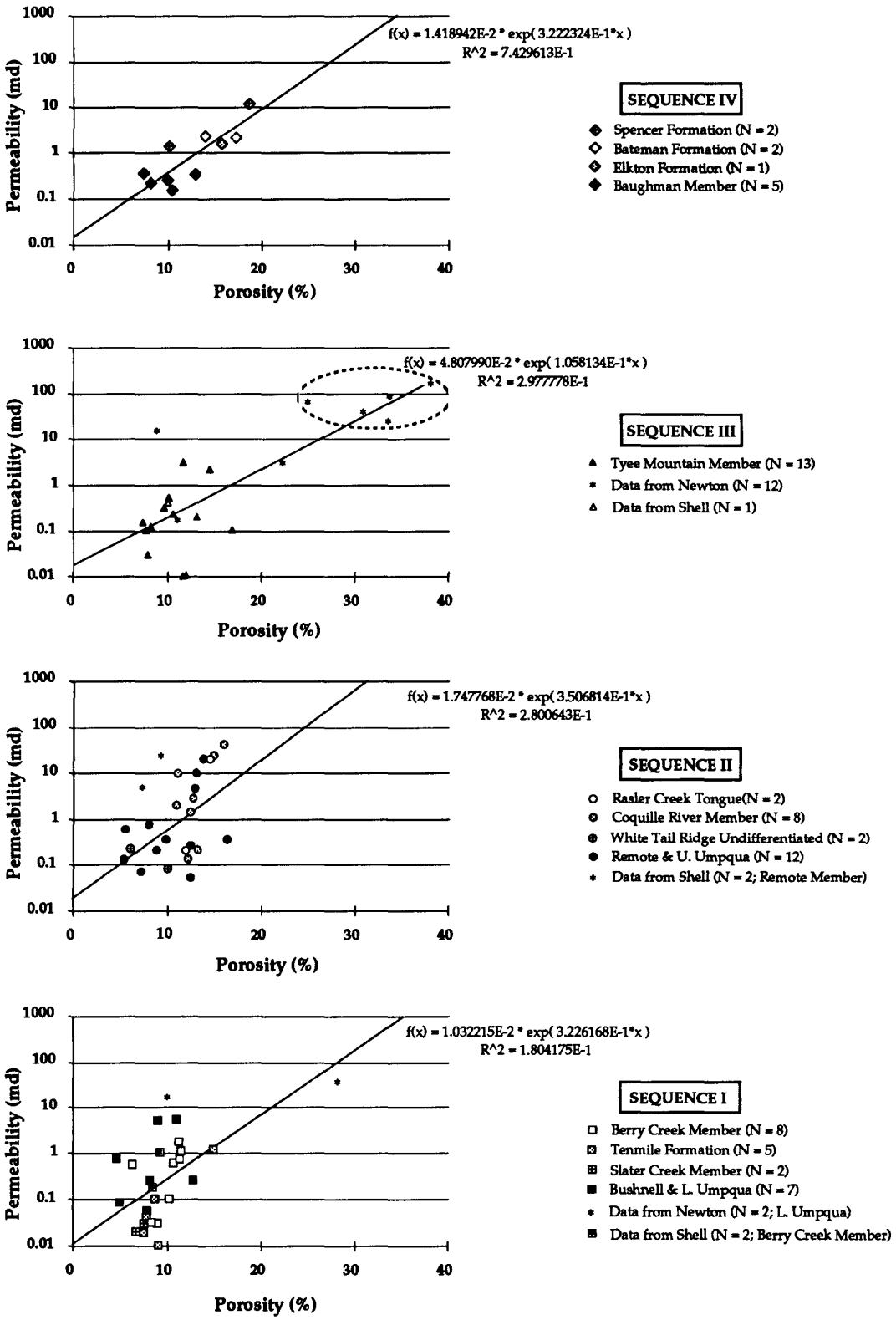

Figure 3.2 Cross-plots of porosity versus permeability for Eocene sandstones of the Tyee basin. Solid lines and correlation index (R^2) values are computer-generated "best fit" of data. Anomalous data points within a circle represent the Tyee Mountain Member sandstones from the northwestern part of the study area.

and that diagenetic processes (i.e., compaction and cementation) have not significantly modified the primary porosity. The lower correlation coefficients in sequences I, II, and III, however, suggest that the relationship of porosity and permeability in these sequences which is non-linear and is more likely a result of diagenetic processes of mechanical compaction and cementation than depositional processes (Fig. 3.2).

Petrographic analysis confirms that mechanical compaction and cementation played a dominant role in controlling the distribution and abundance of porosity and permeability in sandstones of the southern Tyee basin. Major reduction of porosity and permeability has occurred through: (1) mechanical compaction of ductile grains, such as micas and phyllites (particularly in the older and more deeply buried Umpqua Group units); (2) chemical alteration and mechanical compaction of volcanic grains to form pseudomatrix (e.g., Tyee Mountain Member of the Tyee Formation); (3) precipitation of smectite/chlorite clay rim cements in primary interparticle pores and pore throats (e.g., Baughman Member of Tyee Formation); (4) filling of the remaining pore space with zeolites (e.g., Baughman Member of Tyee Formation; or (5) precipitation of early calcite cements. The porosity and permeability of some units has been non-linearly enhanced by: (1) partial dissolution of plagioclase grains and chemically unstable framework grains (e.g., Tyee Mountain Member of Tyee Formation); (2) dissolution of pre-existing pore-filling cements (e.g., White Tail Ridge Formation); or (3) development of microfractures due to tectonic movement (e.g., Bushnell Rock Formation). In addition, some secondary and remaining primary porosity and permeability are further reduced by precipitation of late-stage quartz and calcite cements (e.g., Umpqua Group units).

Potential Reservoir Units and Their Areal Distribution

Compared to the gas-producing deltaic Cowlitz Formation of the Mist Gas Field in northwestern Oregon (average porosity 25% and average permeability 200 md; Armentrout and Suek, 1985), most units in the southern Tyee basin have low to very low porosity and permeability (Table 2.2). Tyee basin sandstones could be called tight sandstones based on the definition of tight sandstones by Law and Spencer (1993). Tight sandstones, such as these, could potentially produce commercial quantities of gas from deeper parts of the basin (Law and others, 1994).

In examination of outcrop samples, the stratigraphic units with the highest reservoir potential in the Tyee basin are members of the White Tail Ridge Formation; i.e., the more permeable and friable delta front sandstones of the Coquille River Member (average porosity 12.90%; permeability 9.59 md for 8 samples) and the Rasler Creek Tongue (average porosity 13.20%; permeability 9.35 md for 2 samples) (Fig. 3.1). Some fluvial distributary channel lithic arkosic sandstones of the Remote Member (13.0% of porosity and 9.6 md of permeability) and delta front sandstones of the Berry Creek Member may be additional, deeper reservoir targets.

The 1,000- to 4,300-foot thick deltaic White Tail Ridge Formation occurs only in the southern part of the basin (i.e., Myrtle Point-Sutherlin subbasin of Ryu and others, 1992) and is well-exposed along Oregon Highway 42 between the towns of Tenmile and Remote (Figs. 3.3 and 3.4; Plates 2B and 2C). The best permeabilities in the unit are in the vicinity of and north of Remote on the west side of the basin. However, some members wedge out over the Reston high (Ryu and others, 1992). Therefore, these units have limited potential as exploration targets in the subsurface near this buried high. They are also locally developed north of the high near Lookingglass Valley (several miles northeast of the Reston high and south of Melrose) (Figs. 3.3 and 3.4; Plates 2B and 2C). A thick section of White Tail Ridge Formation is exposed in the Glide area. These units project beneath the Tyee escarpment and beneath the western Cascade Mountains. They have been recently traced as far north as Tyee Mountain, west of Sutherlin (R. E. Wells, 1994, pers. commun.).

Sandstones of the Coquille River Member were deposited as a tide-dominated, delta-front facies. The tide-dominated facies consists of several thinning-upward parasequences of thick to very thick beds of massive to hummocky cross-bedded, arkosic (quartzo-feldspathic) sandstone (Ryu and others, 1992). The parasequences thin upward to subordinate mollusk-bearing lagoonal or estuarine mudstone, bioturbated mollusk-bearing silty sandstone, and numerous

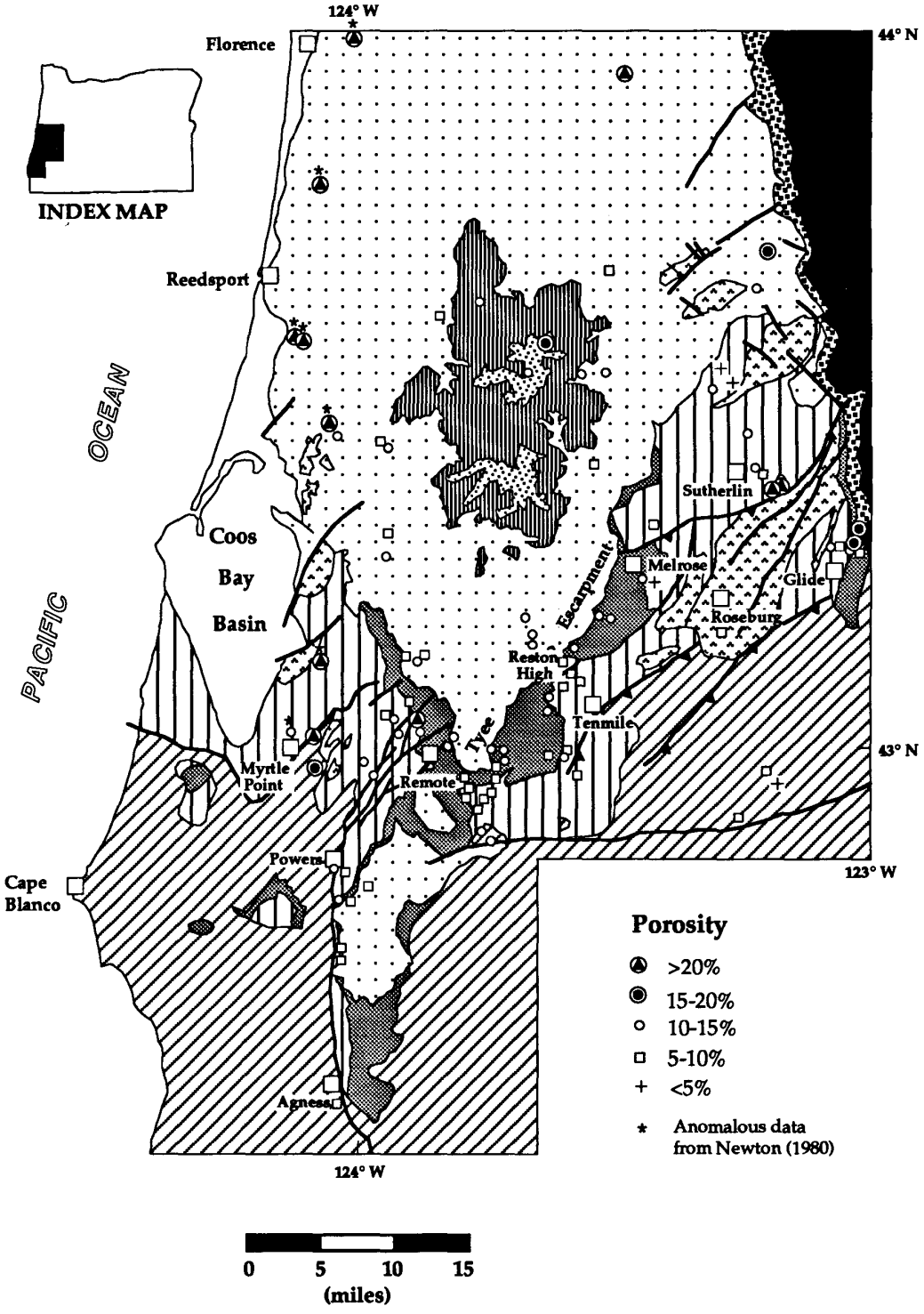

Figure 3.3 Porosity distribution map of Eocene Tyee basin.

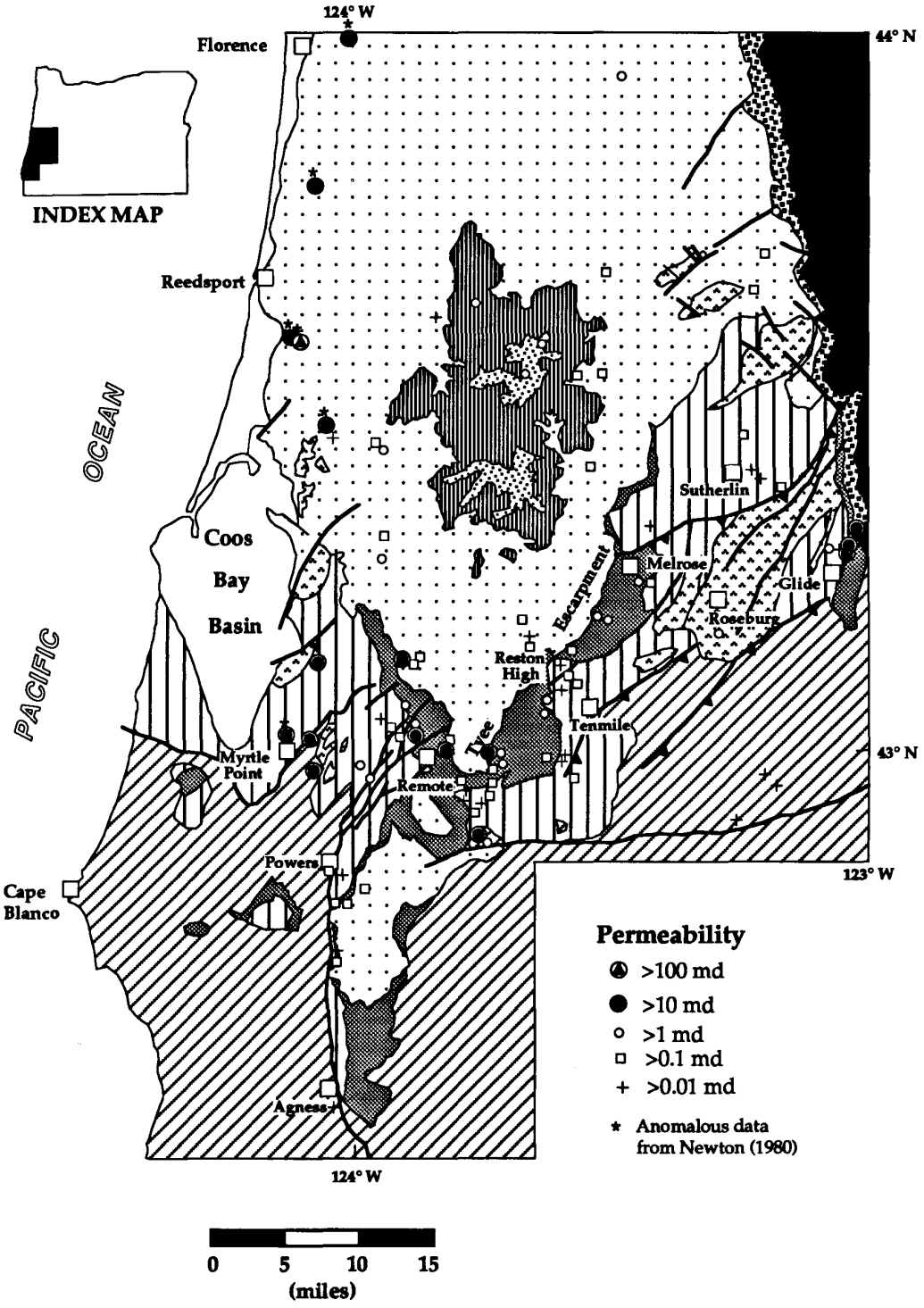

Figure 3.4 Permeability distribution map of Eocene Tyee basin.

Figure 3.5 Exposure of tide-dominated delta front and delta plain sandstone with estuarine coal beds (arrows) of Coquille River Member along Oregon Highway 42 (column number 9 in fence diagram) west of Camas Valley. Coal bed is overlain by distributary mouth bar sandstone. 3-foot traffic poles for scale.

Figure 3.6 Exposure of wave-dominated delta front Rasler Creek Tongue sandstone near Rasler Creek (column number 6 in fence diagram). Ten- to thirty-foot thick thickening-upward parasequences that are encased in thick bioturbated mudstone are well-developed. Geologist for scale.

subbituminous coals (Fig. 3.5). Potential reservoir sandstones in this facies are medium- to coarse-grained, moderately sorted, and thick- to very thick-bedded (5 to 6 feet thick). They were probably deposited in distributary channels. The distributary channel sandstones pinch out laterally and cut into the underlying coal beds.

Sandstones of the Rasler Creek Tongue were deposited as a wave-dominated delta front facies which prograded over the middle to outer shelf muds of the Camas Valley Formation (Ryu and others, 1992). They consist of several 10- to 30-foot thick thickening-upward parasequences which are encased in thick bioturbated mudstone beds. Each thickening-upward parasequence is composed of medium to thick beds of hummocky bedded to trough and planar cross-bedded, lithic arkosic sandstone and thin to very thin beds of wave-ripple laminated siltstone (Fig. 3.6). Potential reservoir sandstones in this facies are medium- to coarse-grained, moderately sorted, and thick-bedded (1 to 2 feet thick) shoreface sandstones. Petrographic analysis indicates that secondary porosity (enlarged interparticle pores) is common in these potential reservoir sandstones (Fig. 2.22).

The Remote and Berry Creek members are possible deeper reservoir targets. Coarse-grained fluvial distributary quartzo-lithic (metamorphic) sandstones in these members are tightly cemented by silica and clay in outcrop in the vicinity of the Tyee escarpment. However, along the Umpqua River near Glide, they are fairly friable and less indurated (Figs. 3.3 and 3.4; Plates 2B and 2C). The porosity and permeability of distributary sandstones in the Remote Member near Glide are 13.7% and 18.5 md which is better than the porosity and permeability of outcrop samples near the Tyee escarpment (Figs. 3.3 and 3.4; Plates 2B and 2C).

Near Glide, potential reservoirs in the Berry Creek Member form a 600-foot thick section of thickening-upward fine- to medium-grained delta front parasequences overlain by medium- to very coarse-grained, cross-bedded, pebbly distributary channel sandstones capped by a thick coal of the Remote Member. These sandstone-dominated units, together with the overlying deltaic to fluvial arkosic Spencer sandstone, dip gently eastward beneath the volcanic rocks of the western Cascade Mountains. The White Tail Ridge sandstones also have been recently traced northward to Nonpareil (Wells, 1994, pers. commun.). South of Glide toward the margin of the Klamath Mountains, fluvial conglomerate (bearing boulders and cobbles of granodiorite) and coarse-grained arkosic sandstone equivalent to the White Tail Ridge Formation are locally intercalated between younger Cascade volcanic rocks and pyroclastic flows and an underlying pre-Tertiary granodiorite (A. Jayko, 1994, pers. commun.).

Another potential reservoir unit is the 1,100-foot thick upper Eocene Spencer Formation (average porosity 14.45%; permeability 6.70 md for 2 samples) (Fig. 3.1). The Spencer Formation is composed of several hundred feet of friable, fluvial to deltaic, medium- to very thick-bedded, highly carbonaceous sandstone (Ryu and others, 1992) (Figs. 3.7 and 3.8). There also are a few thin (one to several foot thick) subbituminous coal beds and thicker, laminated carbonaceous siltstone beds in the unit. Some shallow-marine sandstone beds (which are bioturbated and fossiliferous) have been recognized (Hoover, 1963). The Spencer is probably equivalent to the deltaic, coal-bearing Bateman Formation in the center of the Tyee forearc basin. The Bateman also contains highly friable, porous and permeable arkosic micaceous sandstone (Weatherby, 1991) (Figs. 3.3 and 3.4; Plates 2B and 2C). The possible reservoir in the Spencer is a friable, micaceous, well-laminated to cross-bedded, and fine- to very coarse-grained distributary channel sandstone. This "clean" arkosic micaceous sandstone is exposed locally along the eastern margin of the basin adjacent to the Cascade volcanics from Glide northward to Cottage Grove (Figs. 3.3 and 3.4; Plates 2B and 2C) (Walker and MacLeod, 1991). The sandstone generally dips gently eastward beneath the Cascade volcanics except where locally faulted. Spencer sandstones have abundant primary interparticle porosity which is partially filled with smectite pore-lining clay. Many samples from exposures are too friable for porosity and permeability measurements.

Micaceous arkosic Spencer sandstone has been a target of exploration in the Willamette Valley, locally producing commercial quantities of gas (e.g., near Lebanon, OR) (Baker, 1988). It is equivalent to the middle and upper Eocene Cowlitz Formation (Clark and Wilson sandstone) which produces commercial quantities of gas at Mist in the northern Oregon Coast Range

Figure 3.7 Two thick to very thick beds of Spencer sandstone with interbed of carbonaceous overbank mudstone northeast of Glide. The lower sandstone bed is fine-grained, highly carbonaceous, micaceous and well-laminated.

(Newton, 1979; Alger, 1985). This coarse-grained delta plain-fluvial unit in the southern Tyee basin appears to be a previously unrecognized facies that prograded northwestward and southwestward. The provenance probably was an unidentified Idaho batholith source east of the Cascade Mountains. It may be equivalent to the Eocene Payne Cliffs Formation described by McKnight (1971) in the Medford-Ashland area. How far these sandstones extend beneath the Western Cascades is unknown.

An unnamed pre-Tertiary(?) unit that crops out near Myrtle Point (T29S, R12W) also has relatively high porosity (16.0% for 1 sample) and permeability (16.0 md for 1 sample) (Figs. 3.3 and 3.4; Plates 2B and 2C). The unit is a friable arkosic micaceous cross-bedded pebbly sandstone possibly deposited during the Late Cretaceous or Paleocene (Figs. 3.3 and 3.4; Plates 2B and 2C). Mobil (1980) also reported sandstones and conglomerates with possible reservoir potential (average porosity 15.5%; permeability 23.13 md for 3 samples) near Myrtle Point and southeast of Remote (T31S, R9W) in a large faulted inlier of the Cretaceous-Jurassic Myrtle Group of the adjacent northern Klamath Mountains (Figs. 3.3 and 3.4; Plates 2B and 2C). Most Myrtle Group sandstones and conglomerates, however, appear to be tightly cemented in outcrop. Another potential reservoir within the northern margin of the Klamath Mountains is a "clean", arkosic biotite- and muscovite-bearing pebbly, trough cross-bedded sandstone that occurs either unconformably on top of or within the Dothan Formation (as at Hoover Hill; Peterson, 1957). The reservoir potential of these units is low because they crop out discontinuously, and most appear to be tightly cemented by zeolites (A. Jayko, 1994, pers. commun.).

Most sandstones and conglomerates in the lower Umpqua Group and Bushnell Rock Formation are too well-indurated and tightly cemented in outcrop to be reservoirs (Figs. 3.3 and 3.4; Plates 2B and 2C). However, Newton (1980) reported relatively high porosity (average 19.15% for 2 samples) and permeability (average 24 md for 2 samples) for lower Umpqua turbidite sandstones near Myrtle Point (Figs. 3.3 and 3.4; Plates 2B and 2C). The difference between the porosity and permeability values reported in this study and the high values reported by Newton (1980) (Figs. 3.3 and 3.4; Plates 2B and 2C) may

be a result of variations in technique used by different laboratories.

Some of the high values of porosity and permeability in the lower Umpqua Group and Bushnell Rock Formation may be due to fracture porosity. Petrographic descriptions (see previous section) indicate that there is some fracture porosity in the sandstones of these units. In other structurally deformed convergent margin basins (e.g., Eocene and Cretaceous Great Valley basin and Tertiary Los Angeles basin of California), commercial quantities of gas are produced from fracture porosity in tightly cemented lithic graywackes and quartzo-feldspathic sandstones. Fracture porosity can be produced by tectonism, particularly on thrust-related structures (such as in crests of fault-propagation folds). Such structures are present within the southern part of the basin (e.g., Bonanza fault zone). Seismic-reflection profiles also show that such structures occur beneath the Tyee forearc basin sequence (Peter Hales, Weyerhaeuser, 1989, pers. commun.). Several oil shows, for example, have been reported in unpublished descriptions of cores of fractured Bushnell Rock conglomerate and Umpqua turbidite sandstone from the Scott well drilled in the Bonanza fault zone (Niem and Niem, 1990; see Source Rocks section). Where the Bonanza fault zone crosses the Umpqua River, lower Umpqua sandstones are isoclinally folded and backthrust-faulted. The rocks are intensively jointed and fractured, and traces of thermogenic gas have been measured in these fractures during atmospheric lows (Bill Seeley, Mobil Oil Corp., 1989, pers. commun.).

Mobil geologists found light-colored, more friable sandstones in the Umpqua Group southeast of Sutherlin which they interpreted as a cleaner deltaic facies of the Umpqua submarine fan (Seeley, 1989, pers. commun.) (Fig. 3.3). They reported porosities of 22 to 28% in these sandstones which were a target of Mobil's Sutherlin Unit No. 1 well. This investigation, however, interprets those sandstones as the mid to upper fan facies of a submarine fan which appear to have been hydrothermally altered and bleached white. Unfortunately, most Umpqua turbidite sandstone beds in the Mobil Sutherlin and Union Liles wells were tight.

Thick- to very thick-bedded turbidite sandstones of the Tyee Mountain Member (Tyee Formation) are well-indurated and have

Figure 3.8 Close-up of the upper sandstone bed in Figure 3.7, showing a fluvial or distributary channel that cuts into underlying overbank mudstone and dark coal bed.

relatively low reservoir potential (average porosity 10.88%; permeability 0.53 md for 13 samples). However, Newton (1980) reported that some Tyee turbidite sandstones in the northern part of the study area have very high porosity (average 30.68% for 6 samples) and permeability (average 59.80 md for 6 samples) (Figs. 3.3 and 3.4; Plates 2B and 2C). These anomalous values may result from either formation of secondary porosity or extensive surface weathering. Alternatively, the disparity is due to laboratory variability because the lithology of Tyee sandstones varies little throughout the basin.

Porosities estimated from FDC-CNL logs for the Sawyer Rapids well are not high and are on the magnitude of measured porosities of surface samples in this investigation. This subsurface porosity information also indicates that there is a zone of higher porosity in the lower part of the Tyee Mountain Member in the well (Fig. 2.23). The Long Bell, B-1, F-1, and Harris 1-4 wells, which penetrated thick sections of the Tyee Mountain Member in the northern and central part of the study area, encountered generally tight, well-indurated sandstone with only minor gas shows (Ryu and others, 1992). Our petrographic study of a few samples indicates development of diagenetic secondary porosity in the lower part of the Tyee Mountain Member (i.e., basin-floor fan facies; see Ryu and others, 1992). Thus, the lower part of the Tyee Mountain Member may warrant further investigation. Most porosity and permeability analyses of Tyee Mountain sandstones in this study were concentrated in the southern and central part of the study area (Figs. 3.3 and 3.4; Plates 2B and 2C). Newton's (1980) data hint that the unit may be more porous in the northwestern part of the study area. The reservoir potential of this unit could not be eliminated because of the possibility that secondary porosity has developed locally.

In summary, the units with the highest reservoir potential are sandstones of the White Tail Ridge Formation, especially the Coquille River Member and the Rasler Creek Tongue and to a lesser extent the Remote and Berry Creek members. Spencer Formation sandstones appear to be the second best potential reservoir sandstone in the basin. In addition, some of the pre-Tertiary sandstones and the lower Umpqua sandstones (or the Bushnell Rock Formation) may serve as possible reservoir rock in the basin, if fracture porosity is well-developed (e.g., beneath the Tyee escarpment). However, the distribution of the pre-Tertiary sandstones is very discontinuous and may be difficult to explore. Also, the lower part of the Tyee Mountain Member may have reservoir potential in the deeper northern part of the basin, provided that secondary porosity is developed. Sandstones of other units (e.g., Slater Creek, Baughman, Elkton, and Bateman sandstones) have very limited reservoir potential due to the lack of effective permeability (Figs. 3.1 and 3.4). The low permeability is mainly attributed to extensive burial diagenesis which has clogged pores and pore throats through mechanical compaction and pore water chemical reactions in the sandstones. The friable, clean, micaceous arkosic sandstones of the Bateman delta plain, distributary, and delta front facies are an attractive reservoir. However, this unit has been breached by erosion and is restricted to the synclinal center of the Tyee forearc basin. The Baughman Member also has been largely exposed by erosion, and Baughman sandstones are too tightly cemented by zeolites and smectitic clays to have much reservoir potential other than fracture porosity.

Some Tyee basin sandstones (e.g., Tyee Mountain Member, lower Umpqua Group) could be called tight gas-reservoirs. Law and Spencer (1993) defined tight gas-sandstones as sandstones that have low permeability (<0.1 md) (exclusive of fracture permeability) and low porosity (2 to 12%). Tight gas sandstones and shales have produced large quantities of natural gas from Paleozoic sandstones in the Appalachians and the Black Warrior basin, from Mesozoic sandstones in several Rocky Mountain foreland basins and the Great Plains of Colorado, Nebraska, Kansas, and North and South Dakota, and from Tertiary strata of east Texas and northern Louisiana. Some wells in the Tyee basin (e.g., Long Bell) appear to be overpressured (see source rock section). Fracturing and horizontal drilling may be necessary to produce gas from the tight Tyee basin sandstones (Law and Spencer, 1993).

SOURCE ROCKS

Sample Distribution and Lithologies

More than 190 samples were collected and submitted for source rock analysis during the course of this investigation. They include all Eocene units in the Tyee basin and several pre-Tertiary units in the adjacent Klamath Mountains (Fig. 4.1). Most well cuttings and outcrop samples are fresh dark to medium gray mudstone, coal and carbonaceous mudstone; several are carbonaceous deltaic and turbidite sandstone and one is from a block of micritic limestone in the pre-Tertiary (Cretaceous) mélange. Source rock analyses include total organic carbon (TOC), Rock-Eval pyrolysis, and some vitrinite reflectance (% R_o) and thermal alteration index (TAI) measurements as well as visual kerogen typing. These analyses were performed by Paul Lillis, Ted Daws, and Mark Pawlewicz of the U. S. Geological Survey organic geochemistry laboratory in Denver, Colorado (Lillis and others, 1995) and by the DGSI in Woodlands, Texas, for samples provided to Dave Long for a Portland State University master's thesis (Long, 1994). In addition, source rock data for more than 1625 outcrop and well samples from earlier reports (e.g., Amoco (1983, 1985), Browning and Flanagan (1980), Brown and Ruth (1983), Law and others (1984), Mobil (1980), and Newton (1980)) are also incorporated in this study (Figs. 4.1 and 4.2; see distribution maps in Niem and Niem, 1990). The analytical methods applied to these samples are described in these references. These data also include TOC, Rock-Eval pyrolysis, vitrinite reflectance, thermal alteration index, visual kerogen analyses, and some C_{15}^+ extraction with chromatography. Most of the 193 samples collected for this study are keyed to the measured stratigraphic sections and the exploration wells described by Ryu and others (1992) (Plate 3A).

Source Rock Evaluation

Source rock generative potential

Most of the 1869 surface and subsurface samples contain low to very low total organic carbon (Fig. 4.3A). The average TOC value is approximately 0.85 weight percent. The overall distribution of TOC of Tyee basin units is skewed towards lower values (< 0.5 weight percent) with approximately 95 percent of all samples falling into the poor to fair (non-source to marginal) source rock category (i.e., < 1.0 weight percent TOC). Most of the non-source or marginal source samples are shallow-marine mudstone, mudstone interbeds between turbidite sandstone and conglomerate beds, and some overbank mudstone in fluvial and fan delta facies (Fig. 4.4).

Only 59 samples (< 4% of samples analyzed) have TOC values > 1.0 weight percent, which rate these as good to very good source rocks (Fig. 4.3A). Most of these samples are estuarine carbonaceous mudstone, very fine-grained carbonaceous sandstone, and silty coal from deltaic sequences in sequences II and IV (White Tail Ridge Formation, Baughman Member, Bateman Formation, and Spencer Formation; 21 samples), some slope mudstone from the transgressive deep-marine intervals of sequences II, III, and IV (Camas Valley Formation, Hubbard Creek Member, and Elkton Formation; 13 samples), and a few deep basinal mudstones from turbidite sequences in sequence I (the Umpqua Group; 13 samples) (Figs. 4.4 and 4.5; Plate 3B). Some pre-Tertiary Klamath Mountain terrane samples also have > 1.0 weight percent TOC (carbonaceous shale in Cretaceous Whitsett Limestone; 1 sample: undifferentiated Myrtle Group mudstone; 5 samples) (Figs. 4.4 and 4.5).

The S_1 and S_2 yields liberated during pyrolysis are a useful measurement to evaluate the generative potential of source rocks (Peters, 1986; Law and others, 1984). Approximately 95 percent of the samples analyzed have < 1.0 mg HC/g rock (Fig. 4.3B). Pyrolysis $S_1 + S_2$ yields < 6.0 mg HC/g rock are generally considered to be source rocks with poor to fair generative potential; yields > 6.0 are common in known hydrocarbon source rocks (Peters, 1986). Thus, Rock-Eval pyrolysis $S_1 + S_2$ yields also indicate that most Tyee basin samples analyzed are poor in generative potential, including some basinal and slope mudstone units that rated as good and very good source rock based on TOC (i.e., 2 to 3%;

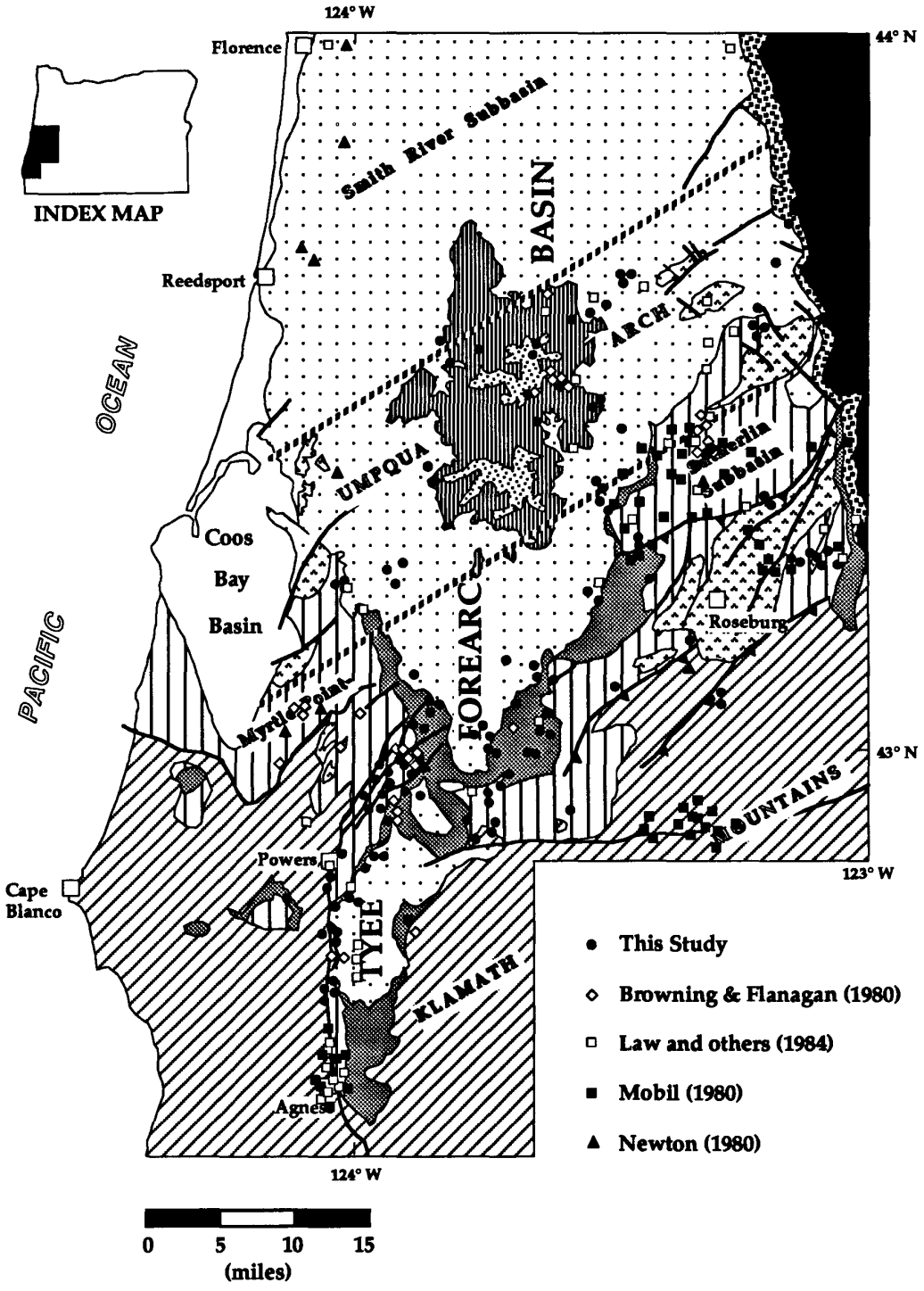

Figure 4.1 Distribution of mudstone, carbonaceous mudstone, and coal samples for source rock analyses from Eocene Tyee basin. Solid circles represent the locations of 193 samples analyzed for this study. Source rock sample locations from earlier investigations are plotted on the map using different symbols.

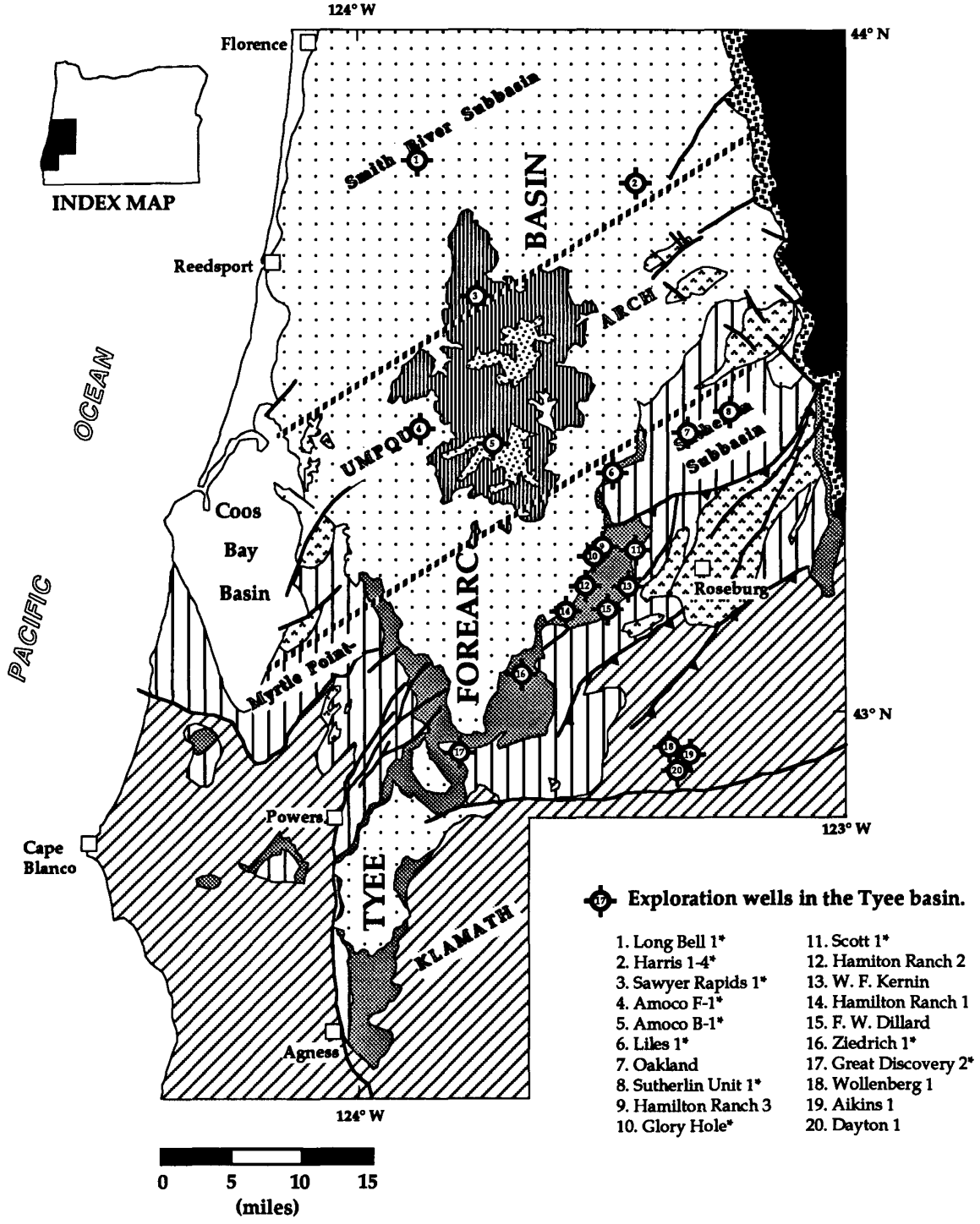

Figure 4.2 Location map of exploration wells in the Tyee basin. Wells marked with an asterisk were analyzed for source rock potential and maturity.

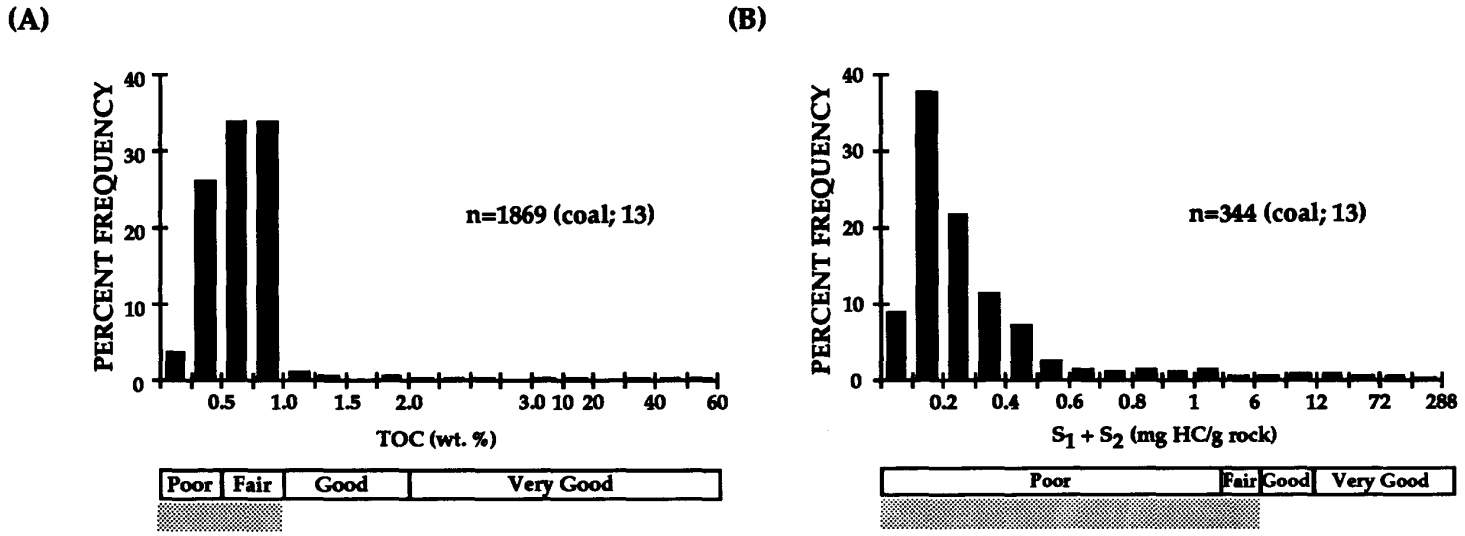

Figure 4.3 (A) Summary of distribution of Total Organic Carbon (TOC) for all Tyee basin samples(B) Pyrolysis $S_1 + S_2$ yields. Approximately 95% of samples fall in the poor to fair categories (Peters, 1986). Stippled area represents 95% distribution of samples.

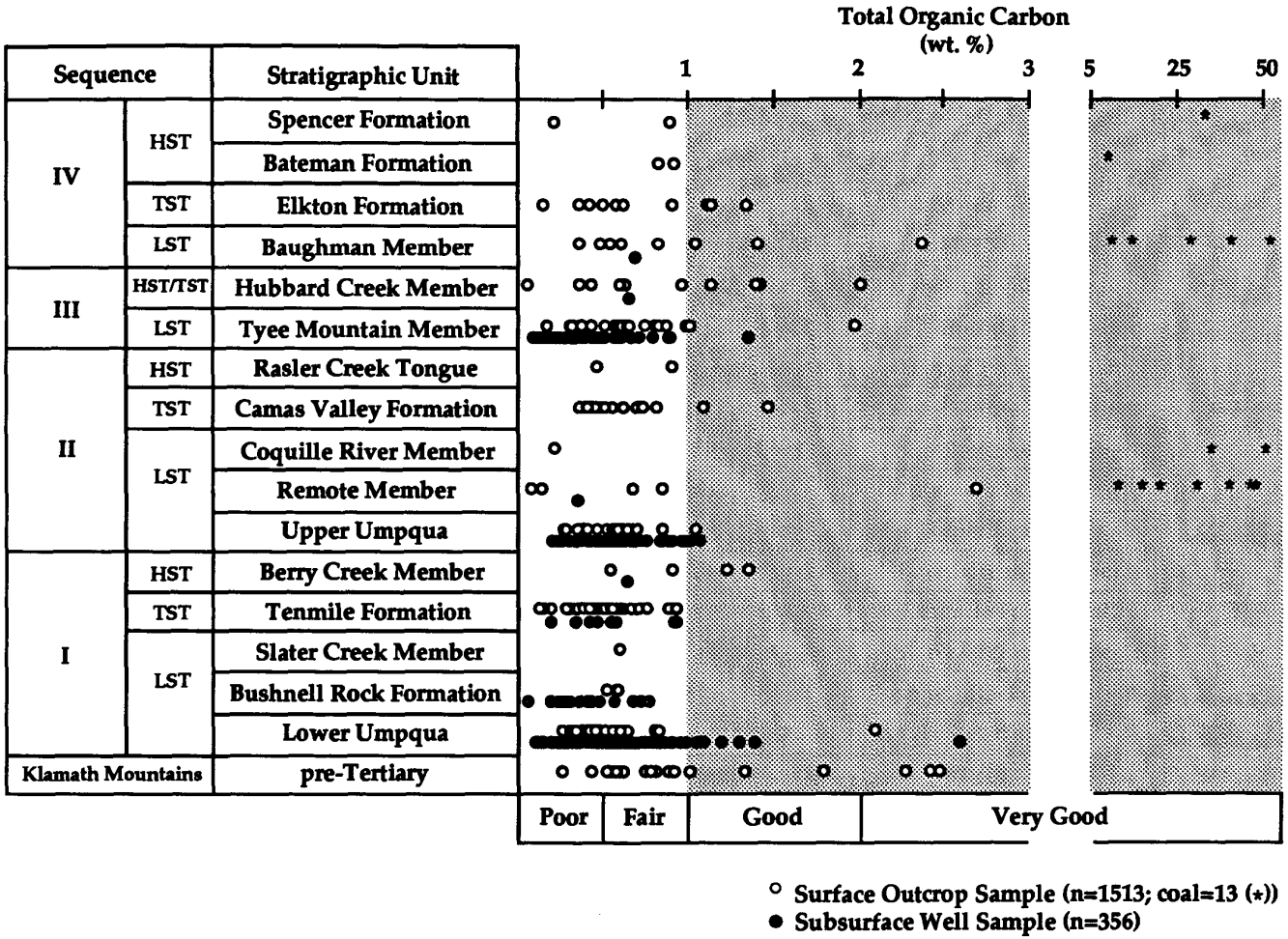

Figure 4.4 TOC values as a function of stratigraphic unit. Coals and carbonaceous mudstones (*) of deltaic sequences commonly rate as good to very good potential source rock in the Tyee basin. Some deep basinal mudstone sequences of the Umpqua Group include good to very good potential source rock. Pre-Tertiary organic-rich source rocks (>1% TOC) are from the Cretaceous Whitsett Limestone and Cretaceous/Jurassic Myrtle Group.

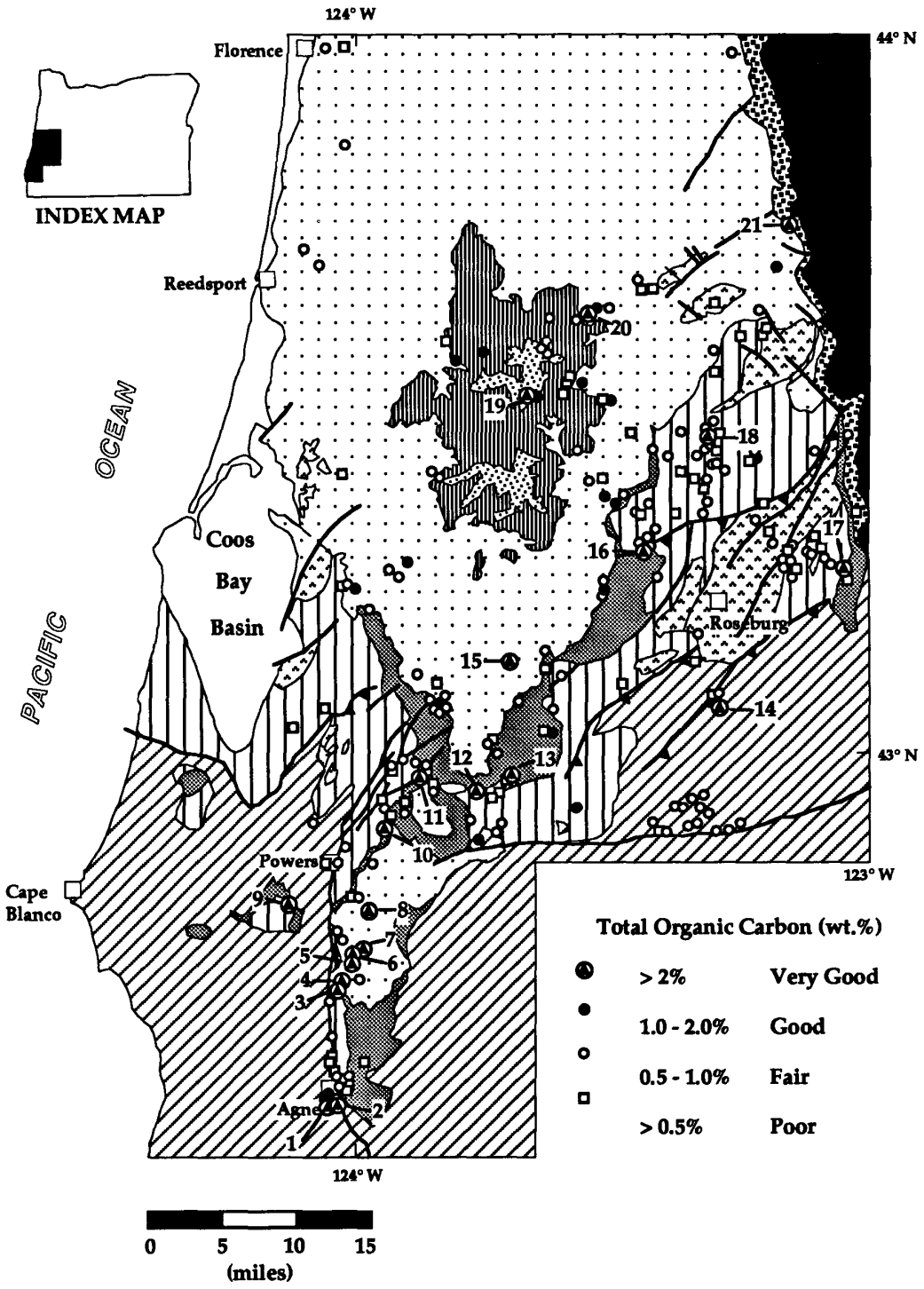

Figure 4.5 Total Organic Carbon (TOC) distribution map of Eocene Tyee basin. Most samples have < 1.0 weight percent TOC (poor to fair; Peters, 1986). Only 59 samples rate as good to very good source rock (Peters, 1986). These samples are carbonaceous mudstones and coals from deltaic units in Sequences II and IV (e.g., White Tail Ridge Formation, Baughman Member, and Bateman and Spencer formations). Some pre-Tertiary Klamath Mountains samples also have > 1.0 weight percent TOC. The samples with the highest TOC (numbered) are listed in Table 4.2.

compare Figs. 4.4 and 4.6). Although high in total organic carbon, much of this carbon is inert and does not yield much free hydrocarbon upon pyrolysis (or heating). Therefore, those samples are rated as poor source rocks.

Tyee basin samples that have the highest potential as source rocks, as indicated by $S_1 + S_2$ values > 6.0 (shaded area of Fig. 4.6), are all coals. These data reaffirm the importance of coals as potential source rocks in the Tyee basin first recognized by Niem and Niem (1990) and Law and others (1984). Coal beds and carbonaceous mudstones are widespread in deltaic sequences of the White Tail Ridge Formation and Baughman Member in the southern part of the basin, in the Bateman Formation in the center of the basin, and in the Spencer Formation on the eastern margin of the basin (Ryu and others, 1992; Figs. 4.1 and 4.5). They range from a few inches thick to as much as 13 feet thick, and some underlie tens of square miles (e.g., Eden Ridge coal field; Lesher, 1914; Duell, 1957; US Bureau of Land Management, 1983; Niem and Niem, 1990). Coal in the Eden Ridge field, for example, contains over 50% TOC and sufficient volatile organic matter (23 to 58%) to generate dry and/or biogenic gas (Niem and Niem, 1990). Two seams have a calculated total reserve of as much as 50 million tons (Duell, 1957; US Bureau of Land Management, 1983).

The coals and carbonaceous mudstones in the White Tail Ridge Formation (Coquille River and Remote members) are a locus of biogenic and thermogenic gas seeps in the basin (Niem and Niem, 1990; Kvenvolden and others, 1995). However, these rocks comprise only a small percentage (1 to <5%) of the total volume of strata in the basin and, thus, are limited sources. Additional beds of thin coal, carbonaceous mudstone, and overbank mudstone and sandstone were discovered recently in the Spencer Formation between the towns of Nonpareil and Glide (R. E. Wells, 1994, pers. commun.; Figs 3.7, 3.8, 4.1, and 4.5). In northwestern Oregon, coals and slope mudstone in the upper Eocene deltaic Cowlitz Formation in the Willamette (Nehalem) basin may be the source of the gas produced commercially in the Mist gas field (Armentrout and Suek, 1985; Stormberg, 1992).

Type of hydrocarbon generated

A binary plot of whole rock hydrogen indices (S_2/TOC) and oxygen indices (S_3/TOC) can be used to classify the dominant type of organic matter (i.e., gas- or oil-prone) in potential source rocks (Tissot and Welte, 1978; Fig. 4.7). Most of 320 surface and subsurface samples plot in the field of very low hydrogen indices and low oxygen indices. This suggests that the organic matter in nearly all Tyee basin samples is Type IV (very limited or marginal potential for gas) or Type III (gas-prone) organic matter. Fifteen samples, however, plot in the field between Type II (oil-prone) and Type III (gas-prone) organic matter. These samples include: Bateman Formation, 1 sample; Baughman Member, 2 samples; Hubbard Creek Member, 1 sample; Tyee Mountain Member, 1 sample; Coquille River Member, 3 samples; Remote Member, 4 samples; Slater Creek Member, 1 sample; Bushnell Rock Formation, 1 sample; Whitsett Limestone; 1 sample. Most samples that contain a mixture of oil- and gas-prone organic matter are coals from the deltaic facies (e.g., White Tail Ridge, Remote, and Baughman). The van Krevelen diagram may overestimate the oil and liquid hydrocarbon generative potential of the Tyee basin coals. Coals are generally composed mainly of gas-prone Type III organic matter. According to Peters (1986), concentrated Type III organic matter in coals (with HI values <300 mgHC/g rock and with S_2/S_3 ratio >5) does not respond during Rock-Eval pyrolysis in the same manner as dispersed Type III organic matter (e.g., as in the mudstones). Coals typically plot between Type II and Type III organic matter area of the van Krevelen diagram.

Rock-Eval pyrolysis studies indicate, however, that high oxygen index with low hydrogen index and low TOC (<0.5%) in argillaceous or mud-rich samples is directly influenced by a variety of variables such as CO_2 released from carbonate minerals in the matrix or absorption of oxygen by clay minerals (Peters, 1986). Outcrop samples are likely to show higher S_3 and lower S_1 and S_2 values due to oxidation during weathering, resulting in high values for oxygen index (Durand and Monin, 1980). This is not the case for Tyee basin outcrop samples which have the same distribution of HI and OI as the well samples. Most well samples (e.g., Umpqua Group in Mobil's Sutherlin well, Tyee Mountain Member and Umpqua Group in the

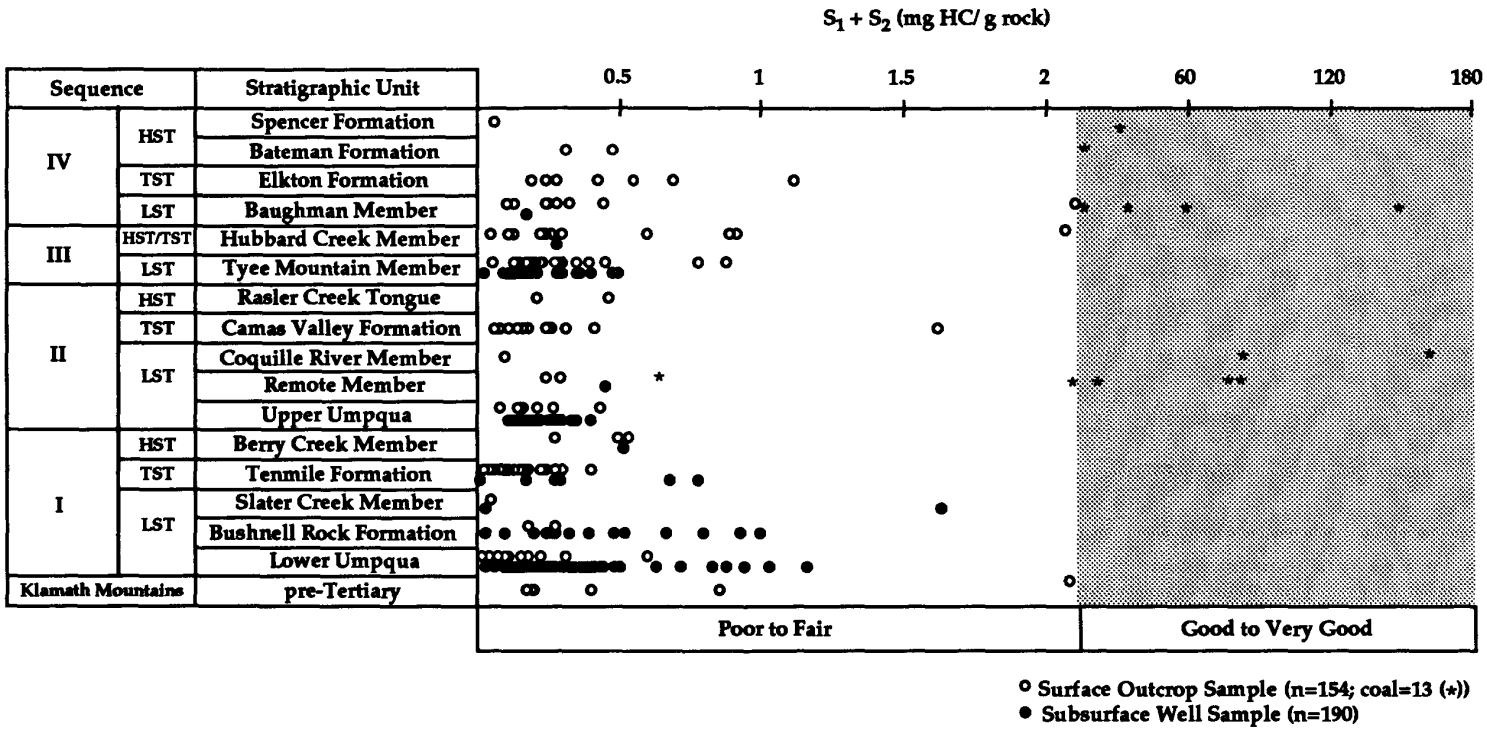

Figure 4.6 Pyrolysis $S_1 + S_2$ yields as a function of stratigraphic unit. Coals and carbonaceous mudstones (*) in the deltaic members of Sequences II and IV rate as good to very good potential source rocks (stippled area) in the Tyee basin.

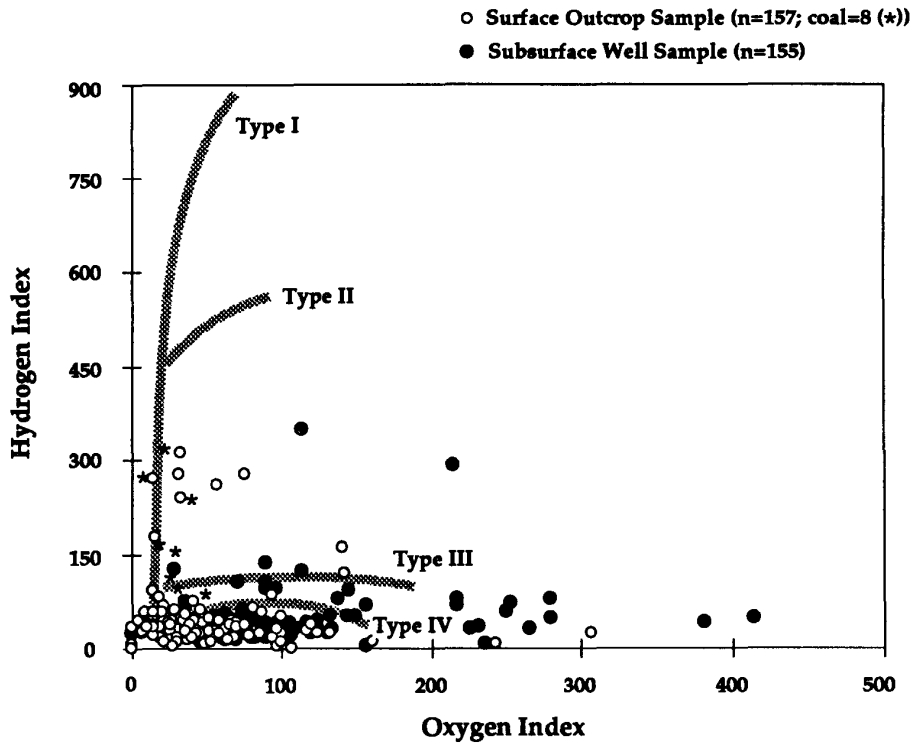

Figure 4.7 Van Krevelen diagram (Hydrogen Index (HI) versus Oxygen Index (OI)), showing the hydrocarbon-generative type. Most Tyee basin samples plot in the Type III (gas-prone) and Type IV (very limited or marginal potential for gas) fields, but a few samples plot in the field between Type II (oil-prone) and Type III (gas-prone).

Long Bell well, and Umpqua Group in Amoco F-1 well) are also depleted in hydrogen (i.e., have a low hydrogen index), have low TOC (Fig. 4.4), and have high oxygen index. These data indicate that the organic matter was highly oxidized during transport before deposition and/or was oxidized by groundwater during early burial and diagenesis (Brown and Ruth, 1983). As a result, this oxidized Type IV organic matter can show a high Tmax value (Peters, 1986).

In order to avoid the possible inaccuracy of oxygen index values, the type of organic matter is now generally classified on hydrogen index only. The distribution of hydrogen index values for all Tyee basin samples is shown in Figure 4.8A. Approximately 75 percent of the samples analyzed has a hydrogen index < 50. A hydrogen index of 50 is typical of organic matter with very limited to marginal potential to generate dry gas (methane). This fraction falls in or close to the field of Type IV organic matter, which is residual organic matter (i.e., inertinite) recycled from older strata (Tissot and others, 1974). The remaining 20 percent of samples plots between hydrogen index values of 50 and 150, indicating the potential for dry gas only (Type III, Tissot and others, 1974). Only five percent of the samples has a hydrogen index > 150, typical of organic matter with the potential to generate oil or wet gas (Type II or Type III organic matter, Tissot and others, 1974). These graphs confirm that potential source rocks in the Tyee basin have only limited ability to produce natural dry gas. A similar conclusion was reached by Law and others (1984) and by Niem and Niem (1990) based on fewer samples. Stratigraphic distribution of hydrogen index values shows that oil- and wet gas-prone organic matter occurs mostly in coal-bearing deltaic sequences (sequences II and IV) and in a few thin mudstones of the Bushnell Rock Formation, Slater Creek Member, Tyee Mountain Member, and Hubbard Creek Member (Fig. 4.9). The Cretaceous Whitsett limestone is also considered a source rock capable of generating oil and wet

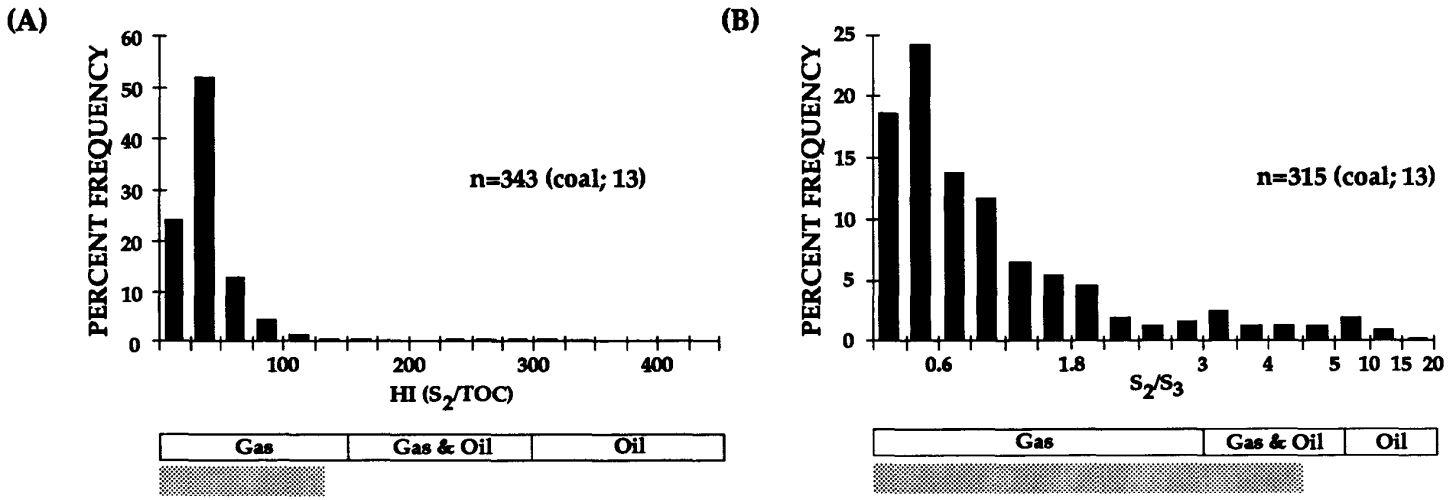

Figure 4.8 (A) Overall distributions of hydrogen index and (B) pyrolysis S_2/S_3 yields. Most samples are gas-prone, but a few samples are oil- and gas-prone (Peters, 1986). Stippled area represents 95% distribution of Eocene Tyee basin samples.

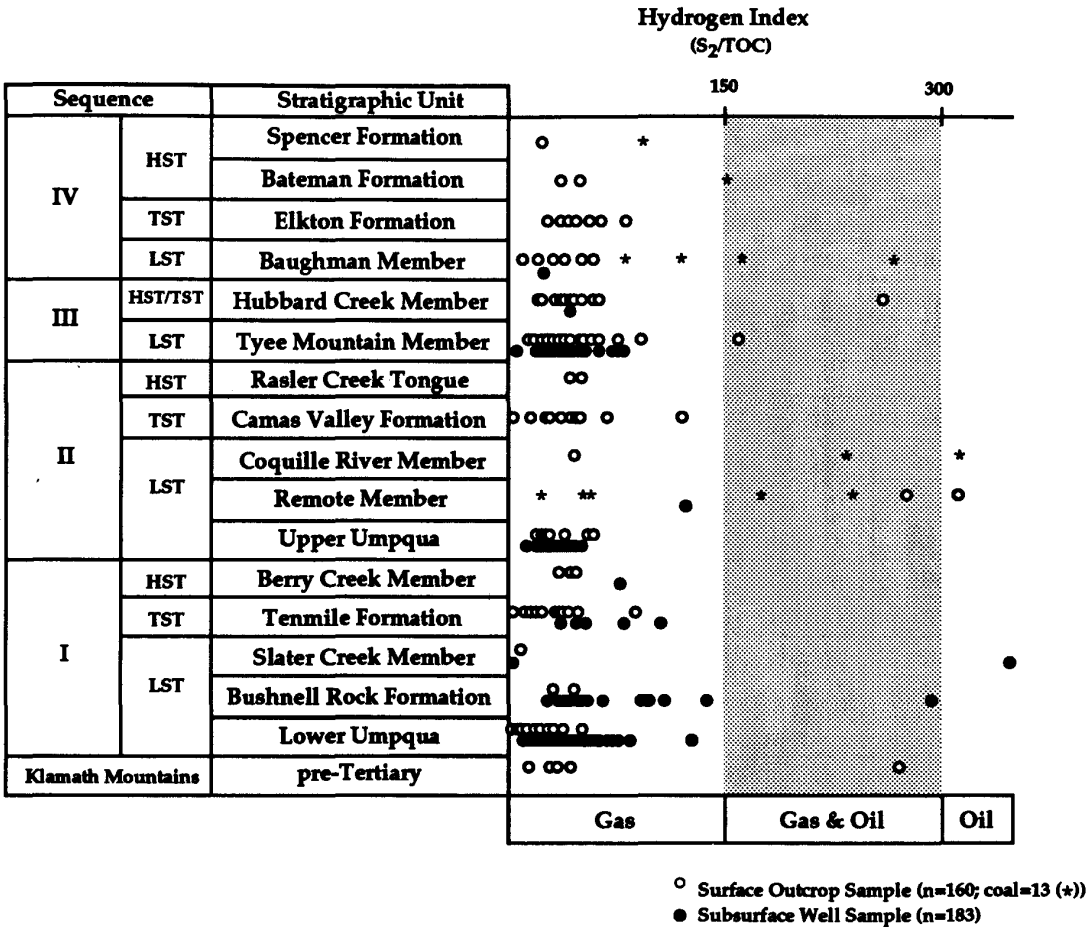

Figure 4.9 Hydrogen Index values as a function of stratigraphic unit. Most samples are gas-prone, but a few samples plot in the gas- and oil-prone area (Peters, 1986). Gas- and oil-prone source rocks of Sequence III (Tyee Mountain and Hubbard Creek members) are deep-marine mudstones in the northern part of the basin (Loon Lake and Elkton areas). Also two subsurface samples from the Scott and Great Discovery wells indicate that some mudstones in the Bushnell Rock Formation and Slater Creek Member are oil-prone. Also a carbonaceous mudstone interbed in the Cretaceous Whitsett Limestone is gas- and oil-prone. Note coals and carbonaceous mudstones (*) of deltaic members of Sequences II and IV are generally gas- and/or oil-prone.

gas. Unfortunately, the potential of this unit as a source rock is limited because it is present only as isolated blocks in Mesozoic mélange (Dothan Formation of Ramp, 1972) (Diller, 1898). Most other samples (lower Umpqua, Bushnell Rock, Tenmile, Camas Valley, Tyee Mountain, Hubbard Creek, Elkton, Bateman, and Spencer) are only gas-prone.

Pyrolysis S_2/S_3 yield is also a useful parameter to determine the type of organic matter in potential source rocks. Rocks with S_2/S_3 yield less than 3.0 are generally considered dry gas-prone source rocks; values of S_2/S_3 between 3.0 and 5.0 are considered to be typical of source rocks with potential to generate oil and wet gas condensate; and values of S_2/S_3 greater than 5.0 are common in oil-prone source rocks (Peters, 1986). More than 90 percent of Tyee basin samples are dry gas-prone source rocks (Fig. 4.8B). The remaining 10 percent of samples are oil- and wet gas-prone source rocks. Based on pyrolysis S_2/S_3 yields, carbonaceous mudstone and coal beds in deltaic units of sequences II and

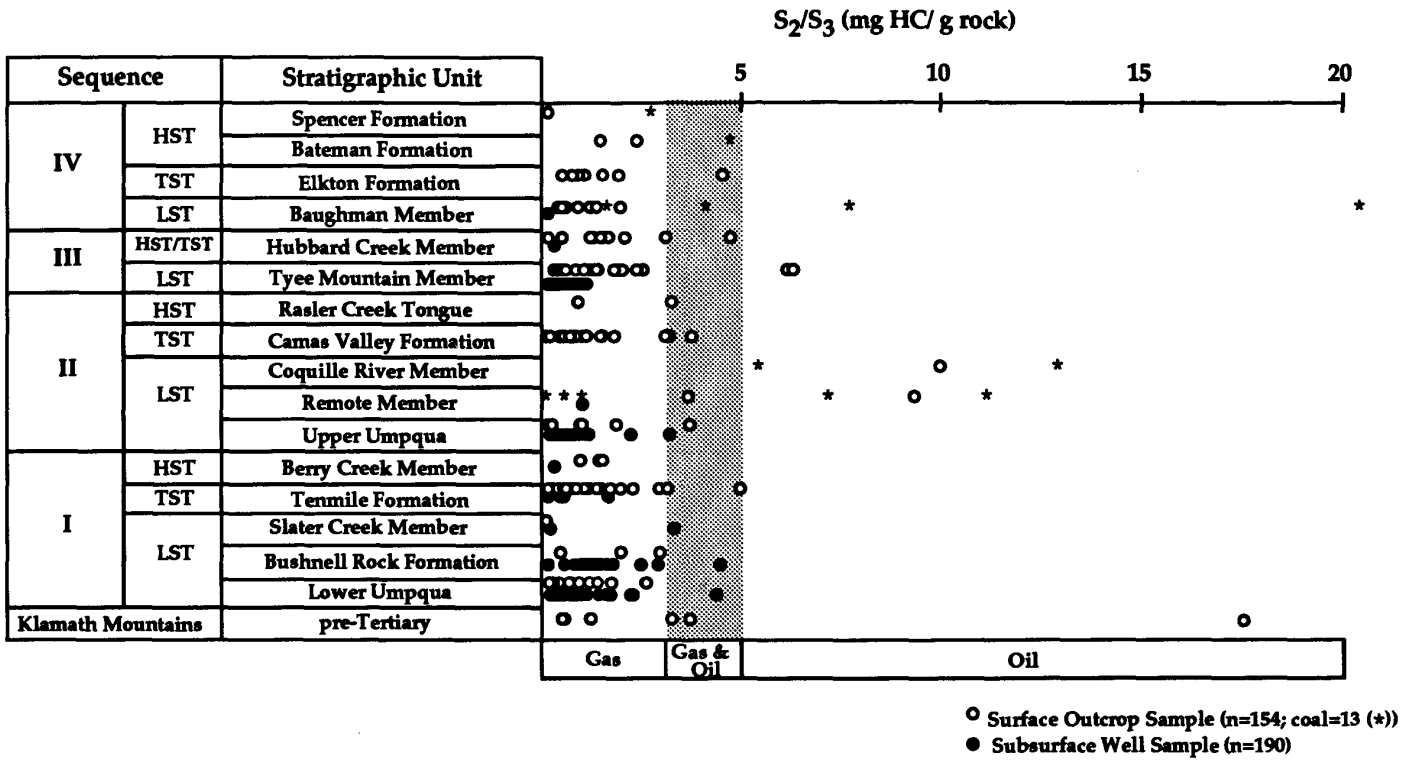

Figure 4.10 Pyrolysis S_2/S_3 yields as a function of stratigraphic unit. Two deep-marine mudstones of Tyee Mountain Member from northern part of the basin (Loon Lake and Elkton areas) are oil-prone. Also a carbonaceous mudstone interbed in the Cretaceous Whitsett Limestone is oil-prone. Note some coals and carbonaceous mudstones of deltaic members of Sequences II and IV are oil-prone.

IV (Remote, Coquille River, and Baughman members) appear to represent better oil-prone source rocks than any of the marine and non-marine mudstone units in the basin (Fig. 4.10). Although coals, in general, tend to be principally gas-prone terrestrial macerals, some coal basins produce petroleum because the coals contain high proportions of algal matter (alginite); for example, in China and Australia. Many Tyee basin coals accumulated in estuarine or paralic settings and, therefore, may include more alginite. Detailed coal petrography would be needed to determine whether these coals do contain more alginite. Although some Tyee basin coals are oil-prone, any oil that might be formed, given proper burial depth, might not be able to migrate out of the coal as readily as gas (P. Lillis, U.S. Geological Survey, 1994, pers. commun.).

Other source rock analyses to determine the types of hydrocarbons which could be generated are visual kerogen typing and C_{15}^+ extract with gas chromatography (Figs. 4.11 and 4.12). These analyses were conducted by petroleum company and by geochemistry consultants on fewer samples and mostly on lower Umpqua Group and Tyee Mountain Member samples from wells (Table 4.1 in Appendix). Microscopic inspection indicates that most kerogen in marine and non-marine mudstone samples is terrestrial herbaceous pollen and structured woody material (Brown and Ruth, 1983; Long, 1994; Fig. 4. 11). This type of kerogen is mainly vitrinite which tends to be gas-prone (Tissot and Welte, 1978).

Oil- and wet gas-prone alginite, inertinitė, and amorphous kerogen are typically minor and variable components. Some deep-marine mudstone in the lower Umpqua Group has higher concentrations of oil-prone alginite and exinite. Some lower Umpqua samples have high concentrations of inertinite (i.e., 60 to 80% in Mobil Sutherlin Unit #1 well), suggesting recycling of organic matter. Browning and Flanagan (1980) reported Upper Cretaceous pine pollen in several units. In addition, Eocene strata penetrated by exploration wells generally contain low amounts (average 319 ppm) of extractable C_{15}^+ bitumen (Fig. 4.12A). A few (<5%) have C_{15}^+ extracts > 1000 ppm. The bitumen is high in asphaltene and non-soluble organic compounds (NSO), and this nonhydrocarbon fraction routinely amounted to 65 to 85% of the total C_{15}^+ extractable (Table 4.1 in Appendix and Fig. 4.12B). This kind of nonhydrocarbon fraction is usually abundant in shallow immature petroleum and decreases with increasing depth and subsequent cracking (Tissot and Welte, 1978). This suggests that only minor generation of petroleum has occurred. For example, the bitumen extracted from Eocene Tyee basin strata is low in saturated and aromatic hydrocarbons compared to average values for crude oils or "typical" source rock bitumens compiled by the French Petroleum Institute (Tissot and Welte, 1978) (Fig. 4.12B). In many Umpqua Group and Tyee Mountain samples, noticeable sterane and terpane components are present as long-chain normal paraffins > C_{25} (Haykus in Newton, 1980) (Fig. 4.13). A high pristane and phytane ratio (generally > 2) in most marine mudstone units encountered in wells (Table 4.1 in Appendix) and occurrence of terrestrial waxes (n-alkanes with mainly odd-carbon numbers from C_{25} to C_{33} in the Amoco Weyerhaeuser F-1 and Mobil Sutherlin Unit #1 wells) also suggest a dominantly terrestrial origin of the Tyee basin organic matter (Brown and Ruth, 1983).

In summary, the bitumen extracts indicate substantial input of terrestrial organic matter during Eocene deposition in the Tyee basin (Tissot and Welte, 1978; Waples, 1980). In a few cases (e.g., Long Bell well cuttings from 4560, 6880, and 8120 feet; lower Umpqua Group, Brown and Ruth, 1983), the C_{15}^+ saturated hydrocarbon distributions are similar to very mature hydrocarbon, i.e., low pristane and phytane ratios, along with no predominance of odd-carbon-numbers (i.e., low carbon preference index values) (Table 4.1 in Appendix and Fig. 4.14). Also the amount of saturated hydrocarbons in these C_{15}^+ extracts for a few Umpqua samples is high relative to the total bitumen content (average 20%; Table 4.1 in Appendix). It suggests that some mature hydrocarbons could be generated locally as deep, basin center gas from some Umpqua Group deep-marine mudstone; for example, in the Smith River subbasin (Law and others, 1994).

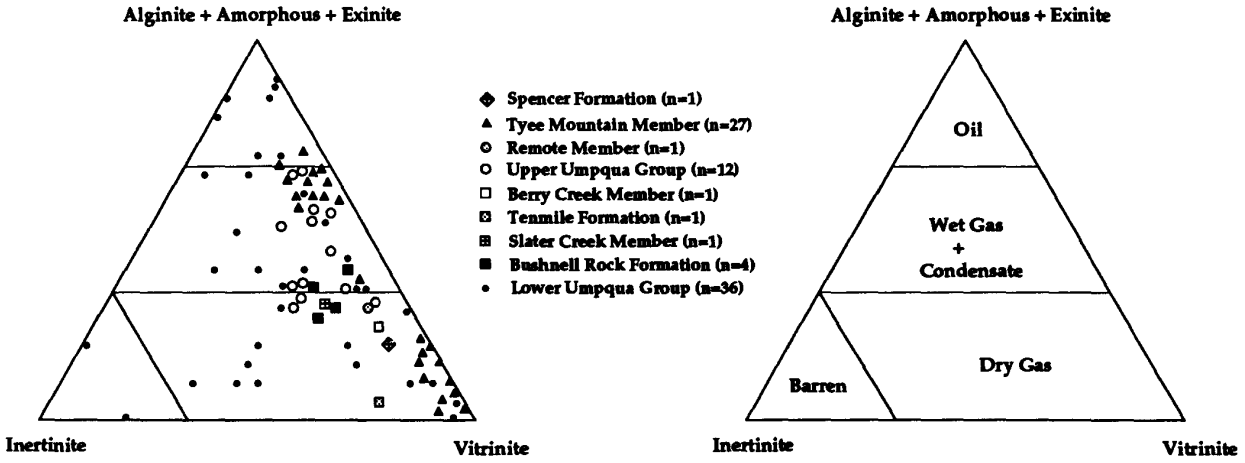

Figure 4.11 Visual kerogen analyses from 84 Tyee basin samples. Most samples are from exploration wells (Long Bell #1, Amoco Weyerhaeuser F-1, Union Liles, Mobil Sutherlin #1, Glory Hole, Scott #1, Great Discovery #2). Comparison of these data with the reference diagram (Tissot and Welte, 1978) indicates that most organic matter in Eocene strata are dry gas-prone and wet gas-prone. However, a few samples of lower Umpqua Group are oil-prone.

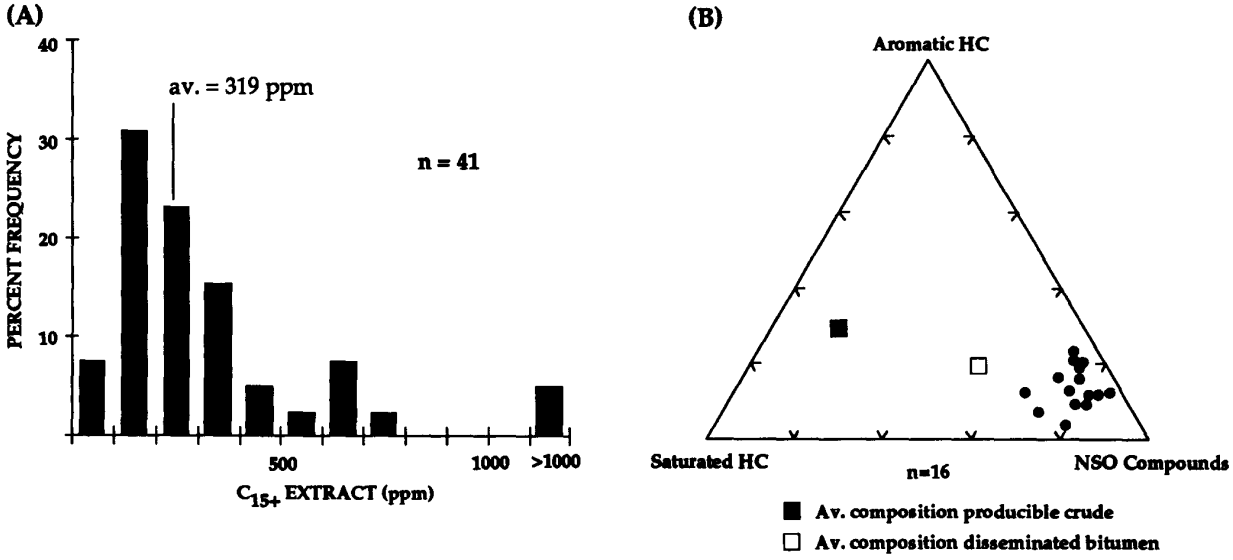

Figure 4.12 (A) C15+ extract levels of Tyee basin samples from five exploration wells (Long Bell #1, Harris 1-4, Weyerhaeuser F-1 and B-1, and Mobil Sutherlin #1) and (B) General composition of C15+ bitumen extracts. Tyee basin strata (mainly Tyee Mountain Member and lower Umpqua Group) contain low amounts of extractable C15+ bitumen. Two samples (3590 ft (lower Umpqua Group) in the Mobil Sutherlin #1 well and 1050 ft (Tyee Mountain Member) in the Harris 1-4 well) contain high amounts (>1,100 ppm) of extractable C15+ bitumen. Note the bitumens from Tyee basin are low in aromatic and saturated hydrocarbons compared to the average values of gross composition of crude oils or "typical" source rock bitumens compiled by the French Petroleum Institute (Tissot and Welte, 1978).

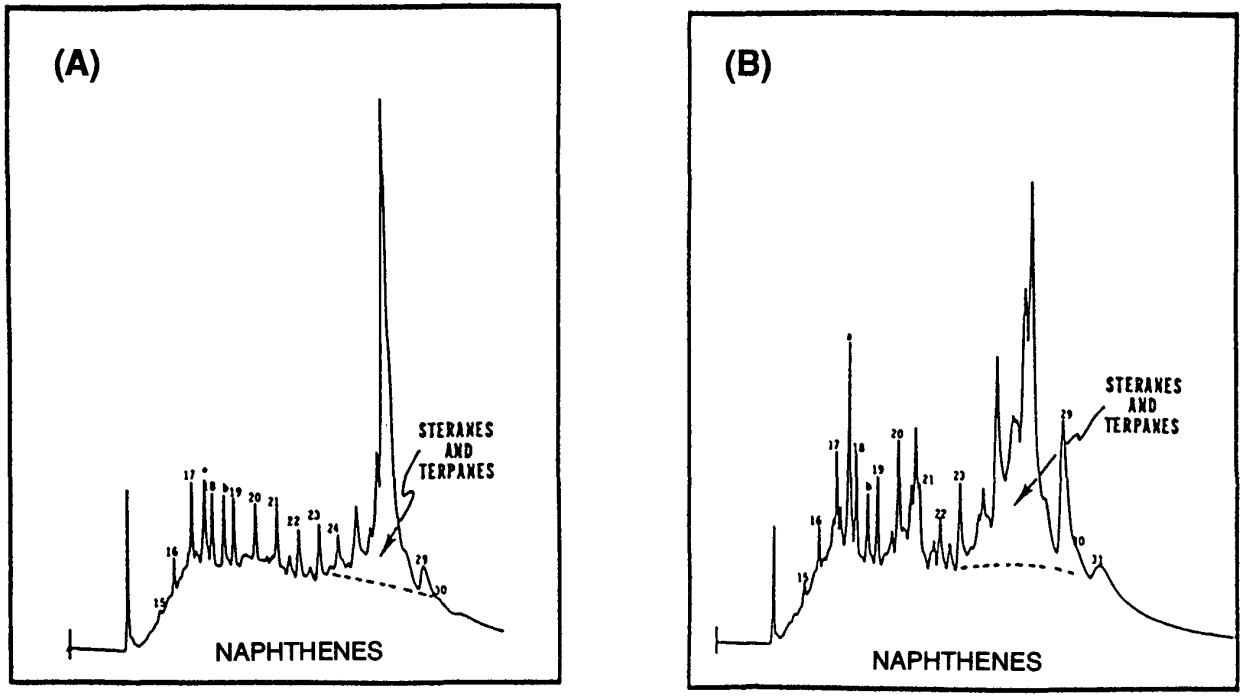

Figure 4.13 Gas chromatograms of Umpqua mudstones. A) lower Umpqua mudstone and B) upper Umpqua mudstone. The organic matter in Umpqua mudstones is mainly steranes and terpanes which are also typical of thermally immature sedimentary strata (from Tybor, in Newton, 1980).

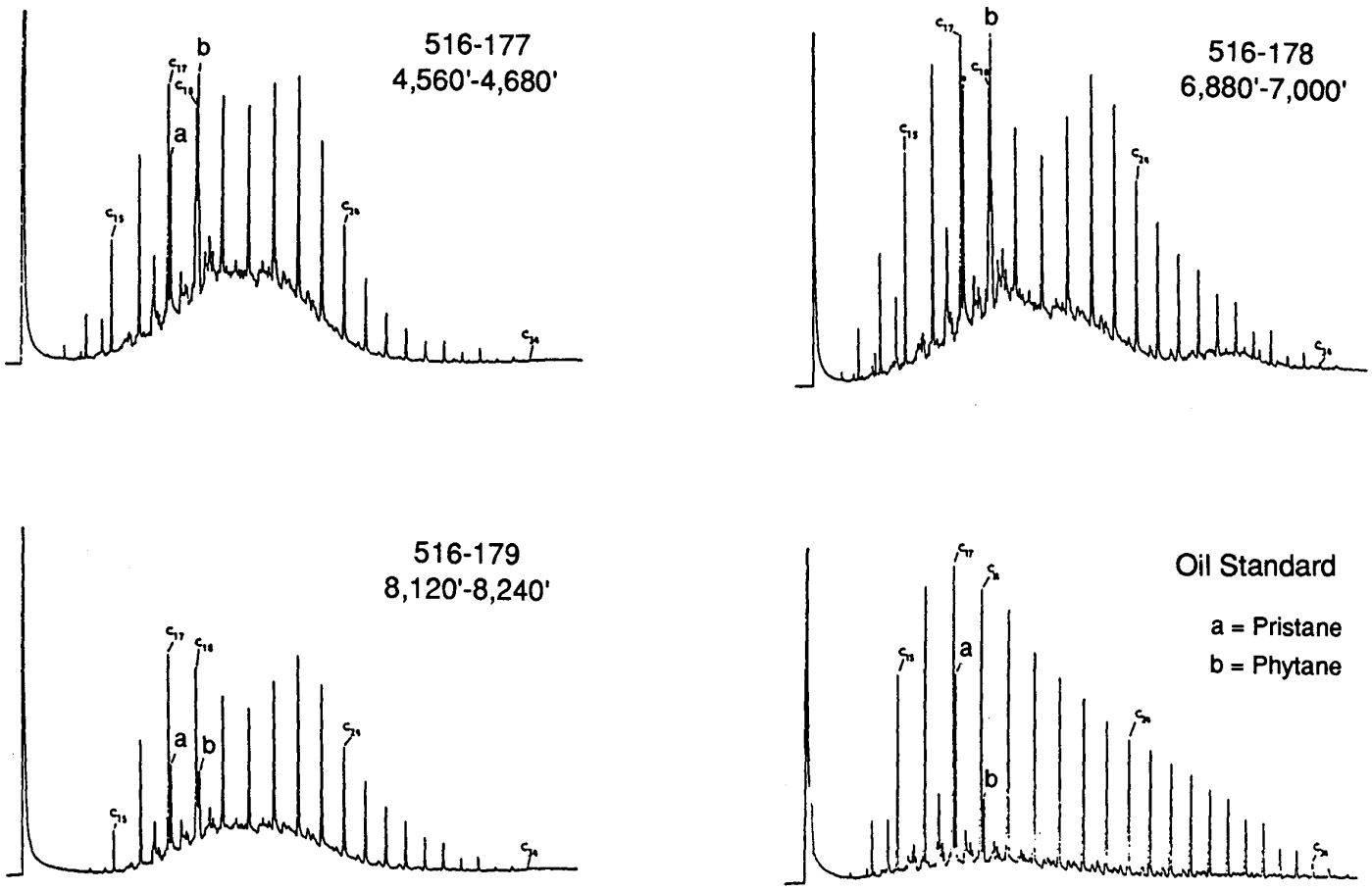

Figure 4.14 Bitumen chromatograms of three deep-marine Umpqua mudstones compared to oil standard (from Long Bell well, from Brown and Ruth, 1983).

Level of thermal maturity

Most Tyee basin samples (95%) show vitrinite reflectance values < 0.8% R_0 (Fig. 4.15A). They generally cluster around 0.5 to 0.7% R_0, merely marginal levels of oil and wet gas generation and significantly below the generation level of dry gas at 1.0% R_0 for Type III organic matter (Fig. 4.15A). The top of the maturation window varies with the type of organic matter from 0.5 to 1.0% R_0; the bottom of the window varies from 1.4 to 3.5% R_0 (Tissot and Welte, 1978; Espitalié, 1985). Thermogenic (metagenic) dry gas is thought to be generated at vitrinite reflectance values above 1.0% R_0 for woody or terrestrial Type III kerogen. The distribution of vitrinite reflectance (% R_0) data suggests that most Eocene Tyee basin units and some pre-Tertiary units are not sufficiently mature to generate thermogenic (metagenic) gas and are marginally mature for oil and wet gas (condensate). However, vitrinite reflectance values for some samples are > 0.7, which indicates that Type II and Type III kerogens are sufficiently thermally mature to produce wet gas and oil (Figs. 4.15A, 4.16, 4.17, 4.18).

Generally, vitrinite reflectance values increase with depth due to increase in geothermal gradient and increasing absolute age of the rock with depth (e.g., Figs. 4.16 and 4.18). White Tail Ridge and post-White Tail Ridge strata (sequences II, III, and IV) are largely immature, whereas pre-White Tail Ridge strata (sequence I) are marginally mature to immature for Type II and Type III kerogen (Fig. 4.16). Deeper burial, attributable to underthrusting, may also have resulted in maturing some of these subduction zone strata (i.e., sequence I). Other exceptions to the generalization that Tyee basin units are immature and submature, however, do occur (Figs. 4.16, 4.17, and 4.18A). For example, two mudstone samples of lower and upper Umpqua Group have very high vitrinite reflectance values of 2.4 and 2.1 (Figs. 4.16, 4.17, and 4.18A). These two samples are mudstones baked by basaltic sills (1) at a depth of 5595 feet in the Long Bell well (column 1 in fence diagram) and (2) in an exposure near Dickinson Mountain (column 22 in fence diagram) (Figs. 4.16, 4.17, and 4.18; Plate 3C).

Thermal maturity of organic matter in Tyee basin samples is also evaluated based on the Tmax of the S_2 peak (Fig. 4.15B). The maturation range of Tmax varies for different types of organic matter (Tissot and Welte, 1984). The range of variation of Tmax is narrow for Type I kerogen, wider for Type II, and much wider for Type III kerogen due to the increasing structural complexity of the organic matter (Tissot and others, 1987). The maturation level

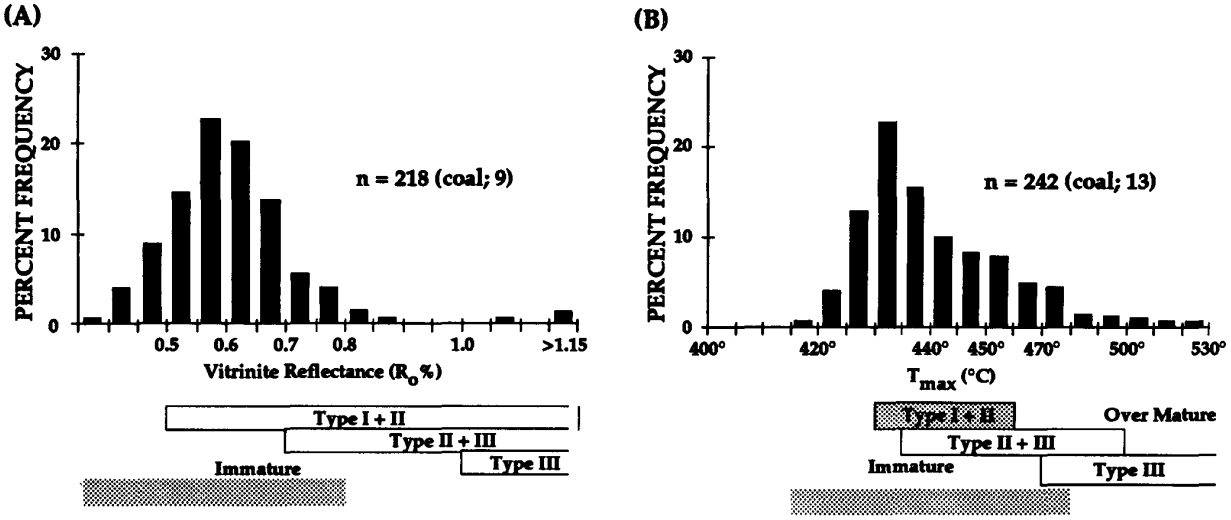

Figure 4.15 Overall distribution of Vitrinite Reflectance (A) and T_{max} (B) for Tyee basin samples. Stippled area represents 95% distribution of samples. ▭ *= maximum maturation range for different types of organic matter (Type I = highly oil-prone, Type II = oil-prone, and Type III = gas-prone). Maturation scale from Espitalié (1985).*

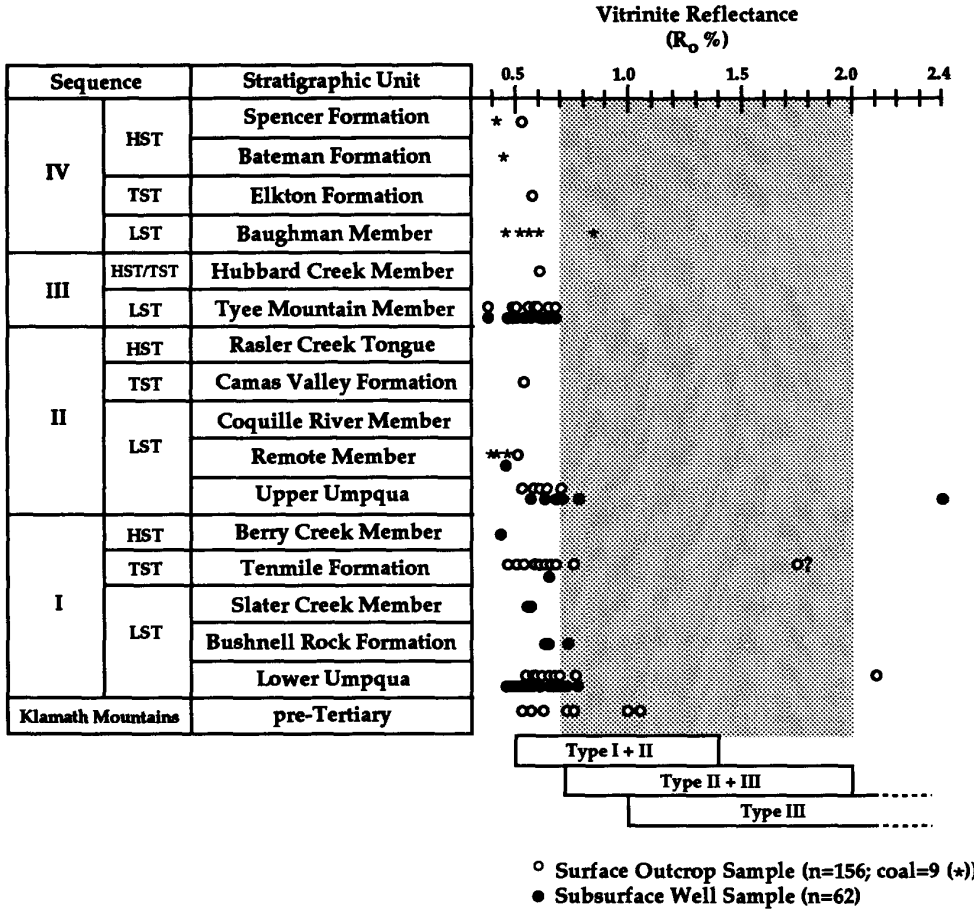

Figure 4.16 Vitrinite reflectance values as a function of stratigraphic unit and increasing depth. Note the vitrinite reflectance value increases with depth. High vitrinite reflectance values (2.1 and 2.4 %R_O) of lower and upper Umpqua Group are due to basaltic intrusions (e.g., Long Bell #1 well). Data point for 1.75 %R_O in the Tenmile Formation is from Law and others (1984), but exact location is not available and stratigraphic unit is questionable. Stippled area represents maturation level for Type II and Type III organic matter.

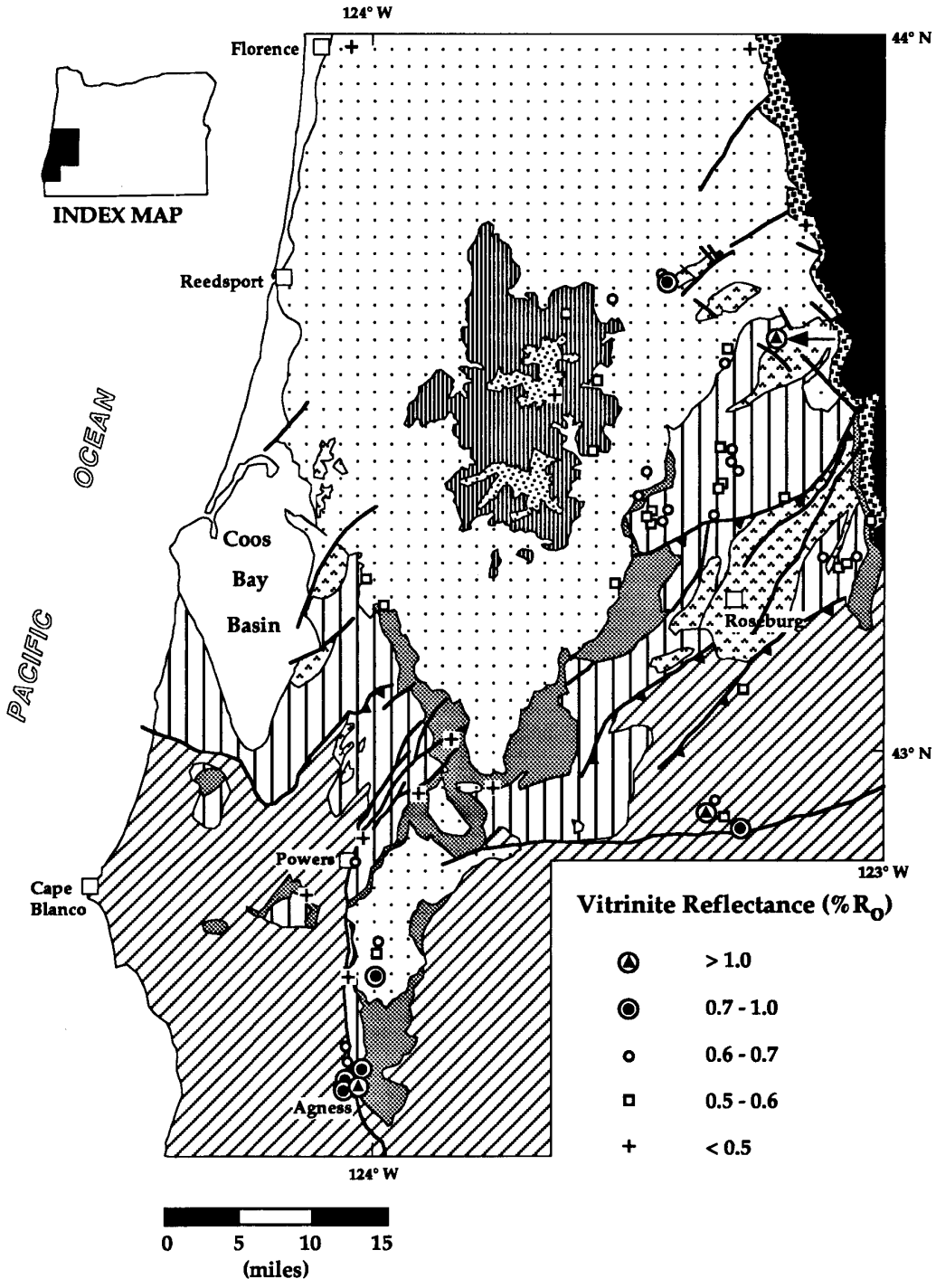

Figure 4.17 Distribution of vitrinite reflectance (% Ro) data. Most Eocene Tyee basin units are not sufficiently mature to generate thermogenic gas (Ro < 0.7). Only nine samples (circled) are thermally mature to generate oil and wet gas (Ro > 0.7). Arrow indicates Umpqua mudstone baked by basaltic sill near Dickinson Mountain.

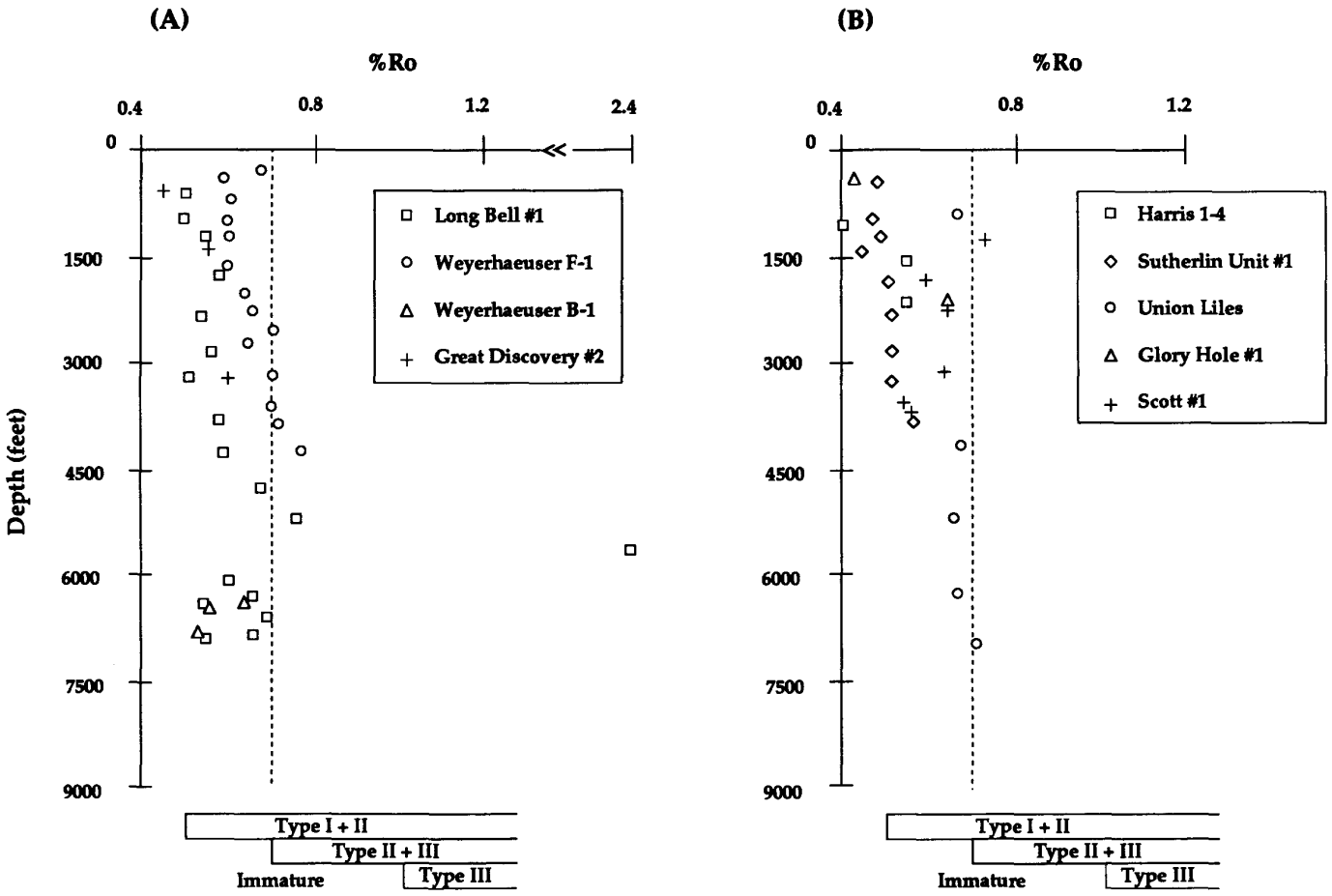

Figure 4.18 Downhole maturity profiles based on vitrinite reflectance for wells in the western area (A) and the eastern area (B) of the Eocene Tyee basin. Most Tyee basin units are thermally immature to generate dry gas from Type III organic matter. However, R_o values for some samples (e.g., Weyerhaeuser F-1 well) are greater than 0.7 $\%R_o$ (dotted line), which indicates that Type II and Type III organic matter are marginally mature to produce wet gas and oil.

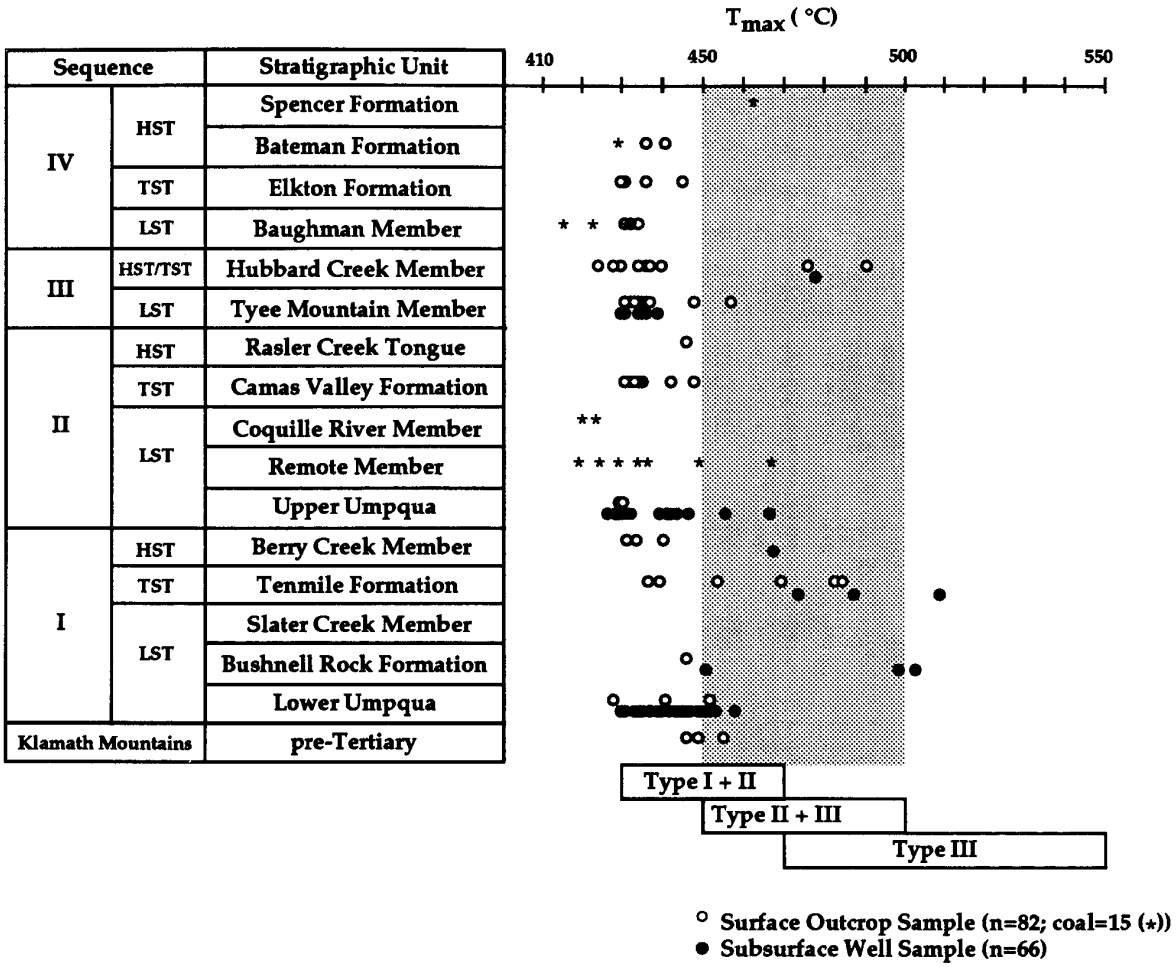

Figure 4.19 Pyrolysis T_{max} values of Tyee basin units as a function of stratigraphic unit and depth. Stippled area represents maturation level for Type II and Type III organic matter. Reliable T_{max} values only (S_2 > 0.2; TOC > 0.5).

of Type I and II organic matter ranges from 430°C to 470°C; this range also represents " the oil window" (Tissot and others, 1987; Peters, 1986). The onset of maturity for Type III terrestrial organic matter is 465°C to 470°C; Tmax > 470°C represents the dry gas-zone (Tissot and others, 1987; Peters, 1986). Most Tyee basin samples (95%) in Rock-Eval pyrolysis yielded Tmax values < 470°C (Fig. 4.15B). They generally group from 425°C to 445°C, significantly below the maturation window of dry gas-prone terrestrial Type III organic matter (Fig. 4.15B). Therefore, almost all Tyee basin units are thermally immature to generate dry gas from Type III organic matter. However, locally in some deep wells and in outcrop (Figs. 4. 19, 4.20, and 4.21) Umpqua Group units are marginally mature for Type II and Type III organic matter (e.g., Scott #1 and Glory Hole #1 wells) whereas the same units farther north and overlain by thicker sections of sedimentary rock are thermally immature (Fig. 4.29 and Plate 3D). These data suggest that areas in the southern part of the basin were once more deeply buried but have been subsequently uplifted and stripped of overlying sedimentary rock (e.g., Coos Bay upper Eocene to middle Miocene (?) strata).

Tmax values of Tyee basin samples generally increase as a result of increasing burial depth (i.e., older, more deeply buried rocks have higher Tmax values) (Figs. 4.19 and 4.21). In general,

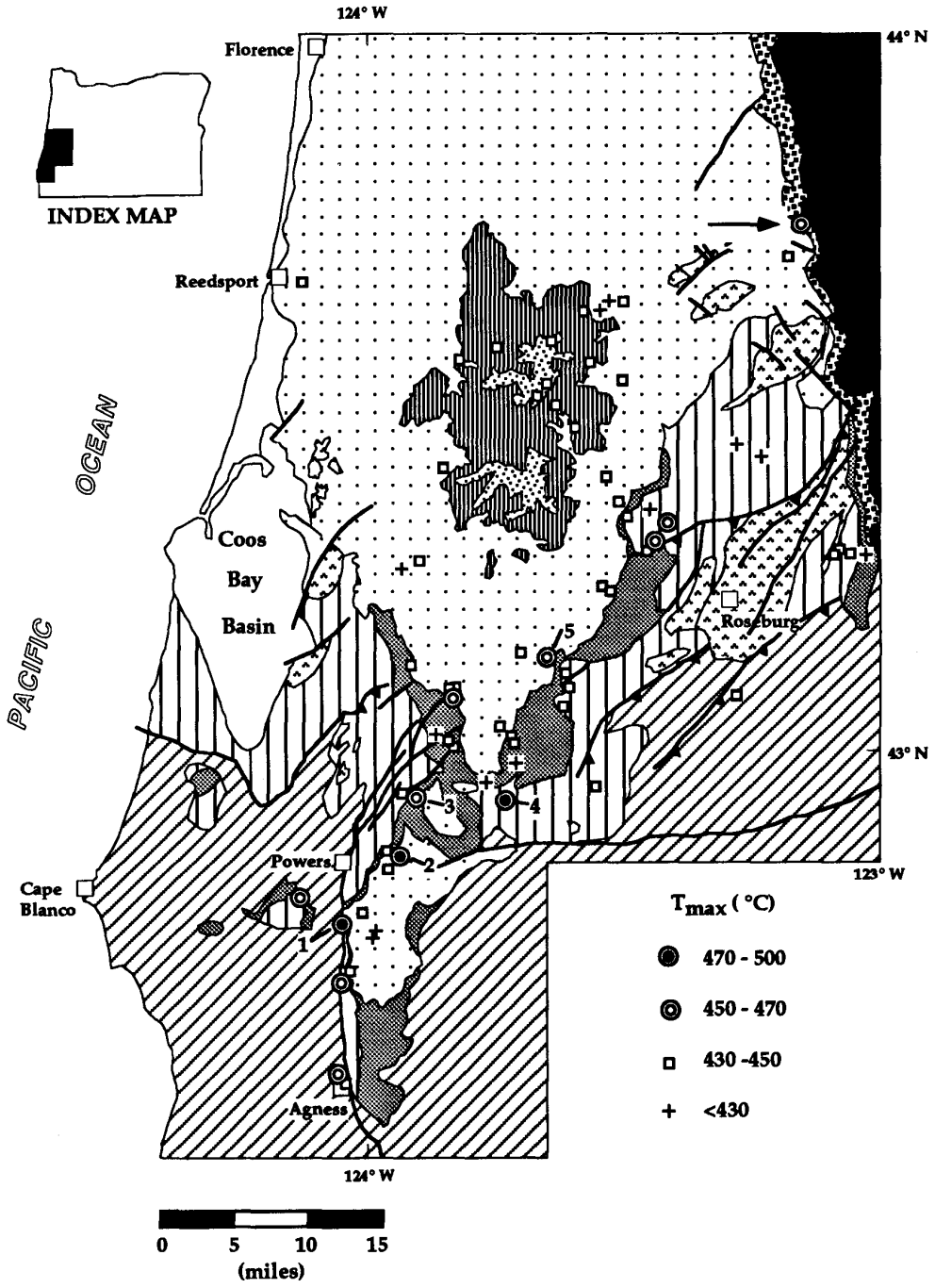

Figure 4.20 Distribution of reliable T_{max} (S_2 > 0.2; TOC > 0.5) data. Almost all Tyee basin units are thermally immature to generate thermogenic gas (T_{max} < 450°C) from Type II and Type III organic matter. Only eleven samples (circled) are thermally mature, but the same units farther north are thermally immature. These data suggest that southern part of the basin was once more deeply buried but has been subsequently uplifted and stripped of overlying sedimentary rocks (e.g., Coos Bay basin strata). The Spencer coal bed (arrow) is thermally mature due to heating by a Western Cascades pluton. Note pre-Tertiary mudstone near the Agness is also thermally mature to generate oil and wet gas. Five samples (numbered 1 to 5) have the best maturity in the basin (see Table 4.3).

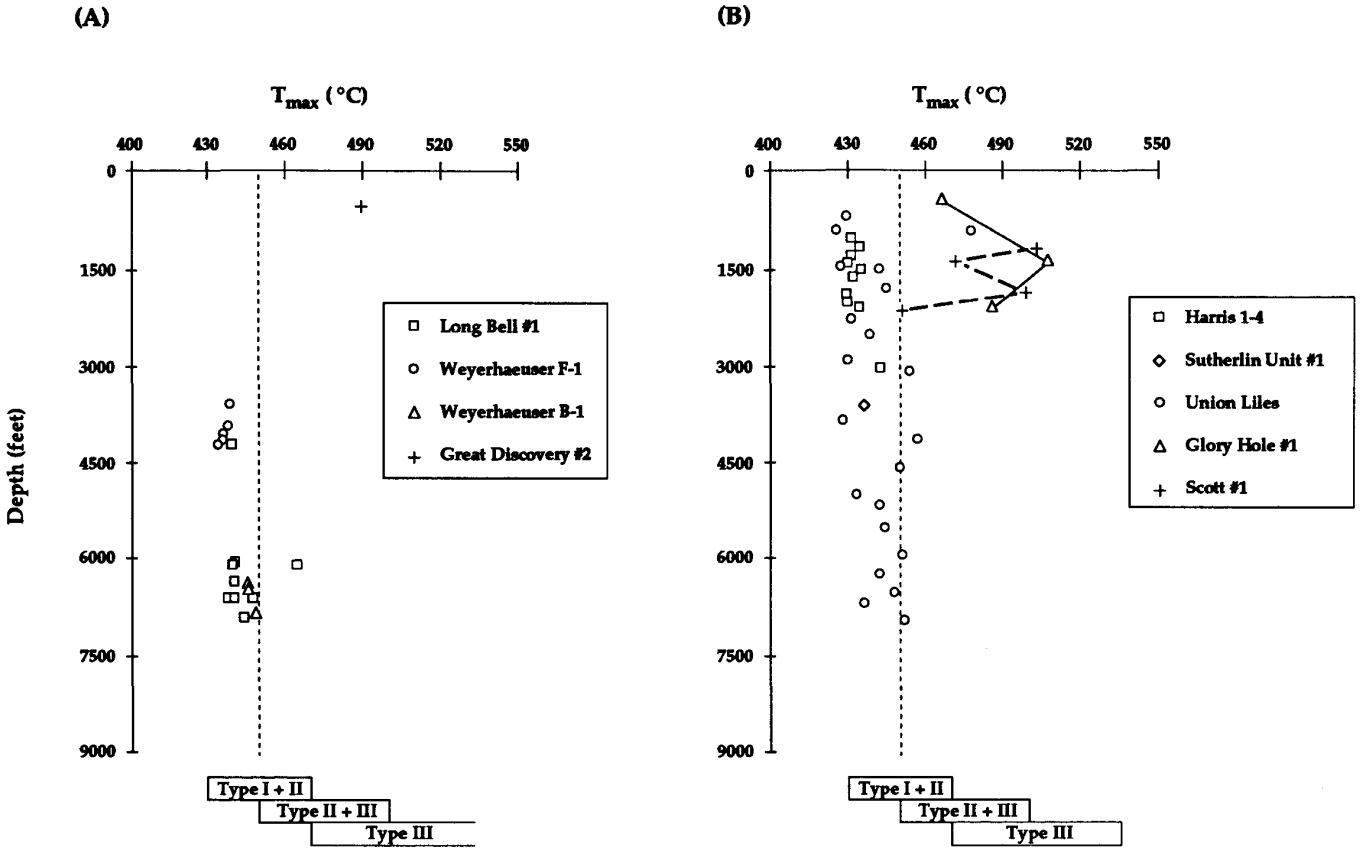

Figure 4.21 Downhole maturity profiles based on reliable T_{max} ($S_2 > 0.2$; TOC > 0.5) value for wells in the western area (A) and the eastern area (B) of the Eocene Tyee basin. Most Tyee basin samples are thermally immature with respect to Type II and Type III organic matter. However, T_{max} values of some wells (e.g., Scott #1 and Glory Hole #1 wells) are greater than 450°C, which indicates that Type II and Type III organic matter are thermally mature to generate wet gas or possibly oil. Note the reversal in the maturity trend of T_{max} in the Scott #1 and Glory Hole #1 wells. The general reversal may be due to thrust faults. Thrusts may have emplaced thermally more mature strata over thermally less mature strata or the higher T_{max} values may be due to migration of hydrothermal fluids along faults. Dotted line represents top of maturation level for Type II and Type III organic matter (T_{max} = 450°C).

the trend of increasing Tmax is similar to the vitrinite reflectance. That is, the older White Tail Ridge and pre-White Tail Ridge strata are marginally mature to mature, and all of the younger post-White Tail Ridge strata are dominantly immature to marginally mature with respect to Type II and Type III kerogen (Fig. 4.19).

Although thermal maturity (i.e., R_0 and Tmax) usually increases linearly with depth and with higher burial temperatures, anomalous variations can result from unconformities, faults, erosion of overlying units, and other local factors (e.g., flash heating by intrusion of basalt sills; Fig. 4.18) and from changes in the relative abundance and type of organic matter (e.g., recycled) (Peters, 1986). The Scott # 1 well, for example, shows a reversal in the maturity trend of Tmax at depths of 2200 to 2800 feet and at a depth of 1200 feet (Fig. 4.21). This suggests the thermal influence of a thrust fault which has brought a plate of more deeply buried, matured strata over immature to marginally mature shallow-buried strata. The Glory Hole # 1 well also shows a reversal in the maturity trend at a depth of 1400 feet (Fig. 4.21). These two wells are on strike with the Bonanza thrust fault zone and probably intersected these thrusts (Fig. 4.2).

Source rock potential and maturation mechanism

The samples with the highest total organic carbon content (> 2.0 weight percent) are listed in Table 4.2. The samples are grouped by formation and ranked by generative potential. All the coals and carbonaceous mudstones in the deltaic units rate as very good potential source rock for gas and possibly oil based on the total organic carbon content (Table 4.2). Also one sample from the Whitsett Limestone is ranked as potential source rock (Table 4.2). The dark micrite containing pelagic foraminifers and coccoliths emits a petroliferous odor when broken and is interbedded with carbonaceous mudstone. However, these Cretaceous (Albian - Aptian) limestones occur as isolated scattered small blocks in the Mesozoic mélange and thus are geographically limited as source rock.

For an organic-rich source rock to become an effective source rock, it must have reached a maturity level sufficient to generate hydrocarbons (Tissot and Welte, 1978). Two

UNIT	SAMPLE NO.	ROCK TYPE	TOC	HI (S2/TOC)	Tmax	Ro	LOCATION
Spencer	R-92-027	Coal	Very Good	Gas	Immature	Immature	*21
Bateman	R-89-172	Coal	Very Good	Gas & Oil	Immature	N/A	*19
Baughman	Law & others	Coal	Very Good	Gas & Oil	Immature	Immature	*6
Baughman	N-92-1001	Coal	Very Good	Gas	Immature	N/A	*8
Baughman	Law & others	Coal	Very Good	Gas & Oil	Immature	Immature	*7
Baughman	B & F	Coal	Very Good	?	Immature	N/A	*5
Baughman	R-89-044	Coal	Very Good	Gas	Immature	N/A	*15
Baughman	B & F	?	Very Good	?	Immature	N/A	*5
Hubbard Creek	RN-90-144	Siltstone	Very Good	Gas & Oil	Immature	N/A	*20
Coquille River	N-90-358	Coal	Very Good	Gas	Immature	N/A	*17
Coquille River	RN-91-099	Coal	Very Good	Gas & Oil	Immature	N/A	*13
Remote	RN-91-270	Coal	Very Good	Gas & Oil	Mature	Immature	*10
Remote	KL-93-14-1	Coal	Very Good	Gas & Oil	Immature	Immature	*11
Remote	Law & others	Coal	Very Good	Gas	Immature	Immature	*12
Remote	R-92-017	Coal	Very Good	Gas	Mature	Immature	*9
Remote	N-91-116	Coal	Very Good	Gas	Immature	N/A	*16
Remote	KL-93-13-1	Coal	Very Good	Gas	Immature	Immature	*3
Remote	RN-91-391	Coal	Very Good	Gas	Immature	N/A	*4
L. Umpqua	Harris 3000'	Mudstone	Very Good	Gas	Immature	N/A	Fig. 4.2 (#2)
L. Umpqua	N-91-131	Mudstone	Very Good	Gas	Immature	N/A	*18
Pre-Tertiary	Law & others	Mudstone	Very Good	Gas	Immature	Immature	*1
Pre-Tertiary	Law & others	Mudstone	Very Good	Gas	Immature	Immature	*2
Pre-Tertiary	KL-93-11-5	Limestone	Very Good	Gas & Oil	Immature	Immature	*14

*See Figure 4.5 for location

Table 4.2. Source rock samples that have the best generative potential in the Tyee basin.

binary plots of hydrogen index versus maturation (i.e., Tmax and R_0) show the hydrocarbon-generative type (i.e., gas or oil or mixed) of potential source rocks and levels of maturation (Figs. 4.23A and 4.23B). Most Tyee basin samples are thermally immature, (i.e., below the stippled areas on Fig. 4.23), including samples with the highest HI (Table 4.2), such as coals which, although organic-rich, have not been buried or heated sufficiently to generate either oil or gas. Only twelve samples are mature and within the generation window for each type of organic matter (Type I, II, and III) to generate oil, oil and gas, and/or dry gas only. Thermally mature samples are from the Hubbard Creek Member (3 samples), Remote Member (1 sample), Tenmile Formation (5 samples), Bushnell Rock Formation (2 samples), and Umpqua Group (1 sample). Some are associated with thrusts or basaltic sills. However, the source rock generative potential of these thermally mature samples is generally poor to fair (i.e., too lean to produce much hydrocarbon) (Table 4.3 in Appendix).

In summary, source rock analyses of Tyee basin strata indicate that the best generative potential is found in coals and carbonaceous mudstones in the deltaic units of the upper Umpqua Group (e.g., Coquille River and Remote members) and the overlying forearc basin units, such as the Baughman Member of the Tyee Formation, and the Bateman and Spencer formations (Fig. 4.22). Rocks that have sufficiently high levels of thermal maturation to produce oil and thermogenic gas are generally organically lean deep-marine and shelf/slope mudstones of the underlying lower Umpqua subduction zone units (e.g., Bushnell Rock Formation, Slater Creek Member, Tenmile Formation, and Berry Creek Member) (Fig. 4.22). Cretaceous pelagic limestone and coals and carbonaceous mudstones of the deltaic Remote Member represent the most effective source rocks in the Tyee basin and northern margin of the Klamath Mountains in terms of source rock generative potential and thermal maturity (Fig. 4.22).

Sequence		Unit	Generative Potential	Maturity
IV	HST	Spencer Formation*		*
		Bateman Formation		
	TST	Elkton Formation		IMMATURE to SUBMATURE
	LST	Baughman Member	GOOD to VERY GOOD	
III	HST/TST	Hubbard Creek Member		
	LST	Tyee Mountain Member	Gas or Gas & Oil	
II	HST	Rasler Creek Tongue		
	TST	Camas Valley Formation	(mainly coal-bearing strata)	
	LST	Coquille River Member		
		Remote Member		MARGINALLY MATURE to MATURE
		Upper Umpqua		
I	HST	Berry Creek Member		
	TST	Tenmile Formation	POOR to FAIR	
	LST	Slater Creek Member		Gas or Gas & Oil
		Bushnell Rock Formation		
		Lower Umpqua		(mainly thrust-related)
Klamath Mountains		pre-Tertiary		

* only in Western Cascade foothills near sills and/or where hydrothermal fluids have migrated up faults.

Figure 4.22 Source rock generative potential and maturity of each stratigraphic unit of the Tyee basin. Stippled pattern indicates units that have both good generative potential as source rock and those that have been locally matured enough to generate hydrocarbons.

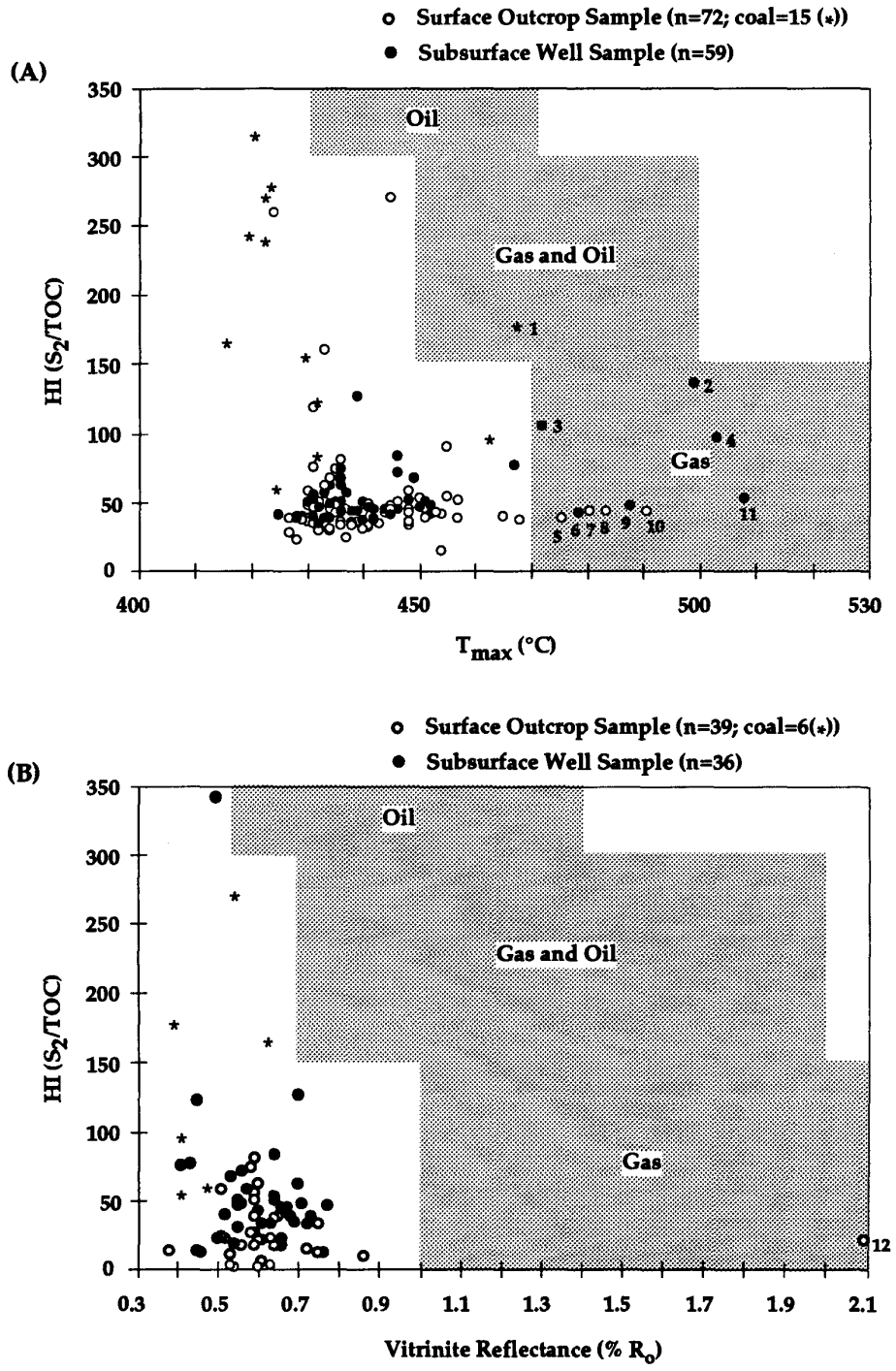

Figure 4.23 Plots of (A) Hydrogen Index (HI) versus pyrolysis T_{max} values and (B) Hydrogen Index (HI) versus vitrinite reflectance values showing the hydrocarbon-generative type and level of maturation of Tyee basin samples. Stippled pattern represents the range of values that are mature for each hydrocarbon-generative type. Most samples plot on the field of gas-prone and thermally immature, but 12 samples plot on the mature fields of oil-prone, gas- and oil-prone, and/or gas-prone only. These twelve samples are listed in Table 4.3.

Natural Gases in the Tyee Basin

Natural gas or oil has been reported from 42 localities in the Tyee basin (Table 4.4 in Appendix and Table 4.5; Fig. 4.24). Niem and Niem (1990) compiled 34 seeps and shows; 8 additional gas seeps were found during the course of this investigation (see also Kvenvolden and others, 1995). Many seeps issue from coal-bearing units (e.g., White Tail Ridge Formation) and from lower Umpqua and Klamath Mountains marine units (Table 4.5 and Fig. 4.24). Some dry water wells which have been capped display strong flows of gas under pressure (e.g., S5 and S7 on Table 4.5). When lighted, these produce flames a few feet long which burn vigorously. Eventually the well loses pressure, suggesting that these are small pockets of gas.

Many seeps are clustered in water wells near the towns of Melrose and Lookingglass in the farm and ranch land of Flournoy and Camas valleys west of Roseburg. The gas appears to be methane from coals and carbonaceous overbank mudstone and sandstone in the White Tail Ridge Formation (e.g., water wells on Fig. 4.24 and coal core holes on Table 4.5). Oil and gas shows also are reported in these valleys in the Kerrin, Dillard, Scott #1, Ziedrich #1, and Glory Hole exploration wells (Fig. 4.24; Niem and Niem, 1990). A drill stem test in the Ziedrich #1 well yielded 8 to 10 Mcfd. Additional gas shows would probably be reported in tcoal-bearing White Tail Ridge strata and in the Baughman Member on the west side of the Tyee forearc basin (i.e., from Agness to Remote to east of Reedsport) if that area were more densely populated (two shows were noted in Baughman and Remote coals; S22 and S17 on Table 4.5).

Other shows and seeps of gas and oil have been reported in roadcut exposures and in water wells that penetrated lower Umpqua Group strata. The locus of these shows and seeps occurs in the Bonanza fault zone between Nonpareil and Melrose and in the Reston fault zone between Lookingglass and Roseburg (Fig. 4.24). For example, fluorescing "oil" was reported in slickensided fractures in cores of Tenmile mudstone and Bushnell Rock conglomerate and sandstone in the Scott No. 1 exploration well which is on strike with the Bonanza fault zone (Niem and Niem, 1990; Ryu and others, 1992). Mobil reported several ppm of flammable gas along the strike of the Bonanza fault zone near Gassy Creek, east of Nonpareil (S1 and S2 on Table 4.5; Seeley, 1989, pers. commun. in Niem and Niem, 1990). Natural gas seeps probably occur in lower Umpqua strata along the continuation of the Bonanza fault zone west of the Tyee escarpment between Remote, Powers, and Myrtle Creek (Fig. 4.24), but the lack of population and water wells in that area limits detection.

North of the Bonanza fault zone, gas seeps occur in water and exploration wells and in fractures in tlower Umpqua turbidites and slope mudstone in anticlines and homoclines. The Mobil Sutherlin No. 1 tested 28 Mcfd at 3,000 feet in Umpqua turbidite strata in the Oakland anticline (Fig. 4.24). The axis of the anticline, which most likely is a fault-propagation fold, is locally tightly folded and faulted and fractured in outcrops east of Sutherlin.

Natural gas also was detected in the Mesozoic terranes of the northern Klamath Mountains (e.g., Dothan Formation and Myrtle Group of Ramp, 1972; Wells and others, in prep.). Gas appears as bubbles in shallow water wells (<200 ft deep) and issues from fractures in Dothan Formation southeast of Roseburg near Glengary and near Agness. The Dothan Formation is a mélange of sheared mudstone which contains blocks of intensively fractured and jointed turbidite sandstone. The blocks range in size from <100 ft to >600 ft long. There are a few building-size tectonic blocks of petroliferous carbonaceous shale and limestone (e.g., Whitsett limestone) within this mélange. Mark Pawlewicz of the U.S. Geological Survey reports bitumen in these limestone samples (Kvenvolden and others, 1995). Two exploration wells in less deformed Myrtle Group sandstones also reported some shows of natural gas (Fig. 4.24; Niem and Niem, 1990). Gas seeps are probably more numerous and widespread in the tectono-sedimentary terranes of the northern Klamath Mountains, but low population density also results in few water wells and few observations of seeps.

Results of recent gas chromatograph and isotopic studies of natural gases collected in several water and exploration wells and from fresh exposures of coals and mudstone in the Tyee basin and adjacent areas are reported by Kvenvolden and others (1994, 1995). These gases have a narrow molecular composition. The gases

Locality No.	Location	SEC. TS. RW	Source of Data	Comments	Rock Unit	Type of Seep
S1	Nonpareil	32, 24, 03	Mobil (1980)	7.14 ppm flammable gas in air	Lower Umpqua Group	crack in rock
S2	Nonpareil	25, 24, 04	Mobil (1980)	7.86 ppm flammable gas in air	Lower Umpqua Group	crack in rock
S3	Melrose	21, 26, 06	Olmstead (1989)	light oil seen rising on gas bubble	Lower Umpqua Group	crack in rock
S4	Melrose	26, 26, 07	Olmstead (1989)	Strong flow of petroleum gas	White Tail Ridge Formation	water well
S5	Melrose	35, 26, 07	Newton (1980)	methane (biogenic): C1 (522,000 ppm), C2 (750 ppm), C3 (72.4 ppm), & C4 (36 ppm)	White Tail Ridge Formation	water well
S6	Melrose	36, 26, 07	BLM (1989)	gas	White Tail Ridge Formation	dry water well
S7	Melrose	36, 26, 07	Niem (1990)	methane (biogenic): C1 (522,000 ppm), C2 (750 ppm), C3 (72 ppm), & C4 (37.2 ppm)	White Tail Ridge Formation	water well
S8	Edenbower	09, 27, 06	Stewart (1954)	gas	White Tail Ridge Formation	water well
S9	Edenbower	21, 27, 07	Olmstead (1989)	gas at 605 ft (TD 1,109 ft)	White Tail Ridge Formation	coal core hole
S10	Lookingglass	32, 27, 07	Treasher (1942)	strong flow of gas at 615 ft	White Tail Ridge Formation	coal core hole
S11	Lookingglass	03, 28, 07	Olmstead (1989)	small amount of light oil and gas	White Tail Ridge Formation	water well
S12	Winston	02, 28, 06	Mobil (1980)	gas at 75 ft	Lower Umpqua Group	crack in rock
S13	Agness	13, 35, 12	Mobil (1980)	11.79 ppm flammable gas in air	Dothan Formation	crack in rock
S14	Tenmile	11, 29, 08	Kvenvolden & others (1995)	methane (biogenic); 49 ppm, iC4	Tenmile Formation	water well
S15	Camas Valley	16, 29, 08	Kvenvolden & others (1995)	methane; 87 ppm	White Tail Ridge Formation	water well
S16	Camas Valley	3, 30, 09	Kvenvolden & others (1995)	thermogenic gas C1, C2 (230 ppm), C3, C4, & C5	White Tail Ridge Formation	outcrop fractures or cleats
S17	Remote	28, 29, 10	Kvenvolden & others (1995)	methane; 29 ppm	White Tail Ridge Formation	outcrop crushed coal sample
S18	Glengary	32, 28, 05	Kvenvolden & others (1995)	thermogenic gas C1 (13,500 ppm), C2 (7.4 ppm), C3 (0.6 ppm), iC4, & nC4	Dothan Formation	bubbling water well
S19	Glengary	33, 28, 05	Kvenvolden & others (1995)	methane (thermogenic); C1 (2,300 ppm), C2 (1.5 ppm), & iC4	Dothan Formation	bubbling water well
S20	Hubbard Creek	20, 25, 07	Wells (1994, pers. commun.)	report of bubbling, flammable gas	White Tail Ridge Formation	water well
S21	Sutherlin	20, 25, 05	Wells (1994, pers. commun.)	report of flammable gas in dry well	Lower Umpqua Group	water well
S22	Powers	21, 32, 11	Newton (1980)	gas reported	Baughman Member	coal core hole
S23	Agness	07, 35, 11	Seeley (1989, pers. commun.)	detectable flow of natural gas during atmospheric lows	Tenmile Formation	fracture in rock
S24	SW of Sutherlin	19, 26, 06	Seeley (1989, pers. commun.)	detectable flow of natural gas during atmospheric lows	Lower Umpqua Group	fractures and joints in rock
S25	SW of Sutherlin	04, 26, 06	Seeley (1989, pers. commun.)	detectable flow of oil	Lower Umpqua Group	small pipe in stock well
S26	Coles Valley	26, 26, 07	Kvenvolden & others (1995)	methane; 30.2 ppm	Lower Umpqua Group	abandoned water well
S27	Reedsport	02, 22, 12	Kienle (1989, pers. commun.)	black asphaltic or tarry? substance in fractures and joints	Tyee Mountain Member	new landfill site
S28	Glengary	20, 28, 05	Kvenvolden & others (1995)	petroliferous odor from thin-bedded micritic limestone and carbonaceous shales when broken	Whitsett Limestone	quarry

Table 4.5. Oil and gas shows in water wells and natural seeps.

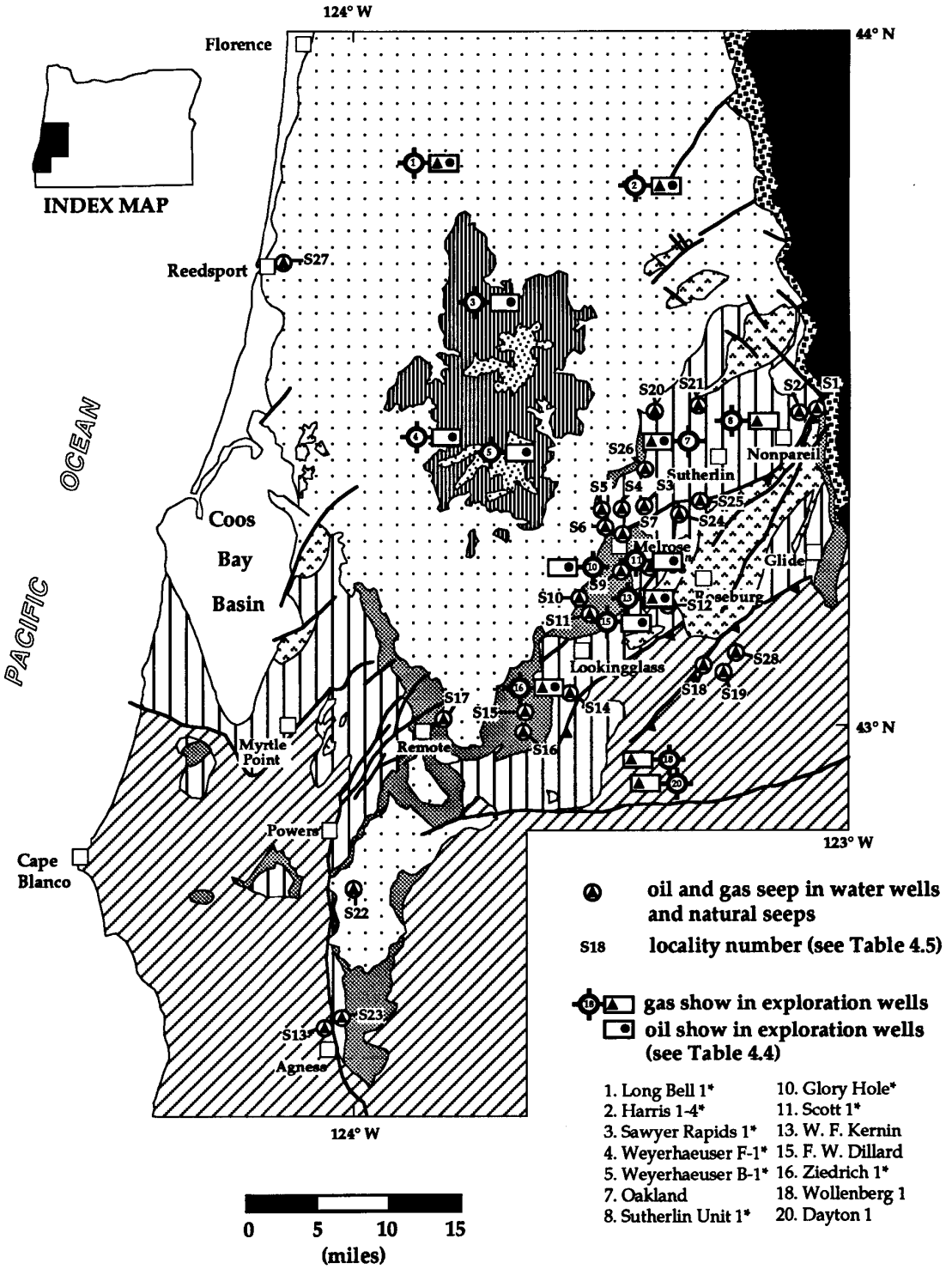

Figure 4.24 Location map of oil and gas shows in wells and natural seeps in Tyee basin (from Niem and Niem, 1990; Kvenvolden and others, 1995).

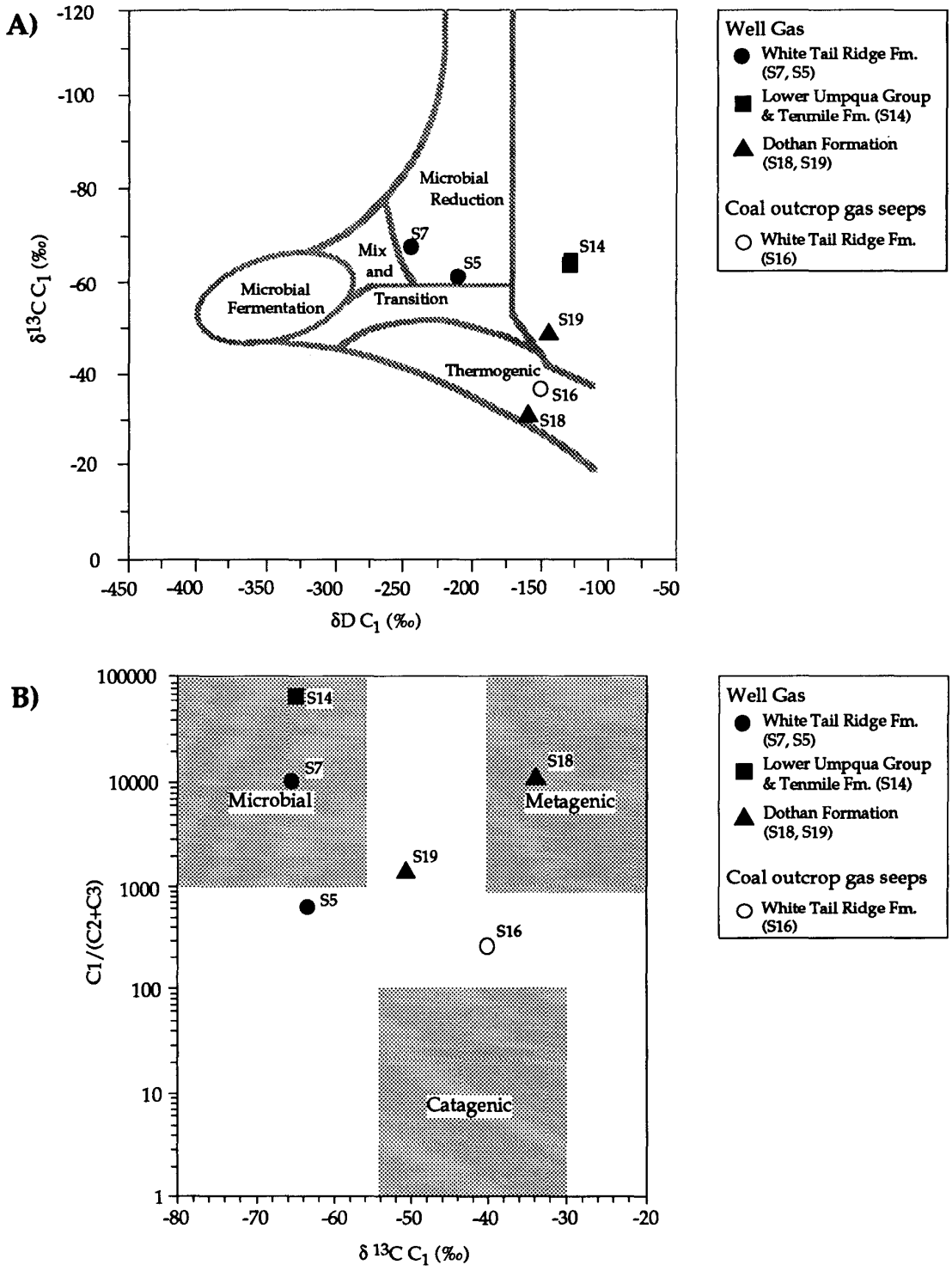

Figure 4.25 (A) $\delta^{13}C\ C_1$ (‰) versus $\delta D\ C_1$ (‰) plot of thermogenic and biogenic methane from natural seeps and water wells, Tyee basin. (B) C_1/C_2+C_3 versus $\delta^{13}C\ C_1$ (‰) plot of Tyee basin methane from natural seeps and water well gas samples, showing peak generation areas of microbial (biogenic), metagenic, and catagenic gases (from Kvenvolden and others, 1995).

are predominantly methane (C_1; >99.8%, typical of very dry gas; Scott, 1993) and contain minor to trace amounts of C_2, C_3, C_4, C_5 and carbon dioxide. The C_1/C_2+C_3 ratios of these gases are high (i.e., 290 to >100,000; Fig. 4.25B). The methane displays a wide range of isotopic compositions (carbon $\delta^{13}C$ and deuterium δD; Figs. 4.25A and 4.25B). The isotopes suggest that both thermogenic and biogenic methane are present and that some gas samples are mixtures of both thermogenic and biogenic methane.

One thermogenic gas sample was collected from a water well drilled in pre-Tertiary mélange and broken formation (Dothan Formation [Sixes River terrane of Kvenvolden and others, 1995]) in the northern Klamath Mountains (S18 on Fig. 4.24). It contained isotopically heavy methane ($\delta^{13}C$ value of -33.3 and δD value of -155). Another Klamath Mountains water well gas sample has an isotopic composition that appears to be a mixture of biogenic and thermogenic methane (i.e., $\delta^{13}C$ of -50.6 and δD of -134; Fig. 4.25B). The isobutane to normal butane ratios of gas samples from these two shallow (<100 ft) Klamath Mountains water wells are similar to absorbed gas released by crushing Klamath Mountains turbidite sandstone, mudstone, and limestone samples from nearby outcrops (Kvenvolden and others, 1995). This similarity suggests that the thermogenic gases from the shallow water wells were derived *in situ* from these pre-Tertiary marine rocks which were formerly more deeply buried and which have been intensely deformed and fractured during the subduction and accretion process. In the southern Tyee basin, thrust faults which bound tectonic blocks of locally mélanged and broken formation (Dothan strata) and/or deeply subducted lower Umpqua turbidite sandstone and mudstone may serve as conduits for migration of thermally mature gas into the overlying, less deformed, thermally immature strata of the Tyee and Coos Bay forearc basins (Kvenvolden and others, 1995). Some natural gas issues from fractures and joints in lower Umpqua turbidite strata associated with these thrusts (e.g., S23, Table 4.5) (Seeley, 1989, pers. commun. in Niem and Niem, 1990).

Dry thermogenic methane derived from Type II and Type III organic matter normally requires a higher level of thermal maturation (i.e., R_o >0.8; Scott, 1993) than normally present in outcrop and exploration well samples of the Tyee basin and northern Klamath Mountains. For example, one gas sample extracted from cleats in a fresh roadcut exposure of thermally submature coal in the gently deformed White Tail Ridge Formation (upper Umpqua Group)(i.e., R_o <0.6% and T_{max} <435°C) contains isotopically heavy methane (S16 on Fig. 4.25A). This thermogenic gas could have migrated up faults and microfractures from underlying thrust blocks of thermally matured Klamath Mountains mélanged strata and/or from more deeply buried and subducted lower Umpqua turbidites and slope mudstone (Kvenvolden and others, 1994, 1995). Similarly, in the upper Eocene strata (Coaledo Formation) of the Coos Bay forearc basin, thermally immature coals (i.e., R_o <0.4) cored in an exploration well at depths of 1200 and 1260 ft released dry methane that displays thermogenic carbon and deuterium isotopic signatures (Pappajohn, 1993, pers. commun.; Kvenvolden and others, 1994; Kvenvolden and others, 1995). Alternatively, the apparent thermogenic or heavy isotopic signature of these dry methane samples (Fig. 4.25A and 4.25B) may be the result of heretofore unexplained isotopic fractionation related to desorption, diffusion, and/or bacterial metabolic processes which generated these gases *in situ* from these thermally immature coals after uplift and erosion (Scott, 1993).

Biogenic methane and carbon dioxide are prevalent in the coal-bearing members of the White Tail Ridge Formation in Lookingglass Valley and Camas Valley, especially west of Melrose (e.g., S5 and S7 on Fig. 4.24). Small pockets of methane are encountered by shallow water wells (i.e., <200 ft deep). The biogenic gas appears to be coalbed gases derived *in situ* from subbituminous coals and carbonaceous mudstones in the gently deformed deltaic Remote and Coquille River members of the White Tail Ridge Formation (upper Umpqua Group) (Kvenvolden and others, 1995). Microbial dry methane also occurs in thin-bedded slope mudstone and turbidites of the Tenmile Formation in Camas Valley (S14 on Figs. 4.25B and 4.24). These biogenic gases from water wells in the Tyee basin are characterized by isotopically light methane; i.e., $\delta^{13}C$ values of -64.8, -63.9, and -64.9‰ and δD values of -245, -207, and -123‰ (Figs. 4.25A and 4.25B). The biogenic gases probably formed *in situ* through secondary or late-stage microbial reduction

associated with groundwater flow after uplift and erosion of these shallow-buried thermally immature coals and carbonaceous overbank mudstone (Fig. 4.25A).

Similar late-stage or secondary dry gases composed largely of isotopically light methane are common in the U.S., China, and elsewhere in the world (Rice, 1993; Scott, 1993). These gases occur in the zone of alteration (shallow burial; tens to thousands of feet) associated with active groundwater flow in regional coal aquifers. These conditions favor aerobic oxidation of the coal and carbonaceous organic matter (in the adjacent sandstone and mudstone beds) which produces food for methanogens (anaerobic bacteria) that metabolize and form methane when dissolved oxygen in the groundwater in the coals is depleted (Rice, 1993; Scott, 1993). Thus, the biogenic gas in the Tyee basin could have been generated by degradation of organic matter in coal in the late stage of geologic history (i.e., last 10,000 to 100,000 years) after uplift and erosion of the Coast Range and in association with groundwater flow. It may still be forming today. The natural gas may have migrated short distances from the coals and carbonaceous mudstone into adjacent sandstone beds by desorption and diffusion as meteoric water pressure was reduced by uplift and erosion and/or by pumping water wells.

Alternatively, this biogenic methane may have been generated by methanogens in deltaic coals of the White Tail Ridge, Tyee, Spencer, and Bateman formations during the early stages of coalification at shallow burial depth and at low temperatures in the Eocene. Scott (1993), however, thinks that much of this early-stage biogenic methane is lost to the atmosphere or is lost by dissolution in groundwater migrating through the porous peats and lignites.

Dry methane with a broad range and mixture of both thermogenic and biogenic isotopic signatures similar to gases sampled in the Tyee basin is common in exploration and water wells throughout the Pacific Northwest, including the Mist Gas Field of northwestern Oregon (e.g., Armentrout and Suek, 1985; Snavely and Kvenvolden, 1988; Kvenvolden and others, 1989; Stormberg, 1992; Johnson and others, 1993). The principal source rocks appear to be coals and/or lean mudstone source rocks of marine origin in which the organic matter is mostly gas-prone terrestrial Type III and Type II similar to Tyee basin strata.

Recently, Mango and others (1994) suggested from experimental studies that natural gas (largely methane) with a wide variation of isotopic compositions (as displayed by Tyee basin gas samples) can be generated from carbonaceous sedimentary rocks under relatively shallow burial and mild temperatures (approx. 200°C) due to catalytic action of transition metals. This catalytic process could explain the wide variation of isotopic compositions and mixtures of both "thermogenic" and "biogenic" dry methane in seemingly thermally immature carbonaceous source rocks, coals, and adjacent reservoir sandstones in the Tyee basin and other basins of the Pacific Northwest. This explanation would eliminate the elaborate deep burial generative processes and migration pathways for production of thermogenic natural gas (methane) as proposed here and for other Pacific Northwest basins (e.g., Stormberg, 1992; Kvenvolden and others, 1989). Ongoing studies of Pacific Northwest carbonaceous and coal samples are now being tested under laboratory conditions to determine if this is the case (Mango, 1995, pers. commun.). It is important to note that, regardless of whether this gas (methane) is thermogenic or biogenic in origin, it can accumulate in commercial quantities in Eocene deltaic reservoir sandstones in the Pacific Northwest, as in the Mist Gas Field of northwest Oregon.

BASIN SUBSIDENCE HISTORY AND KINETIC MODEL FOR HYDROCARBON GENERATION

In the preceding section, the source rock potential of Tyee basin units is evaluated in terms of source rock generative potential, type of hydrocarbon generated, and level of thermal maturity. The timing of hydrocarbon generation and expulsion (if any) from these source rocks can be evaluated further by reconstructing the geohistory of basin subsidence and uplift. A computer program, BasinMod, which was developed recently by Pratt River Associates, Inc., models the burial history of stratigraphic units and uses a kinetic model approach. This kinetic model simulates the evolution of hydrocarbons from three different types of organic matter (Type I, II, and III) against burial depth and geologic time, and provides a quantitative evaluation of the types of hydrocarbons that could (if any) have been generated during basin subsidence and later uplift. It also identifies which stratigraphic unit(s) could generate hydrocarbons.

A composite section representing 45 measured sections and 11 oil and gas exploration wells of Ryu and others (1992) was used to reconstruct the burial history of the southern Tyee basin. Table 5.1, in the Appendix, lists the stratigraphic thicknesses, ages, lithologies, porosities and permeabilities, and paleobathymetry entered as data from which the program calculated and drew this subsidence model. Thicknesses of stratigraphic units were decompacted using the Falvey and Middleton (1981) equation; a residual subsidence curve, derived by assuming Airy isostacy, adjusted for isostatic rebound. Paleobathymetry and age of various Tyee basin units are based on analysis and interpretation of assemblages of benthonic foraminifers, mollusks, and coccoliths (McKeel, Moore, and Bukry, 1989-94, written communications) and on radiometric dates.

The burial subsidence model created from the composite section suggests that rapid deposition of Tyee basin sediment was initiated at 54 Ma. The time-depth history of the sediment, since deposition, is shown by the solid lines in Figure 5.1. The burial history consisted of very rapid rates of subsidence and sediment deposition in the early and middle Eocene (i.e., most Tyee basin units) until 37 Ma, at which time there was a brief period of uplift. Uplift was followed by renewed subsidence at a slower rate during deposition of upper Eocene to lower Miocene Coos Bay basin strata. At 15 Ma, uplift of the southern Coast Range began at a rapid rate in the late-middle Miocene (6,000 to 10,000 ft). According to Niem and others (1992c), the uplift rate slowed in the Pliocene and Pleistocene but continues today. The Tyee basin sediment is now (time=0) at a depth of 0 to 20,000 feet. However, because the locus of sediment deposition changed during the history of the basin (i.e., in the early to middle Eocene; Ryu and others, 1992), this composite thickness overgeneralizes the total subsidence of the basin. Exploration wells penetrate <15,000 feet of strata overlying the Siletz River Volcanics. The overlying Coos Bay basin strata and Western Cascades volcanics which had overlaid the Eocene Tyee basin strata were entirely eroded off due to continual uplift after 15 Ma (Fig. 5.1). Today, the Coos Bay basin strata are only partially preserved in a structural downwarp along the western margin of the Tyee basin. Western Cascades arc volcanics form a major topographic high on the eastern flank of the Tyee basin.

The second aspect of the BasinMod burial subsidence model is reconstruction of the temperature history of the basin. The subsurface temperature must be specified for every depth throughout the geologic past. The simplest way to do this is to determine the present geothermal gradient by using bottom-hole temperatures from exploration wells in the basin and assume that the temperature history of the basin has been constant throughout the time interval covered by the burial subsidence model. Bottom hole temperatures from 10 exploration wells in the Tyee basin were used to calculate the average geothermal gradient for each well and a regional

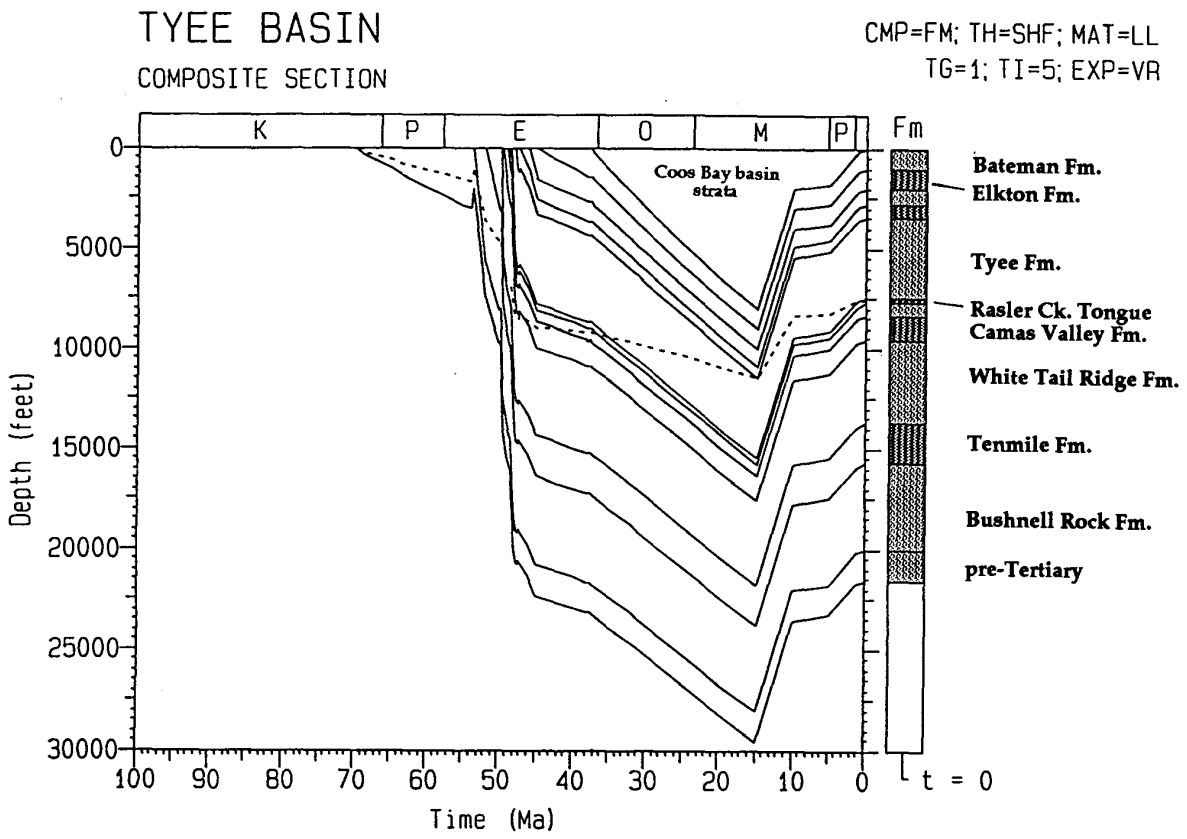

Figure 5.1 Burial subsidence model of Tyee basin stratigraphic units using a composite section (Ryu and others, 1992). Dotted line represents tectonic subsidence curve. Stratigraphic units were decompacted using Falvey and Middleton (CMP=FM) equation (1981). Thermal history (TH) is calculated using a steady state heat flow (SHF). Maturity (MAT) was derived from Lawrence Livermore National Laboratories Easy %Ro (LL). TG is thermal gain. TI is time interval for calculation of maturity and expulsion. Expulsion (EXP) is based on vitrinite reflectance (VR).

gradient was calculated as an average of all 10 wells (Table 5.2 in Appendix; Fig. 5.2). The average regional geothermal gradient in the Tyee basin is 1.27°F/100 feet. This value is higher than the average geothermal gradient from uncorrected bottom-hole temperatures of other wells in the Pacific Northwest and the world average geothermal gradient of forearc basins applied by Brown and Ruth (1983). This higher than expected geothermal gradient might be due to the anomalously high values of 1.81°F/100ft, 1.54°F/100ft, and 1.46°F/100ft in the Scott, Amoco F-1, and Harris 1-4 wells (Table 5.2 in Appendix). There may also not have been sufficient time after drilling ceased for the drilling mud to cool before these bottom hole temperatures were taken. If these wells are excluded from the data base, the average

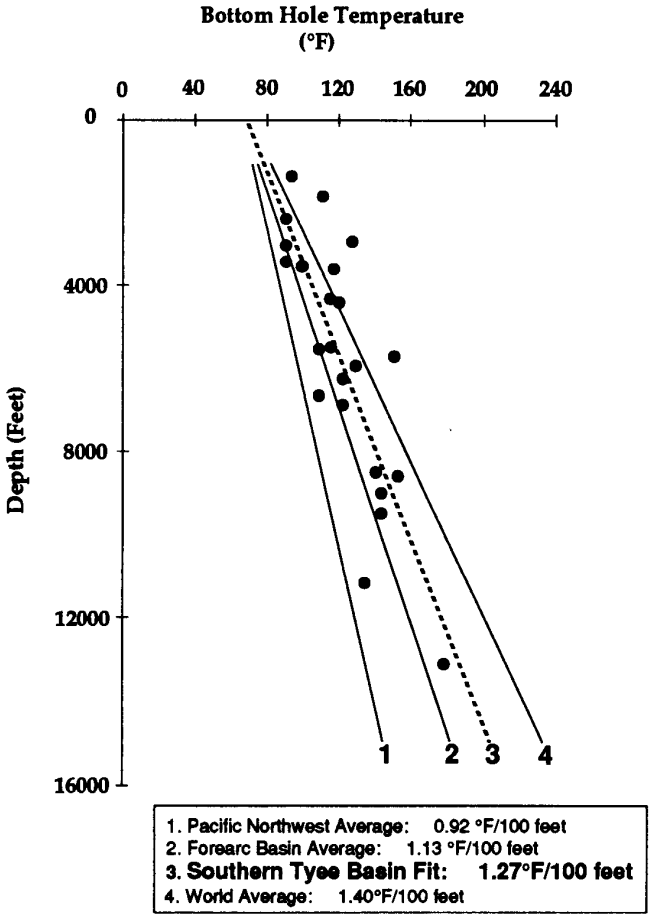

Figure 5.2 Linear plot (dashed line) of the average geothermal gradient for the Tyee basin (1.27°F/100 feet) based upon bottom-hole temperature measurements (solid circles) at known depths of 10 wells in the basin. Bottom-hole temperatures were obtained from electric-log header data from the wells. Other lines are for comparison with geothermal gradients elsewhere in the world (modified from Brown and Ruth, 1983).

gradient for Tyee basin wells is 1.12°F/100ft which is closer to the forearc basin average. The average geothermal gradient of 1.27°F/100ft is µsed, however, to reconstruct thermal history in the basin and is plotted on the burial subsidence and kinetic models as an isotherm (Fig 5.3). The isotherms (dotted lines) in Figure 5.3 thus represent the subsurface temperature during geologic time.

Time and temperature are important factors in modeling hydrocarbon generation and expulsion from potential source rocks in a basin (Lopatin, 1971). These two factors are interchangeable; high temperatures acting for a short time can have the same effect on thermal maturation of potential source rocks as a lower temperature acting over a longer time. Lopatin (1971) assumed that the relationship of maturity to time is linear; that is, doubling the cooking time at a constant temperature doubles the maturity (i.e., R_0 and Tmax). Using the average geothermal gradient and the geologic age of each Tyee basin unit, the maturation level of each stratigraphic unit (i.e., Time Temperature Index, abbreviated TTI) can be calculated, assuming that the maturity reaction doubles for every 10°C increase in temperature (Lopatin, 1971). The resulting TTI value is then converted to vitrinite reflectance value and a maturity model is

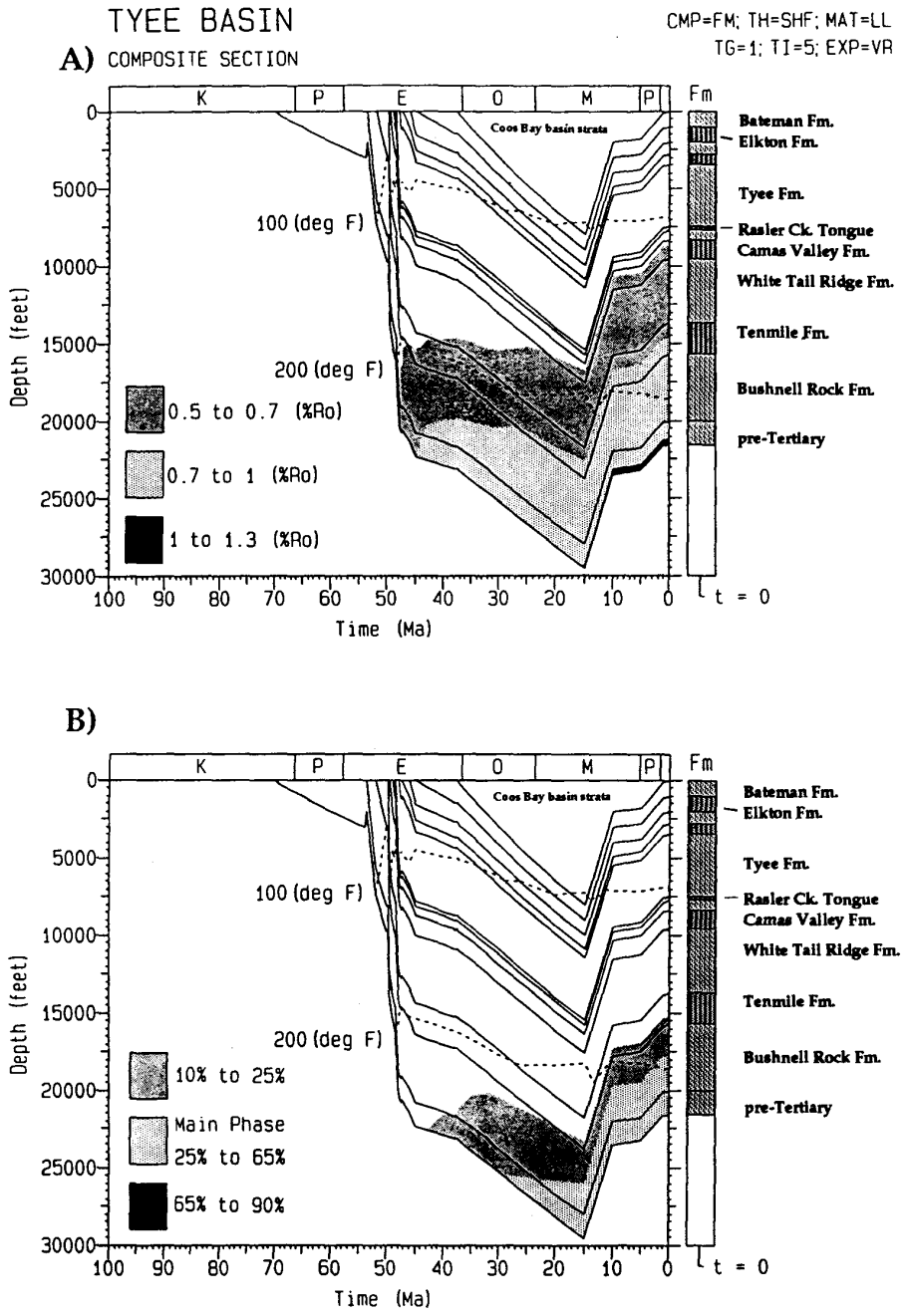

Figure 5.3 Maturity model (A) and kinetic model (B) superimposed on the burial subsidence model for the composite section of Tyee basin. Dotted lines represent isotherms. The maturity model shows that, at a depth of 14,500 feet, potential source rocks would generate oil and wet-gas if they contain Type II and Type III organic matter. The kinetic model indicates that the middle part of the Bushnell Rock Formation and pre-Tertiary units would be in the main phase of hydrocarbon generation and expulsion.

constructed showing the level of maturation of each unit (Fig. 5.3A). This maturity model derived from TTI value is adjusted (as necessary due to the geothermal gradient) until the calculated vitrinite reflectance values match the measured vitrinite reflectance values.

The maturity model suggests that lower Umpqua strata (e.g., Bushnell Rock Formation) first attained a vitrinite reflectance value of 0.7 $\%R_0$ during the middle Eocene (43 Ma). The model predicts that this level of maturity is now encountered in the middle part of the Tenmile Formation at a depth of 14,500 feet (Fig. 5.3A). Deeper than 14,500 feet, source rocks reached sufficiently high levels of thermal maturity (0.7 to 1.0 $\%R_0$) to have generated thermogenic wet-gas. Also source rocks at depths of 8,750 to 14,500 feet (White Tail Ridge and Camas Valley formations) are sufficiently mature (0.5 to 0.7 $\%R_0$) to generate oil. However, potential source rocks overlying the Camas Valley Formation (e.g., Rasler Creek Tongue and Tyee, Elkton, and Bateman formations) have not been buried deep enough to generate significant amounts of thermogenic wet gas or oil even though some units contain organic rich coals and carbonaceous mudstones (Fig. 5.3A).

Combining calculated vitrinite reflectance values with total organic carbon content (TOC) and type of organic matter (Type I, II, or III), the expulsion efficiency (the amount of hydrocarbons expelled from a given source rock), is calculated to construct the kinetic model for the basin as shown in Figure 5.3B. Because the organic matter is predominantly Type III in the Tyee basin, the hydrocarbons expelled from source rocks would be mainly thermogenic dry-gas (methane). This model does not include shallow-burial biogenic methane. The kinetic model indicates that, at present (t=0), the lower part of the Bushnell Rock Formation and pre-Tertiary mudstones are in the main phase of thermogenic gas generation and expulsion at depths greater than 17,500 feet (Fig 5.3B). The gas generation and expulsion from these units started at a burial depth of 22,500 feet during late-middle Eocene time (43 Ma). There is no evidence that these rocks were ever buried to such a depth based on Tmax and R_0 measurements and thickness of stratigraphic sections (Ryu and others, 1992). The only exceptions are the pre-Tertiary units and some Umpqua strata that may have been subducted to great depth beneath the Klamath terranes in the early Eocene. However, that also is speculation. More realistic results might be obtained by using specific wells to generate the models rather than using a composite section for this tectonically active setting. For example, the locus of sediment deposition shifted through geologic time, and there were periods of uplift in the late-middle Eocene and late Eocene. Neither of these is factored into these simplified computer-generated models (see discussion in the next section).

PETROLEUM SYSTEMS OF THE TYEE BASIN

Magoon (1988) developed the concept of the **"petroleum system"** which emphasizes or implies the genetic relationship between a particular source rock and the resulting petroleum (or natural gas) accumulation. In contrast, basin analysis concerns a study of a structural or sedimentary depression and the lenticular body or prism of sedimentary rocks within that depression, regardless of any relationship to hydrocarbon accumulations. A petroleum system may occur within a part or all of the sedimentary basin or may extend beyond the borders of a basin into the adjacent geologic provinces.

A **play**, according to Magoon (1988), tells whether the existing trap is detectable with geological, geophysical, or geochemical technology. A play need not include all the elements of a petroleum system. A **prospect** is a drillable trap within a play. The Petroleum Geology Branch of the U.S. Geological Survey has utilized the petroleum system (Magoon, 1988, 1990, 1992) and more recently the play concept in that agency's assessment of the petroleum potential of the United States, including the Pacific Northwest (Gautier and Varnes, 1993).

In order to better organize and synthesize source rock, maturation, porosity, permeability, and structural data to understand the oil and gas potential of this study area, we have followed Magoon's (1988) methodology for identifying petroleum systems and plays in the Tyee basin. We believe that the source rocks, maturation, migration paths, potential traps, and reservoir rocks are more likely to exist in some areas within the basin, in areas overlapped by the adjacent Western Cascades volcanic arc, and beyond the basin limits in the Mesozoic Dothan Formation of the northern Klamath Mountains borderland. Thus, we do not restrict our approach to basin analysis.

The elements of a petroleum system, according to Magoon (1988) include: (1) a source rock for petroleum; (2) migration path(s); (3) reservoir rock; (4) seal; (5) trap; and the geologic processes that form these elements. All these elements must be appropriately arranged in space and time such that organic matter in the source rock can be matured or converted to petroleum and migrate into petroleum accumulations. The areal extent of a petroleum system can be delineated by a line which circumscribes both mature source rock and oil or gas accumulations (Fig. 6.1).

Magoon (1988) proposed the following conventions for naming petroleum systems. The system name should consist of the name of the source rocks, followed by the name of the major reservoir rock, followed by a symbol that indicates the level of certainty.

Magoon (1988) classified petroleum systems into three levels of certainty: known, hypothetical, and speculative. In a known petroleum system, there is a good geochemical match between the source rocks and the existing oil or gas accumulation. In a hypothetical petroleum system, there are geochemical data that identify a source rock but don't match the source rock to a known oil or natural gas accumulation (e.g., Mist Gas Field, northwest Oregon). In a speculative petroleum system, geological or geophysical evidence is used to postulate the existence of a link between source rocks and potential oil and/or gas accumulations.

If a petroleum system can be identified for a geographical area, it then can be classified into one of 12 categories based upon: (a) type of source rock (i.e., I, II, or III); (b) reservoir rock composition; and (c) whether the system is purebred or a hybrid (Magoon, 1988). In a purebred system, the structural framework did not change during the geologic existence of the system. In a hybrid system, there is a major structural reorientation from that which created the petroleum system.

The level of certainty for any petroleum system is indicated by a punctuation mark within parentheses following the name of the system. For example, the name of a known petroleum system is followed by an exclamation point within parentheses; i.e., (!). Similarly, a hypothetical petroleum system is indicated by (.) following the name; and a speculative system is indicated by (?) following the name.

Following Magoon's (1988) petroleum systems methodology, we have identified three speculative petroleum systems in the southern Tyee basin: Umpqua-Dothan-White Tail Ridge(?) hybrid petroleum system; Umpqua-lower Tyee Mountain(?) petroleum system; and Spencer-White Tail Ridge-Western Cascade Arc(?) petroleum system. Figs. 6.1, 6.2, and 6.3 are a map and schematic cross sections of the Tyee-Umpqua basin and bordering geologic provinces. These figures depict the hypothetical or speculative areal extent of petroleum systems and potential plays within each system. A heavy boundary line circumscribes the hypothetical or speculative petroleum deposits and the location of the source rocks that could have generated hydrocarbons in those accumulations.

Umpqua-Dothan-White Tail Ridge(?) Hybrid Petroleum System

Figure 6.1 is a map of the southern Tyee basin and surrounding geologic provinces; Figure 6.2 is a NNW-SSE cross section in late Eocene time, showing the production of dry gas (methane) from two sources. Biogenic methane is produced *in situ* from coal and overbank carbonaceous mudstone source beds (largely Type III organic matter) in deltaic units, such as the Remote Member of the lower Eocene White Tail Ridge Formation. This natural gas may have migrated into stratigraphic traps in adjacent distributary channel sandstone and into up-dip pinch outs of delta front sandstone (e.g., Berry Creek and Coquille River members). Seals include neritic shelf/slope mudstone of the Camas Valley Formation. Isotopic and field studies indicate that biogenic gas in water wells in these deltaic-coastal plain units is largely derived from degassing of coals and disseminated plant debris in overbank carbonaceous mudstone and fine-grained sandstone (Kvenvolden and others, 1995). Coals also could act as fractured gas reservoirs for coalbed gases (e.g., methane and CO_2) particularly if matured to bituminous grade (Pappajohn, 1994, pers. commun.). The other source for dry gas (methane) is deeply buried lower Eocene-Paleocene and pre-Tertiary sedimentary units.

A maturity model (Lopatin diagram) was computed from the Twelvemile Creek measured section of Ryu and others (1992) (Fig. 6.4A). This model indicates that below a depth of 8,500 feet potential source rocks in the lower Umpqua Group (lower part of the Tenmile Formation and Bushnell Rock Formation) and pre-Tertiary Klamath terranes would have reached sufficiently high levels of thermal maturity (>0.7%) by the middle Eocene to have generated wet-gas and oil (Fig. 6.4A). Gas-prone Type III organic matter in pre-Tertiary strata would have had an R_0 of 1.0 to 1.3 at depths greater than 14,500 feet by the middle Miocene (Fig. 6.4A). The kinetic model predicts that, at present, the lower part of the Bushnell Rock Formation and pre-Tertiary Dothan Formation are in the main phase of gas generation and expulsion at depths greater than 11,750 feet (Fig. 6.4B).

Lower Umpqua Group strata may be more deeply buried in thrust slices interleaved with thrust slices of Mesozoic Dothan Formation and mélange beneath the northern margin of the Klamath Mountains as a result of partial subduction or underthrusting (Figs. 6.1 and 6.2). Carbon and deuterium isotopic studies of natural gas from water wells which were drilled in Mesozoic mélange indicate that the dry gas is thermogenic (metagenic) and was generated from Type III terrestrial organic matter (Kvenvolden and others, 1994). The gas could have migrated up along thrust faults into overlying deltaic White Tail Ridge sandstone and coal beds (Fig. 6.2). Field data suggest that small quantities of natural gas are migrating and seeping out of fractured rocks associated with these thrusts (e.g., Bonanza fault zone; Fig. 4.24); some seeps emit thermogenic gas (e.g., S16 on Fig. 4.24, 4.25A, and 4.25B).

The metagenic dry gas could also have been formed earlier in the Late Cretaceous to Paleocene during mélanging and subduction of Mesozoic to lower Eocene potential source rocks (Types II and III organic matter). This dry gas could then migrate into the overlying thermally immature to submature upper Umpqua deltaic reservoir sandstone (i.e., White Tail Ridge Formation) and possibly into fractured and jointed sandstone and conglomerate reservoirs in the Bushnell Rock, Tenmile, and lower Umpqua turbidite strata. The Camas Valley mudstone and diagenetically tight sandstone and mudstone of the Tyee Formation could act as a seal for natural gas accumulations west of the Tyee escarpment (Figs. 6.1 and 6.2).

Some potential sandstone reservoir bodies in the deltaic White Tail Ridge Formation (i.e.,

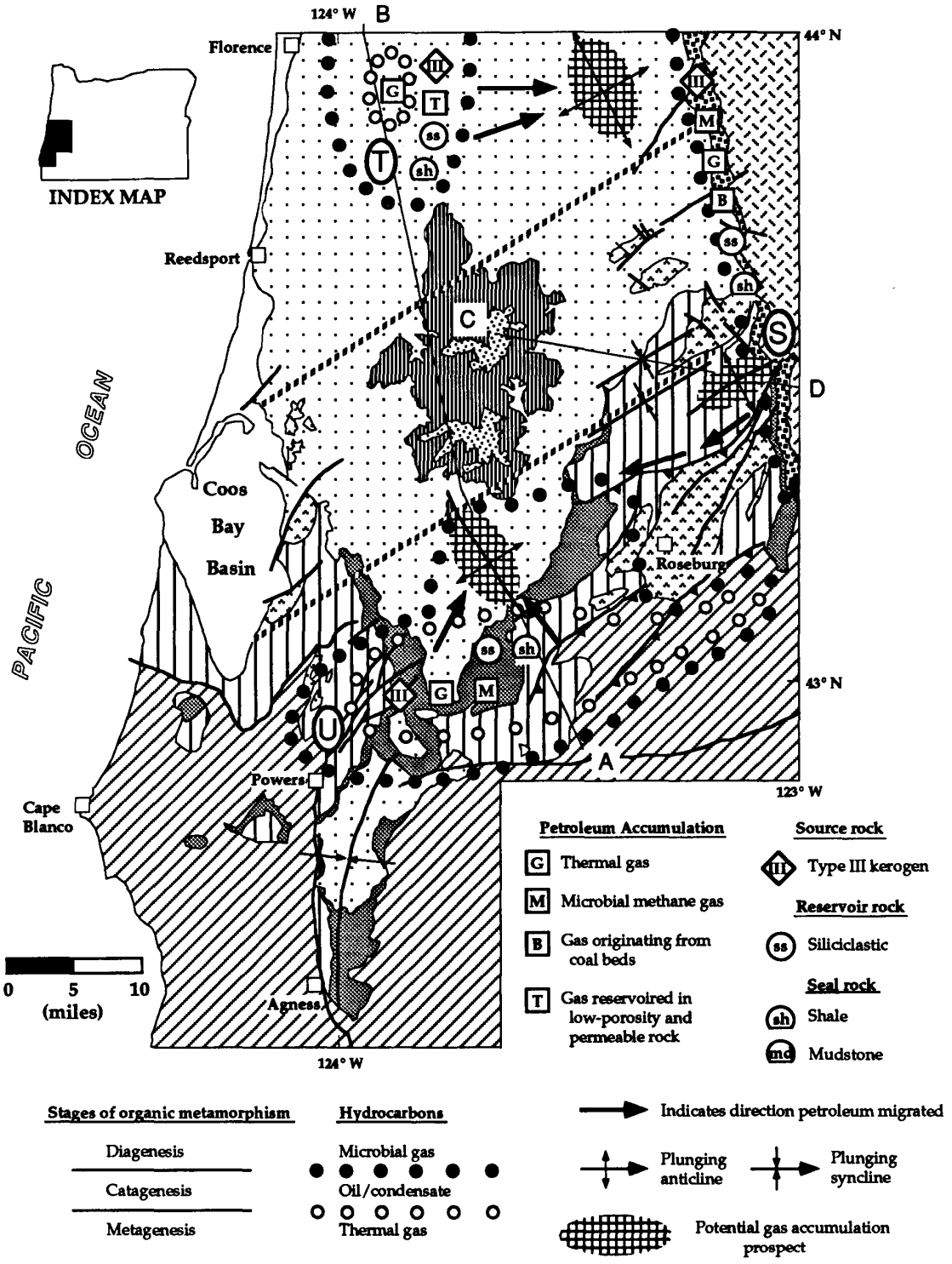

Figure 6.1 Generalized geologic map of the southern Tyee basin and surrounding geologic provinces (i.e., Western Cascade arc, Coos Bay basin, and Klamath Mountains), showing the areal extent of speculative(?) petroleum systems: (U) Umpqua-Dothan-White Tail Ridge(?) hybrid petroleum system; (T) Umpqua-lower Tyee Mountain(?) petroleum system; and (S) Spencer-White Tail Ridge-Western Cascade Arc(?) petroleum system. Lines AB and CD indicate schematic cross sections AB and CD in Figs. 6.2 and 6.3.

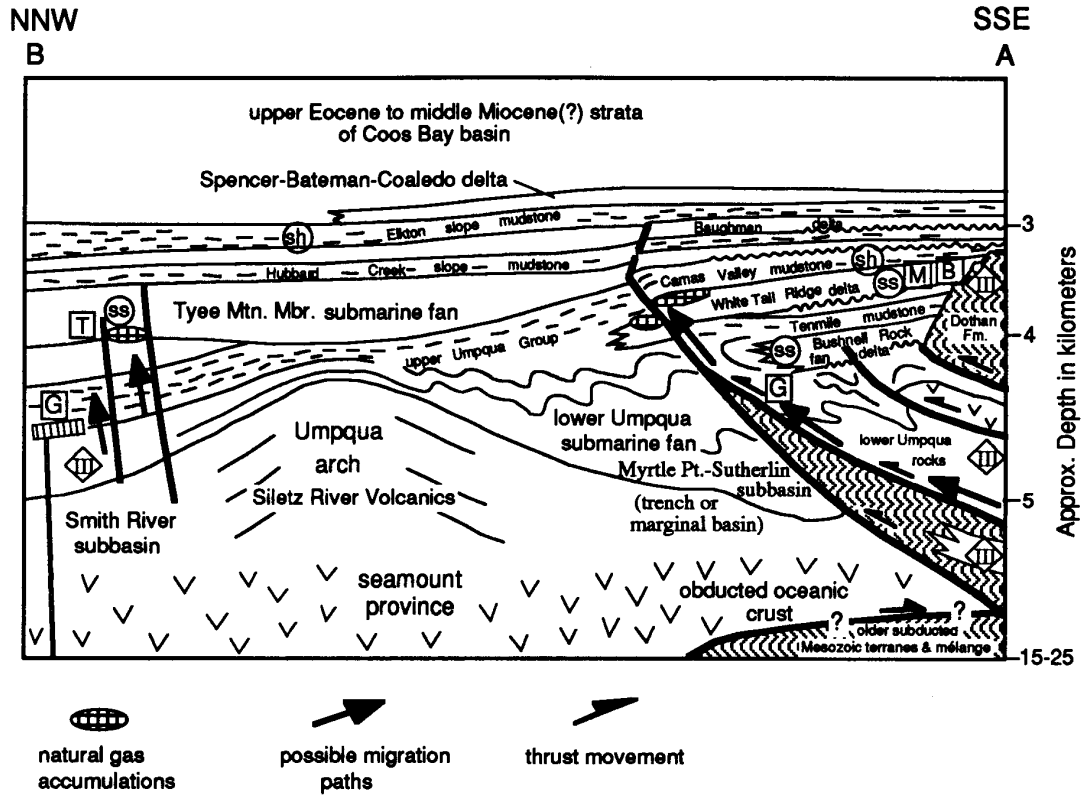

Figure 6.2 Schematic geologic cross section showing the Umpqua-Dothan-White Tail Ridge(?) hybrid petroleum system and the Umpqua-lower Tyee Mountain(?) petroleum system in the southern Tyee basin at the end of the late Eocene to the late-middle Miocene.

Coquille River Member) are also involved in or overlie fault-propagation folds associated with renewed movement on blind thrusts (e.g., Reston high of Ryu and others, 1992) that were formed during underthrusting or subduction as the Umpqua Group and Siletz River Volcanic crust were accreted to North America (i.e., Mesozoic Klamath Mountains). These structural traps were created prior to subsidence of the Tyee forearc basin and deposition of the upper White Tail Ridge (Remote Member and Rasler Creek Tongue), delta/submarine fan of the Tyee Formation, Elkton slope mudstone, and Bateman-Spencer-Coaledo formations and younger Coos Bay basin siliciclastic strata (3,000 m, upper Eocene to upper Miocene).

Metagenic natural gas in the Umpqua-Dothan-White Tail Ridge (?) petroleum system was generated and started to migrate in the late-early Eocene during early deformation of the Umpqua basin associated with accretion. Later, subsidence created the Tyee forearc basin which trends obliquely across the strike (Ryu and others, 1992; Figs. 4.1 and 6.2). Therefore, this system would be classified as a hybrid petroleum system. In addition, because there is no known connection between the potential source rocks and potential reservoir rocks/traps and no large accumulations of natural gas (i.e., commercial gas pools) are known to exist, the Umpqua-Dothan-White Tail Ridge(?) petroleum system is speculative.

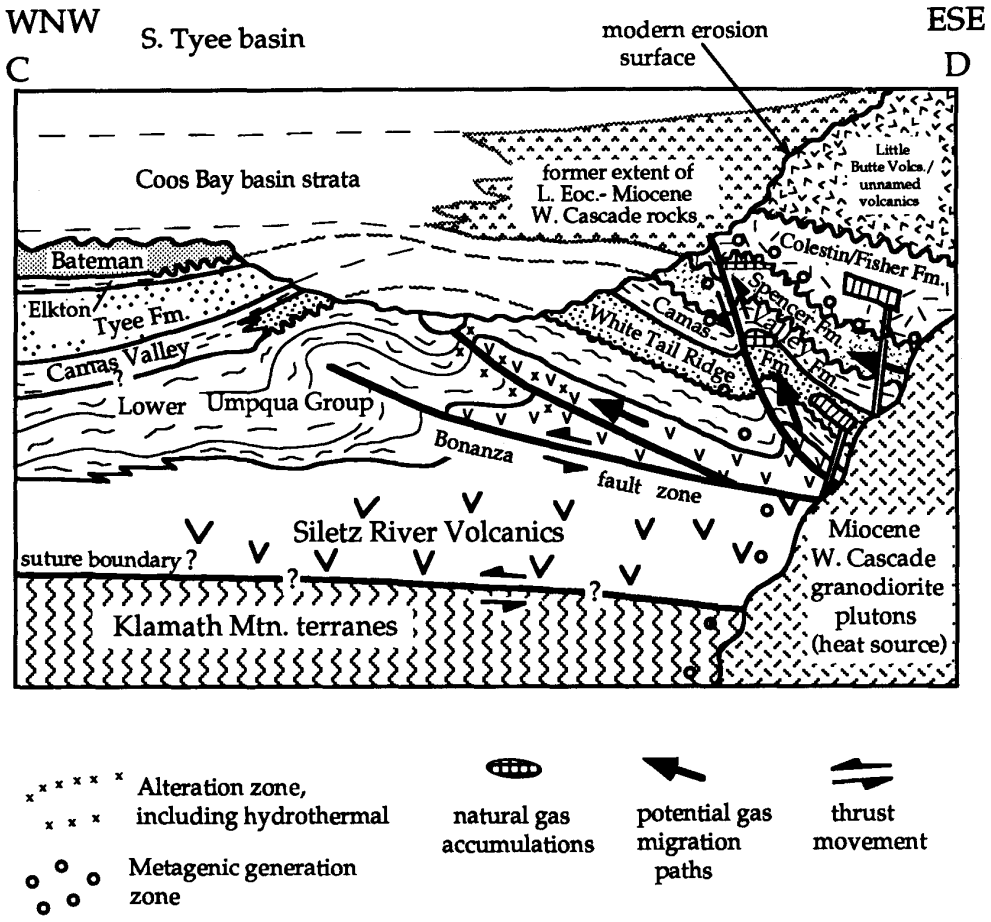

Figure. 6.3 Schematic geologic cross section showing White Tail Ridge-Spencer Western Cascades arc(?) hybrid petroleum system in the southern Tyee basin in late Miocene time.

Except for the area west of the Tyee escarpment, much of the Umpqua-Dothan-White Tail Ridge (?) petroleum system has been breached by erosion since uplift of the southern Coast Range which began in the late-middle Miocene; only gas seeps remain (see Kvenvolden and others, 1995) (Fig. 6.1). Some oil shows also are reported in thrusts and fractured, thermally matured Bushnell Rock and Tenmile strata in the Scott No. 1 well near Melrose in the southern part of the Umpqua basin. There are also possible subthrust Umpqua plays beneath the northern margin of the Klamath Mountains and less likely some untested NE-SW-trending anticlines and blind thrusts in the lower Umpqua Group between Roseburg and Yoncalla north of the Umpqua arch and between Remote and Coquille (Fig. 6.1)

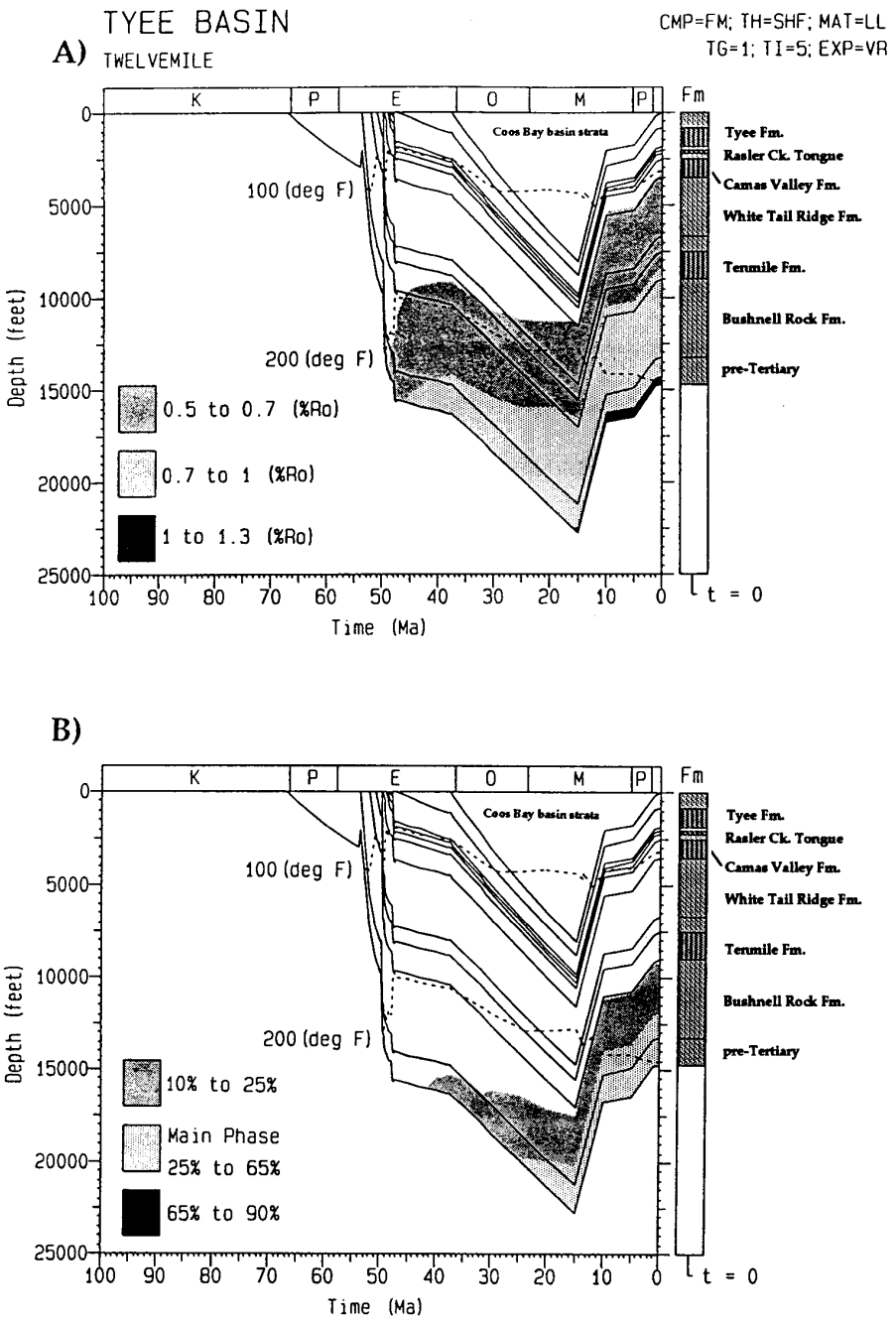

Figure 6.4 Maturity model (A) and kinetic model (B) for Umpqua-Sixes River-White Tail Ridge (?) hybrid petroleum system. Stratigraphic section for burial subsidence was measured along Twelvemile Creek south of the Reston High. Bottom-hole temperature of the nearby Great Discovery well is used to calculate a geothermal gradient for reconstruction of temperature history. Refer to Figure 5.1 for abbreviations in the upper right corner.

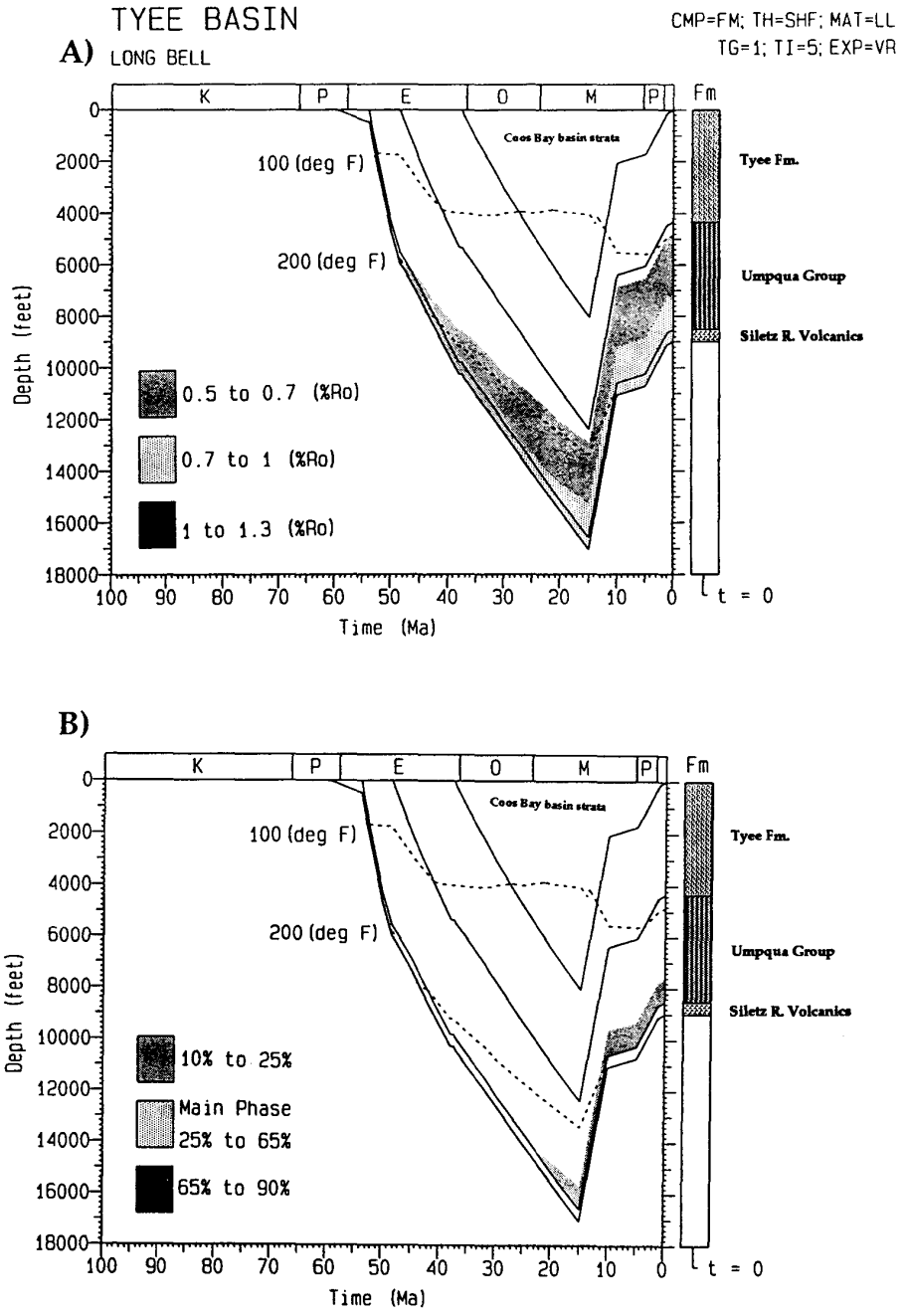

Figure 6.5 Maturity model (A) and kinetic model (B) for lower Umpqua-Tyee Mountain (?) hybrid petroleum system. These models were created with the BasinMod program, using data from the Long Bell well drilled in the Smith River subbasin of Ryu and others (1992). Thickness of Coos Bay basin strata are projected from the Coos Bay basin. Diagrams show that, at a depth of 9,000 feet in the late Eocene, lower Umpqua mudstones had reached sufficiently high levels of thermal maturity (>0.7% Ro) to have generated wet-gas and possibly oil but not metagenic dry gas. Refer to Figure 5.1 for abbreviations.

Umpqua-lower Tyee Mountain(?) Petroleum System; Basin Center Gas (?)

A second more speculative petroleum system may exist in the center of the Smith River subbasin of Ryu and others (1992) and is named the Umpqua-lower Tyee Mountain(?) petroleum system. This petroleum system may include a tight-gas sandstone reservoir. According to Law and Spencer (1993), "**tight-gas reservoirs** are gas-bearing rocks that usually have an *in-situ* permeability to gas of less than 0.1 md".

Maturity and kinetic models for the Smith River subbasin were created, using data from the Long Bell well (Figs. 6.5A and 6.5B). These models show that the lower Eocene Umpqua mudstone (Type III terrestrial gas-prone organic matter) could have been buried sufficiently deep to generate thermogenic wet-gas and oil at peak generation. Umpqua Group mudstone may have been buried by several thousand feet of submarine fan facies of the middle Eocene Tyee Mountain Member and by upper Eocene strata of the Coos Bay basin during the Oligocene. In addition, flash heating caused by basalt sills (e.g., at a depth of 5,595 feet in the Long Bell well; Figs 4.16 & 4.18) could have matured the gas-prone deep basinal Umpqua mudstones. The kinetic model for the Long Bell well suggests that the lower Umpqua Group entered the early phase of thermogenic gas generation in the Oligocene when burial depth exceeded 14,000 feet (Fig. 6.5B). The model predicts that, at present, the lower Umpqua Group is in the early phase of thermogenic gas generation at depths greater than 7,650 feet.

Gas could migrate up along faults and fractures to charge small accumulations in lower Tyee Mountain turbidite sandstones in which some secondary porosity and permeability has been noted (see Reservoir Potential section of this report; and Figs. 3.1 and 6.2). Mudstone beds and less permeable turbidite sandstones in the Tyee Mountain Member could act as seals although a seal and structural or stratigraphic traps are not necessary in tight-gas sandstone reservoirs (Law and Dickinson, 1985; Law and others, 1994; Law and Spencer, 1993). These accumulations may occur in untested anticlines which were formed in the Tyee Mountain Member in the late-middle Miocene in the northeastern part of the study area (see Tyee Mountain anticlinal plays in the Structural and Stratigraphic Plays section of this report). One of these structures was drilled by Florida Exploration (Harris 1-4 well; Fig. 4.2). The Umpqua arch, a buried seamount of Siletz River Volcanics southeast of the Long Bell well, has been drilled by three wells (i.e., Amoco Weyerhaeuser F-1, Amoco Weyerhaeuser B-1, and Northwest Exploration Sawyer Rapids). Only shows of gas were reported in those wells (Figs 4.24 and Table 4.4 in Appendix).

In addition to a basin-center tight-gas sandstone reservoir in the lower Tyee Mountain Member, an unconventional overpressured tight-gas mudstone reservoir is possible in the Umpqua Group in the Smith River subbasin. Law and others (1994) have suggested that an unconventional basin-center tight-gas reservoir mudstone or tight sandstone (permeability <0.1 md) may be present in the Tyee basin and in other Pacific Northwest basins. Tight-gas sandstone and mudstone reservoirs produce large quantities of natural gas in other North American basins (Law and others, 1994; Law and Dickinson, 1985; Law and Spencer, 1993). These tight-gas reservoirs are abnormally pressured (either underpressured or overpressured), low permeability (<0.1 md), low porosity (<1%), blanket and lenticular, marine, gas-bearing sandstone, mudstone (shale), and chalk. They can be characterized by overpressured zones, R_o >0.7% and gas-prone source rock with a kinked vitrinite reflectance profile (Spencer, 1987). In many cases, the source of the gas is interbedded shales and coals. There is no definable structural or stratigraphic trap, but the gas reservoir occurs in the deep basin-center downdip from water-bearing strata which act as an unconventional seal (Law and Dickinson, 1985).

An overpressured zone is present at a depth of 6,970 feet in the Long Bell well in the deeper part of the basin (Fig. 6.6). A projected vitrinite reflectance value at the top of the overpressured zone is approximately 0.7 to 0.95% which is sufficient to generate thermogenic wet-gas. Although the projected R_o value of >0.7% is high enough to generate gas from Type III organic matter and there is a kinked vitrinite reflectance profile that typifies overpressured gas reservoirs (Law and others, 1989), no measurements of R_o have been made of rocks within the overpressured zone.

According to Law and Spencer (1993), tight-gas reservoirs almost always require artificial

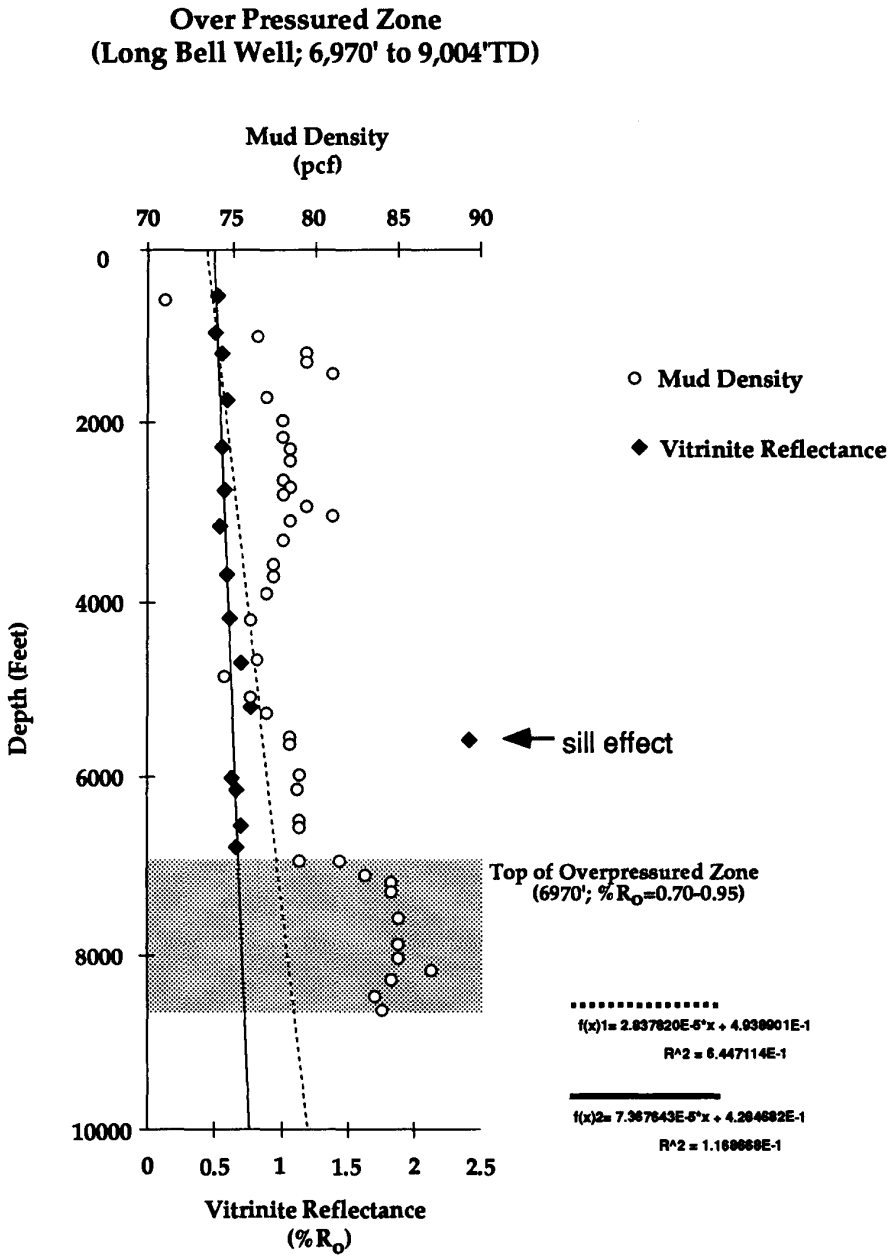

Figure 6.6 Mud-weight profile for the Long Bell well. Note the overpressured zone (stippled area) from 6,970 ft to 9,004 ft TD based on an abrupt increase in the density of the drilling mud (weight); data from mud log. Solid line represents the best fit of measured $\%R_O$ values (Brown and Ruth, 1983) without the baking effect of a basaltic sill at a depth of 5,595 ft. The dotted line represents best fit of measured $\%R_O$ values with a basaltic sill. Abrupt increase of mud density at a depth of 6,970 ft indicates the top of the overpressured zone. Projected vitrinite reflectance values at the top of overpressured zone are approximately 0.7 $\%R_O$ (without the effect of the sill) and 0.95 $\%R_O$ (with the effect of the sill).

stimulation (i.e., hydraulic fracturing) or special drilling (e.g., horizontal drilling) and completion in order to produce commercial quantities of gas because production depends on the presence of natural fractures. In the Tyee Formation, fractures are generally vertical and, therefore, would not be efficiently intersected by a vertical well bore. This may also be true for overpressured tight-gas sandstones in the White Tail Ridge Formation in the Umpqua-Dothan-White Tail Ridge(?) petroleum system discussed above.

Spencer-White Tail Ridge-Western Cascade Arc(?) Petroleum System

A third speculative petroleum system is the Spencer-White Tail Ridge-Western Cascade arc(?) system (Figs. 6.1 and 6.3). In this hybrid system, the source rocks are coals and carbonaceous overbank mudstone and sandstone of the Spencer Formation and White Tail Ridge Formation (Coquille River and Remote members). Less likely, lean to marginal source rocks (Type II and Type III organic matter) include the underlying lower Umpqua/Tenmile deep-marine mudstone and Camas Valley slope mudstone. The reservoirs would be fluvial cross-bedded arkosic sandstones in the delta plain facies (Remote Member and Spencer Formation) and fluvial-deltaic and delta front sandstones in the Coquille River and Berry Creek members (Ryu and others, 1992). These units dip homoclinally eastward beneath several thousand feet of upper Eocene to Miocene volcaniclastics, basalt and basaltic andesite lavas, and ash flow tuffs of the Western Cascades arc (Fig. 1.1). The volcanic sequence probably extended farther westward prior to erosion (Fig. 6.3).

Biogenic gas could be sourced from the coals and carbonaceous strata which contain Type III gas-prone organic matter. Thermogenic dry gas is likely to have been generated beneath the Western Cascades because of deep burial, because of heating by Western Cascades arc plutons (e.g., >1,000-ft thick andesite-basaltic andesite sills intrude these units in the Glide and Nonpareil area), and because of a generally higher geothermal gradient in the Western Cascade arc during the late Eocene to Miocene.

The maturity model for the Glide section predicts that potential source rocks in the Spencer, Camas Valley, White Tail Ridge, and Tenmile formations, buried by Western Cascade rocks below 14,000 feet, would have reached sufficiently high levels of thermal maturity (i.e., >0.7% R_o) to generate wet-gas and oil by the Miocene (Fig. 6.7A). Dry metagenic gas could be produced from Tenmile (lower Umpqua Group) source rocks at depths of 16,500 feet. The kinetic model indicates that, at present, the lower part of the White Tail Ridge Formation and upper part of the Tenmile Formation are in the main phase of wet-gas and oil generation and expulsion at depths ranging from 15,500 to 17,750 feet (Fig. 6.7B).

Several types of structural traps are possible. Reactivation of some thrusts in the Bonanza fault zone and associated fault-propagation folds in the late Eocene to Oligocene(?) deformed the friable Spencer deltaic reservoir sandstone into large asymmetrical folds (partly breached) in the Nonpareil-Glide area along the eastern margin of the Tyee basin (Fig. 6.3 and see Structural and Stratigraphic Plays section of this report). Faults recently mapped in the foothills of the Western Cascades by Wells and Niem, 1996; Wells, 1996b) may have created untested structures with natural gas accumulations (Fig. 6.3). The seal could be carbonaceous mudstone in the Spencer Formation or Camas Valley neritic mudstone over delta front and distributary channel White Tail Ridge reservoir sandstone. Thick, diagenetically altered, upper Eocene pyroclastic debris flow deposits, basaltic sandstone and conglomerate, tuffaceous strata, and ash flow tuffs could also act as seals.

Metagenic dry gas could be generated by Western Cascades granodioritic plutons and local thick andesitic sills intruding Spencer and White Tail Ridge coal-bearing strata at depth; the dry gas could then migrate updip (westward) through those units (Fig. 6.3). Similarly, Miocene and Oligocene(?) mercury sulfide (cinnabar)-, quartz-, and pyrite-bearing hydrothermal fluids from such plutons have apparently migrated westward updip and flowed through porous units under pressure in the Bonanza fault zone. The heat from these hydrothermal fluids resulted in alteration and mineralization of the fractured sedimentary rock along and above this fault zone for several miles along the eastern margin of the Tyee basin (Figs. 4.29 and 4.31)(e.g., Bonanza and Nonpareil mines; Wells and Waters, 1934). Field mapping by Wells (1996c) shows that hydrothermal fluids and associated sills and

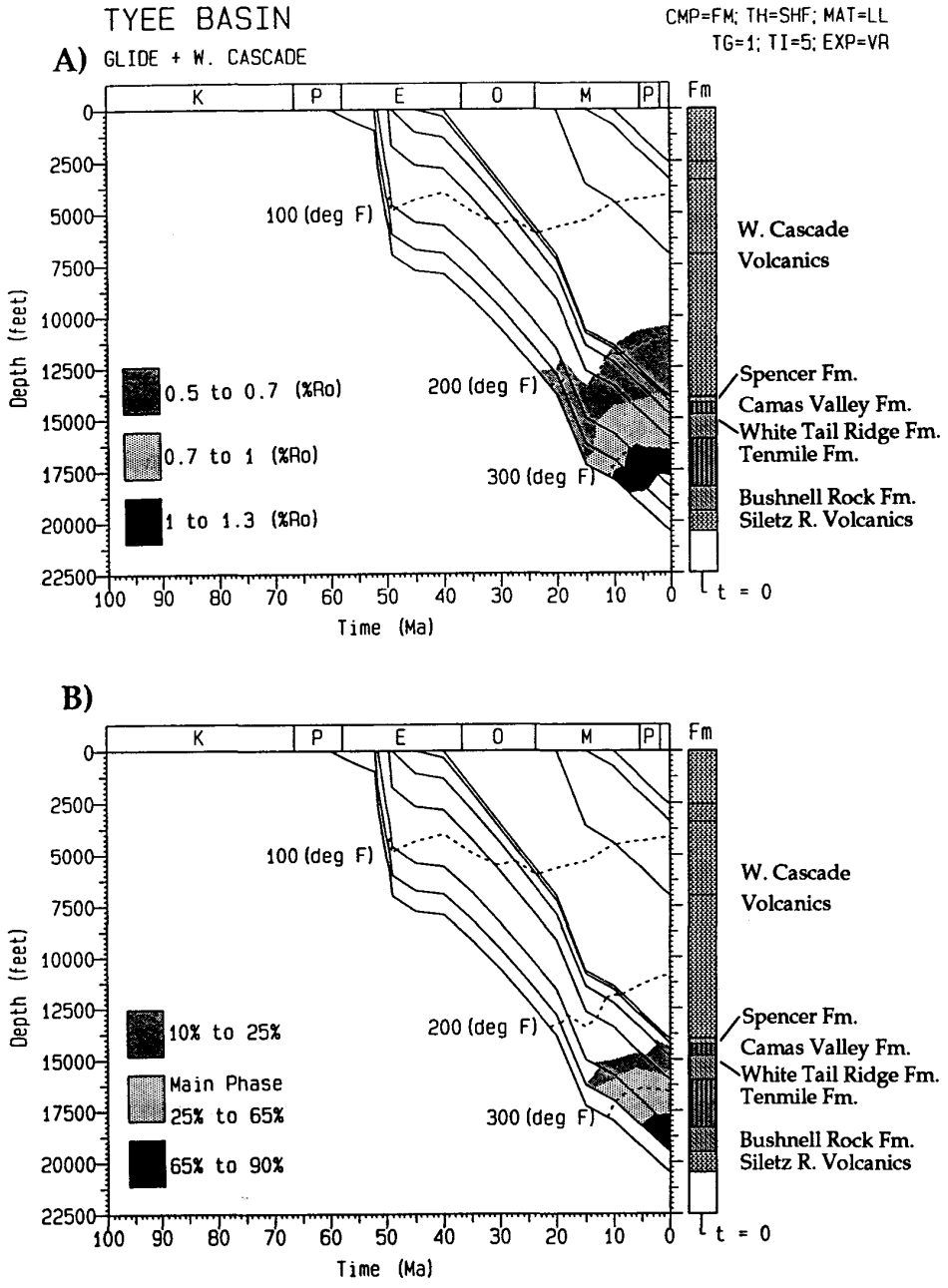

Figure 6.7 Maturity model (A) and kinetic model (B) for Spencer-White Tail Ridge-Western Cascade arc (?) hybrid petroleum system. Thicknesses of Eocene sedimentary units are from a stratigraphic section measured along the Umpqua River near Glide. An average geothermal gradient (1.27°F/100 feet) and a higher average heat flow value (65 mW/m2; Black, personal communication) are applied for Eocene sedimentary rocks and Western Cascades volcanic rocks, respectively. Refer to Figure 5.1 for abbreviations.

dikes have also baked (and probably matured) coal-bearing source rocks in the Spencer and White Tail Ridge formations for hundreds of feet in the Nonpareil area.

Flash heating by sills could have generated local accumulations of gas along the eastern margin of the basin. Some gas seeps are present along and near these mineralized fault zones near Nonpareil and Gassy Creek (see Niem and Niem, 1990 and Source Rocks section of this report). This metagenic gas and possibly some oil? may have migrated in an artesian flow system as far west as Melrose (e.g., Scott and Glory Hole wells) where there are numerous gas seeps (Natural Gases in the Tyee basin section in this report).

This is a hybrid speculative petroleum system. The Eocene strata which comprise the source rocks and reservoir rocks in the system dip eastward beneath the Western Cascades and are deformed to various degrees by early Eocene, late Eocene, and Oligocene thrust faults. They are truncated by an unconformity over which upper Eocene to Miocene volcanic flows and pyroclastic rocks of the Western Cascades were deposited. The volcanic units are largely unaffected by the thrusting but were intruded by Oligocene-late Eocene mafic and intermediate sills and by Miocene granodioritic plutons and were tilted by faulting in the Western Cascades (Walker and MacLeod, 1991).

Other petroleum systems may have existed in the southern Tyee basin. For example, biogenic methane may have been present in the Baughman Member of the Tyee Formation, in the coals and deltaic arkosic sandstone of the Bateman Formation, and locally in the Jurassic-Cretaceous Myrtle Group and younger Upper Cretaceous/Paleocene(?) sandstones. However, these units and structures have been uplifted and largely breached by erosion; it is unlikely that commercial quantities of natural gas remain. Until a drilling program is undertaken, all these petroleum systems will remain speculative as did the Mist Gas Field of northwest Oregon until 1979 when the discovery well was drilled (Newton, 1979; Armentrout and Suek, 1985).

STRUCTURAL AND STRATIGRAPHIC PLAYS

by Alan R. Niem, Ray E. Wells, and In-Chang Ryu

Structural and stratigraphic plays in the southern Tyee basin are being redefined by new detailed geologic mapping of stratigraphic units, faults, and folds. In 1990, Niem and Niem compiled a geologic map (scale 1:125,000), showing a preliminary interpretation of the structure and rock units. Geologists of the Oregon Department of Geology and Mineral Industries (DOGAMI) have mapped eight 7.5-minute quadrangles from Lookingglass Valley on the east to the settlement of Dora on the west (Black, 1990, 1994a, 1994b; Black and Priest, 1993; Wiley and Black, 1994; Wiley and others, 1994; Wiley, 1995). Detailed geologic mapping of eighteen 7.5-minute quadrangles and a map of the Roseburg 30-minute by 60-minute quadrangle (at a scale of 1:100,000) is in progress by the U.S. Geological Survey in the Umpqua basin and Klamath Mountains borderland in the Roseburg, Coquille, and Remote areas (Jayko, 1995a, 1995b; Jayko and Wells, 1996; Wells, 1996a-i; Wells and others 1996a, 1996b). Preliminary structural data from the new mapping are compiled on page-size maps in this report (Figs. 7.2, 7.3, 7.4, 7.5, and 7.6). A compilation map of the southern Tyee basin, revising the map of Niem and Niem (1990), is in preparation by Wells and by Black and others and will synthesize much of the new mapping and structure on a 1:100,000 base. Thus, additional structural traps and plays will be better defined as those projects are completed.

Our improved understanding of stratigraphic facies and their syntectonic relationship to progressive folding and thrusting in the basin have allowed us to define several promising structural and stratigraphic plays. Many potential traps occur on or above NW-trending structural culminations transverse to both the dominant NE-trending thrusts in the Umpqua Group and the younger N-S-, NE-, and NW-

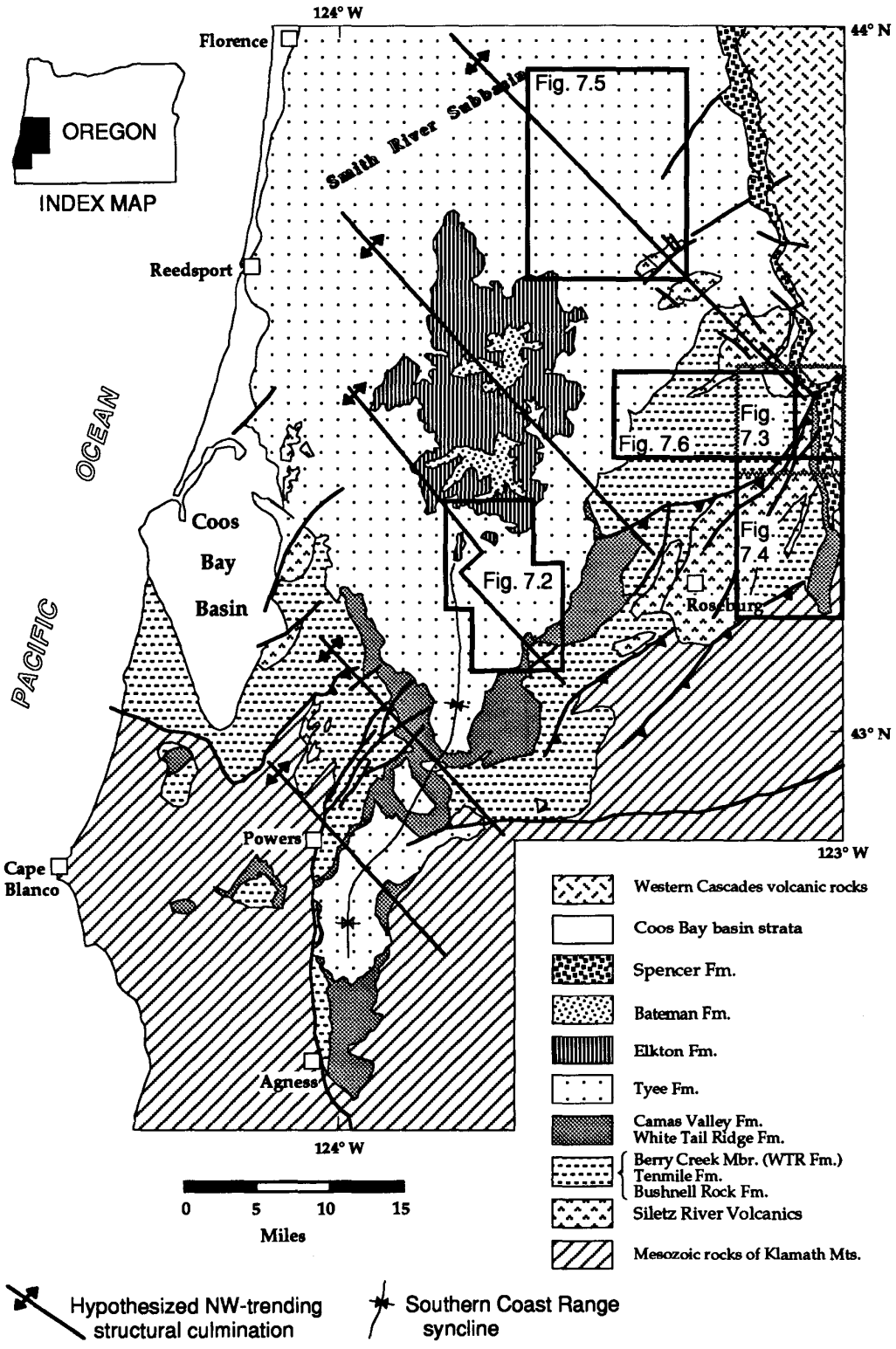

Figure 7.1 Index map of structural plays. Note the NW-trending structural culminations.

trending folds in the Tyee and younger formations. A prominent example of this is the northwest alignment of the culminations of the Jack Creek, Drain, and Dickinson Mountain anticlines (Figs. 1.1 and 7.1); others are buried beneath and subtly reflected in the Tyee and younger formations (see compilation map of Niem and Niem, 1990).

These potential structural plays are ranked by the size and closure of the structure, the position relative to potential source rocks, seals, and reservoir rocks, and the timing of formation relative to the timing of migration of potential generated hydrocarbons. Identified structural plays (Fig. 7.1), in order of potential to produce hydrocarbons, are:

(1) Williams River-Burnt Ridge anticlines and underlying thrusts, south-central part of southern Tyee basin;
(2) Western Cascades plays and Bonanza thrust near Nonpareil;
(3) Klamath Mountains subthrust play, Glide area;
(4) Tyee Mountain anticlinal plays, northeastern part of study area;
(5) Anticlinal and subthrust plays in the Myrtle Point-Sutherlin subbasin.

Williams River-Burnt Ridge Anticlinal Plays

The Williams River anticline (Fig. 7.2) is a complex domal structure in the Tyee Formation northwest of the settlement of Reston in the Mt. Gurney, Cedar Creek, and Tioga 7.5-minute quadrangles (Wiley and others, 1994; Wells, 1996a and unpub. mapping). The structure apparently formed by interference of NNW- and ENE-trending folds, possibly related to reactivation of NE-trending thrust faults at depth during east-west shortening of the Tyee, Elkton, and Bateman formations. The axis of this NNW-trending fold is deflected by NW-trending oblique-slip faults along the Williams River (Wells, 1996a). The Z-shaped trace of the Williams River anticline and adjacent synclines also suggests some right-lateral slip on NE-trending faults at depth. This structure is large, several miles across, and may have closure afforded by the gentle plunge of the fold to the north and by E-W crosscutting folds and NW-trending faults (Fig. 7.2). Closure on the south is lacking, but the axis may merge with the Burnt Ridge anticline (Fig. 7.2).

Wiley and others (1994) and Wiley (1995) mapped the NW-trending S-shaped Burnt Ridge anticline in the Mt. Gurney, Dora, and Sitkum 7.5-minute quadrangles. The northern end of the fold is yet to be mapped. Closure on the south is partially lacking because the Tyee and Camas Valley formations are breached by erosion in the Tyee escarpment (Fig. 7.2). The Burnt Ridge anticline appears to be the northwest continuation of the older Reston basement high that forms a re-entrant in the Tyee escarpment (Figs. 7.1 and 7.2). An EW- to NE-trending fault truncates the northern end of the Reston high, downdrops the Tyee and Camas Valley formations in the north block, and may create some closure in the underlying Umpqua units.

In a north-south seismic-reflection profile shot along the Williams River (Plate 1), the Williams River anticline appears to overlie and trend obliquely across an older NE-SW-trending fault-propagation fold in the underlying Umpqua Group turbidites (potential source rocks) and Siletz River Volcanics. The older fault-propagation fold is associated with a blind thrust (labelled Fault A on Plate 1) which is likely part of the Bonanza fault zone mapped to the northeast (Niem and Niem, 1990; Wells, 1996b, d, h, and i; Wells and others, 1996a). The older structure consists of a basement high of Siletz River Volcanics thrusted northwestward along Fault A over a wedge of lower Umpqua Group turbidites and possible White Tail Ridge deltaic strata. This high lies on trend with the Oakland or Heavens Gate anticlines mapped by Wells (1996g, 1996h). There is relatively little net slip on the blind thrust. Natural gas could be trapped in the southward-dipping lower Umpqua strata in the footwall beneath Siletz River Volcanics in the hanging wall. Potential seals in the older structure are the Camas Valley Formation and undifferentiated Umpqua Group mudstones which can be traced north on the seismic-reflection profile into the Amoco Weyerhaeuser B-1 well (Plate 1). Above the older structure, WNW-trending high-angle reverse or tear faults associated with the northwestward-verging thrust (Fault A on Plate 1) may project to the surface and truncate the Hubbard Creek Member in Williams Canyon (Fig. 7.2). Northward dipping upturned White Tail Ridge sandstone truncated by this high-angle fault (Plate 1) could be a potential structural trap. Overlying Camas Valley mudstone could act as a seal.

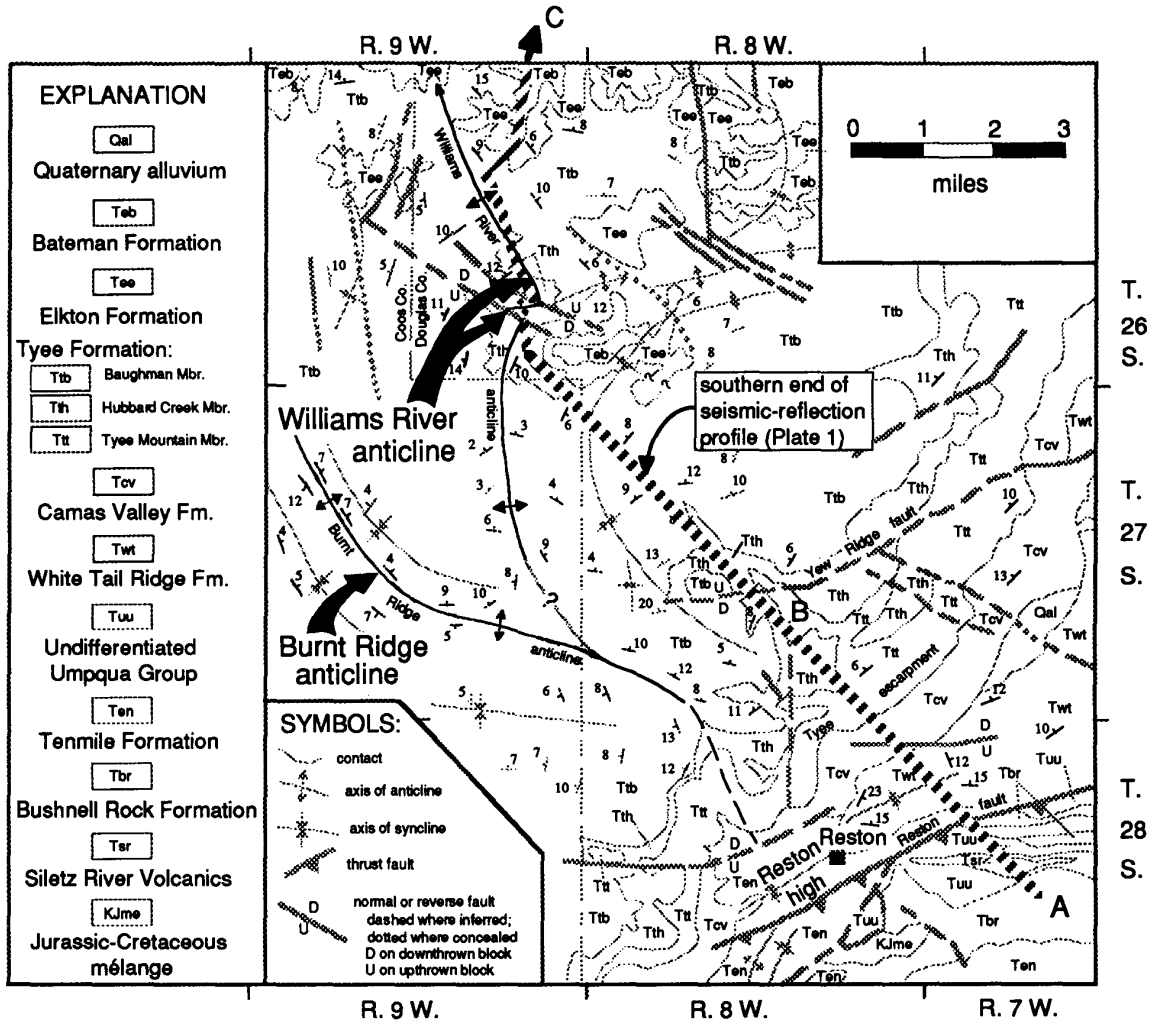

Figure 7.2 Generalized geologic map northwest of Reston, illustrating the Williams River-Burnt Ridge anticlinal plays (map derived from Wells, 1996a, unpub. mapping; Wiley, 1995; Wiley and others, 1994; and Black, 1990).

Similarly, the Yew Ridge fault (Plate 1 and Fig. 7.2) which is an ENE- to NE-trending high-angle reverse fault or reactivated back thrust(?) associated with a northwestward-verging thrust (Fault B on Plate 1) truncates the Hubbard Creek and Baughman members along the Williams River on the surface (Fig. 7.2). The Yew Ridge fault crosses the Williams River and may continue toward the Burnt Ridge anticline. The underlying NE-SW-trending volcanic basement structural high may have deflected the axis of the Burnt Ridge anticline to an east-west trend in this area. The Yew Ridge fault and thrust fault B, like fault A and the associated high-angle fault, may produce structural traps in the upturned lower Umpqua Group and White Tail Ridge Formation.

The Reston fault (Fig. 7.2 and south of B on Plate 1) is an outcrop expression of the buried NE-trending imbricate thrust fault and fold belt system (i.e., Bonanza fault zone). Field mapping in the Reston area by Black (1990) shows that these uplifted thrust faulted basement highs are composed of folded Bushnell Rock conglomerate and lower Umpqua Group turbidites (e.g., Tenmile Formation) overlying and flanking cores of Siletz River Volcanics (Fig. 7.2 and Plate 1).

Possible reservoir rocks and stratigraphic traps in the Williams River and Burnt Ridge anticlines are fluvial and delta front sandstones of the White Tail Ridge Formation (i.e., Remote and Coquille members). Seals include mudstone of the Camas Valley Formation and the Hubbard Creek Member of the Tyee Formation as well as tightly cemented turbidite sandstone and mudstone within the Tyee Mountain Member. Although the White Tail Ridge Formation pinches out to the north, these folds lie south of the mapped pinchout (Ryu and others, 1992; Wells, 1996h; Black and others, in prep.). White Tail Ridge deltaic strata, however, probably thin over and pinch out on the southern flank of the uplifted blocks of Siletz River Volcanics and also on the Umpqua arch (Plate 1)(Niem and Niem, 1990; Ryu and others, 1992). For example, mapping by Black (1990) shows that White Tail Ridge deltaic strata abruptly thin over the nearby Reston high. White Tail Ridge pebbles in a locally pebbly sandstone in the lower part of the Tyee Mountain Member west of Reston were apparently derived from erosion of White Tail Ridge strata off the Reston high (Tom Wiley, 1994, pers. commun.). These pinchouts and local unconformities create potential stratigraphic traps on the limbs of folds and on the flanks of the basement highs.

The thrust faults also represent potential migration paths for natural gas (see Natural Gases section of this report). Fracture porosity is possible in Umpqua Group turbidites and White Tail Ridge strata affected by this early Eocene thrusting. Secondary porosity in the turbidite sandstones in the lower part of the Tyee Formation represents a low potential reservoir target in these two folds (see Reservoir section of this report).

The timing of formation of structural traps is critical to hydrocarbon accumulation. The Reston and Bonanza thrusts and associated basement highs appear to have formed prior to deposition of the Tyee Mountain turbidites and Camas Valley mudstone in the middle Eocene (Fig. 7.2; Plate 1). Field mapping suggests that some NE-SW-trending thrusts and associated tear faults of the Bonanza fault zone were reactivated in post-White Tail Ridge time because these faults truncate and fold White Tail Ridge strata (see maps of Black and others, in prep.; Wiley and others, 1994; Wells and Niem, 1996). Many fold axes and faults terminate at the basal contact of the Tyee Formation or Camas Valley Formation; other faults cut the Tyee Mountain Member as well (Fig. 7.2; Plate 1). The Williams River and Burnt Ridge anticlines reflect progressive deformation over these older structures which may have been accentuated during the late-middle Miocene and younger folding and uplift of the Oregon Coast Range (Niem and Niem, 1990; Niem and others, 1992c). This should have allowed ample time for migration of hydrocarbons (mainly methane) along thrust faults up into the anticlinal structure and into subthrust plays. Migration of gas is ongoing today as indicated by gas seeps (mainly thermogenic methane) along faults in the Bonanza fault zone (see Natural Gases section of this report and Niem and Niem, 1990).

In addition, coal beds, carbonaceous mudstone, and fluvial-overbank siltstone and sandstone in the Remote Member of the White Tail Ridge Formation which emit biogenic methane in water wells (e.g., in the Melrose and Lookingglass valley area) represent another source of gas in the Williams River and Burnt Ridge anticlines and underlying thrusted basement structures (see Natural Gas section of this report).

Other anticlinal folds in the Tyee Formation with possible underlying fault traps exist in the area between the settlements of Dora, Remote, and Reston (Black, 1994b; Wiley and others, 1994; Wiley, 1995). The best reservoir rocks (i.e., White Tail Ridge deltaic facies) are buried by the Camas Valley and Tyee formations that could act as seals (see Reservoir section of this report). White Tail Ridge reservoir units also overlie and are involved in basement thrusts of the Bonanza fault zone (Niem and Niem, 19990; Black and others, in prep.). High-angle reverse, normal, and oblique-slip faults in the Tyee Formation and younger units may provide additional closure and act as structural traps.

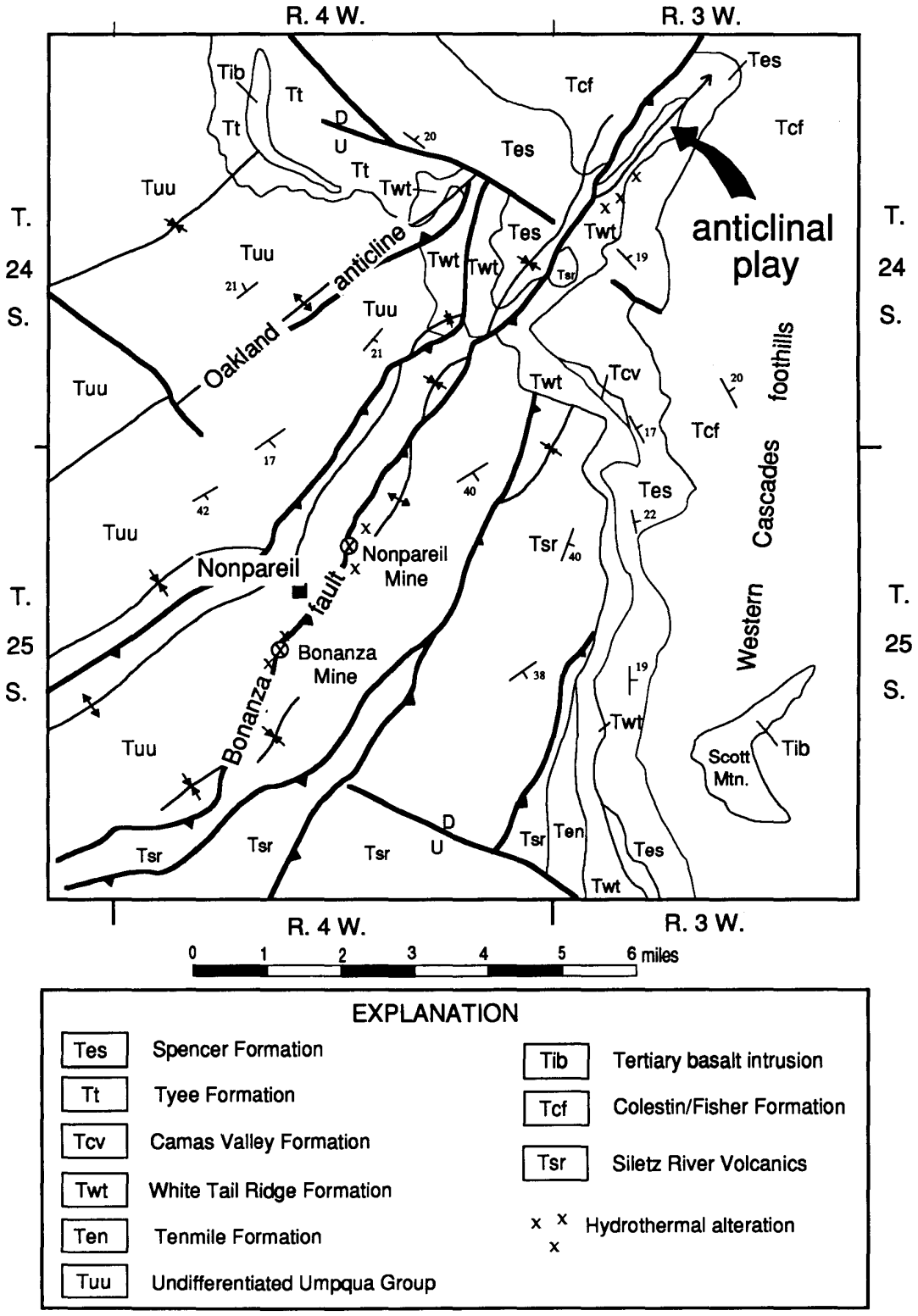

Figure 7.3 Generalized geologic map northeast of the town of Nonpareil, illustrating a NE-SW-trending anticline (large arrow) truncated by the Bonanza thrust fault (from Wells, 1996b; Walker and MacLeod, 1991).

Western Cascades Plays and Bonanza Thrust near Nonpareil

Recently, Wells (1996b; Wells and Niem, 1996) has mapped faults of the Bonanza fault zone into the foothills of the Western Cascades, as far as 8 miles northeast of the settlement of Nonpareil east of Sutherlin (Fig. 7.3). The SE-dipping Bonanza thrust fault truncates a NE-SW-trending asymmetrical anticline which involves sandstones of the Spencer and White Tail Ridge formations. The north limb of the fold is vertical to overturned; the south limb is gently dipping. A companion asymmetrical syncline in the footwall below the thrust suggests that the anticline is a fault-propagation fold. The fault was originally mapped by R. O. Brown of the U.S. Geological Survey (Wells, 1994, pers. commun.; unpublished mapping) and appears on the geologic map of Oregon by Walker and MacLeod (1991). The vertical to overturned north limb of the anticline includes volcanic pebble conglomerate, sandstone, and tuffaceous strata in the basal part of the upper Eocene and Oligocene Colestin/Fisher Formation of the Western Cascades, suggesting that compressional activity on this thrust was renewed during or after the latest Eocene or Oligocene. The fault appears to die out into folded Colestin/Fisher Formation to the northeast in the Western Cascades. Closure on the fold is accomplished by the Bonanza fault to the southwest. Evidence of closure on the southeast is buried by volcanic rocks of the Western Cascades. Some closure may be afforded by a NW-trending fault.

Potential reservoir rocks in this asymmetrical anticline include the 1100- to 1700-ft thick, moderately indurated to friable, medium- to coarse-grained micaceous arkosic sandstone of the Spencer Formation (unit Tes on Fig. 7.3). These distributary channel, delta front, and fluvial sandstones are time-equivalent to the gas-producing C&W sandstone of the upper Eocene Cowlitz Formation of the Mist Gas Field in northwestern Oregon. Another, potential reservoir unit in this fold is the underlying, less permeable, delta front and distributary channel, pebbly, non-micaceous sandstone beds of the White Tail Ridge Formation (unit Twt on Fig. 7.3). A possible younger reservoir is the basal 100 to 200 feet of the Colestin/Fisher Formation. These beds overlie an erosional unconformity on the Spencer Formation and consist of friable, micaceous arkosic sandstone (reworked from the Spencer) and beds of moderately consolidated volcanic pebble-cobble conglomerate. Potential source rocks (for biogenic and thermogenic methane) are the several one to six-foot thick coal beds and laminated, highly carbonaceous fine-grained sandstone and overbank mudstone within the Spencer Formation and possibly the underlying deep-marine undifferentiated Umpqua and Camas Valley mudstones. Seals for the White Tail Ridge Formation include some thin Camas Valley mudstone. Seals for the Spencer Formation would be the very thick, diagenetically altered "tight", basaltic sandstone and conglomerate, altered tuffs, and debris flow deposits of the Colestin/Fisher Formation (unit Tcf on Fig. 7.3).

This play lies in the foothills of the Western Cascades arc, and there is abundant evidence of local hydrothermal fluid activity in the vicinity of Nonpareil. Two mines, the Bonanza and Nonpareil mines, produced cinnabar from hydrothermal mineralized deposits in altered, bleached white Umpqua turbidites along the Bonanza thrust fault (Fig. 7.3). Extensive hydrothermal alteration is also recognized in White Tail Ridge and Spencer sandstones in the core of the anticlinal fold adjacent to the thrust just before it plunges beneath the Western Cascades volcanic rocks (Wells, 1996b; Wells and Niem, 1996). The alteration zone can be traced in outcrop for hundreds of feet. The hydrothermal fluids were associated with thick, mafic to andesitic Western Cascades sills and dikes or with undetected Miocene granodioritic plutons farther east beneath the Western Cascades (Wells and Waters, 1934). The heat from these fluids could have thermally matured potential source rocks. Gas shows also have been reported along the fault near Gassy Creek (see Mobil Oil Corp. data in Niem and Niem, 1990).

Another possible heat source for thermal maturation of Spencer coals and carbonaceous strata is flash heating by thick (>1,000 ft) upper Eocene-Oligocene sills or Miocene intrusions of the Western Cascades (see Source Rock section of this report).

Originating from or near intrusions in the topographically high Western Cascades, gas-charged hydrothermal fluids could have migrated along the strike of thrust faults southwestward into the Tyee basin. Artesian pressure may have forced the fluids up the fault zone to the surface,

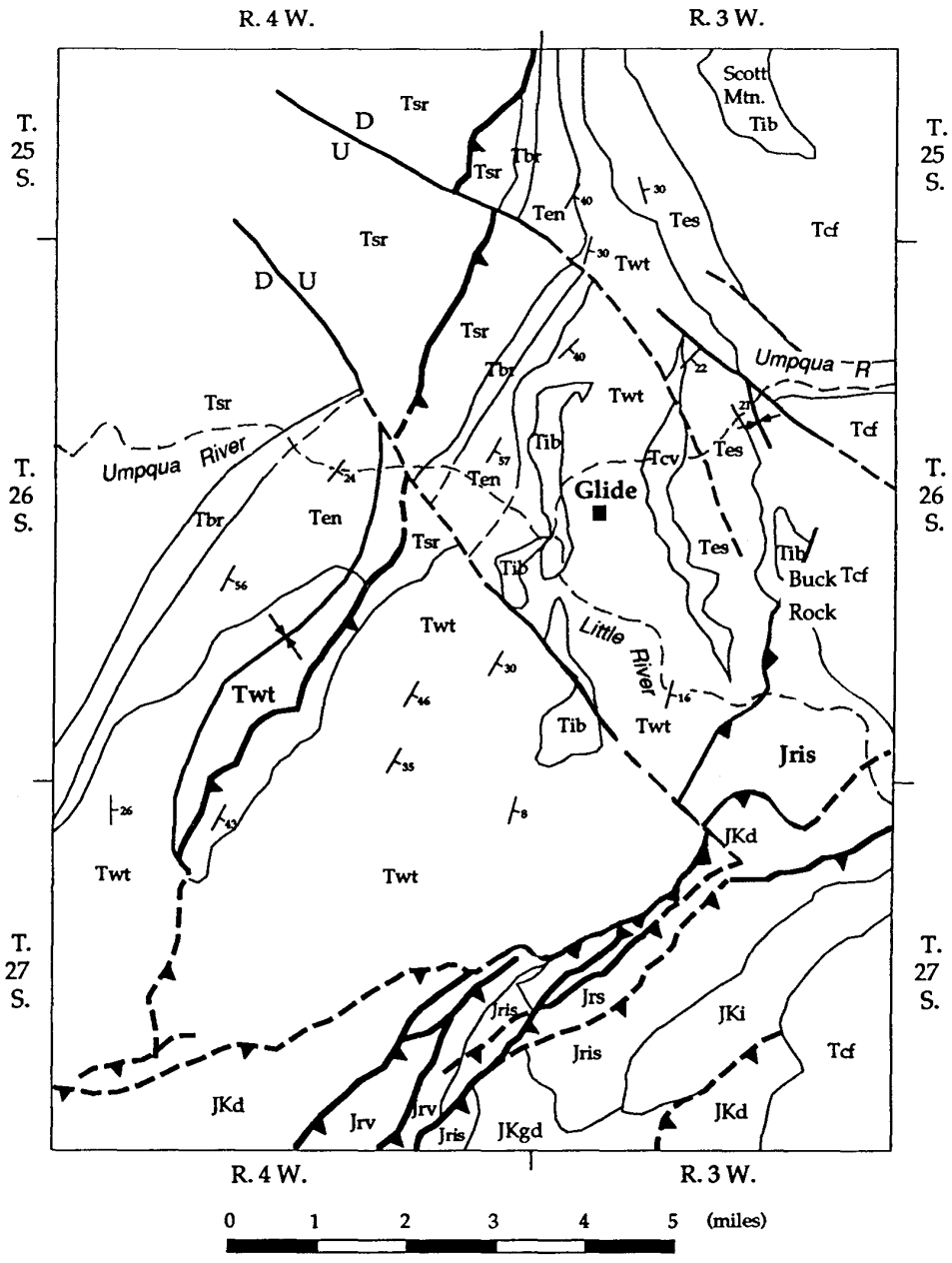

EXPLANATION

Tertiary units:		Mesozoic units:	
Tib	Basalt intrusion	pre-T	Undifferentiated Mesozoic rocks
Tcf	Colestin/Fisher Formation	JKd	Jurassic-Cretaceous Dothan Formation
Tes	Spencer Formation	JKi	Jurassic-Cretaceous intrusive rocks
Tcv	Camas Valley Formation	JKgd	Jurassic-Cretaceous granodiorite
Twt	White Tail Ridge Formation	Jris	Jurassic serpentinite
Ten	Tenmile Formation	Jrs	Sedimentary rocks of the Rogue Formation
Tbr	Bushnell Rock Formation	Jrv	Volcanic rocks of the Rogue Formation
Tsr	Siletz River Volcanics		

Figure 7.4 Generalized geologic map of the Glide area, illustrating homoclinal Eocene sequence which dips under Western Cascades rocks (Colestin/Fisher Formation) and Mesozoic rocks thrust over White Tail Ridge Formation (from Wells and Niem, 1996; Jayko, 1995a; unit Tcv mapped by A. R. Niem).

baking and mineralizing White Tail Ridge and lower Umpqua strata in the process. A gaseous envelope of methane may have formed in front of the hydrothermal fluids as the hot fluids thermally matured sedimentary source rocks in their path.

Numerous gas seeps have been reported in the Bonanza fault zone (Niem and Niem, 1990), and gas may have seeped along this zone beneath the Western Cascades rocks. Spencer sandstone is a potential gas reservoir in this area, and the overlying impermeable, clay-altered volcanic rocks of the Colestin/Fisher Formation could be a seal. Coal beds and overbank carbonaceous sandstone and mudstone in the Spencer Formation contain Type III organic matter and are potential source rocks. Thus, reservoir units, source rocks, seals and structural traps were in existence before the Miocene. During the Miocene, hydrothermal fluids, derived from Western Cascades intrusions, flowed through and altered rocks of the eastern Tyee basin (Wells and Waters, 1934). Those fluids may also have matured the potential source rocks to produce natural gas.

Other Western Cascades Plays-- The principal reservoir in any structural or stratigraphic play in the foothills of the Western Cascades is the Spencer Formation although the extent of this unit beneath the Western Cascades is unknown. The Spencer Formation is exposed from Glide to Cottage Grove along the eastern flank of the southern Tyee basin. It includes coarse-grained, fluvial to distributary channel arkosic micaceous sandstone and is coal-bearing. In contrast, the type Spencer near Eugene and northward to Corvallis in the Willamette Valley is fine-grained, is more marine, and locally contains basaltic sandstone and volcanic conglomerate (Baker, 1988). Therefore, it is unlikely that the Spencer Formation near Glide was derived from the Spencer facies to the north. Instead, it represents a separate deltaic-fluvial-coastal plain system which was probably once laterally continuous with the Bateman Formation (in the center of the southern Tyee basin) (Weatherby, 1991) and with the Coaledo Formation of the Coos Bay basin (Dott, 1966). A possible correlative micaceous arkosic unit is the Eocene Payne Cliffs Formation in the Ashland area which also contains white mica derived from the Idaho batholith (McKnight, 1971; Heller and others, 1992; T. Wiley, 1994, pers. commun.). A few paleocurrent measurements, however, indicate a southwestward paleocurrent dispersal pattern, suggesting that the Spencer fluvial system and nearshore and deltaic facies of the Tyee Formation (Snavely and Wagner, 1963) may extend farther east beneath the volcanic rocks of the Western Cascades.

Other structural traps (faults and folds) exist north and south of Nonpareil in the foothills of the Western Cascades (e.g., extension of the Oakland anticline south of Ben More Mountain; Fig. 7.3). These faults were mapped by Wells (1996b; Wells and Niem, 1996) and by MacLeod in Walker and MacLeod (1991). Spencer sandstone could be drag folded along these faults to form small anticlinal structural traps similar to the Cowlitz Formation in structural traps in the Mist gas field (Niem and others, 1994).

Near Glide along the Umpqua River, hundreds of feet of friable (reservoir quality), arkosic sandstone and some coal beds of the White Tail Ridge Formation (Berry Creek and Remote members) dip homoclinally beneath Western Cascades rocks (Fig. 7.4). The overlying Camas Valley mudstone which is hundreds of feet thick could act as a seal for the White Tail Ridge Formation (Fig. 1.3, section 14). Overlying the Camas Valley mudstone, friable Spencer sandstone (a younger potential reservoir) dips eastward beneath Colestin/Fisher mudflows and altered tuffs (potential seals). Fault traps could be created by a NW-trending high-angle fault mapped by R. E. Wells north of Buck Rock (Fig. 7.4). Maturation could have been accomplished by flash heating by very thick sills (basaltic and andesitic). For example, thick sills intruded into the White Tail Ridge Formation are exposed at Colliding Rivers State Park; at Buck Rock and Scott Mountain (southeast and northeast of Glide, respectively) sills intruded the Colestin/Fisher Formation.

Between Glide and Nonpareil, the White Tail Ridge, Camas Valley, and Spencer formations are currently mapped on a reconnaissance level as a largely unfaulted homoclinal sequence. An angular unconformity at the base of the White Tail Ridge Formation locally cuts out thousands of feet of Tenmile turbidites and Bushnell Rock Formation such that White Tail Ridge strata rest on older Siletz River Volcanic highs (Hoover, 1963; R. E. Wells, 1994, pers. commun.) (Fig. 7.3). Further definition of faults or folds in the

Western Cascades foothills will require additional mapping or geophysical surveys before a structural play is developed in this potential target area. One problem with a Spencer/White Tail Ridge play beneath the Western Cascades is that these potential reservoir units may be cut out entirely in the subsurface by a post-Spencer/pre-Colestin-Fisher erosional unconformity. For example, mapping by A. Jayko of the U.S. Geological Survey southeast of Canyonville shows that both units are missing and that Colestin/Fisher Formation overlies Mesozoic rocks of the Klamath Mountains (Jayko, 1994, pers. commun.). In addition, one or both units may be cut out by faults beneath the Western Cascades. The depth of burial of these eastward-dipping arkosic units beneath the thick Western Cascades volcanic sequence limits drilling targets to within a few miles of the western margin of the highly dissected Western Cascade foothills.

Klamath Mountains Subthrust Plays

The boundary between the Coast Range and Klamath Mountains has been interpreted as a faulted boundary; that is, Mesozoic Klamath Mountains rocks are thrust over Tertiary Coast Range rocks (Heller and Ryberg, 1983; Carayon, 1984; Carayon and others, 1984). Therefore, a possible play is to drill through thrust slices of Mesozoic rocks into the underlying Tertiary strata. One such subthrust play could exist within a few miles south of the Wildlife Safari fault. Another possible play is a few miles southeast and southwest of Glide (Fig. 7.4).

South of Glide, Jurassic-Cretaceous Dothan Formation (broken formation), Mesozoic volcanic rocks, and granodiorites are thrust over thousands of feet of delta front and fluvial, pebbly arkosic sandstone of the White Tail Ridge Formation along the Wildlife Safari and subparallel thrust faults. The NNE-trending fault near Buck Rock is also a thrust, suggesting that a subthrust play also exists southeast of this fault in the vicinity of Little River (Fig. 7.4). The White Tail Ridge Formation is a potential reservoir unit. Fracture porosity may enhance the reservoir characteristics of this unit if it is involved in folding at depth. Potential source rocks are coals in the Remote Member (possible biogenic gas) and slope mudstone of the Tenmile Formation. Some thrust slices of Dothan Formation might also be source rock (see Natural Gases section in this report). The Klamath Mountains mélange and broken formation in upper thrust slices could also act as partial seals. Thermogenic gas generated from thrust slices of Umpqua and pre-Tertiary strata appear to be still migrating to the surface in seeps and in water wells (e.g., in the northern margin of the Klamath Mountains and along thrust faults in the Umpqua basin; see Natural Gases section in this report; Kvenvolden and others, 1994; Kvenvolden and others, 1995). Gas seeping from Klamath Mountains pre-Tertiary rocks could alternatively have been formed *in situ* through heating by hydrothermal fluids migrating along faults from the nearby Western Cascades arc.

Wells and Snavely (1989) offered an alternative interpretation to the subduction zone model of Heller and Ryberg (1983). They suggested that the Siletz River Volcanics were erupted in a rifted continental marginal basin. Later, minor, oblique subduction of the Farallon plate beneath North America seaward of this basin caused telescoping of this basin against the northern Klamath Mountains in the late-early Eocene to produce the compressional folds and thrusting. The lack of widespread, thick Paleocene-Eocene mélange and broken formation between the Klamath Mountains and the southern Coast Range, which would represent an accreted subduction zone complex, argues in favor of the rifted marginal basin model of Wells and Snavely (1989). This model could also explain local intercalation of the upper part of the Siletz River pillow lavas with polymict conglomerate and lithic (metamorphic) turbidite sandstone (Bushnell Rock Formation and undifferentiated lower Umpqua Group) that were derived from Klamath Mountains sources.

The exploration implications of the rift model are important. If underthrusting along the suture has been minor, then there are no deep, major subducted wedges of Umpqua Group strata beneath the northern margin of the Klamath Mountains and a subthrust play is unlikely. This model also implies that Umpqua Group strata matured by deep burial through underthrusting are not the source for the thermogenic dry gas in some seeps and water wells in the Umpqua basin and northern Klamath Mountains (Kvenvolden and others, 1994, 1995).

Also, if net slip or thrusting is minor, then reservoir rocks of the deltaic White Tail Ridge

Formation below the thrusts would exist only within a few miles south of the Coast Range/Klamath Mountains suture. Further deep refraction, reflection, gravity, or magnetic profiling across this suture zone could reveal if Umpqua Group strata are caught in thrust slices that extend far beneath the northern margin of the Klamath Mountains.

Tyee Mountain Anticlinal Plays

Several untested anticlines are mapped in the Tyee Mountain and Baughman members of the Tyee Formation (see Niem and Niem, 1990; Black and others, in prep.). The foremost of these, the Burnt Ridge and Williams River anticlines, were discussed above. Three wells drilled on the Umpqua arch (the Amoco Weyerhaeuser B-1 and F-1 wells and the Northwest Exploration Sawyer Rapids well) failed to produce commercial quantities of hydrocarbons. Some gas and oil shows were reported in Tyee Mountain and Baughman sandstones in these wells, but these diagenetically altered sandstones have insufficient permeability to act as reservoirs and/or have been breached by erosion.

A basement high northwest of the Drain anticline was tested without success by the Florida Harris well which drilled through 1,500 feet of Tyee Formation and 800 feet of Umpqua mudstone into the Siletz River Volcanics. The Weyerhaeuser B-1 well, located near the crest of the Umpqua arch, drilled through nearly 7,000 feet of Elkton Formation, Tyee Formation, and undifferentiated Umpqua Group mudstone before drilling >4,000 feet of Siletz River Volcanics (Plate 1 and Fig. 1.3; Ryu and others, 1992). These volcanics appear on the seismic-reflection profile (Plate 1) to be composed of a well-bedded sequence of acoustically transparent palagonitic volcanic breccia and strongly reflecting pillow lavas. The arch may be a seamount paleohigh that projects northeastward toward the Dickinson Mountain anticline which is cored by submarine and subaerial Siletz River Volcanics (Niem and Niem, 1990). The angular unconformity at the base of the Tyee and Camas Valley formations is evident as a distinct truncation of Siletz River flows and of lower Umpqua Group strata(?) and as thinning or onlap of those strata onto the arch. Thus, stratigraphic traps are possible on the flanks of this subsurface structure. North of the Umpqua arch, the seismic-reflection profile (Plate 1) shows a broad downwarped structure which would project northeastward into the NE-SW-trending Hardscrabble Creek syncline. Several reverse faults lie between this downwarped structure and Northwest Exploration's Sawyer Rapids well. The Sawyer Rapids well drilled a NNE-trending surface anticline mapped in the Elkton Formation and penetrated >5,000 feet of Tyee Formation (Fig. 1.3; Niem and Niem, 1990; Ryu and others, 1992).

North-south trending folds in Tyee, Elkton, and Bateman strata in the northern part of the study area probably formed during a compressional stage starting in the late-middle Miocene (Niem and Niem, 1990). This younger structural fabric is superimposed on the older NE-SW-trending structure, creating closure. The compilation map of Niem and Niem (1990) shows that these north-south axes gradually become NE-SW-trending, subparallel to the older structural trend on the eastern flank of the basin. The Long Bell and Sawyer Rapids wells were drilled on north-northwest-trending anticlines mapped in the Tyee Mountain Member.

One largely untested anticlinal structure is centered near Stony Point (northwest quadrant of T. 19 S., R. 6 W.), 10 miles northwest of the Florida Harris well (R.E. Wells, 1994, pers. commun.). The axis of this NNW-trending fold subparallels the Siuslaw River in the northeastern part of the study area (Fig. 7.5). It shows up subtly by strikes and dips in the Tyee Mountain Member on the compilation map by Niem and Niem (1990) although the fold axis was not drawn. The structure was mapped in detail on a proprietary map by R.E. Wells and colleagues for Mobil Oil Corporation in the 1970s (R.E. Wells, 1994, pers. commun.). The fold shows 10 to 15 miles of closure on the southwest, northeast, and northwest, but not obviously on the southeast flank where it may merge into the older NE-SW-trending Jack Creek anticline (R.E. Wells, 1994, pers. commun.).

The stratigraphy in the Florida Harris well which was drilled on the southern plunging nose of this structure is an indication of the lithologies and thicknesses that could be expected structurally higher on this anticline (Fig. 7.5). In that well, a thick section of impermeable turbidite sandstone and mudstone (Tyee Mountain Member mid-fan facies) and thinner

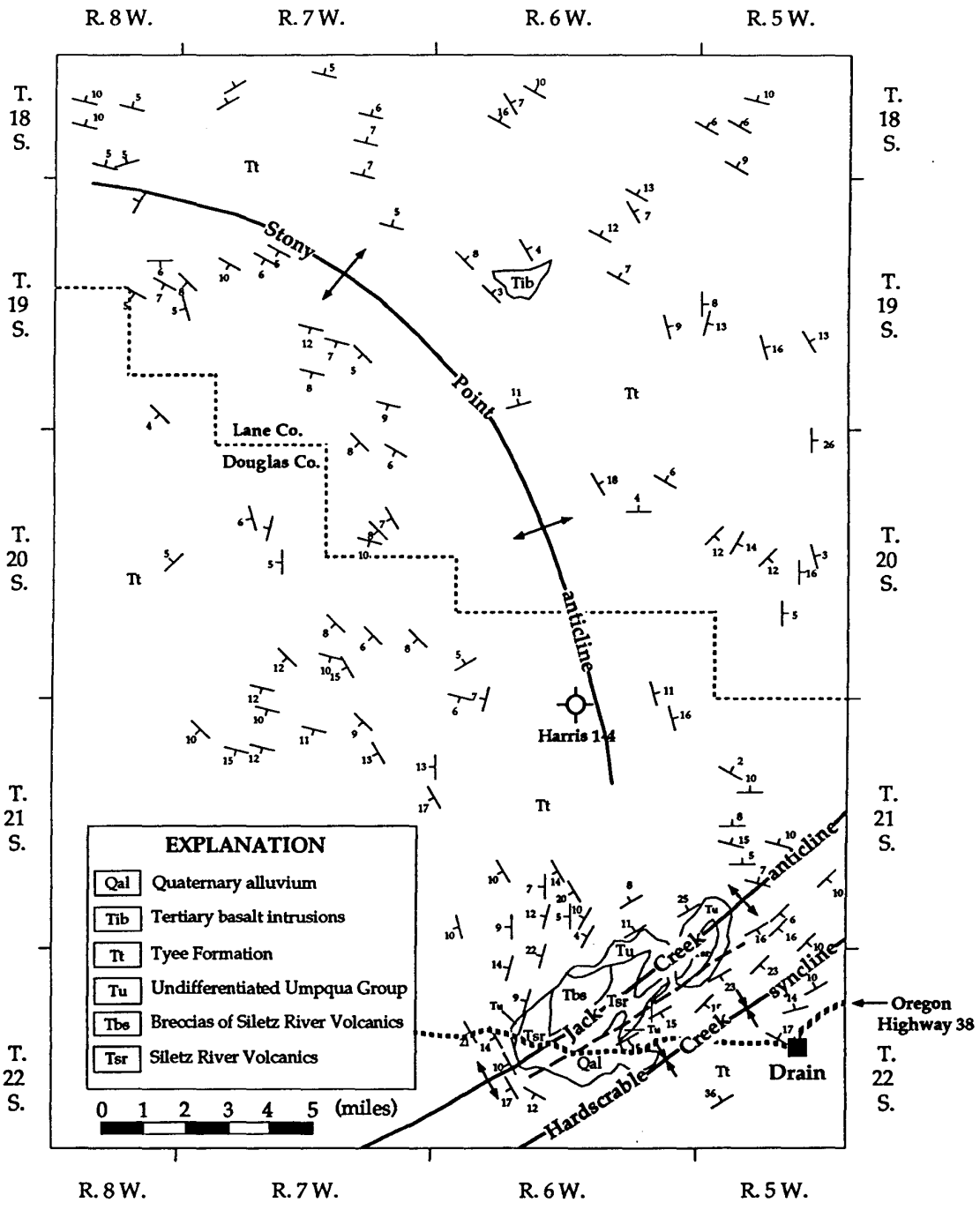

Figure 7.5 Generalized geologic map of the Stony Point anticline area northwest of Drain (after Niem and Niem, 1990).

section of Umpqua basinal mudstone overlie Siletz River Volcanics. There is a problem of finding good reservoir rock in this structure and other structures in the northern part of the study area because the permeable delta front sandstone of the White Tail Ridge Formation pinches out south of this area (Fig. 1.3; Ryu and others, 1992; Wells, 1996h; Black and others, in prep.). Fracture porosity is limited in Tyee Mountain Member turbidite sandstones (Penoyer and Niem, 1975). Diagenetically altered (zeolites and smectite clay) Tyee Mountain turbidite sandstone and mudstone higher in the section could act as seals in the Stony Point domal structure.

Secondary porosity in Tyee Mountain sandstone in this structure and in the more deeply buried part of the Smith River subbasin, however, could create a limited reservoir. Newton (1980) reported secondary porosity (as much as 15%) in some turbidite sandstones in the lower part of the Tyee Mountain Member from outcrops on the western flank of the basin. This secondary porosity is due to dissolution of feldspar grains and volcanic rock fragments and has been reported in lower Tyee Mountain Member sandstones in the Long Bell well, 20 miles west-southwest of the Stony Point structure (see Diagenesis section in this report).

Several other northward plunging anticlines and NE- and NW-trending faults are mapped in the northern part of the study area (see Niem and Niem, 1990; Black and others, in prep.). For example, the Long Bell well was drilled on the east limb of a doubly plunging north-south-trending fold. Reservoir rocks, however, are scarce. Turbidite sandstones in the lower Umpqua Group in the Myrtle Point-Sutherlin subbasin also pinch out in this direction due to a facies change, distance from the source, and barrier effects of the Umpqua arch (Fig. 1.3). The unit which is the best potential reservoir, the White Tail Ridge Formation, does not extend this far north.

On the other hand, Umpqua basinal mudstones penetrated by the Long Bell well in the Smith River subbasin (Fig. 1.3) are lean to moderately organic-rich (mainly gas-prone Type III organic matter; see Source Rock Evaluation section of this report). In the lower part of the well, they are nearly at the top of the oil/dry gas window. These more deeply buried mudstones could act as source rocks for unconventional basin center gas (Law and others, 1988; Law and others, 1994). A computer-generated model (i.e., BasinMod; see Basin Subsidence History section of this report) shows that basin center gas could have been generated initially in the middle Miocene if the thick upper Eocene to middle Miocene section of the adjacent Coos Bay basin were deposited on top of the Tyee Formation in the northwest corner of the study area. Unfortunately, the structure on which the Long Bell well was drilled may have formed in the late-middle Miocene after maximum burial, peak generation, and migration of basin center gas. It is possible that, due to the lag time between generation and migration, some gas may have migrated into these folds. However, undeformed nepheline syenite (30 Ma) and basalt dikes cut across parts of the fold, suggesting that this structure formed earlier during the late Eocene or Oligocene (P. D. Snavely, Jr., 1995, pers. commun.).

Even though untested structures exist, the hydrocarbon potential of the northern part of the study area is low, compared to the southern part of the basin, due to a general lack of maturation, lack of organic-rich source rock (e.g., coals), and "tight" reservoir rocks.

Anticlinal and Subthrust Plays in the Myrtle Point-Sutherlin Subbasin

In the Roseburg-Sutherlin-Glide area, imbricate thrust faults, some back thrusts, and associated anticlinal and synclinal folds deform turbidite fan strata and slope mudstone of the lower Umpqua Group, Bushnell Rock submarine channels, and deltaic strata of the White Tail Ridge Formation in the Myrtle Point-Sutherlin subbasin (Fig. 7.6; Wells, 1996g, 1996h, 1996i; Wells and others, 1996a). Some folds may be underlain by blind thrusts and may be fault-propagation folds. North of the thrust faults, from Sutherlin to Drain, Umpqua turbidite sandstone and mudstone beds are folded into broad anticlines and synclines that trend northeast-southwest. The anticlines are cored by Siletz River Volcanics.

One such anticline, the Oakland anticline, was drilled by Mobil Oil Corporation (Sutherlin Unit No. 1) five miles northeast of Sutherlin. The Sutherlin well penetrated <4,000 feet of Umpqua outer and middle fan turbidite strata overlying Siletz River subaerial and submarine tuff

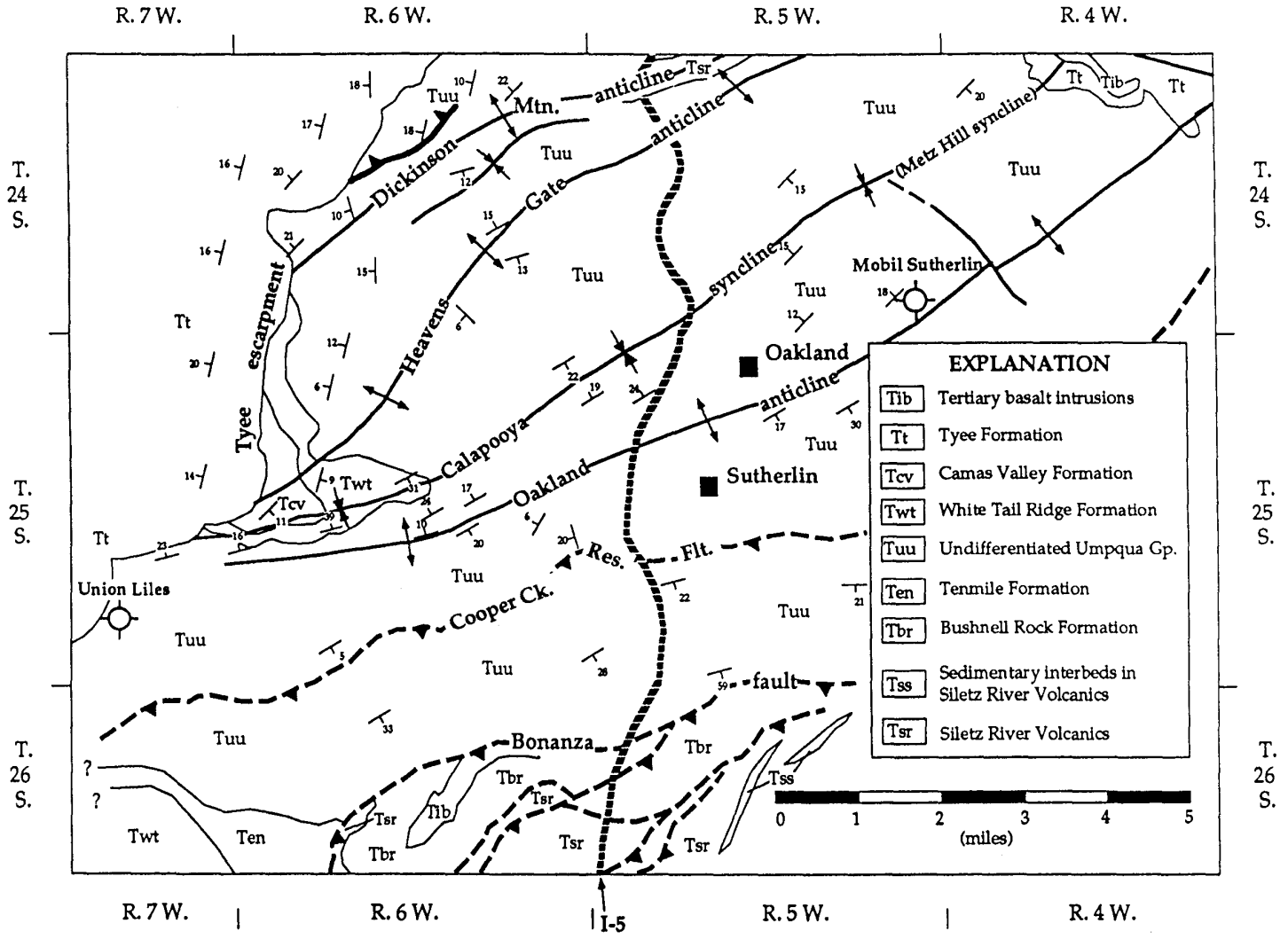

Figure 7.6 Generalized geologic map of the Sutherlin area, illustrating folds in lower Eocene rocks between the Bonanza fault zone and the Dickinson Mountain anticline (from Wells, 1996g, 1996h, 1996i; Wells and Niem, 1996).

breccias, pillow lavas, and flows (Fig. 1.3; Ryu and others, 1992). The axis of the symmetrical anticline is definable by surface attitudes and by seismic-reflection profiles. Dips of the broad fold, measured at the surface, range from 10° to 30°, and the axis of the fold is exposed in a roadcut along the I-5 one-quarter mile north of Sutherlin. However, near faults, the dips of the limbs are steeper, ranging from 40° to 70°. Several subparallel high-angle faults formed by flexural slip along bedding planes.

The southwest-plunging nose of the Oakland anticline crosses the Umpqua River south of Tyee Mountain and disappears beneath the Tyee escarpment (Fig. 7.6). It was unsuccessfully drilled by Union Oil Company of California (Liles No. 1). That well penetrated several thousand feet of tight, thin- to medium-bedded Umpqua turbidite strata. It may also have encountered a repeated section (recognized by repetition of foraminiferal zones B1 and C; McKeel, 1992, pers. commun.) probably due to a thrust fault (see section #8 on Fig. 1.3 and in Ryu and others, 1992). Gas shows were encountered in "tight" lithic turbidites of the lower Umpqua Group in both the Sutherlin and Liles wells, but there was no commercial production. Gas (methane) issues from a water well drilled on the axis of the fold near the Liles well (see Natural Gases section of this report).

An untested anticline north of the Oakland anticline, the Heavens Gate anticline, was defined in recent mapping by R.E. Wells (1996g, 1996h) (Fig. 7.6). The NE-SW-trending symmetrical anticline occurs south of the Dickinson Mountain anticline and north of the Calapooya syncline (Metz Hill syncline of Wells, 1996g, 1996h). The Heavens Gate anticline involves generally impermeable outer and middle fan turbidite sandstone, slope mudstone, and thick basin plain mudstone of the lower Umpqua Group. These strata presumably overlie a thin section of well-indurated basaltic sandstone and subaerial flows of Siletz River Volcanics similar to those exposed along the I-5 in the core of the Dickinson Mountain anticline. Some gas seeps are reported in water wells on the axis of the Heavens Gate fold (see Natural Gases section of this report).

These folds and faults were formed in the late-early Eocene which may pre-date generation of hydrocarbons (see Basin Subsidence History section of this report). However, the Umpqua mudstones in this area are thermally immature, contain low TOC (generally <0.5%; see Source Rock Evaluation section of this report), and are unlikely to be significant source rocks. The rhythmically bedded, outer and middle fan lithic turbidite sandstone beds in the Umpqua Group generally would be poor reservoirs because they are thin and contain abundant silica, zeolite (laumontite), and clay (corrensite) cements which fill pores (see sections on diagenesis and porosity and permeability in this report). The Heavens Gate fold plunges to the southwest. In the area between the Umpqua River and Dodge Canyon, this fold involves White Tail Ridge sandstone (Wells, 1996g, 1996h). Unless fracture porosity is developed in Umpqua and White Tail Ridge strata beneath the Tyee forearc basin sequence west of the Tyee escarpment, this fold would be a low priority play.

The area between the Bonanza fault zone and Wildlife Safari fault presents low priority possibilities for subthrust plays and untested anticlines in the Myrtle Point-Sutherlin subbasin (Fig. 1.1). Several gas seeps are reported along the thrust faults and in the associated drag folds. The Scott No. 1 well near Melrose drilled through several thrust plates of the Umpqua Group and reported oil shows (fluorescence) in fractures in the Bushnell Rock conglomerate, Tenmile turbidite sandstone, and Siletz River Volcanics (driller's report; see Niem and Niem, 1990). Small, non-commercial quantities of gas were present. This well and the nearby Glory Hole well are both on strike with the Bonanza fault zone. Several seeps of biogenic gas are reported from water wells drilled in the deltaic coal-bearing White Tail Ridge Formation near Melrose (see Natural Gases section in this report).

Any subthrust or stratigraphic pinchout play in the Myrtle Point-Sutherlin subbasin must take into account that Bushnell Rock conglomerates and lower Umpqua Group (Tenmile) turbidites have low porosity and permeability and, therefore, do not have good potential as reservoirs (see porosity and permeability section of this report). However, fracture porosity is locally developed in these units along back thrusts and fault-propagation and drag folds (e.g., along the Umpqua River northwest of Roseburg).

Potential source rocks are deeply buried broken formation and mélange of the Mesozoic Dothan Formation and other Klamath Mountains sedimentary units in thrust slices interleaved with thrust plates of lower Umpqua strata to the south (e.g., near Bushnell Rock, south of Tenmile, and west of Remote; Wiley and Black, 1994; Black, 1994b; see cross section in Niem and Niem, 1990). Lower Eocene Umpqua Group turbidites and deep-marine mudstone may also have been thermally matured by deep burial as thrust slices beneath Klamath Mountains rocks or by hydrothermal fluids from the Western Cascades (see other plays discussed above).

Several younger sandstone-dominated units (upper Umpqua Group) in the Myrtle Point-Sutherlin subbasin could be reservoirs, including the delta front and distributary sandstone and pebbly conglomerate of the Remote, Coquille River, and Berry Creek members of the White Tail Ridge Formation.

Another possible, but limited, reservoir unit is the clean Cretaceous(?) or Paleocene(?) arkosic-quartzose micaceous sandstone which is exposed in widely scattered outcrops along the Wildlife Safari fault (e.g., near Winston and Hoover Hill; see Niem and Niem, 1990). This locally cross-bedded to laminated, pebbly sandstone contains clasts derived from the Klamath Mountains (Wells, 1994, pers. commun.). It is locally several hundred feet thick and was deposited in shallow-marine(?) or fluvial conditions. The permeability of the unit is widely variable. At some localities, it has excellent permeability and would make a good reservoir (see Reservoir section of this report). Elsewhere, it is well-cemented (tight) biotite-muscovite sandstone which appears to be part of the Dothan Formation (Jayko and Wells, 1994, pers. communs.). It is most friable two miles northeast of Myrtle Point along the East Fork of the Coquille River where it either lies on top of or is included in an isolated klippe of Dothan mélange (Niem and Niem, 1990). Because of the scattered distribution of this unit, it would be difficult to predict where this potential reservoir sandstone would occur in the subsurface in subthrust plays in the Myrtle Point-Sutherlin subbasin.

Other units in the northern margin of the Klamath Mountains that could be reservoir rocks in thrust slices interleaved with lower Umpqua Group strata are the pre-Tertiary Days Creek and Riddle formations of the Myrtle Group (see cross sections in Ramp, 1972; and Niem and Niem, 1990). Conglomerate and sandstone beds in these units have moderately high permeability and porosity although they appear "tight" in outcrop (see porosity and permeability section in this report). The mudstone/shale interbedded with the sandstone in these units is generally immature and has moderately low TOC and, therefore, would be marginal source rock at best (see Source Rock Evaluation section of this report). These units, however, represent possible, but limited, reservoir targets in subthrust plays.

Additional subthrust plays and oblique-slip fault plays will be better defined in the next few years as new geologic mapping is completed by the US Geological Survey (R.E. Wells and Bob McLaughlin) and by DOGAMI (T. Wiley and J. Black) in the Myrtle Point-Sutherlin subbasin west of Remote, Powers, and Dora (Fig. 1.1). Several NE-SW-trending oblique-slip faults, steep-limbed anticlines, high-angle reverse faults, and thrusts emerge from beneath the Tyee forearc basin sequence in this area and some reverse faults involve the White Tail Ridge Formation (Black, 1994a). The details of the structural relationships of the Umpqua Group and Klamath Mountains terranes in the southwestern part of the Myrtle Point-Sutherlin subbasin remain to be determined.

SUMMARY AND CONCLUSIONS

Application of sequence stratigraphic concepts, together with a basinwide surface-to-subsurface fence diagram, seismic-reflection records, and microfossil and log data from several exploration wells and new geologic mapping (by DOGAMI and the US Geological Survey) refines previous Tyee basin lithostratigraphy. These approaches have resulted in a better understanding of the geometry of units, facies distribution, geologic evolution, structure, and oil and gas potential of this basin.

Lithostratigraphic and structural conclusions are:

(a) Four depositional sequences (I through IV) are defined in the 25,000-ft thick composite Paleogene section. Each sequence is bounded by local unconformities which are conformable basinward.

(b) Fan delta conglomerate, slope mudstone, and submarine fan turbidites of sequence I (lower Umpqua Group, Bushnell Rock and Tenmile formations) were deposited in the early Eocene as a syntectonic accretionary wedge in a marginal rift basin or "trench". These well-indurated, graded, lithic sandstones and conglomerates were sourced largely from uplifted Mesozoic terranes of the Klamath Mountains to the south. The southern part of the Umpqua marginal basin (which now trends NE-SW) was intensely folded, thrusted, and partially subducted in the late-early Eocene during plate convergence of the underlying thick Paleocene-lower Eocene Siletz River oceanic basalt basement and seamount terrane with the North American continent (represented by Mesozoic terranes of the Klamath Mountains).

(c) Northward prograding, Klamath Mountain-derived, wave- and tide-dominated deltas of sequence II (upper Umpqua Group, White Tail Ridge Formation) filled irregular basin lows and thinned over submarine highs (e.g., Reston high) created by reactivation of the northwestward verging imbricate thrust faults.

(d) Farther north in the less deformed central part of the basin, coal-bearing deltaic and deep-marine lithic and lithic arkosic turbidite sandstones of sequences I and II thin rapidly, pinch out, and onlap seamounts and oceanic basaltic islands of Siletz River Volcanics (i.e., Umpqua arch). These sequences are represented by a 200-ft thick condensed section of deep-marine mudstone over the high. The section thickens northward in the subsurface into the Smith River subbasin.

(e) By the middle Eocene (50 Ma), after accretion, a new subduction zone formed on the present outer continental shelf and slope of Oregon. Renewed subsidence created the Tyee forearc basin which, with the Umpqua basin and northern Klamath Mountains, was concurrently rotated clockwise. This mildly deformed basin presently trends north-south, obliquely across the older folded and thrusted Umpqua marginal basin. Wave- and tide-dominated coal-bearing middle and late Eocene deltas of sequences III and IV and a sandy deep-sea fan of sequence III (Tyee, Elkton, Bateman, and Spencer formations) prograded northward down the axis of the forearc basin. The micaceous lithic arkosic sandstones of these formations were sourced from rivers draining the granitic Idaho batholith and middle Eocene Clarno(?) volcanic arc terrane and from the Klamath Mountains.

(f) Renewed mild east-west compression formed gentle north-south, northwest-, and northeast-trending folds in the middle Eocene sequences III and IV, as the southern Oregon Coast Range was uplifted starting in the late-middle Miocene. Some high-angle reverse (back thrusts?) and oblique-slip strike-slip (tear) faults reflect reactivation of Umpqua basement structures.

Conclusions regarding the oil and gas potential of the basin are:

(a) In general, the southern Tyee basin has low to moderate petroleum potential. This study, however, has identified several promising areas that merit further exploration for natural gas.

(b) Organic geochemistry of numerous samples (including analyses of Rock-Eval, TOC, R_O, and TAI) indicates that most potential source rocks (e.g., shelf, slope, and overbank mudstones)

are thermally immature to submature although some potential source rocks are locally mature (i.e., R_O 0.7 to 1.0). Most sedimentary rock units would likely produce limited quantities of only or primarily natural gas (methane) because most potential source rocks in these units are organically lean (<1% TOC) and because the organic matter is dominantly gas-prone terrestrial Type III kerogen.

(c) Some deltaic sedimentary units (e.g., White Tail Ridge and Spencer formations), however, contain thin, widespread beds of coal and carbonaceous overbank mudstone (i.e., TOC 2 to 50%) which could act as sources for methane. In addition, some pre-Tertiary deep-marine mélanged mudstone and pelagic limestone in the adjacent Klamath Mountains represent restricted potential source beds. Both biogenic and thermogenic methane, identified by isotopic and molecular gas compositions, were sampled in numerous natural seeps, exploration wells, and water wells in the southern part of the basin and adjacent Klamath Mountains. Possible seals include the Camas Valley Formation, intraformational mudstone, and overlying tightly cemented sandstone units.

(d) A computer-generated maturation model (BasinMod) predicts that, by the Oligocene, some lower Umpqua Group strata may have been matured in parts of the basin that were more deeply buried. Other mechanisms that have created local thermal maturation include flash heating by intrusion of thick basaltic sills, migration of hydrothermal fluids and/or frictional heating along thrust faults, and deep burial by thrusting during early Eocene subduction and accretion.

(e) Reservoir-quality porosity and permeability are present locally in some delta front sandstone parasequences and delta plain channel sandstone facies of the White Tail Ridge Formation and Spencer Formation. In general, however, a complex burial diagenesis of zeolite (laumontite-clinoptilolite), clay (smectite-corrensite), and quartz cements has destroyed much of the primary porosity in many potential arkosic and lithic reservoir sandstone and conglomerate units (typically <5% porosity and <5 md permeability). Minor secondary dissolution and fracture (jointing) porosity have locally enhanced the reservoir potential of some turbidite sandstones in the lower Tyee Mountain Member in the northern part of the basin. Minor secondary fracture porosity is also locally developed in tightly folded and thrusted Umpqua Group turbidite sandstones in fault-propagation folds.

Three speculative petroleum systems (Magoon, 1988) identified within the Tyee basin include five structural and stratigraphic plays:

(a) A hybrid petroleum system in the southern part of the Tyee basin consists of potentially mature lower Eocene Umpqua Group strata in thrust slices with locally subducted, mature source rocks of the Klamath Mountains. Thermogenic natural gas may have migrated up along thrust faults into fault-propagation folds of tectonically fractured, thermally immature Umpqua turbidite sandstone reservoirs and into the overlying less deformed White Tail Ridge deltaic sandstone reservoir. These reservoirs, which pinch out to the north, could be sealed by transgressive mudstone of the Camas Valley Formation and by intraformational mudstone and diagenetically "tight" sandstone beds of the Tyee Mountain Member.

(b) A second speculative hybrid petroleum system lies along the eastern border of the basin beneath the foothills of the Western Cascades volcanic arc. Locally, gas-prone potential source rocks (beds of coal and carbonaceous mudstone in the Spencer and White Tail Ridge formations) may have been thermally matured by flash heating near thick sills or by hydrothermal fluids associated with mid-Tertiary volcanism and plutonism in the Western Cascades arc. Hydrothermal fluids could have migrated through a fracture system associated with thrust faults and high-angle faults into overlying anticlinal folds involving reservoir-quality delta front and channel sandstone of the Spencer and White Tail Ridge formations and sealed by Camas Valley mudstone, intraformational overbank mudstone, and/or younger units of the Western Cascades arc.

(c) Basin-center tight-gas sandstone-mudstone reservoirs are possible in the deeply buried northern part of the basin in overpressured zones in the lower Tyee Mountain Member and lower Umpqua Group (i.e., Smith River subbasin). Anticlinal and fault traps are possible.

Proposed structural plays include the Williams River-Burnt Ridge anticlinal plays, Western Cascades play and Bonanza thrust, Klamath Mountains subthrust plays, and Tyee Mountain anticlines.

REFERENCES CITED

Alger, M. P., 1985, Geology; *in* Olmstead, D. L., ed., Mist gas field; exploration and development, 1979-84: Oregon Dept. of Geology and Mineral Industries Oil and Gas Investigation 10, p. 6-9.

Ahmad, Raisuddin, 1981, Stratigraphy, structure and petrology of the Lookingglass and Roseburg formations, Agness-Illahe area, southwestern Oregon: Eugene, OR, University of Oregon, M.S. thesis, 150 p.

Amoco Production Company, Research Center, 1983, Source rock evaluation: Eocene cuttings, Florida Exploration No. 1-4 Harris, Douglas County, Oregon, 2 p. + tables.

Amoco Production Company, Research Center, 1985, Oil correlation evaluation: Drilling mud analysis, Amoco No. B-1 Weyerhaeuser well, Douglas County, Oregon, 2 p. + tables.

Armentrout, J. M. and Suek, D. H., 1985, Hydrocarbon exploration in western Oregon and Washington: American Association of Petroleum Geologists Bulletin, v. 69, no. 4, p. 627-643.

Baker, L. J., 1988, The stratigraphy and depositional setting of the Spencer Formation, west-central Willamette Valley, Oregon; a surface-subsurface analysis: Corvallis, OR, Oregon State University, M.S. thesis, 171 p.

Baldwin, E. M., 1974, Eocene stratigraphy of southwestern Oregon: Oregon Dept. of Geology and Mineral Industries Bulletin 83, 40 p.

Baldwin, E. M., 1984, The origin of olistostromes in the Roseburg Formation in southwestern Oregon: Oregon Geology, v. 46, no. 7, p. 75-76, 82.

Baldwin, E. M. and Beaulieu, J. D., 1973, Geology and mineral resources of Coos County, Oregon: Oregon Dept. of Geology and Mineral Industries Bulletin 80, p. 9-40.

Baldwin, E. M. and Hess, P. D., 1971, Geology of the Powers quadrangle,Oregon: Oregon Dept. of Geology and Mineral Industries Geologic Map Series GMS-5, scale 1:62,500.

Baldwin, E. M. and Perttu, R. K., 1980, Paleogene stratigraphy and structure along the Klamath borderland, Oregon; *in* Oles, K. F., Johnson, J. G., Niem, A. R., and Niem, W. A., eds., Geologic field trips in western Oregon and southwestern Washington: Oregon Dept. of Geology and Mineral Industries Bulletin 101, p. 9-37.

Baldwin, E. M. and Perttu, R. K., 1989, Eocene unconformities in the Camas Valley quadrangle, Oregon: Oregon Geology, v. 51, no. 1, p. 3-8.

Black, G. L., 1990, Geologic map of the Reston quadrangle, Douglas County, Oregon: Oregon Dept. of Geology and Mineral Industries Geologic Map Series GMS-68, scale 1:24,000.

Black, G. L., 1994a, Geologic map of the Kenyon Mountain quadrangle, Douglas and Coos counties, Oregon: Oregon Dept. of Geology and Mineral Industries Geologic Map Series GMS-83, scale 1:24,000.

Black, G. L., 1994b, Geologic map of the Remote quadrangle, Coos County, Oregon: Oregon Dept. of Geology and Mineral Industries Geologic Map Series GMS-84, scale 1:24,000.

Black, G. L. and Priest, G. R., 1993, Geologic map of the Camas Valley quadrangle, Douglas and Coos counties, Oregon: Oregon Dept. of Geology and Mineral Industries Geologic Map Series GMS-76, scale 1:24,000.

Black, G. L., Molenaar, C. M., Niem, A. R., Niem, W. A., Priest, G. R., Ryu, I., and Wells, R. E., in prep., Geologic map of the Tyee basin, southern Coast Range, Coos and Douglas counties, Oregon: Oregon Dept. of Geology and Mineral Industries Open-File Report

Blake, M. C., Jr., 1984, Tectonostratigraphic terranes in southwestern Oregon; *in* Nilsen, T. H., ed., Geology of the Upper Cretaceous Hornbrook Formation, Oregon and California: Pacific Section, Society of Economic Paleontologists and Mineralogists, v. 42, p. 159-165.

Blake, M. C., Jr., Engebretson, D. C., Jayko, A. S., and Jones, D. L., 1985, Tectono-stratigraphic terranes in southwest Oregon; *in* Howell, D. G., ed., Tectono-stratigraphic terranes of the Circum-Pacific region: Circum-Pacific Council on Energy and Mineral Resources, Earth Science Series, v. 1, p. 145-157.

Bodine, M. W. and Madsen, B. M., 1987, Mixed-layer chlorite/smectites from a Pennsylvanian evaporite cycle, Grand County, Utah: Proceedings, International Clay Conference 1985, Denver, CO, p. 85-96.

Boles, J. R., 1982, Active albitization of plagioclase, Gulf Coast Tertiary: American Journal of Science, v. 282, p. 165-180.

Boles, J. R. and Coombs, D. S., 1975, Mineral reactions in zeolite Triassic tuff, Hokonui Hills, New Zealand: Geological Society of America Bulletin, v. 86, p. 163-173.

Boles, J. R. and Coombs, D. S., 1977, Zeolite facies alteration of sandstone in the Southland Syncline, New Zealand: American Journal of Science, v. 277, p. 982-1012.

Brown and Ruth Laboratories, Inc., 1983, Regional petroleum geochemistry of the onshore and offshore sediments of Washington and Oregon: geochemical reports on General Petroleum Long Bell No. 1, Sutherlin Unit No. 1, and Amoco Weyerhaeuser F-1 wells: unpublished reports on file in offices of Oregon Dept. of Geology and Mineral Industries, Portland.

Browning, J. L. and Flanagan, T., 1980, Source rock study of the lower Tertiary formations of southwestern Oregon: Consultant's report, 96 p.

Bukry, David and Snavely, P. D., Jr., 1988, Coccolith zonation for Paleogene strata in the Oregon Coast Range; *in* Filewicz, M. V. and Squires, R. L., eds., Paleogene stratigraphy, west coast of North America: Pacific Section, Society of Economic Paleontologists and Mineralogists, West Coast Paleogene Symposium, v. 58, p. 251-263.

Burns, L. K. and Ethridge, Frank, 1979, Petrology and diagenetic effects of lithic sandstone: Paleocene and Eocene Umpqua Formation, southwest Oregon; *in* Scholle, P. A. and Schluger, P. R., eds., Aspects of

diagenesis: Society of Economic Paleontologists and Mineralogists Special Publication 26, p. 307-317.

Carayon, Veronique, 1984, Étude geologique de l'extremité septentrionale de la chaine des Klamath, sud-ouest Oregon (U.S.A.): Ph.D. dissertation, 3rd Cycle, Pierre and Marie Curie University, University of Paris VI, 186 p., map scale 1:62,500.

Carayon, Veronique, de Wever, Patrick, and Raoult, J. F., 1984, Étude des blocs calcaires contenus dans les series franciscaines du Sud-Ouest de l'Oregon (U.S.A.): consequences sur l'age des mélanges franciscains: Comptes Rendus de l'Academie des Sciences, v. 298, Series II, no. 16, p. 709-714.

Chan, M. A., 1982, Comparison of sedimentology and diagenesis of Eocene rocks, southwest Oregon: Madison, Wisconsin, University of Wisconsin-Madison, Ph.D. dissertation, 322 p.

Chan, M. A., 1985, Correlations of diagenesis with sedimentary facies in Eocene sandstones, western Oregon: Journal of Sedimentary Petrology, v. 55, no. 3, p. 322-333.

Chan, M. A. and Dott, R. H., Jr., 1983, Shelf and deep-sea sedimentation in Eocene forearc basin, western Oregon--fan or non-fan?: American Association of Petroleum Geologists Bulletin, v. 67, no. 11, p. 2100-2116.

Chan, M. A. and Dott, R. H., Jr., 1986, Depositional facies and progradational sequences in Eocene wave-dominated deltaic complexes, southwestern Oregon: American Association of Petroleum Geologists Bulletin, v. 70, no. 4, p. 415-429.

Dickinson, W. R., 1970, Interpreting detrital modes of graywacke and arkose: Journal of Sedimentary Petrology, v. 40, p. 695-707.

Dickinson, W. R. and Suczek, C. A., 1979, Plate tectonics and sandstone compositions: American Association of Petroleum Geologists Bulletin, v. 63, p. 2164-2182.

Dickinson, W. R., Beard, L. S., Brakenridge, G. R., Rejavec, J. R., Inman, K. F., Knepp, R. A., Lindberg, F. A., and Ryberg, P. T., 1983, Provenance of North American Phanerozoic sandstones in relation to tectonic setting: Geological Society of America Bulletin, v. 94, p. 222-235.

Diller, J. S., 1898, Roseburg folio: U.S. Geological Survey Geologic Atlas of the United States, Folio No. 49.

Dott, R. H., Jr., 1966, Eocene deltaic sedimentation at Coos Bay, Oregon: Journal of Geology, v. 74, p. 373-420.

Duell, G. A., 1957, The Eden Ridge coal field, Coos County, Oregon--A preliminary study: consulting report prepared for Pacific Power and Light Company, 24 p. + tables and lithology logs; courtesy of U.S. Bureau of Land Management, Portland.

Durand, B. and Monin, J. C., 1980, Elemental analysis of kerogens (C, H, O, N, S, Fe); *in* Durand, B., ed., Kerogen: Paris, Editions Technip, p. 113-142.

Espitalié, J., 1985, Use of Tmax as a maturation index for different types of organic matter - comparison with vitrinite reflectance; *in* Burrus, J., ed., Thermal modeling in sedimentary basins: Paris, Editions Technip, p. 475-496.

Falvey, D. and Middleton, M. F., 1981, Passive continental margins; evidence of prebreakup deep crustal metamorphic subsidence mechanism: Oceanologica Acta, Colloquium C3, 26th International Geological Congress, p. 103-104.

Folk, R. L., 1974, Petrology of sedimentary rocks: Austin, TX, Hemphill Publishing Co., 170 p.

Gautier, D. L. and Varnes, K. L., 1993, Plays for assessment in Region II, Pacific Coast as of October 4, 1993; 1995 National assessment of oil and gas: U.S. Geological Survey Open-File Report 93-596-B, 11 p.

Gold, P. B., 1987, Textures and geochemistry of authigenic albite from Miocene sands, Louisiana Gulf Coast: Journal of Sedimentary Petrology, v. 57, p. 353-362.

Heller, P. L., 1983, Sedimentary response to Eocene tectonic rotation in western Oregon: Tucson, Arizona, University of Arizona, Ph.D. dissertation, 343 p.

Heller, P. L. and Dickinson, W. R., 1985, Submarine ramp facies model for delta-fed, sand-rich turbidite systems: American Association of Petroleum Geologists Bulletin, v. 69, no. 6, p. 960-976.

Heller, P. L., Renne, P. R., and O'Neil, J. R., 1992, River mixing rate, residence time, and subsidence rates from isotopic indicators: Eocene sandstones of the U.S. Pacific Northwest: Geology, v. 20, no. 12, p. 1095-1098.

Heller, P. L. and Ryberg, P. T., 1983, Sedimentary record of subduction to forearc transition in the rotated Eocene basin of western Oregon: Geology, v. 11, no. 7, p. 380-383.

Heller, P. L., Peterman, Z. E., O'Neill, J. R., and Shafiqullah, M., 1985, Isotopic provenance of sandstones from the Eocene Tyee Formation, Oregon Coast Range: Geological Society of America Bulletin, v. 96, p. 770-780.

Helmold, K. P. and Van de Kamp, P. C., 1984, Diagenetic mineralogy and controls on albitization and laumontite formation in Paleogene arkoses, Santa Ynez Mountains, California; *in* MacDonald, D. A. and Surdam, R. C., eds., Clastic diagenesis: American Association of Petroleum Geologists Memoir 37, p. 239-276.

Hoover, Linn, 1963, Geology of the Anlauf and Drain quadrangles, Douglas and Lane counties, Oregon: U.S. Geological Survey Bulletin 1122-D, 62 p.

Hower, J., 1981, Shale diagenesis; *in* Longstaffe, F. J., ed., Clays and the resource geologist: Mineralogical Association of Canada, Short Course, v. 7, p. 60-80.

Iijima, A., 1978, Geological occurrences of zeolites in marine environments; *in* Mumpton, F. A., and Sand, L. B., eds., Natural zeolites: occurrences, properties, use: New York, Pergamon, p. 175-198.

Ingersoll, R. V., 1978, Petrofacies and petrologic evolution of the late Cretaceous fore-arc basin, northern and central California: Journal of Geology, v. 86, p. 335-353.

Jayko, A. S., 1995a, Geologic map of the Lane Mt. 7.5' Quadrangle, Oregon: U. S. Geological Survey Open File Report 95-20.

Jayko, A. S., 1995b, Geologic map of the White Rock 7.5' Quadrangle, Oregon: U. S. Geological Survey Open File Report 95-18.

Jayko, A. S., and Wells R. E., 1996, Geologic map of the Dixonville 7.5' Quadrangle, Oregon: U. S. Geological Survey Open File Report 96-XXX, in prep.

Johnson, V. G., Graham, D. L., and Reidel, S. P., 1993, Methane in Columbia River Basalt aquifers: isotopic and geohydrologic evidence for a deep coal-bed gas source in the Columbia Basin, Washington: American Association of Petroleum Geologists Bulletin, v. 77, no. 7, p. 1192-1207.

Koler, T. E., 1979, Stratigraphy and sedimentary petrology of the northwest quarter of the Dutchman Butte quadrangle, southwest Oregon: Portland, OR, Portland State University, unpublished master's thesis, 72 p.

Kugler, R. L., 1979, Stratigraphy and petrology of the Bushnell Rock Member of the Lookingglass Formation, southwestern Oregon Coast Range: Eugene, OR, University of Oregon, unpublished master's thesis, 118 p.

Kvenvolden, K. A., Golan-Bac, M., and Snavely, P. D., Jr., 1989, Preliminary evaluation of the petroleum potential of the Tertiary accretionary terrane, west side of the Olympic Peninsula, Washington: C. Composition of natural gas seeps, outcrops and a test well: U.S. Geological Survey Bulletin 1892, p. 39-45.

Kvenvolden, K. A., Lorenson, T. D., and Niem, A. R., 1994, Natural gas occurrences in the Coast Range of southern Oregon: Geological Society of America Abstracts and Programs, v. 26, no. 7, p. 36.

Kvenvolden, K. A., Lorenson, T. D., and Niem, A. R., 1995, Natural hydrocarbon gases in the Coast Range of southern Oregon: U.S. Geological Survey Open-File Report 95-93, 19 p.

Law, B. E. and Dickinson, W. W., 1985, Conceptual model for origin of abnormally pressured gas accumulations in low-permeability reservoirs: American Association of Petroleum Geologists Bulletin, v. 69, p. 1295-1304.

Law, B. E. and Spencer, C. W., 1993, Gas in tight reservoirs - an emerging major source of energy; *in* Howell, D. G., ed., The future of energy gases: U.S. Geological Survey Professional Paper 1570, p. 233-252.

Law, B. E., Anders, D. E., Fouch, T. D., Pawlewicz, M. J., Lickus, M. R., and Molenaar, C. M., 1984, Petroleum source rock evaluation of outcrop samples from Oregon and northern California: Oregon Geology, v. 46, p. 77-81.

Law, B. E., Nuccio, V. F., and Barker, C. E., 1989, Kinky vitrinite reflectance well profiles: evidence of paleopore pressure in low-permeability, gas-bearing sequences in Rocky Mountain foreland basins: American Association of Petroleum Geologists Bulletin, v. 73, p. 999-1010.

Law, B. E., Tennyson, M. E., and Johnson, S. Y., 1994, Basin-centered gas accumulations in the Pacific Northwest: American Association of Petroleum Geologists, 1994 Annual Convention Program (with abstracts), p. 194.

Lesher, C. E., 1914, The Eden Ridge coal field, Coos County, Oregon: U.S. Geological Survey Bulletin 541, p. 399-418.

Lillis, Paul, Daws, T. A., Pawlewicz, M. J., Niem, A. R., and Ryu, In-Chang, 1995, Hydrocarbon source rock characterization and maturity based on Rock Eval pyrolysis and vitrinite reflectance of Eocene strata, southern Oregon Coast Range, Douglas and Coos counties, southwest Oregon: U.S. Geological Survey Open-File Report 95-75G, 27 p.

Long, D. E., 1994, Source rock geochemistry of the southern Tyee basin, southwest Oregon: Portland, OR, Portland State University, M.S. thesis, 136 p.

Lopatin, N. V., 1971, Temperature and geologic time as factors in coalification: Akad. Nauk. Uzb. SSR Izv. Ser. Geol., v. 3, p. 95-106.

Lovell, J. P. B., 1969, Tyee Formation: Undeformed turbidites and their lateral equivalents: Mineralogy and paleogeography: Geological Society of America Bulletin, v. 80, no. 1, p. 9-22.

Magoon, L. B., 1988, Petroleum systems of the United States: U.S. Geological Survey Bulletin 1870, 68 p.

Magoon, L. B., 1990, The petroleum system - status of research and method, 1990: U.S. Geological Survey Bulletin 1912, 88 p.

Magoon, L. B., 1992, The petroleum system - status of research and method, 1992: U.S. Geological Survey Bulletin 2007, 98 p.

Mango, F. D., Hightower, J. W., and James, A. I., 1994, Role of transition-metal catalysis in the formation of natural gas: Nature, v. 368, p. 536-538.

McBride, E. F., Land, L. S., and Mack, L. E., 1987, Diagenesis of eolian and fluvial feldspathic sandstones, Norphlet Formation (Upper Jurassic), Rankin County, Mississippi, and Mobile County, Alabama: American Association of Petroleum Geologists Bulletin, v. 71, p. 1019-1034.

McKnight, Brian K., 1971, Petrology and sedimentation of Cretaceous and Eocene rocks in the Medford-Ashland region, southwestern Oregon: Corvallis, OR, Oregon State University, Ph.D. dissertation, 177 p.

Meissner, F. F., 1978, Patterns of source-rock maturity in nonmarine source rocks of some typical Western Interior basins; *in* Nonmarine Tertiary and upper Cretaceous source rocks and the occurrence of oil and gas in west-central U.S.: Rocky Mountain Association of Geologists Continuing Education Lecture Series, p. 1-37.

Milliken, K. L., 1988, Loss of provenance information through subsurface diagenesis in Plio-Pleistocene sandstones, northern Gulf of Mexico: Journal of Sedimentary Petrology, v. 58, p. 992-1002.

Mobil Oil Corporation, 1980, Source rock data on map of southwest Oregon, courtesy of Lee High, Division Geologist.

Molenaar, C. M., 1985, Depositional relations of Umpqua and Tyee formations (Eocene), southwestern Oregon: American Association of Petroleum Geologists Bulletin, v. 69, no. 8, p. 1217-1229.

Moraes, M. A. S. and DeRos, L. F., 1990, Infiltrated clays in fluvial Jurassic sandstones of Reconcavo basin, northeastern Brazil: Journal of Sedimentary Petrology, v. 60, p. 809-819.

Newton, V. C., Jr., 1979, Oregon's first gas wells completed: Oregon Geology, v. 41, p. 87-90.

Newton, V. C., Jr., 1980, Prospects for oil and gas in the Coos basin, western Coos, Douglas, and Lane counties, Oregon: Oregon Dept. of Geology and Mineral Industries Oil and Gas Investigation 6, 74 p.

Niem, A. R. and Niem, W. A., 1990, Geology and oil, gas, and coal resources, southern Tyee basin, southern Coast Range, Oregon: Oregon Dept. of Geology and Mineral Industries, Open-File Report O-89-3, 11 tables, 3 plates, 44 p.

Niem, A. R. and Snavely, P. D., Jr., 1991, Geology and preliminary hydrocarbon evaluation of the Tertiary Juan de Fuca basin, Olympic Peninsula, NW Washington: Washington Department of Natural Resources, Division of Geology and Earth Resources, Washington Geology, v. 19, no. 4, p. 27-34.

Niem, A. R., MacLeod, N. S., Snavely, P. D., Jr., Huggins, D., Fortier, J. D., Meyer, H. J., Seeling, A., and Niem, W. A., 1992a, Onshore-offshore geologic cross section, northern Oregon Coast Range to continental slope: Oregon Dept. of Geology and Mineral Industries Special Paper 26, 1 plate, 10 p.

Niem, A. R., McKnight, B. K., Meyer, H. J. and Campbell, K. A., 1994, Sedimentary, volcanic, and tectonic framework of forearc basins and the Mist Gas Field, northwest Oregon; *in* Swanson, D. A. and Haugerud, R. A., eds., Geologic field trips in the Pacific Northwest:

1994 Geological Society of America, Annual Meeting, Seattle, v. 1, section F, p. 1-42.

Niem, W. A., Niem, A. R., and Snavely, P. D., Jr., 1992b, Early and Mid-Tertiary oceanic realm and continental margin -- western Washington-Oregon coastal sequence; *in* Burchfiel, B. C., Lipman, P. W., and Zoback, M. L., eds., The Cordilleran Orogen: Conterminous U.S.: Geological Society of America The Geology of North America, volume G-3, p. 265-270.

Niem, W. A., Niem, A. R., and Snavely, P. D., Jr., 1992c, Late Cenozoic continental margin of the Pacific Northwest -- Sedimentary embayments of the Washington-Oregon coast; *in* Burchfiel, B. C., Lipman, P. W., and Zoback, M. L., eds., The Cordilleran Orogen: Conterminous U.S.: Geological Society of America The Geology of North America, volume G-3, p. 314-319.

Noh, J. H. and Boles, J. R., 1993, Origin of zeolite cements in the Miocene sandstones, North Tejon oil fields, California: Journal of Sedimentary Petrology, v. 63, p. 248-260.

Olmstead, D. L., 1989, Hydrocarbon exploration and occurrences in Oregon: Oregon Dept. of Geology and Mineral Industries, Oil and Gas Investigation 15, 78 p.

Penoyer, P. E. and Niem, A. R., 1975, Geology and ground water resources of the Kings Valley area, central Oregon Coast Range, Oregon: Water Resources Research Institute, Bulletin WRRI-39, 92 p.

Personius, S. F., 1993, Age and origin of fluvial terraces in the central Coast Range, western Oregon: U.S. Geological Survey Bulletin 2038, 56 p.

Perttu, R. K., 1976, Structural geology of the northeast quarter of the Dutchman Butte quadrangle, southwest Oregon: Portland, OR, Portland State University, M.S. thesis, 60 p.

Perttu, R. K. and Benson, G. T., 1980, Deposition and deformation of the Eocene Umpqua Group, Sutherlin area, southwestern Oregon: Oregon Geology, v. 42, no. 8, p. 135-140.

Peters, K. E., 1986, Guidelines for evaluating petroleum source rock using programmed pyrolysis: American Association of Petroleum Geologists Bulletin, v. 70, p. 318-329.

Peterson, N. V., 1957, The geology of the southeast third of the Camas Valley quadrangle, Oregon: Eugene, OR, University of Oregon, M.S. thesis, 89 p.

Pittman, E. D., Larese, R. E., and Heald, M. T., 1992, Clay coats: occurrence and relevance to preservation of porosity in sandstones; *in* Houseknecht, D. W. and Pittman, E. D., eds., Origin, diagenesis, and petrophysics of clay minerals in sandstones: Society of Economic Paleontologists and Mineralogists Special Publication 47, p. 241-255.

Posamentier, H. W., Jervey, M. T., and Vail, P. R., 1988, Eustatic controls on clastic deposition I - conceptual framework; *in* Wilgus, C. K., Posamentier, H. W., Ross, C. A., and Kendall, C. G. St. C., eds., Sea-level changes: an integrated approach: Society of Economic Paleontologists and Mineralogists Special Publication 42, p. 109-124.

Ramp, Len, 1972, Geology and mineral resources of Douglas County, Oregon: Oregon Dept. of Geology and Mineral Industries Bulletin 75, 106 p.

Ramp, Len and Moring, Barry, 1986, Reconnaissance geologic map of the Marial quadrangle, southwestern Oregon: U.S. Geological Survey Miscellaneous Field Studies Map MF-1735, scale 1:62,500.

Reynolds, R. C., 1980, Interstratified clay minerals; *in* Brindley, G. W. and Brown, G., eds., Crystal structures of clay minerals and their X-ray identification: Mineralogical Society of London, p. 249-303.

Rice, D. D., 1993, Composition and origins of coalbed gas; *in* Law, B. E. and Rice, D. D., eds., Hydrocarbons from coal: American Association of Petroleum Geologists, AAPG Studies in Geology Number 38, p. 159-184.

Ryberg, P. T., 1984, Sedimentation, structure, and tectonics of the Umpqua Group (Paleocene to early Eocene), southwestern Oregon: Tucson, Arizona, University of Arizona, Ph.D. dissertation, 280 p.

Ryu, In-Chang, 1995, Stratigraphy, sedimentology, and hydrocarbon potential of the lower to middle Eocene forearc and subduction zone strata in the southern Tyee basin, Oregon Coast Range: Corvallis, OR, Oregon State University, Ph.D. dissertation.

Ryu, In-Chang and Niem, A. R., 1993, Sequence stratigraphy in active convergent margins - Eocene Tyee basin, southern Oregon Coast Range: American Association of Petroleum Geologists Bulletin, 1993 Annual Convention Program (with abstracts), p. 175-176.

Ryu, In-Chang and Niem, A. R., 1994, Tectonism-forced transgressive systems tract: a stratigraphic fingerprint of convergent basin tectonics, Eocene Tyee basin, southern Oregon Coast Range: Geological Society of America Abstracts with Programs, v. 26, no. 7, p. 430.

Ryu, In-Chang, Niem, A. R., and Niem, W. A., 1992, Schematic fence diagram of the southern Tyee basin, Oregon Coast Range, showing stratigraphic relationships of exploration wells to surface measured sections: Oregon Dept. of Geology and Mineral Industries Oil and Gas Investigation 18, 1 plate + 28 p.

Schmidt, V. and MacDonald, D. A., 1979, Texture and recognition of secondary porosity in sandstone; *in* Scholle, P. A. and Schluger, P. R., eds., Aspects of diagenesis: Society of Economic Paleontologists and Mineralogists Special Publication 26, p. 209-225.

Scott, A.R., 1993, Composition and origin of coalbed gases from selected basins of the United States: Proceedings of the 1993 International Coalbed Methane Symposium, 16 p.

Shell Oil Company, 1959, Petrographic and field data on Eocene strata of the Tyee basin, research by C. M. Molenaar, provided to the authors by Molenaar with permission of Shell Oil Company.

Snavely, P. D., Jr., 1984, Sixty million years of growth along the Oregon continental margin; *in* Clarke, S. H., ed., Highlights in marine research: U.S. Geological Survey Circular 938, p. 9-18.

Snavely, P. D., Jr., 1987, Tertiary geologic framework, neotectonics, and petroleum potential of the Oregon-Washington continental margin; *in* Scholl, D. W., Grantz, A., and Vedder, J. G., eds., Geology and resource potential of the continental margin of western North America and adjacent ocean basins--Beaufort Sea to Baja California: Circum-Pacific Council for Energy and Mineral Resources Earth Science Series, v. 6, p. 305-335.

Snavely, P. D., Jr. and Kvenvolden, K. A., 1988, Preliminary evaluation of the petroleum potential of the Tertiary accretionary terrane, west side of the Olympic Peninsula, Washington--Geology and hydrocarbon potential: U.S. Geological Survey Open-File Report 88-75, p. 1-26.

Snavely, P. D., Jr., MacLeod, N. S., and Wagner, H. C., 1968, Tholeiitic and alkalic basalts of the Eocene Siletz River Volcanics, Oregon Coast Range: American Journal of Science, v. 266, no. 6, p. 454-481.

Snavely, P. D., Jr. and Wagner, H. C., 1963, Tertiary geologic history of western Oregon and Washington: Washington Division of Mines and Geology Report of Investigation 22, 25 p.

Snavely, P. D., Jr., Wagner, H. C., and MacLeod, N. S., 1964, Rhythmic-bedded eugeosynclinal deposits of the Tyee Formation, Oregon Coast Range: Kansas Geological Survey, Bulletin 169, p. 461-480.

Spencer, C. W., 1987, Hydrocarbon generation as a mechanism for overpressuring in Rocky Mountain region: American Association of Petroleum Geologists Bulletin, v. 71, p. 368-388.

Stewart, R. E., 1954, Oil and gas exploration in Oregon: Oregon Dept. of Geology and Mineral Industries Miscellaneous Paper 6, 53 p.

Stormberg, G. J., 1992, The Mist Gas Field, northwest Oregon: Source rock characterization and stable isotope (C, H, N) geochemistry: Corvallis, OR, Oregon State University, M.S. thesis, 191 p.

Surdam, R. C. and Boles, J. R., 1979, Diagenesis of volcanic sandstones; *in* Scholle, P. A. and Schluger, P. R., eds., Aspects of diagenesis: Society of Economic Paleontologists and Mineralogists Special Publication 26, p. 227-242.

Surdam, R. C. and Crossey, L. J., 1987, Integrated diagenetic modelling: a process-oriented approach for clastic systems: Annual Review of Earth and Planetary Sciences, v. 15, p. 141-170.

Tissot, B. T. and Welte, D. H., 1978, Petroleum formation and occurrence: New York, Springer Verlag, 538 p.

Tissot, B. T. and Welte, D. H., 1984, Petroleum formation and occurrence, second edition: New York, Springer-Verlag, 699 p.

Tissot, B. P., Durand, B., Espitalié, J., and Combaz, A., 1974, Influence of nature and diagenesis of organic matter in formation of petroleum: American Association of Petroleum Geologists Bulletin, v. 58, p. 499-506.

Tissot, B. P., Pelet, R., and Ungerer, P. H., 1987, Thermal history of sedimentary basins, maturation indices, and kinetics of oil and gas generation: American Association of Petroleum Geologists Bulletin, v. 71, p. 1445-1466.

Treasher, R. C., 1942, Camas Valley and Flournoy Valley (west of Roseburg): unpublished report on file at DOGAMI, Portland, 8 p.

Trehu, Anne, Nabelek, J., Azevedo, S., Brocher, T., Mooney, W., Luetgert, J., Clowes, R., Nakamura, Y., Smithson, S., and Miller, K., 1992, A crustal cross section across the Cascadia subduction zone in central Oregon: EOS, v. 73, no. 43, p. 391.

U.S. Bureau of Land Management (USBLM), 1983, Eden Ridge resource recovery and protection plan: unpublished report on file at USBLM, Portland, 24 p.

U.S. Bureau of Land Management (USBLM), 1989, Letter of November 15, 1989, from John F. Kalvels, mining engineer, to Alan Niem.

Van Wagoner, J. C., Mitchum, R. M., Campion, K. M., and Rahmanian, V. D., 1990, Siliciclastic sequence stratigraphy in well logs, cores, and outcrops: concepts for high-resolution correlation of time and facies: American Association of Petroleum Geologists Methods in Exploration Series, No. 7, 55 p.

Walker, G. W. and MacLeod, N. S., 1991, Geologic map of Oregon: U.S. Geological Survey, scale 1:1,500,000.

Waples, D. W., 1980, Time and temperature in petroleum formation; application of Lopatin's method to petroleum exploration: American Association of Petroleum Geologists Bulletin, v. 64, p. 916-926.

Weatherby, D. G., 1991, Stratigraphy and sedimentology of the late Eocene Bateman Formation, southern Oregon Coast Range: Eugene, OR, University of Oregon, M.S. thesis, 161 p.

Wells, F. G. and Peck, D. L., 1961, Geologic map of Oregon west of the 121st meridian: U.S. Geological Survey Miscellaneous Geologic Investigations Map I-325, scale 1:500,000.

Wells, F. G. and Waters, A. C., 1934, Quicksilver deposits of southwestern Oregon: U.S. Geological Survey Bulletin 850, 58 p.

Wells R. E., 1996a, Geologic map of the Cedar Creek 7.5' Quadrangle, Oregon: U.S. Geological Survey Open File Report 96-XXX, in press.

Wells R. E., 1996b Geologic map of the Hinkle Creek 7.5' Quadrangle, Oregon: U.S. Geological Survey Open File Report 96-XXX, in press.

Wells R. E., 1996c, Geologic map of the Nonpareil 7.5' Quadrangle, Oregon: U.S. Geological Survey Open File Report 96-XXX, in press.

Wells R. E., 1996d, Geologic map of the Oak Creek Valley 7.5' Quadrangle, Oregon: U.S. Geological Survey Open File Report 96-XXX, in press.

Wells R. E., 1996e, Geologic map of the Roseburg West 7.5' Quadrangle, Oregon: U.S. Geological Survey Open File Report 96-XXX, in press.

Wells R. E., 1996f, Geologic map of the Roseburg East 7.5' Quadrangle, Oregon: U.S. Geological Survey Open File Report 96-XXX, in press.

Wells R. E., 1996g, Geologic map of the Sutherlin 7.5' Quadrangle, Oregon: U.S. Geological Survey Open File Report 96-XXX, in press.

Wells R. E., 1996h, Geologic map of the Tyee Mountain 7.5' Quadrangle, Oregon: U.S. Geological Survey Open File Report 96-XXX, in press.

Wells R. E., 1996i, Geologic map of the Winchester 7.5' Quadrangle, Oregon: U.S. Geological Survey Open File Report 96-XXX, in press.

Wells R. E., Felger, Tracey, and Abolins, Mark, 1996a, Geologic map of the Garden Valley 7.5' Quadrangle, Oregon: U.S. Geological Survey Open File Report 96-XXX, in press.

Wells, R. E. and Heller, P. L., 1988, The relative contribution of accretion, shear, and extension to Cenozoic tectonic rotation in the Pacific Northwest: Geological Society of America Bulletin, v. 100, p. 325-338.

Wells R. E., and Niem, A.R., 1996, Geologic map of the Glide 7.5' Quadrangle, Oregon: U.S. Geological Survey Open File Report 96-XXX, in press.

Wells R. E., Smith, Brett, and Cherichetti, Lars, 1996b, Geologic map of the Callahan 7.5' Quadrangle, Oregon: U.S. Geological Survey Open File Report 96-XXX, in press.

Wells, R. E. and Snavely, P. D., Jr., 1989, Paleogene geologic history of the Oregon-Washington continental margin: Geological Survey of America Abstracts with Program, v. 21, no. 5, p. 157.

Wells, R. E., Engebretson, D. C., Snavely, P. D., Jr., and Coe, R. S., 1984, Cenozoic plate motions and the volcano-tectonic evolution of western Oregon and Washington: Tectonics, v. 3, no. 2, p. 275-294.

Wells, R. E., Jayko, A., McLaughlin, R., Niem, A. R., and Black, G. L., in prep., Geology of the Roseburg (1:100,000) sheet: U.S. Geological Survey Open-File Report.

Wiley, T. J., 1995, Reconnaissance geologic map of the Dora and Sitkum quadrangles, Coos Co., Oregon: Oregon Dept. of Geology and Mineral Industries: Geologic Map Series GMS-98, scale 1:24,000.

Wiley, T. J. and Black, G. L., 1994, Geologic map of the Tenmile quadrangle, Douglas County, Oregon: Oregon Dept. of Geology and Mineral Industries: Geologic Map Series GMS-86, scale 1:24,000.

Wiley, T. J., Priest, G.R., and Black, G. L., 1994, Geologic map of the Mt. Gurney quadrangle, Douglas and Coos counties, Oregon: Oregon Dept. of Geology and Mineral Industries: Geologic Map Series GMS-85, scale 1:24,000.

Williams, H., Turner, F. J., and Gilbert, C. M., 1954, Petrography: San Francisco, W. H. Freeman, 406 p.

APPENDIX

SEQUENCE	STRATIGRAPHIC UNIT	NUMBER OF SAMPLES	% DETRITAL FRAMEWORK GRAINS								
			QUARTZ		FELDSPAR		LITHIC FRAGMENTS			ACCESSORY MINERALS	
			Qm	Qp	P	K	Lv	Lm	Ls	Micas	Heavy M.
IV	Spencer Formation	2	31.88	0.77	25.10	10.37	24.84	0.13	0.38	5.76	0.77
	Bateman Formation	2	29.48	0.68	26.42	11.00	25.85	1.02	0.68	4.20	0.68
	Elkton Formation	1	28.54	0.71	25.94	10.38	26.89	1.42	0.24	5.19	0.71
	Baughman Member	5	24.24	1.59	22.37	8.92	36.62	0.47	0.14	4.90	0.75
III	Tyee Mountain Member	13	24.68	2.92	23.05	10.65	29.15	1.82	0.49	6.64	0.60
II	Rasler Creek Tongue	2	18.78	15.81	19.86	4.41	22.76	9.59	6.27	1.49	1.03
	Coquille River Member	8	10.95	19.17	14.18	4.83	6.93	19.01	23.28	0.25	1.38
	Remote & Upper Umpqua	12	9.75	24.98	13.29	4.87	7.98	21.44	15.91	0.29	1.49
	White Tail Ridge Formation	2	9.26	19.87	7.79	2.15	9.66	40.54	9.19	0.27	1.28
I	Berry Creek Member	8	18.25	15.42	8.68	2.70	7.93	22.02	23.89	0.59	0.51
	Tenmile Formation	5	16.21	21.11	10.27	2.36	12.49	21.11	15.27	0.66	0.52
	Slater Creek Member	2	4.07	17.78	9.26	2.73	14.69	27.65	22.58	0.62	0.62
	Bushnell & Lower Umpqua	7	3.70	15.03	7.63	2.06	19.21	30.28	20.68	0.69	0.72
Klamath Mtns.	Pre-Tertiary	1	17.90	10.10	12.04	23.12	7.88	10.48	17.88	0.20	0.40
	AVERAGE		17.69	11.85	16.13	7.18	18.06	14.78	11.21	2.27	0.82

*Qm=Monocrystalline Quartz, Qp=Polycrystalline Quartz, P=Plagioclase, K=K-Feldspar,
Lv=Volcanic Rock Fragments, Lm=Metamorphic Rock Fragments, Ls=Sedimentary Rock Fragments.

Table 2.3. Percent abundance of quartz, feldspar, lithic fragments, and accessory minerals.

SEQUENCE	UNIT	SORTING	ROUNDING	GRAIN SIZE	TEXTURAL MATURITY
IV	**Spencer Formation**	Moderate to Well	Subangular to Subrounded	V. Coarse to Medium	Submature to Immature
	Bateman Formation	Moderate to Well	Subangular to Subrounded	V. Coarse to Medium	Submature to Immature
	Elkton Formation	Moderate to Poor	Angular to Subrounded	Medium to Fine, some Coarse	Immature to Submature
	Baughman Member	Poor to V. Poor	Angular to Subrounded	V. Coarse to Medium, locally Pebble Conglomerate	Immature
III	**Tyee Mountain Member**	Moderate to Poor	Subrounded to Angular	Medium to Fine, locally Pebbly to V. Coarse	Immature to Submature
II	**Rasler Creek Tongue**	Moderate	Rounded to Subangular	Coarse to Medium	Mature to Submature
	Coquille River Member	Moderate to Poor	Rounded to Subangular	V. Coarse to Medium	Mature to Submature
	Remote & Upper Umpqua	Poor to V. Poor	Subangular to Angular	Pebble-Cobble Conglomerate, some V. Coarse to Medium	Immature to Submature
I	**Berry Creek Member**	Moderate	Wellrounded to Subrounded	Medium to Fine	Mature to Submature
	Tenmile Formation	Poor to Moderate	Subangular to Angular	Coarse to Medium	Immature to Submature
	Slater Creek Member	Moderate	Rounded to Subrounded	largely Fine, some V. fine	Submature to Mature
	Bushnell & Lower Umpqua	V. Poor to Poor	Subangular to Very Angular	Pebble-Cobble Conglomerate, some V. Coarse to Coarse	Immature to Submature
Klamath Mtns.	**Pre-Tertiary**	Well to Moderate	Wellrounded to Subrounded	Medium to Fine	Mature

Table 2.4. Textural characteristics of Eocene Tyee basin sandstones and conglomerates.

SEQUENCE	Stratigraphic Unit	No. of Samples	Q	F	L	Qm	F	Lt	Qp	Lv	Ls
IV	Spencer Formation	2	35.01	37.94	27.05	34.07	37.94	27.98	3.37	95.09	1.55
	Bateman Formation	2	32.06	39.48	28.47	31.08	39.48	29.44	3.49	92.12	4.39
	Elkton Formation	1	32.58	38.60	28.82	30.33	38.60	31.08	7.26	91.94	0.81
	Baughman Member	5	27.91	33.18	38.91	25.79	33.18	41.04	5.26	94.06	0.67
III	Tyee Mountain Member	13	32.33	36.52	31.15	26.69	36.52	36.79	15.82	84.18	0.00
II	Rasler Creek Tongue	2	49.35	26.15	24.50	19.40	26.15	54.45	54.30	41.57	4.13
	Coquille River Member	8	62.85	19.46	17.69	11.06	19.46	69.47	73.67	10.54	15.79
	Remote & Upper Umpqua	12	62.59	17.50	19.91	9.85	17.50	72.66	73.31	10.70	15.99
	White Tail Ridge Formation	2	66.04	10.21	23.76	9.47	10.21	80.33	70.54	12.38	17.08
I	Berry Creek Member	8	70.73	11.60	17.67	18.44	11.60	69.96	74.85	11.56	13.59
	Tenmile Formation	5	64.69	12.82	22.49	16.46	12.82	70.72	68.09	17.53	14.38
	Slater Creek Member	2	67.59	11.12	21.29	4.12	11.12	84.76	74.89	17.55	7.56
	Bushnell & Lower Umpqua	7	57.75	5.73	36.52	3.68	5.73	90.59	59.86	21.45	18.70
Klamath Mtns.	Pre-Tertiary	1	35.76	34.98	29.26	18.04	34.98	46.98	37.88	19.02	43.01
	AVERAGE		49.80	23.95	26.25	18.46	23.95	57.59	44.47	44.26	11.26

SEQUENCE	Stratigraphic Unit	No. of Samples	Qm	P	K	Lv	Ls	Lm
IV	Spencer Formation	2	47.31	37.39	15.30	97.94	1.58	0.49
	Bateman Formation	2	44.07	39.50	16.43	94.50	2.07	3.43
	Elkton Formation	1	44.00	40.00	16.00	94.21	0.83	4.96
	Baughman Member	5	43.78	40.16	16.07	98.28	0.44	1.29
III	Tyee Mountain Member	13	42.26	39.56	18.18	92.00	1.81	6.19
II	Rasler Creek Tongue	2	42.54	45.56	11.90	49.71	12.83	37.46
	Coquille River Member	8	34.98	49.34	15.68	14.32	46.53	39.15
	Remote & Upper Umpqua	12	36.54	49.80	13.65	12.74	34.52	52.74
	White Tail Ridge Formation	2	47.23	41.60	11.16	16.04	14.14	69.82
I	Berry Creek Member	8	61.71	29.20	9.09	12.20	48.04	39.76
	Tenmile Formation	5	56.13	35.72	8.15	19.89	31.25	48.86
	Slater Creek Member	2	27.07	61.42	11.50	11.91	35.73	52.37
	Bushnell & Lower Umpqua	7	38.68	48.47	12.86	14.02	28.82	57.16
Klamath Mtns.	Pre-Tertiary	1	34.25	22.01	43.74	22.86	49.12	28.02
	AVERAGE		42.90	41.41	15.69	46.47	21.98	31.55

Q=Quartz; F=Feldspar; L=Lithic fragments; Qm=Monocrystalline quartz; Qp=Polycrystalline quartz; Lt=Total lithic fragments;
Lv=Volcanic rock fragments; Ls=Sedimentary rock fragments; Lm=Metamorphic rock fragments; P=plagioclase; K=Potassium feldspar

Table 2.5. Average values of ternary plots for Eocene sandstones.

Well Name	Depth (Feet)	Unit	Source	Total Extract (ppm)	Hydrocarbons (ppm)		Nonhydrocarbons (ppm)		CPI	Pr/Ph
					Saturates	aromatics	Asphaltene	NSO's		
Long Bell 1	4560	Upper Umpqua	Brown & Ruth (1983)	324	70	24	111	119	1.25	0.7
Long Bell 1	6880	Lower Umpqua	Brown & Ruth (1983)	682	150	85	264	183	1.2	0.9
Long Bell 1	8120	Lower Umpqua	Brown & Ruth (1983)	357	60	15	161	121	1.19	1.3
Weyerh. F-1	1220	TMM	Brown & Ruth (1983)	249	*	*	*	*	2.12	4
Weyerh. F-1	1310	TMM	Brown & Ruth (1983)	161	*	*	*	*	2.21	5.6
Weyerh. F-1	1400	TMM	Brown & Ruth (1983)	115	*	*	*	*	2.07	3.6
Weyerh. F-1	1490	TMM	Brown & Ruth (1983)	234	18	27	115	67	2.13	5.6
Weyerh. F-1	1580	TMM	Brown & Ruth (1983)	245	19	37	124	52	2.18	7
Weyerh. F-1	1670	TMM	Brown & Ruth (1983)	160	8	17	89	30	2.17	5.6
Weyerh. F-1	1760	TMM	Brown & Ruth (1983)	225	25	28	129	31	1.87	2.1
Weyerh. F-1	2030	TMM	Brown & Ruth (1983)	98	*	*	*	*	2	2.7
Weyerh. F-1	2300	TMM	Brown & Ruth (1983)	188	5	22	113	36	1.97	6
Weyerh. F-1	2840	TMM	Brown & Ruth (1983)	105	*	*	*	*	1.95	4.8
Weyerh. F-1	3560	Lower Umpqua	Brown & Ruth (1983)	338	38	49	136	75	1.63	3.6
Weyerh. F-1	3740	Lower Umpqua	Brown & Ruth (1983)	621	29	115	240	181	1.48	5.4
Weyerh. F-1	3920	Lower Umpqua	Brown & Ruth (1983)	450	30	91	185	129	1.53	6.3
Weyerh. F-1	4100	Lower Umpqua	Brown & Ruth (1983)	527	34	98	230	153	1.48	6.7
Weyerh. F-1	4190	Lower Umpqua	Brown & Ruth (1983)	374	17	66	169	72	1.45	6.3
Weyerh. B-1	6230	TMM	Amoco (1985)	130	*	*	*	*	1.36	4
Weyerh. B-1	6320	TMM	Amoco (1985)	203	*	*	*	*	1.15	6.17
Weyerh. B-1	6420	Lower Umpqua	Amoco (1985)	269	*	*	*	*	1.68	6
Weyerh. B-1	6510	Lower Umpqua	Amoco (1985)	215	*	*	*	*	2	5.14
Weyerh. B-1	6610	Lower Umpqua	Amoco (1985)	159	*	*	*	*	1.16	5.55
Weyerh. B-1	6700	Lower Umpqua	Amoco (1985)	170	*	*	*	*	1.38	5.5
Weyerh. B-1	6800	Lower Umpqua	Amoco (1985)	74	*	*	*	*	1.19	2.75
Weyerh. B-1	6900	Lower Umpqua	Amoco (1985)	219	*	*	*	*	1.55	5.5
Weyerh. B-1	6940	Lower Umpqua	Amoco (1985)	175	*	*	*	*	0.83	2.71
Weyerh. B-1	9010	Lower Umpqua	Amoco (1985)	166	*	*	*	*	1.67	6.89
Weyerh. B-1	9280	Lower Umpqua	Amoco (1985)	84	*	*	*	*	1.77	4.17
Mobil Sutherlin	1480	Lower Umpqua	Brown & Ruth (1983)	656	78	63	242	273	1.59	2
Mobil Sutherlin	3590	Lower Umpqua	Brown & Ruth (1983)	1322	124	128	438	632	1.32	2.5
Mobil Sutherlin	10500	Lower Umpqua	Brown & Ruth (1983)	743	41	176	153	373	1.56	4.6
Harris 1-4	1020	TMM	Amoco (1983)	1111	97	*	*	*	*	*
Harris 1-4	1500	TMM	Amoco (1983)	403	53	*	*	*	*	*
Harris 1-4	1980	Lower Umpqua	Amoco (1983)	332	64	*	*	*	*	*
Harris 1-4	3000	Lower Umpqua	Amoco (1983)	346	94	*	*	*	*	*
Harris 1-4	3600	Lower Umpqua	Amoco (1983)	128	16	*	*	*	*	*
Harris 1-4	5120	Lower Umpqua	Amoco (1983)	167	29	*	*	*	*	*
Harris 1-4	5480	Lower Umpqua	Amoco (1983)	201	22	*	*	*	*	*
Outcrop	36, T28S, R12W	Lower Umpqua	Newton (1980)	182	*	*	*	*	*	1.15
Outcrop	26, T21S, R12W	TMM	Newton (1980)	185	*	*	*	*	*	3

Table 4.1. Results of C15+ heavy hydrocarbon analysis. TMM=Tyee Mountain Member; CPI=Carbon Preference Index; Pr/Ph=Pristane/Phytane;
*= Not Available

No. in fig. 4.22	UNIT	SAMPLE NO.	ROCK TYPE	TOC	HI (S2/TOC)	Tmax	Ro	LOCATION
5	Hubbard Creek	RN-91-112	Shale	Fair	Gas	*Mature (?)	N/A	Fig 4.20 (5)
6	Hubbard Creek	SR 900'	Mudstone	Fair	Gas	*Mature (?)	N/A	Fig. 4.2 (#3)
10	Hubbard Creek	RN-91-348	Mudstone	Fair	Gas	*Mature (?)	N/A	Fig 4.20 (2)
1	Remote	RN-91-270	Coal	Very Good	Gas & Oil	Mature	Immature	Fig 4.20 (3)
3	Tenmile	SC 1380'	Mudstone	Fair	Gas	Mature	N/A	Fig. 4.2 (#11)
7	Tenmile	RN-91-070	Mudstone	Fair	Gas	Mature	N/A	Fig 4.20 (4)
8	Tenmile	RN-91-354	Mudstone	Fair	Gas	Mature	N/A	Fig 4.20 (1)
9	Tenmile	GH 2130'	Mudstone	Fair	Gas	Mature	N/A	Fig. 4.2 (#10)
11	Tenmile	GH 1410'	Mudstone	Fair	Gas	Mature	Immature	Fig. 4.2 (#10)
2	Bushnell Rock	SC 1860'	Siltstone	Fair	Gas	Mature	Immature	Fig. 4.2 (#11)
4	Bushnell Rock	SC 1200'	Siltstone	Fair	Gas	Mature	N/A	Fig. 4.2 (#11)
12	L. Umpqua	RN-90-322	Mudstone	Poor	Gas	Mature	Mature	Fig. 4.17 (arrow)

*Tmax values are likely to be too high because of adsorption of pyrolytic organic compounds onto the smectitic clay-rich matrix
SR=Sawyer Rapids #1 well; GH=Glory Hole #1 well; SC=Scott #1 well

Table 4.3. Source rocks that have the best maturity in the Tyee basin.

Well No.	Well Name	Depth (feet)	Date Drilled	Comments	Rock Unit
#1	Long Bell 1	4200	1957	Brown stain, fluorescence	Tyee Mountain Member
	Long Bell 1	5345	1957	Slight gas	Umpqua Group
	Long Bell 1	5590	1957	Trace, hydrocarbon cut in core	Umpqua Group
	Long Bell 1	6040	1957	Trace, hydrocarbon cut in core	Umpqua Group
	Long Bell 1	6900	1957	Tar stain, fluorescence	Umpqua Group
#2	Harris 1-4	5962	1982	Gas shows and several oi shows	Siletz River Volcanics
#3	Sawyer Rapids	850	1980	Minor oil	Hubbard Creek Member
	Sawyer Rapids	959	1980	Trace of gold fluorescence	Hubbard Creek Member
	Sawyer Rapids	1050	1980	Minor oil	Tyee Mountain Member
#4	Weyerh. F-1	1000	1985	Oil in mud, slight yellow cut	Tyee Mountain Member
#5	Weyerh. B-1	1400	1985	Oil stain, slight yellow cut	Elkton Formation
	Weyerh. B-1	2100	1985	Oil stain	Baughman Member
	Weyerh. B-1	2900	1985	Oil stain	Hubbard Creek Member
	Weyerh. B-1	5300	1985	Trace crude oil in mud	Tyee Mountain Member
	Weyerh. B-1	11204	1985	Micro show	Siletz River Volcanics
#7	Oakland	2200	1926	Trace oil	?
	Oakland	2234	1926	Considerable gas	?
#8	Sutherlin Unit 1	13177	1979	Tested 28 mcfd at 3000 feet	Siletz River Volcanics
#10	Glory Hole	2980	1983	Pale yellow cut	Tenmile Formation
#11	Scott 1	1500 to 3520	1954	Oil show in cores	Bushnell Rock Formation
	Scott 1	3792	1954	Some oil colors	Umpqua Group
#13	W. F. Kernin	3900	1931 to 1948	Gas and oil shows	?
#15	F. W. Dillard	700	1910	Oil in shale reported	?
#16	Ziedrich 1	1640 to 1655	1955	8 to 10 mcf; oil shows	Remote Member
	Ziedrich 1	4368	1955	Some gas	Tenmile Formation
#18	Wollenberg 1	1100	1956 to 1965	Gas shows	?
#20	Dayton 1	1370	1955 to 1958	Small flow of gas	?

Table 4.4. Oil and gas shows in exploration wells (from Niem and Niem, 1990).

Formation	Age (Ma)	Thickness (Feet)	Lithology			Paleo-Water Depth (Feet)	
			Sandstone	Siltstone	Mudstone		
Bateman	48	1200	85	10	5	0 to 150	IN
Elkton	48.2	1200	5	25	70	1560	ON to UB
Baughman	48.5	1000	95	5	-	0 to 150	IN
Hubbard Ck.	49	600	-	10	90	1560	ON to UB
Tyee Mtn.	49.5	3400	90	5	5	4700	UB to MB
Rasler Ck.	49.6	600	70	10	20	0 to 150	IN
Camas Valley	49.8	1200	-	5	95	4700	ON to MB
WTR	51	4200	70	15	15	0 to150	IN
Tenmile	52	2000	30	30	40	4700	UB to MB
Bushnell Rock	54	4000	90	5	5	0 to150	IN
pre-Tertiary	67	3000	90	5	5	0 to 150	IN
	Initial Porosity (%)		45	55	60		
	Compaction Factor (km-1)		1.75	2.2	2.4		

*IN=Inner Neritic; ON=Outer Neritic; UB=Upper Bathyal; MB=Middle Bathyal
WTR=White Tail Ridge Formation

Table 5.1. Input values for geohistory calculations for Basin Mod program for the Tyee basin.

Well Name	Total Depth (Feet)	Surface Tem. (°F)	Bottom H. Tem. (°F)	*Correction F. (°F)	Gradient (°F/100 feet)
Long Bell	9004	65	143	30	1.1995
Florida Harris	5962	65	129	23	1.4592
Sawyer Rapids	5560	65	108	21.3	1.1565
Weyerh. F-1	4390	65	115	17.4	1.5353
Weyerh. B-1	11300	65	152	32.7	1.0593
Union Liles	6686	65	108	25.1	1.0185
Mobil Sutherlin	13160	65	178	32.5	1.1056
Scott	3684	65	117	14.8	1.8132
U. Ziedrich	3061	65	90	12	1.2088
Great Discovery	3497	65	90	14	1.1152

*Standard AAPG temperature correction (Meissner, 1978) applied **Average = 1.2671 °F/100 feet**

Table 5.2. Modern geothermal gradients calculated by using bottom-hole temperatures from 10 exploration wells in the basin. The average regional geothermal gradient is 1.27 °F/100 feet.

STATE OF OREGON
DEPARTMENT OF GEOLOGY AND MINERAL INDUSTRIES
DONALD A. HULL, STATE GEOLOGIST

PLATE 1 INTERPRETED NORTH-SOUTH SEISMIC-REFLECTION PROFILE ACROSS SOUTHERN TYEE BASIN

The geologic cross section and topographic profile was constructed from geologic maps of Wells (1996a), Wiley and others (1994), and Niem and Niem (1990). Two wells (Amoco Weyerhaeuser B-1 and Northwest Sawyer Rapids) provided subsurface control.

By Peter O. Hales, Weyerhaeuser Corporation, Alan R. Niem, Oregon State University, and In-Chang Ryu, Oregon State University

OGI-19
Oil and Gas Potential of the Southern Tyee Basin, Southern Oregon Coast Range
By Peter O. Hales, Alan R. Niem, and In-Chang Ryu
Plate 1

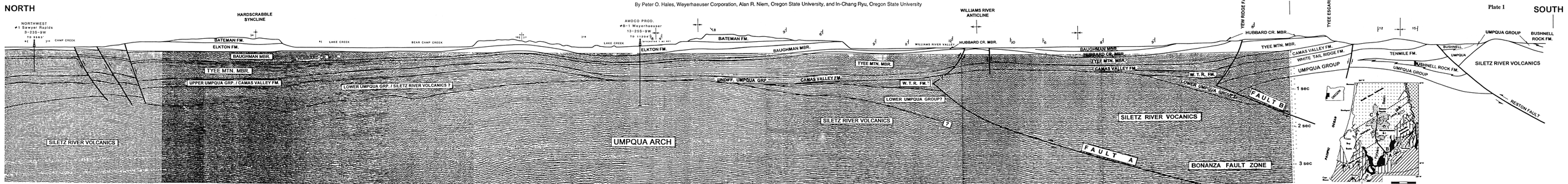

Plate 2A Stratigraphic distribution of sandstone and conglomerate samples

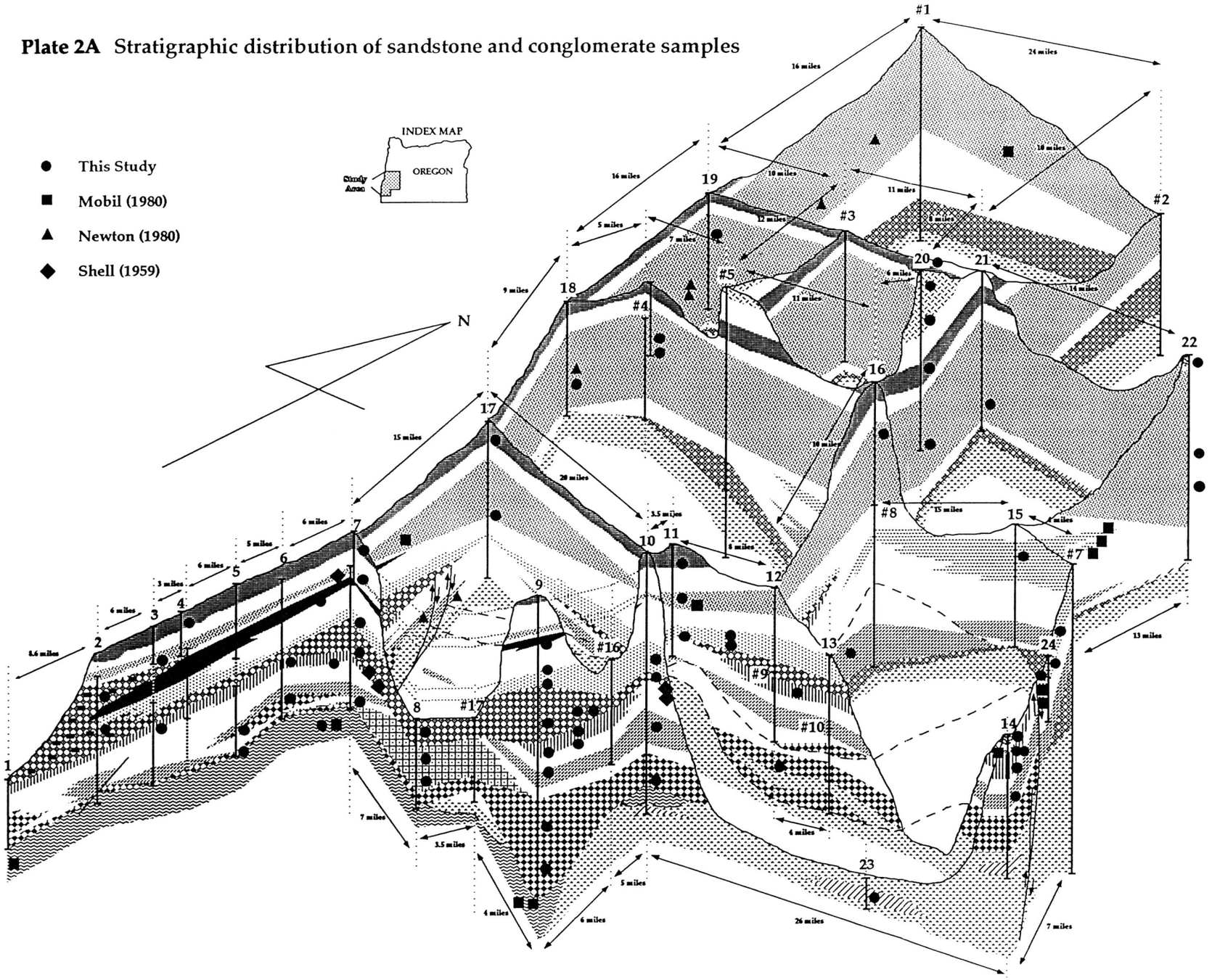

EXPLANATION

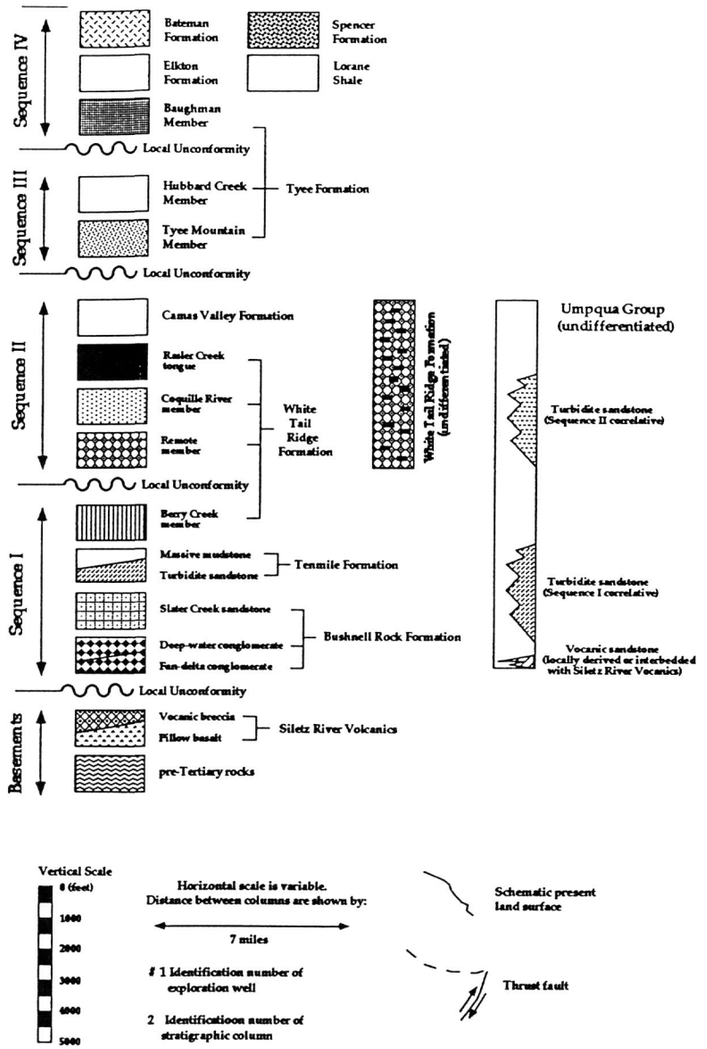

Plate 2B Stratigraphic distribution of porosity

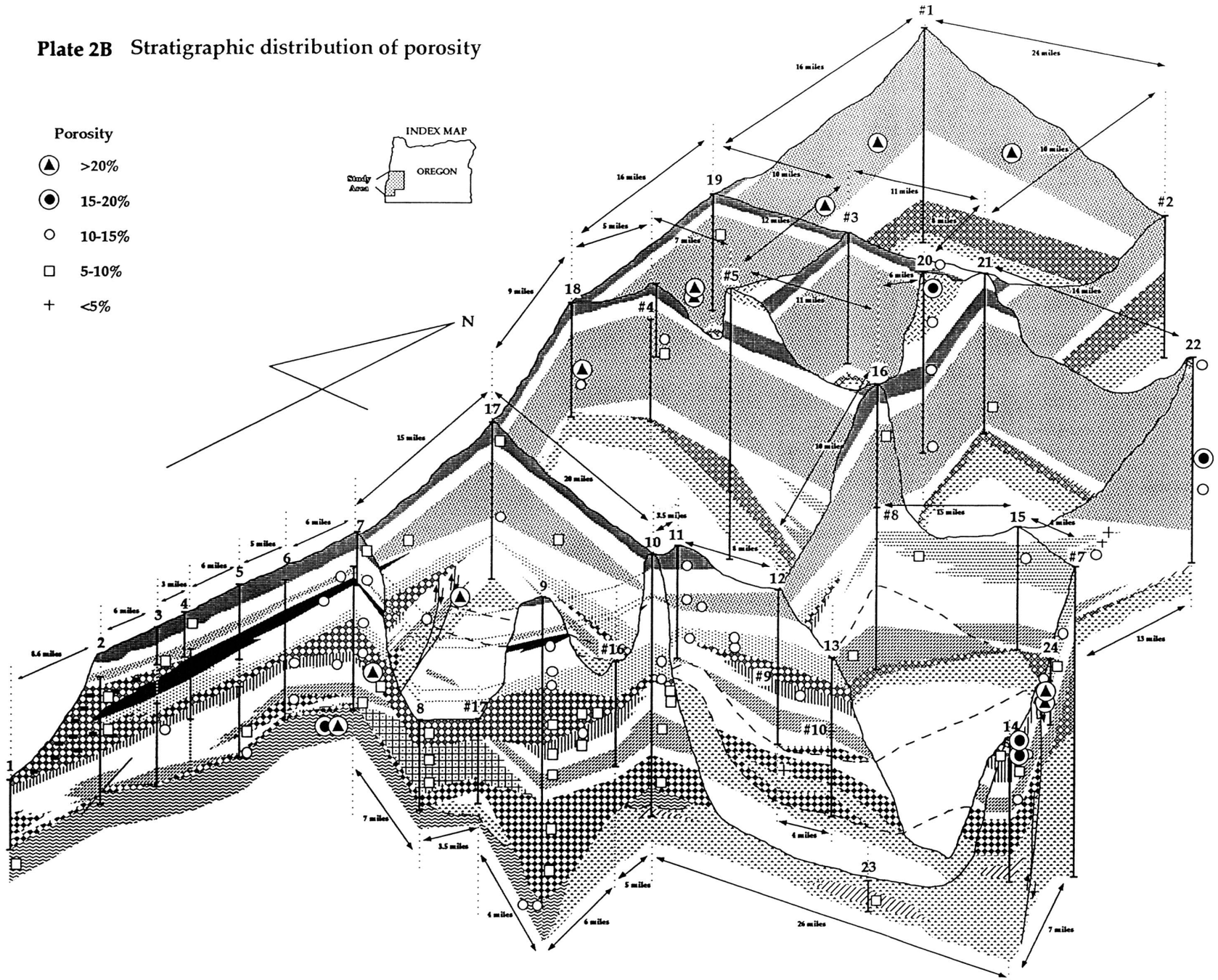

EXPLANATION

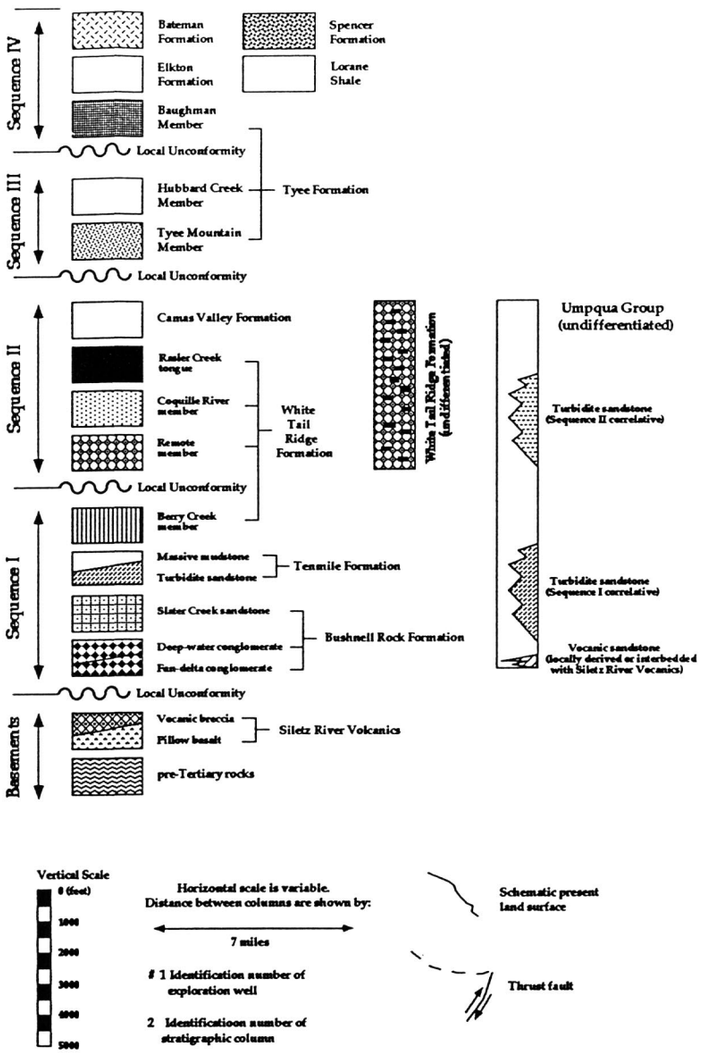

Plate 2C Stratigraphic distribution of permeability

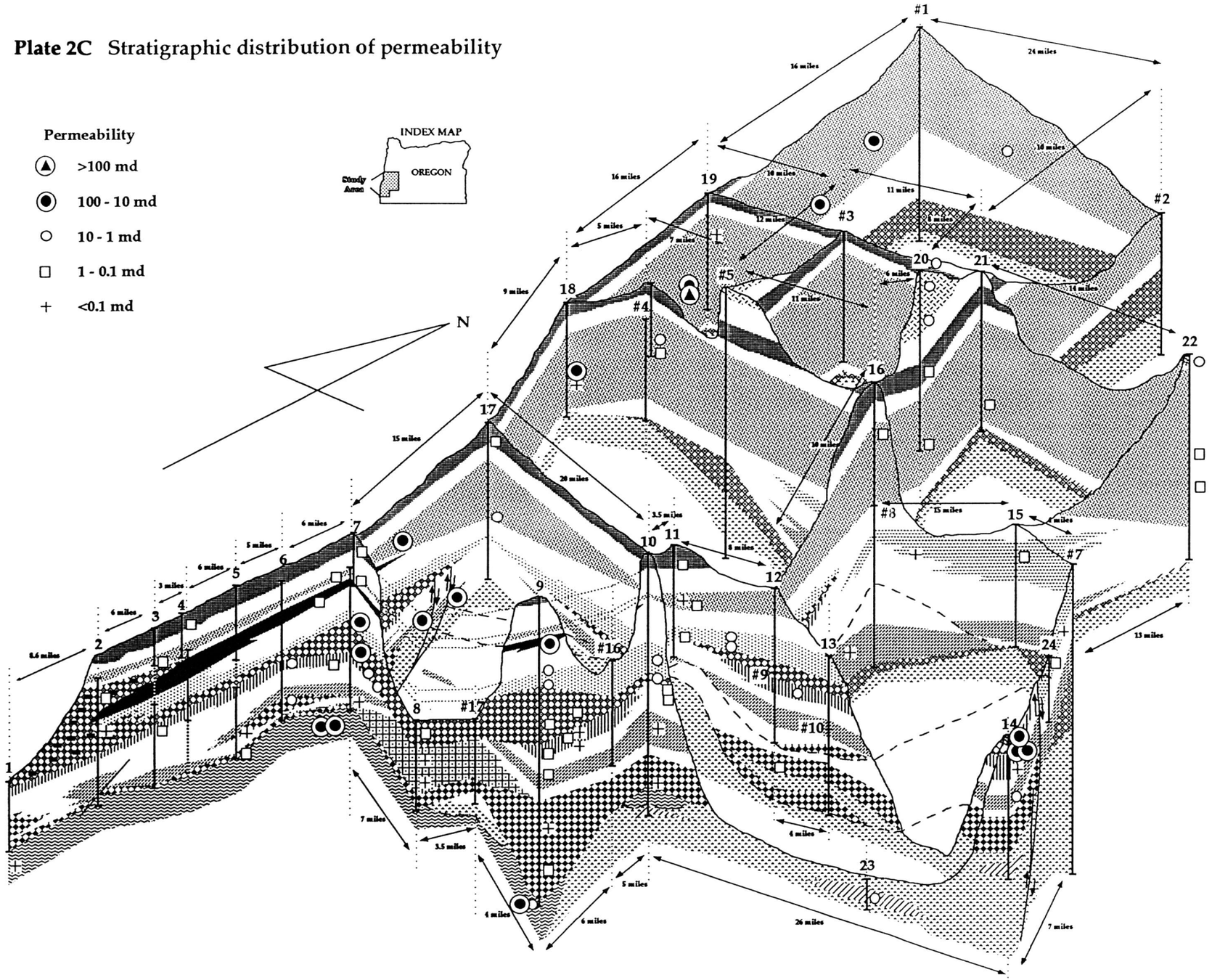

EXPLANATION

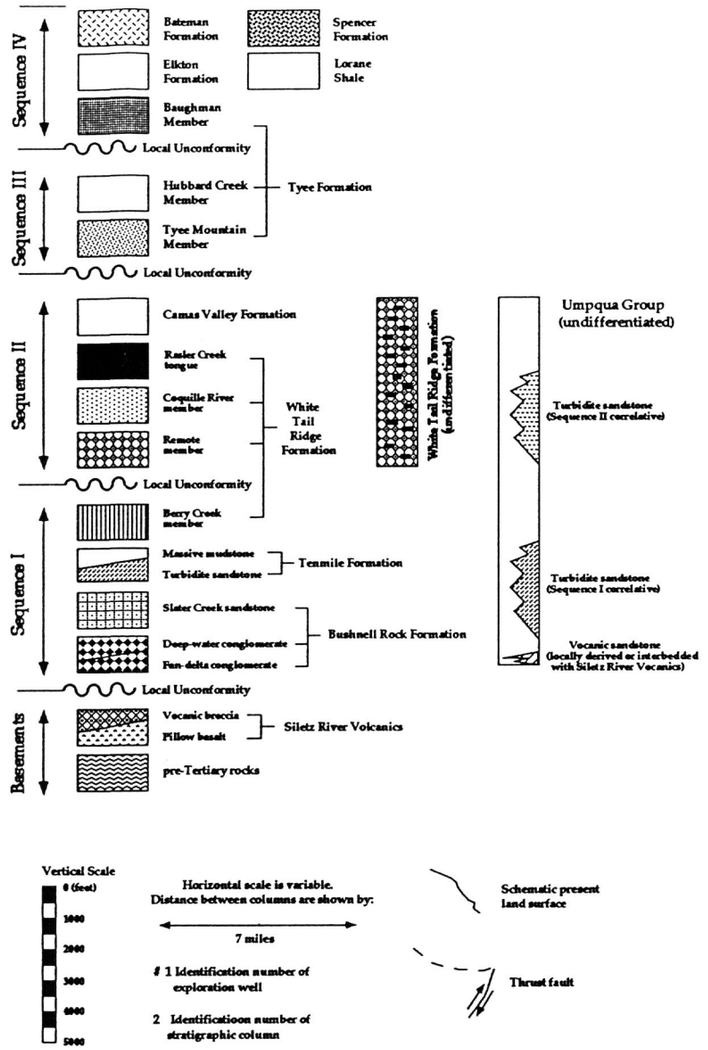

Plate 3A Stratigraphic distribution of source rock samples

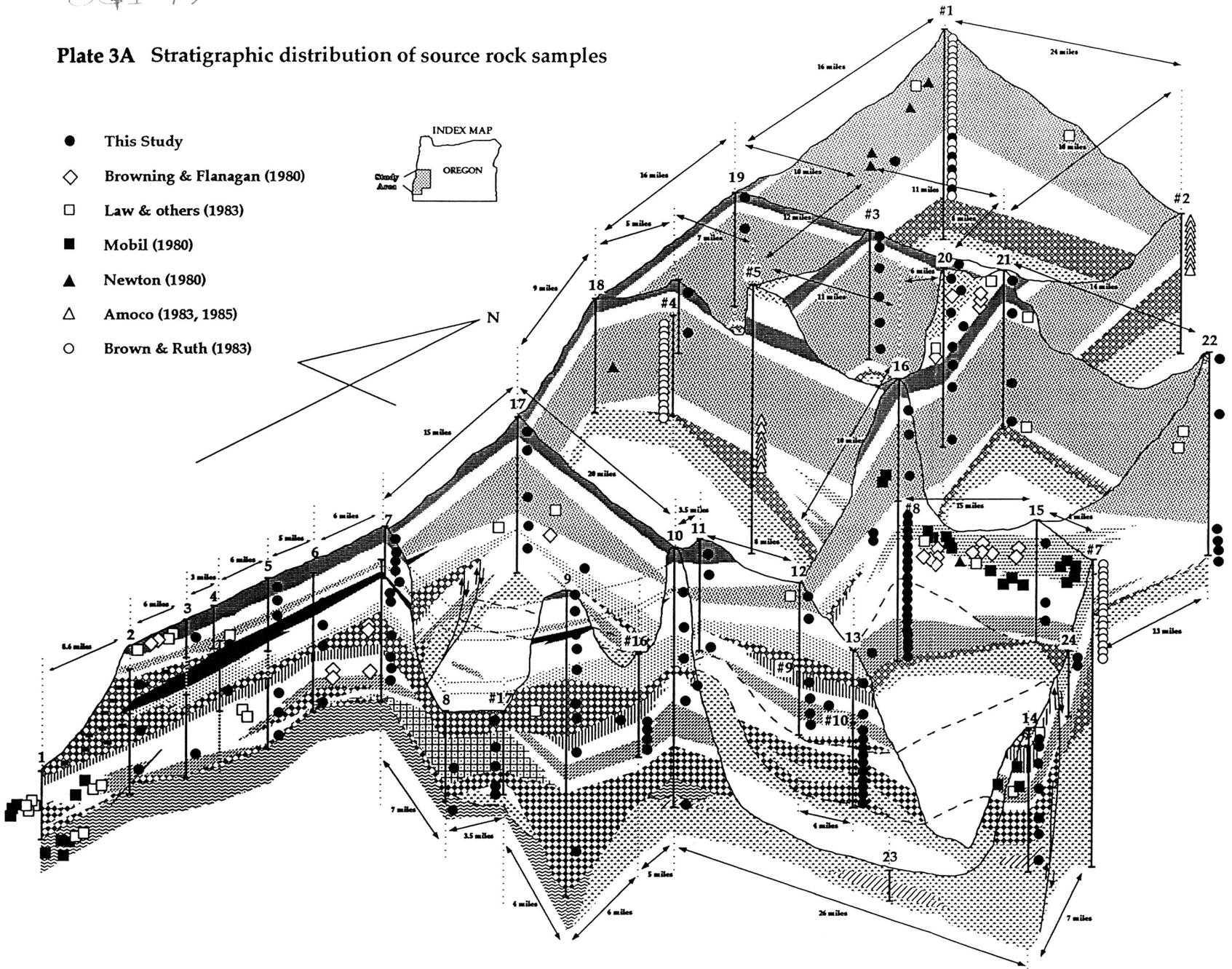

EXPLANATION

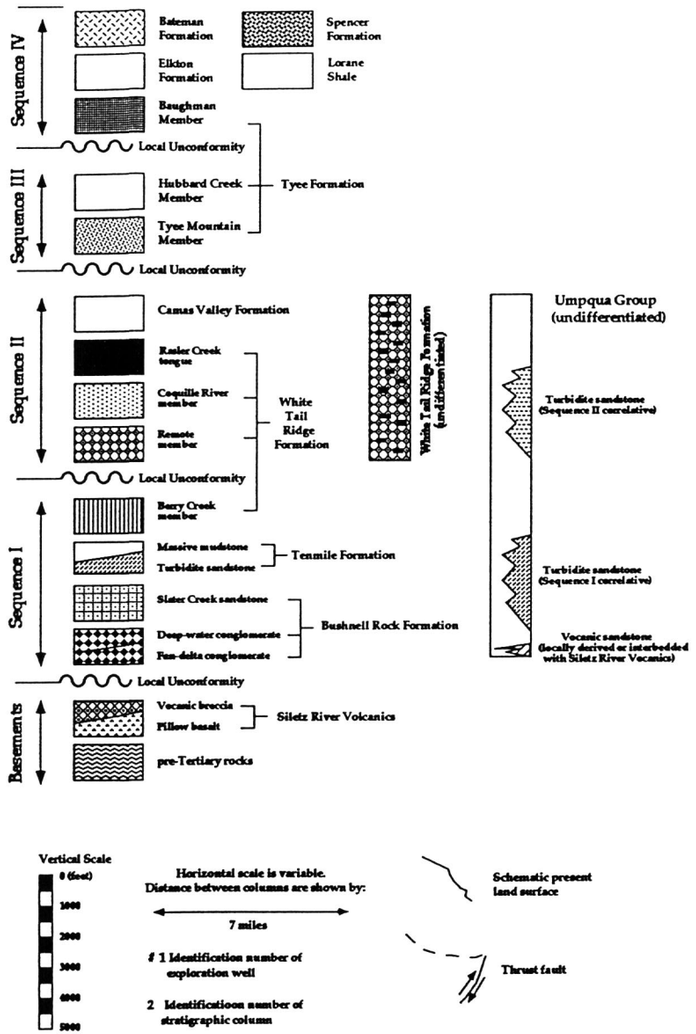

Plate 3B Stratigraphic distribution of TOC

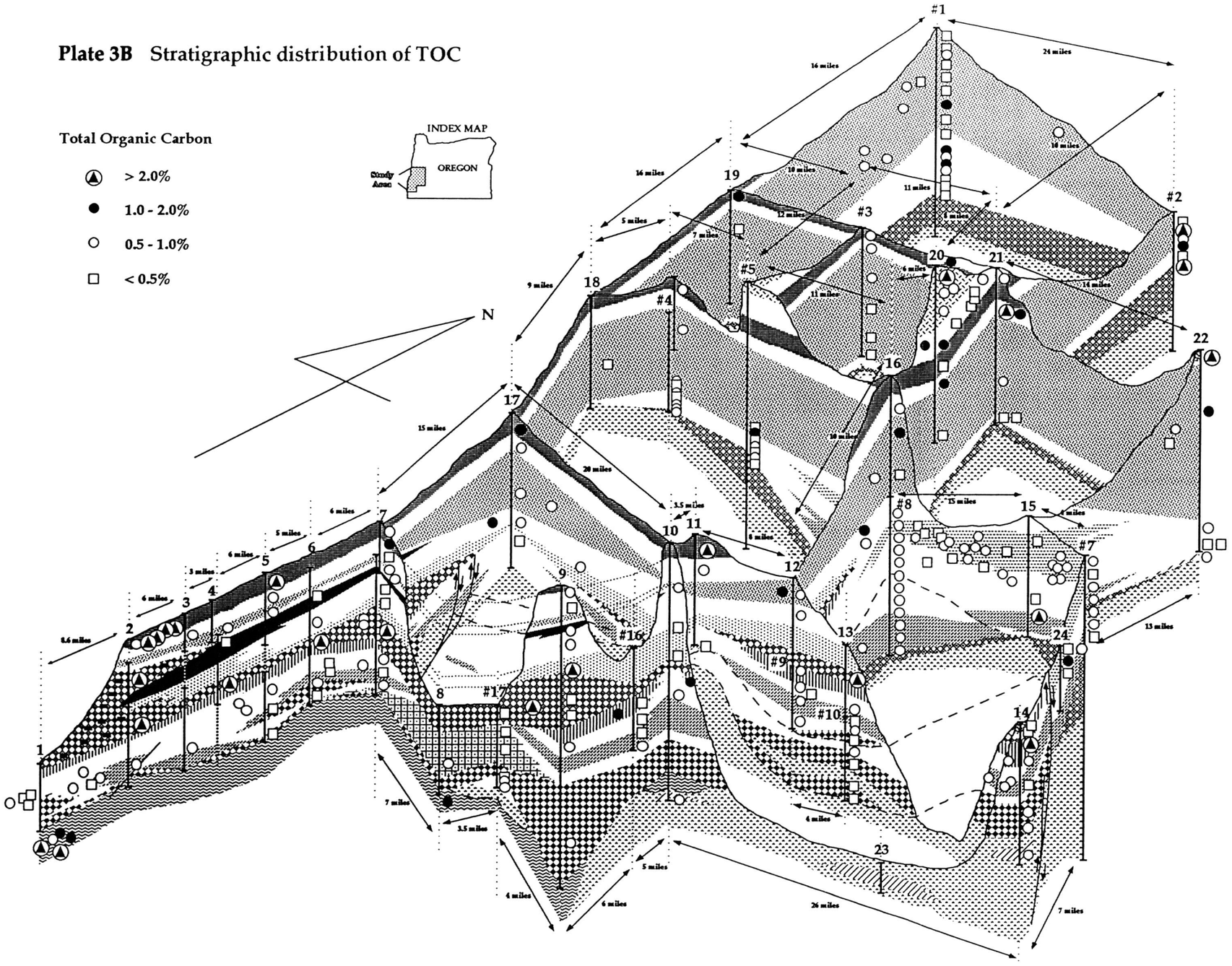

EXPLANATION

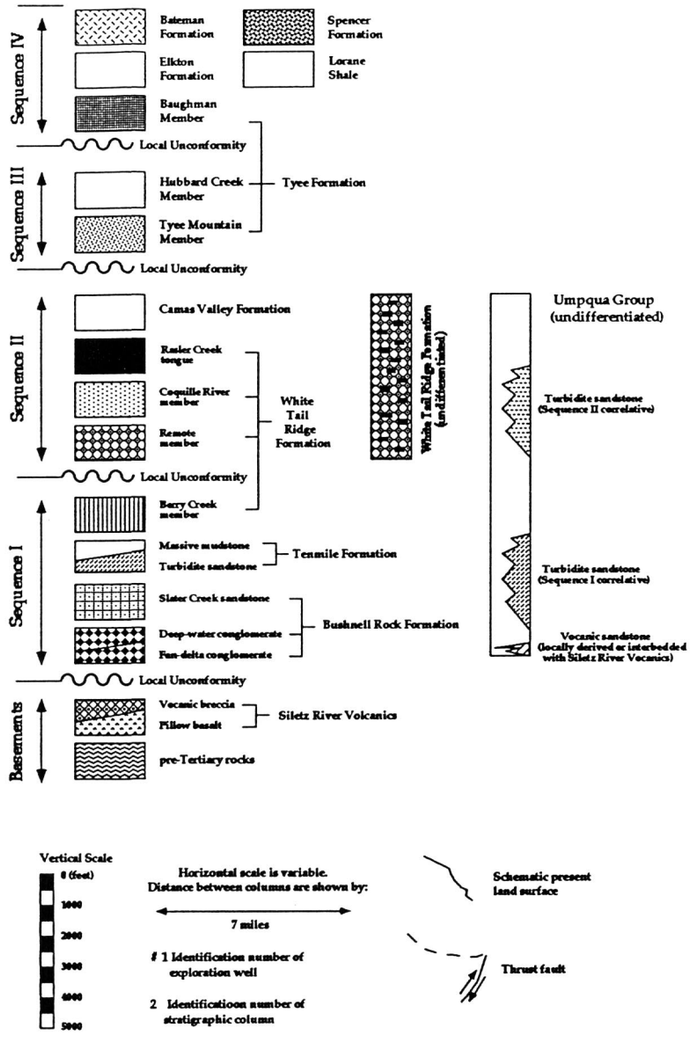

Plate 3C Stratigraphic distribution of vitrinite reflectance (%Ro)

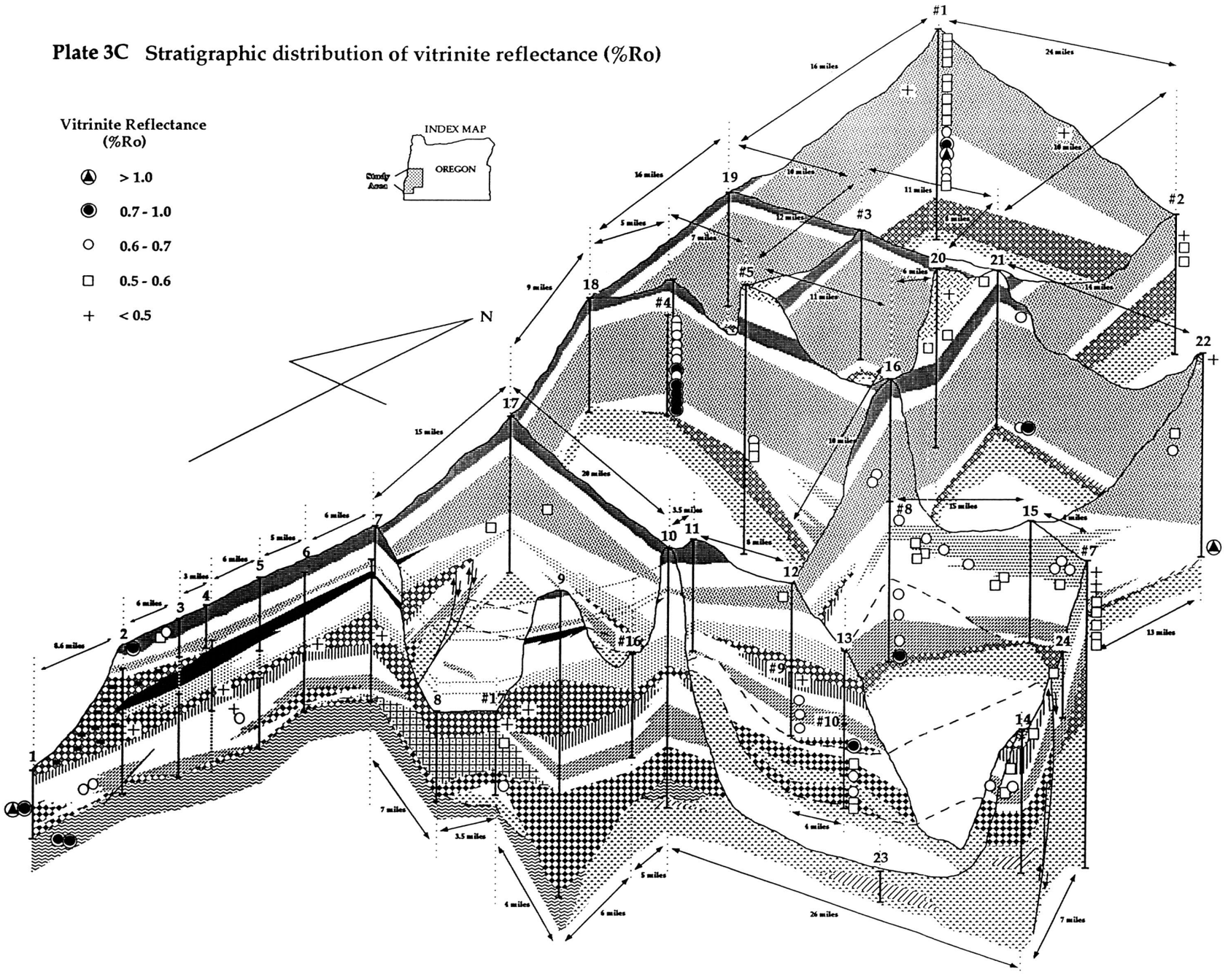

EXPLANATION

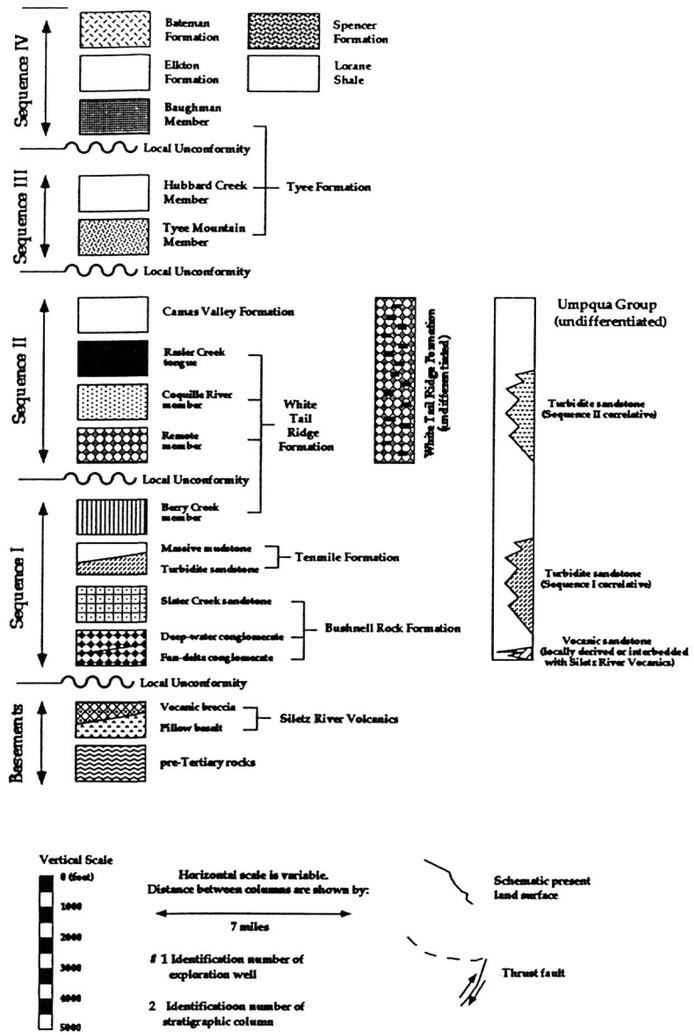

Plate 3D Stratigraphic distribution of Tmax

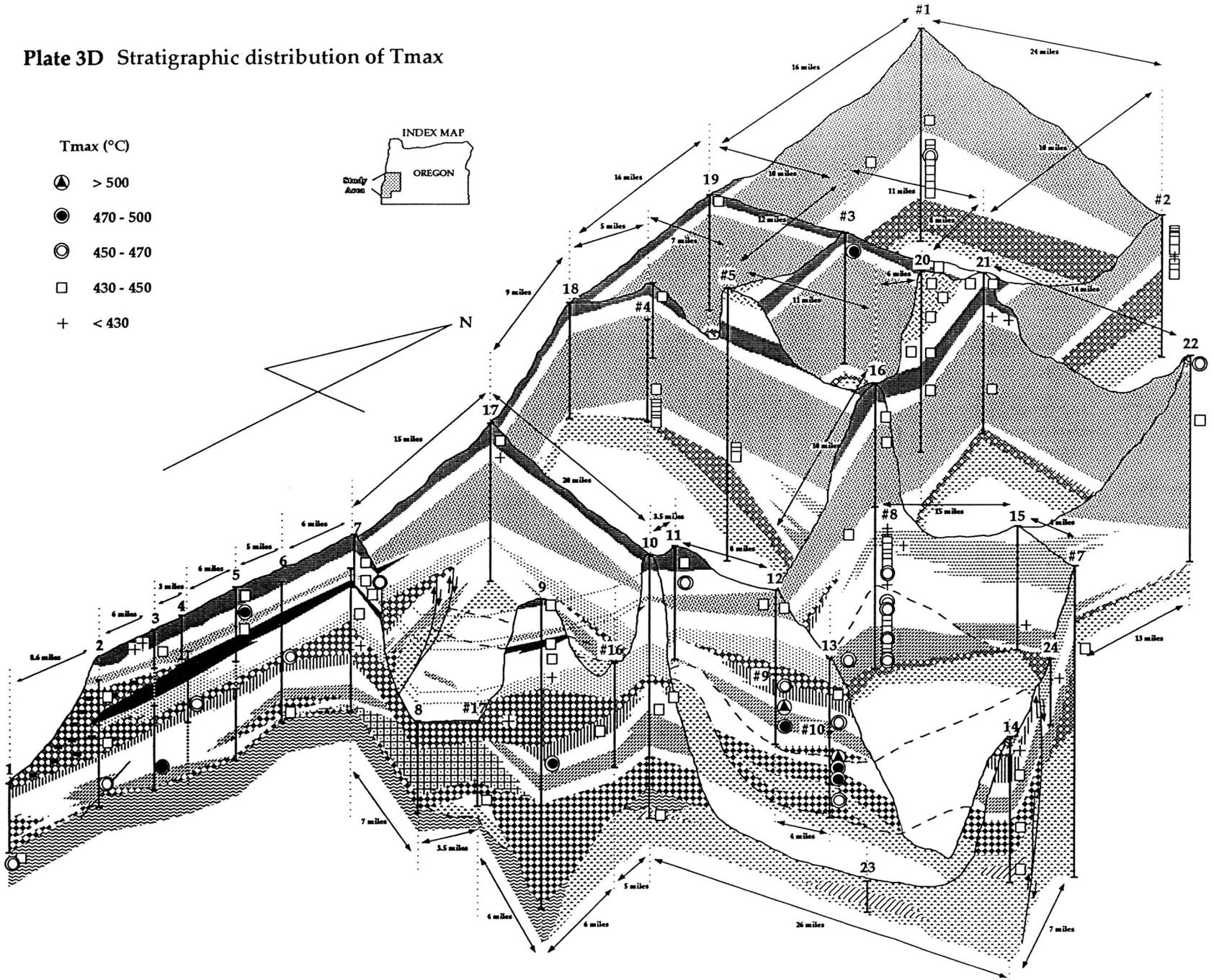

EXPLANATION

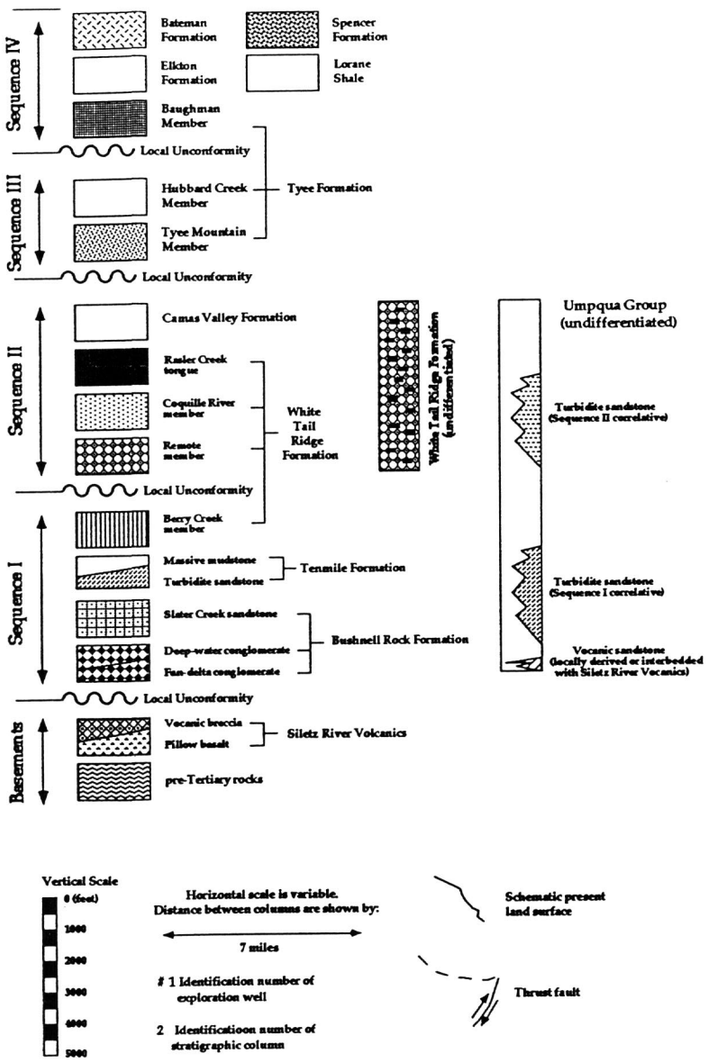

Plate 4 **Index map of fence diagram**

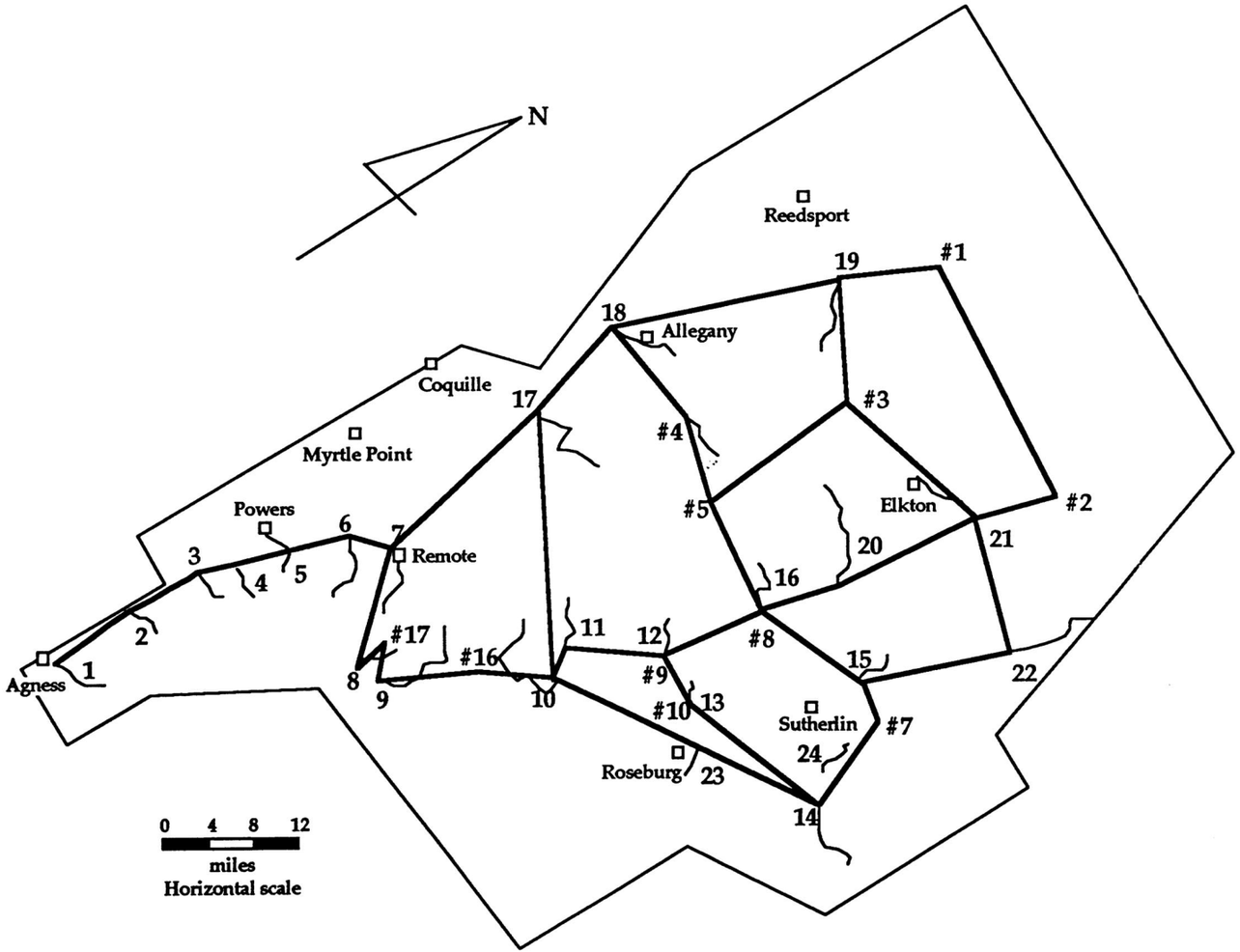

Table I Exploration well numbers and well names

No.	Operator and Well Name	Date Drilled	Total Depth (ft)
#1	General Petroleum Long Bell No. 1	1957	9,004
#2	Florida Exploration Harris 1-4	1982	5,962
#3	Northwest Exploration Sawyer Rapids No. 1	1980	5,562
#4	Amoco Wayerhaeuser F-1	1985	4,428
#5	Amoco Wayerhaeuser B-1	1985	11,330
#7	Mobil Sutherlin Unit 1	1979	13,177
#8	Union Liles No. 1	1951	7,002
#9	Hutchins and Marrs Glory Hole No. 1	1983	2,987
#10	Oil Developers Inc. Scott No. 1	1954	3,693
#16	Uranium Ziedrich No. 1	1955	4,368
#17	Hutchins and Marrs Great Discovery No. 2	1984	3,510

Table II List of measured sections and exploration holes that comprise the stratigraphic columns

Column No.	Measured Sections and Exploration Holes
1	Agness
2	Agness Pass
3	China Flat
4	Coal Creek and Sand Rock Mountain
5	Powers
6	Rasler Creek
7	Remote and Sandy Creek
8	Slater Creek
9	Twelvemile Creek, Oregon Highway 42, and Bingham Creek
10	Reston Road, Suicide Creek, Shield Creek, and Lost Lake
11	Reston Junction and Burnt Ridge
12	Glory Hole well (#9), Lookingglass Road, and Callahan Road
13	Scott well (#10), Cow Hollow, and Melrose
14	Glide
15	Metz Hill
16	Union Liles well (#8) and Tyee Road
17	LaVern Creek and Middle Creek
18	Allegany
19	Loon Lake
20	Kellogg and Waggoner Creek
21	Elkton
22	I-5
23	S. Roseburg
24	Sutherlin Creek